Università degli Studi di Ferrara

DOTTORATO DI RICERCA IN

"FARMACOLOGIA E ONCOLOGIA MOLECOLARE"

CICLO xxv

COORDINATORE Prof. Antonio Cuneo

New insights into the circuitry underlying levodopa-induced dyskinesia in rodent models of Parkinson's disease

Settore Scientifico Disciplinare BIO/14

Dottorando

Dott. Bido Simone

Tutore

Prof. Morari Michele

Anni 2010/2012

Doctoral dissertation

New insights into the circuitry underlying levodopa-induced dyskinesia in rodent models of Parkinson's disease

By
Simone Bido

LEGGE DI FAGIN: il senno di poi è una scienza esatta.

Arthur Bloch

Abstract

Abnormal involuntary movements (AIMs) or dyskinesias are probably the most debilitating side-effect elicited by levodopa pharmacotherapy of Parkinson's disease. Development of levodopa-induced dyskinesias (LID) reflects a processes of sensitization to levodopa taking place primarily in striatum, and leading to the abnormal response to dopaminomimetics. Despite the growing knowledge about the intracellular pathways involved in the development of LID, little is known about the impact of antidyskinetic treatments on the basal ganglia circuitry. In the present thesis, we used microdialysis to investigate the neurochemical and behavioural changes exerted by different antidyskinetic treatments or approaches in basal ganglia. We first found that levodopa evoked AIMs, and simultaneously elevated GABA levels in the substantia nigra reticulata but not globus pallidus of dyskinetic mice and rats, suggesting the involvement of the striato-nigral "direct" GABAergic pathway in both species (Bido et al., J Neurochem 118, 1043-1055, 2011). Amantadine (the only antidyskinetic drug marketed for treating LID) attenuated AIMs expression and prevented the nigral GABA rise (Bido et al., J Neurochem 118:1043-55, 2011), suggesting nigral GABA as a neurochemical correlate of LID. To further investigate which pathway is involved in LID and in the antidyskinetic effect of amantadine, we took advantage from recent studies showing the specificity of Ras-guanine nucleotide-releasing factor 1 and 2 to selectively couple NR2B and NR2A NMDA receptor subunits, respectively. We showed that blockade of striatal expression of Ras-GRF1 using a lentiviral vector carrying a short hairpin RNA (LV Ras-GRF1) caused an attenuation of LID development and expression, which was accompanied by the lack of the increase in nigral GABA. However, in LV Ras-GRF1 mice the antidyskinetic effect of amantadine and its neurochemical correlates were lost, suggesting LV Ras-GRF1 might interfere with the antidyskinetic effect of amantadine by acting on the same target (possibly the NR2B receptor). Conversely, injection of a viral construct expressing a small hairpin directed against RasGRF2 caused only a not significant reduction of LID, and did not prevent the increase of nigral GABA following L-DOPA. In these mice, also the antidyskinetic effect of amantadine remained unaltered (Bido et al., in preparation).

To confirm the involvement of the direct pathway in LID, and dissect out the role of striatal and nigral dopamine D1 and D2 receptors we performed regional perfusion (striatum and substantia nigra pars reticulata) of selective D1 and D2 antagonists simultaneously with systemic L-DOPA

administration. Intrastriatal blockade of D1 receptor attenuated LID and prevented the accompanying rise of nigral GABA levels whereas blockade of D2 receptor was ineffective (Mela et al., Neurobiol Dis 45, 574-583, 2012). When perfused in the substantia nigra, both the D1 and D2 antagonists attenuated LID expression, although only the D1 antagonist prevented the GABA rise.

Overall, the data provide neurochemical evidence that LID is accompanied by activation of D1-receptor expressing striato-nigral GABAergic neurons, and that the antidyskinetic effect of amantadine partly relies on the modulation of this pathway, possibly through NR2B-subunit expressing NMDA receptors. Nonetheless, by using different antidyskinetic approaches we were able to cause only ~50% reduction of LID in face of a complete inhibition of the GABA rise in substantia nigra. This points to the existence of other important neurochemical modulators of LID, possibly also in brain structures outside the basal ganglia.

Table of content

Introduction

Parkinson's disease and L-DOPA-induced dyskinesia

Parkinson's disease (PD) is characterized by prominent loss of dopaminergic neurons in the substantia nigra (SN) and formation of intraneuronal protein inclusions termed Lewy bodies, composed mainly of α-synuclein (Jellinger, 1987). This progressive neurodegenerative process underlies the development of motor and non-motor symptoms. The non-motor manifestations range from dementia (~30% of PD patients) to depression and disturbance to visuo-spatial function as hallucinations, that are frequently owing to the effect of dopaminergic drugs (Fenelon et al., 2000). Depression is a characteristic hallmark of PD can occur at any stages of the disease, and can be use as a diagnostic tool (Noyce et al., 2012). The cardinal features of PD are the motor disturbance, resulting from the dopamine (DA) loss in the midbrain. Tremor is typically at rest and disappears when voluntary movement is performed (Elble, 2000); rigidity is an increase in passive muscle tone in flexor and extensor muscle groups, and is expressed as a defect to obtain a complete muscular relaxation (Delwaide et al., 1986); akinesia is referred as slowness in movement execution (bradykinesia) and the poverty of voluntary movements (hypokinesia; Marsden et al., 1981). Postural instability appears on the late stage of the disease and is associated with the loss of equilibrium and falling (Marsden et al., 1981). In the late 1690s a novel strategy to counteract the motor symptoms of PD has been developed, which is based on the replacement of the DA with the precursor 3,4-dihydroxy-L-phenylalanine (L-DOPA). It was became the gold standard in the therapy of PD. As quickly as the enthusiasm for the new therapy grew, it became evident that were major limitations to L-DOPA treatment. In the early stage of the disease, the response to L-DOPA is excellent (for this reason it is also called the "honey moon" period) and therapeutic benefit is prolonged. However, with the progression of the disease, the therapeutic effect of L-DOPA starts to wear off, both in terms of extent and duration, and the patient start to fluctuate between the "on" and "off" period in which symptoms re-appeared. In order to fully restore the beneficial effect of L-DOPA, the dose has to be increased, and in turn, this induce the development of involuntary movements, the so called dyskinesia, during the "on" period. Thus after ten years of L-DOPA therapy, ~70-80% of patients

develop dyskinesia and almost 100% of patients with early onset of disease is affected by this severe side-effect (Fahn, 1982; Quinn et al., 1987). Dyskinesia is mainly choreiform in nature but dystonia and myoclonus are also present. They are classified according to their onset in relation to L-DOPA intake in: i) “peak-dose” dyskinesia that occurs with high plasma levels of L-DOPA; ii) diphasic dyskinesia that appears during the rise and fall of L-DOPA levels and disappears during the “on” period; iii) several patients con also experience the “off period dystonia” with prolonged muscle spasm affecting feet, arm and face (Luquin et al., 1992).

Main targets of L-DOPA are the medium-sized spiny neurons (MSNs) of the dorsal striatum, which receive a massive innervation from the dopaminergic neurons placed in SN pars compacta (SNc). Studies performed in animal models of L-DOPA-induced dyskinesia (LID) demonstrated that striatum is the scenario of many adaptive changes following DA depletion and chronic administration of L-DOPA. In 1998 Cenci and collaborators (Cenci et al., 1998) showed that chronic L-DOPA treatment affects the striatal neuronal plasticity, inducing long lasting changes in striatal gene expression that highly correlate with the severity of LID. In particular they found an up-regulation of striatal prodynorfin and glutamic acid decarboxylase mRNA and no changes in striatal level of preproenkefalin mRNA in dyskinetic animals with respect to DA-depleted rats (Cenci et al., 1998). Since dynorfin is the neuropeptide released by MSNs (together with γ-aminobutyric acid; GABA) expressing the D1 DA receptor (D1R), these data dragged the researchers attention to the modifications in this particular neuronal pathway. Indeed, studies performed in parkinsonian patients (Tong et al., 2004), and rats (Corvol et al., 2004), revealed an increase of D1R-mediated adenylyl cyclase activity in the DA-depleted striatum. These findings are most likely due to a compensatory process consequent to the loss of striatal DA rather than to changes in D1R affinity as demonstrated by a number of studies (Joyce, 1991; Pifl et al., 1992; Savasta et al., 1988). The enhancement of adenylyl cyclase activity in response to D1R agonists is linked to a clear increase in the levels of Gαolf, a G protein that couples D1R to adenilyl cyclase that which promotes the synthesis of cAMP (Corvol et al., 2004). However, the increase of Gαolf expression cannot be directly responsible for triggering dyskinesia, because if this were the case, LID would appear at the first L-DOPA injection, since D1R hypersensitivity is caused by DA depletion. Conversely, the development of LID takes place after repeated administration for a long period of time. Chronic usage of particular substances

can lead to the onset of plastic modifications through the potentiation of the translational machinery, including the transcription of new genes and the synthesis of new proteins. Long-lasting change in proteins profile needs the expression of stable transcription factors. Indeed, the appearance of LID strongly correlates with the increase of ΔFosB, which is induced in a region specific manner in the brain as a response to varius chronic perturbations (Hope et al., 1994). The increase of ΔFosB immunoreactivity in the brain of parkinsonian animals provides a cellular marker to map the neuronal systems that become activated by chronic dyskinetiogenic treatments with L-DOPA (Andersson et al., 1999). The remarkable stability of ΔFosB and the ΔFosB-related proteins after the discontinuation of chronic dopaminomimetic treatment can account in part for the long-lasting effects on synaptic plasticity produced by L-DOPA (Andersson et al., 2003). An important question requires an explanation: is there any links between the over-expression of Gαolf mediate by the DA depletion and the sustained increase of ΔfosB and ΔfosB-like proteins resulting from chronic L-DOPA treatment? An increase in Gαolf only, i.e., without any changes in the number of D1R is not sufficient to explain the boost effect of L-DOPA on gene expression seen in LID animals. Indeed it is well known that the activity of D1R, as many other receptors, is regulated through the desensitization mediated by G-proteins coupled receptor kinases (GRK; for a review see Beaulieu et al., 2011). Interestingly, Berthet and collaborators found that, D1R is more abundant in the plasma membrane of dyskinetic compared with non-dyskinetic animal (Berthet et al., 2009), which is in line with previous observations that LID is associated with deficiencies in D1R desensitization and trafficking (Bezard et al., 2005; Guigoni et al., 2007). Noteworthy, a very recent study indicates a pathological overexpression of synapses-associated scaffolding protein PSD-95 in the striatum of dyskinetic monkeys that anchoring the D1R to the membrane, reduces the D1R trafficking at the synapses (Porras et al., 2012). However, when the link between the compensatory elevation of Gαolf and the impairment of D1R desensitization is established we observe an enhancement in all the transduction steps ranging from the increased activity of the adenylyl cyclase to the over-activation of protein kinase A (PKA). One of the major targets of PKA in MSNs is the DA and cAMP-regulated phosphoprotein of 32 kDa (DARPP-32; Walaas and Greengard, 1984). PKA catalyzes the phosphorylation of DARPP-32 at Thr 34. This, in turn, converts DARPP-32 into an inhibitor of protein phosphatase-1 (PP-1; Hemmings et al., 1984) thereby suppressing

dephosphorylation of other downstream effector proteins and amplifying PKA-mediated responses (Greengard, 2001). The participation of the cAMP/PKA/DARPP-32 pathways in the generation of LID has been clearly demonstrated in mice. After DA denervation L-DOPA produces large increases in both phospho-Thr34-DARPP-32 and phospho-Ser845-GluR1 (Santini et al., 2007). These changes in responsiveness are most likely attributable to an enhanced sensitivity of D1R, triggered by DA depletion, as previously described. Moreover, it has been shown that striatal DA depletion confers to a D1R agonist the ability to stimulate ERK phosphorylation (Gerfen et al., 2002). Consistently, the administration of L-DOPA is able to promote the increase of ERK1/2 phosphorilation in lesioned mice but not in naïve mice (Santini et al., 2010) specifically in striatal D1R-expressing MSNs (Darmopil et al., 2009). It is noteworthy that in monkeys (Macaca Mulata), the dysregulation of cAMP signaling is maintained during the course of chronic L-DOPA treatment, while the ability of the drug to promote ERK signaling is maximal at the first drug administration and declines during chronic treatment, almost normalizing within three months (Santini et al., 2010). The contribution of phospho-ERK seems to be associated with the priming to L-DOPA, rather than to the maintenance of dyskinesia.

The persistent hyper-phosphorylation of DARPP-32associated with LID has a profound impact on the excitability of MSNs. High frequency stimulation of cortical afferents to striatal MSNs can induce long-term potentiation (LTP), an electrophysiological correlate of synaptic efficiency enhancement (Calabresi et al., 1992). This phenomenon requires DA innervation and is abolished by lesioning dopaminergic neurons (Centonze et al., 1999). LTP can be reversed by low frequency stimulation, which re-establishes normal level of excitability at cortico-striatal synapses and is called depotentiation (Picconi et al., 2003). From a behavioral point of view, the depotentiation is essential to restore the normal synaptic activity, because it acts to erase previous motor program, thus allowing the integration of new motor tasks. Indeed in the rat model of LID, the dyskinetic motor response to L-DOPA is associated with an altered form of synaptic plasticity. After DA denervation, L-DOPA is able to restore LTP in lesioned L-DOPA-injected but not dyskinetic animals, that are unable to depotentiate (Picconi et al., 2003). Blockade of PP-1, a protein phosphatase inhibited by DARPP-32, mimics the lack of depotentiation associated with LID (Picconi et al., 2003), making the involvement of cAMP/PKA/DARPP-32/ERK cascade in the development of LID even more clear. The activation of

ERK, in turn, leads to the sustained phosphorylation of the mitogen and stress-activated kinase 1 (MSK1),a nuclear target of ERK (Santini et al., 2007; Westin et al., 2007). Activated MSK1 phosphorylates the transcription factor cAMP response elements binding protein (CREB; Sgambato et al., 1998) and the increased levels of phosphorilated CREB has been found to correlate with dyskinesia (Oh et al., 2003).

Other important events regulated by the ERK/MSK1 signaling cascade during LID are the phosphorylation of histone H3 (Santini et al., 2009) and the deacetylation of histone H4 (Nicholas et al., 2008). Since chromatine remodeling such as via histone deacetylation and/or phorsphorylation, plays a critical role in gene expression and nuclear reprogramming, it is likely that the abnormal and sustained ERK activation caused by D1R sensitization and DARPP-32 overactivity could modify the protein patterns in MSNs. A study on the regulation of mTORC cascade supports this hypothesis. In mouse model of LID, L-DOPA increases the activity of several effectors of the translational complex, including the initiation factor 4E-binding protein, the p70 ribosomal S6 kinase, and the ribosomal protein S6 (Santini et al., 2009). The role of these proteins, that are known to promote the initiation of process, in the mechanisms underlying LID is confirmed by the antidyskinetic effect of rapamycin, an allosteric inhibitor of mTORC1, when administered in combination with L-DOPA (Santini et al., 2009). These events take place mainly in striatal MSNs. However the plastic changes occurring in the striatum reverberate in many brain structures. For this reason, an overall view on the dynamic interelations between the different nuclei involved in the motor processing is mandatory to better understand the phenomenology of LID. Here below, a brief description of the basal ganglia, the subcortical structures probably most affected in LID.

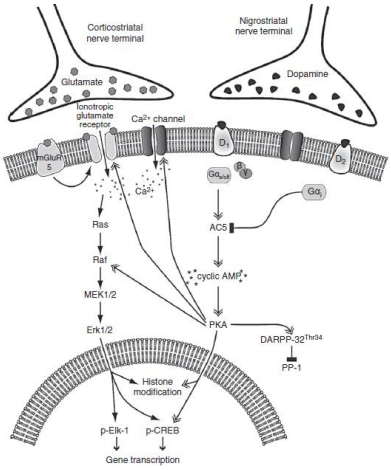

Scheme 1. Signaling cascades underlying LID in MSNs. In particular, cAMP/PKA/DARPP-32 pathway modulates the activity of MAPK-dependent signaling pathways downstream of glutamate receptors and it is influenced by the activity of D1R transduction pathway (Cenci and Konradi, 2010).

The basal ganglia

The basal ganglia are a group of interconnected subcortical nuclei which play an important role in the control of voluntary movements. These structures receive major inputs from wide areas of the neocortex, and send efferents, through the thalamus to prefrontal, premotor and motor cortex. The basal ganglia are able to elaborate a broad range of complex signals, and then convey them to areas of the cortex involved in motor control. Through this information processing , these nuclei are able to regulate the ascending and descending components of the motor system. Basal ganglia are also involved in cognitive functions. In fact, the pathological processes affecting basal ganglia leads to the appearance of neuropsychiatric, behavioral and cognitive disorders. The nuclei that make up the basal ganglia are the SN, the globus pallidus (GP), the subthalamic nucleus (STN) and the striatum (Alexander et al., 1986; Albin et al., 1989; DeLong, 1990; Obeso et al., 2000).

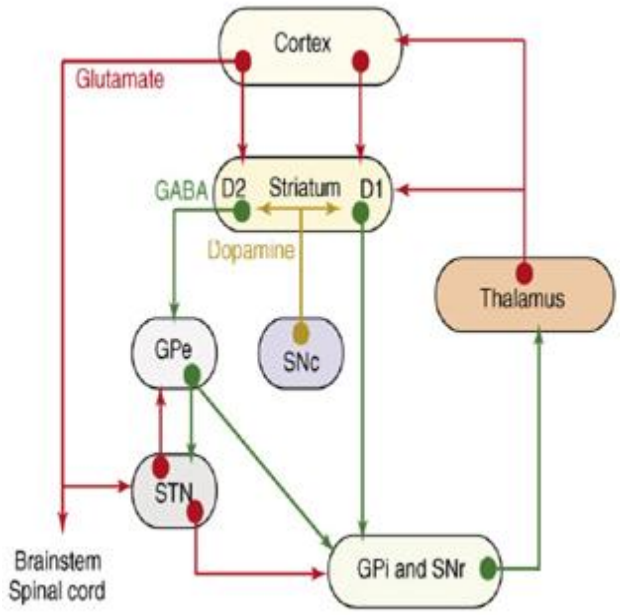

Scheme 2. Schematic representation of basal ganglia connections in the physiological state. DA projections (yellow arrows) exert a modulation of glutamatergic (red arrows) synapses coming from cortex ad thalamus. GABAergic (green arrows) efferents rising from striatum modulate the activity of GPe and GPi/SNr that in turn modify the firing pattern of STN and thalamus, respectively.

Substantia Nigra

SN is divided in two functionally distinct nuclei: the SN pars reticulata, (SNr) and SNc. The SNr receives GABAergic inputs rising from the striatum and GP, glutamatergic afferents from the STN, the cerebral cortex and the peduncolo-pontine nucleus (PPN), and serotonergic innervation from raphe nucleus. The SNr sends GABAergic efferents mainly to the thalamus (ventral anterior, ventral lateral and dorsomedial nucleus), the PPN and the superior colliculus. The SNc is innervated by GABAergic fibers from striatum and GP, and receives glutamatergic projections from STN. SNc provides the striatum, STN and GP with a vast dopaminergic projection. (Parent and Hazrati, 1995b).

Globus pallidus

In humans and primates GP is placed medial to the putamen and lateral to the internal capsule and is divided into an external (GPe) and an internal (GPi) segment. It also includes a portion called the ventral pallidum (GPv). However, in rodents, the nucleus has no subdivisions, and is functionally similar to the GPe of primates and humans. In rodents, the functions of GPi functions are exerted by the entopeduncolar nucleus (EPN). The GP receives its major afferents from the striatum: striatal association areas project preferentially to the dorsal part of the GPe while striatal sensorimotor areas reach the ventral area of the GPi. In addition, GP receives afferent fibers from the STN and to a lesser extent from other structures including the dorsal raphe nucleus, the SNc, the thalamus and PPN. GPe sends its projections mainly to the STN and to a lesser extent the striatum and SN. The GPi projects massively to the ventral and medial nucleus of the thalamus, the centromedian nucleus, and the PPN. GP neurons use GABA as a neurotransmitter (Parent and Hazrati, 1995b).

Subthalamic nucleus

Anatomically STN is placed immediately below the thalamus and above the SN. This nucleus receives inputs from the cerebral cortex, thalamus, SNc and GPe, and projects to striatum, SN and GP. The STN contains a large number of medium-sized neurons that use glutamate as a neurotransmitter, and a limited number of interneurons. Despite its small size the STN exerts a

strong excitatory influence on target structures. Glutamatergic innervations rising from STN are the only excitatory projections of basal ganglia. The dopaminergic fibers innervating the STN control the activity of the nucleus, and the loss of nigral afferents is the root cause of the typical subthalamic hyperactivity that is observed in parkinsonian conditions.

Striatum

The striatum is the principal integrator in the basal ganglia, as well as the site where the phenomena of neuronal plasticity take place. Anatomically, the striatum is divided into three different areas: caudate nucleus, putamen and ventral striatum which includes the nucleus accumbens (NAc). This distribution reflects a different functional organization. In fact, the caudate receives the most part of afferents from associative cortical areas (prefrontal cortex, temporal, parietal, and cingulate), while the putamen is innervated by projections rising from sensorimotor cortex. This fibers use glutamate as a major neurotransmitter. The limbic and paralimbic cortical areas, the amygdala and the hippocampus project to the ventral striatum through cholinergic and glutamatergic pathways. The striatum also receives important dopaminergic projections from SNc, GABAergic, glutamatergic and serotonergic from GP, PPN and dorsal raphe nucleus respectively. The striatal neuronal population is mostly represented (90-95%) by the projecting neurons MSNs, sharing the property to GABA as neurotransmitter. These neurons are characterized by high density of dendritic spines, negative resting membrane potential, and low-frequency discharge in vivo. Although these cells have similar morphological feature, it is possible to classify them into two subtypes, based on their innervation territories, types of DA-expressed receptors and the peptides released as co-transmitters (Parent and Hazrati, 1995a). The remaining 5-10% of neurons consist of striatal interneurons, the so called “fast spiking”, and the “low threshold” spiking neurons. The cholinergic interneurons (which constitute 1-2% of striatal cells) are large aspiny neurons. All these interneurons, although representing a small fraction of the total number of striatal neuronal cells, play a key role in the regulation of MSNs excitability (Kreitzer and Malenka, 2008).

The direct and indirect pathway model

Basal ganglia constitute a highly organized network, involved in motor control, as well as associative learning, planning, working memory, and emotion (Alexander et al., 1986). The classical model of basal ganglia functioning explain the parkinsonian akinesia and LID, as due to an unbalance between two functionally opposing pathways (Albin et al., 1989; Alexander et al., 1986). The striatonigral MSNs that monosynaptically project to the GPi and SNr (direct pathway) preferentially express D1R and produce the neuropeptides dynorphin and substance P whereas the striatopallial MSNs that project to GPe (indirect pathway) express the DA D2 receptor (D2R) and produce enkephalin (Gerfen et al., 1990). More recent studies, revealed a significant number of D1R and D2R-coexpressing MSNs (~5-10%) in rats and monkeys (Le Moine and Bloch, 1995; Aubert et al., 2000). Moreover, anatomical studies show that a single striatofugal axon can arborize in both GPi and GPe (Castle et al., 2005; Nadjar et al., 2006). The dopaminergic terminals rising from SNc exert a modulation of glutamatergic corticostriatal synapses, excite D1R-expressing neurons of direct pathway and inhibit D2R-expressing neurons of the indirect pathway. In this context, the activity of the direct pathway has been proposed to facilitate and select the appropriate movements, whereas the activation of the indirect pathway is associated with the inhibition of unwanted or inappropriate movements (Albin et al., 1989, Alexander et al., 1990). A clear demonstration of the different role of the two pathways has been recently provided using optogenic approaches (Kravitz et al., 2010). The GPe and the STN are classically viewed as part of the indirect pathway. GPe sends GABAergic projections to the STN. As cortex and striatum, the STN is well organized into different territories, and the large dorsoalteral portion corresponds to the motor part of the nucleus (Bevan et al., 2006). Most STN neurons are glutamatergic in nature and provide GPe with an excitatory input (Parent et al., 2000; Castle et al., 2005). GPi and SNr share many histological characteristics as well as afferent and efferent connections. Both nuclei project to the ventral motor thalamus, caudal intralaminar nuclei (Sidibe et al., 2002) and PPN (Grofova and Zhou, 1998). The thalamic nuclei send glutamatergic projections to the motor cortex, thus closing the circuit. According to the model described above, parkinsonism results from an excessive inhibition of components of the motor circuit in the thalamus, cortex and brainstem. These aspects are generally supported by lesioning and inactivation studies, which have shown that inactivation of the sensorimotor portion of the STN

or GPi increases the metabolic activity in cortical motor areas and improves bradykinesia and tremor in patients with PD. Conversely, metabolic imaging and electrophysiological studies in MPTP models have demonstrated that neuronal discharge is increased in STN and GPi, but decreased in GPe (Mink and Thach, 1991; McIntyre et al., 2004; Grafton et al., 2006). These findings prompted the development of a model in which DA depletion leads to the increased activity of the indirect pathway, resulting in increased inhibition of GPe, disinhibition of STN and subsequent increased excitation of GPi/SNr. The net effect of DA loss is an increase of the inhibitory output from GPi and SNr, and the decreased activity in thalamo-cortical neurons (DeLong, 1990; Alexander et al., 1986). In contrast to the situation in PD, the direct pathway appears to be overactive in dyskinesia, resulting in a net reduction in GPi/SNr activity, as clearly demonstrated by in vivo microdialysis studies showing an increase of GABA release in SNr (Mela et al., 2007) and a reduction of GABA levels in thalamus (Marti et al., 2012) after L-DOPA injection in dyskinetic animals. Thus, the model predicts that LID is driven by the hyperactivity of the direct pathway leading to a reduced inhibition of thalamo-cortical neurons and overactivation of cortical motor areas.

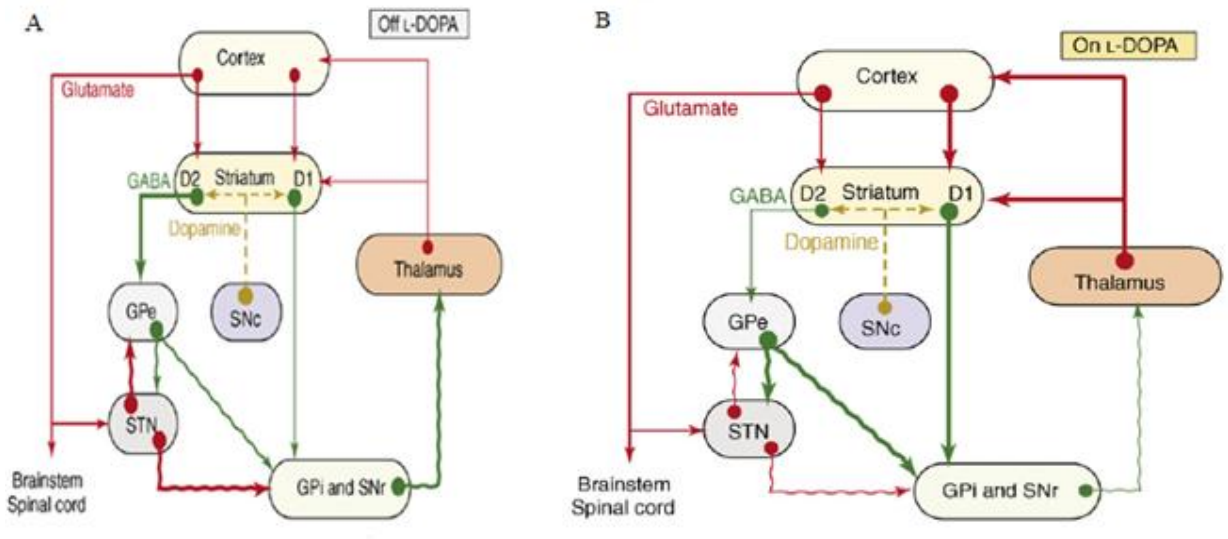

Scheme 3. Representative schemes of basal ganglia functionality in DA-depleted striatum in absence of (A) and in presence of L-DOPA (B). The situation in panel A, describes the situation of the activity of basal ganglia in the parkinsonian state, in which the unbalancing among the direct and indirect pathways in favor of the indirect pathway (green bold line) inhibits the motor activity. In panel B the repetitive administration of L-DOPA triggers the expression of LID through the overactivation of the direct pathway that provoke the disinhibition of thalamic neurons and a excessive prokinetic signal to brainstem.

Pharmacological strategies to reduce L-DOPA induced dyskinesia

LID is caused, at least in part, by the repetitive, intermittent nature of oral L-DOPA administration (Chase, 1998). Continuous intravenous perfusion of the DA precursor is indeed less dyskinetogenic (Colzi et al., 1998). However this approach is limited to patients refractory to other treatments. The use of orally administered controlled-release formulation of carbidopa/L-DOPA or benserazide/L-DOPA (Madopar©), designed to provide minimal fluctuation in L-DOPA levels and thus expected to produce less dyskinesia, was initiated several years ago. The clinical trials have not demonstrated significant reductions of LID in PD patients treated with this formulations (Koller et al., 1999). Agonists selective for either D1R and D2R have been proposed as treatment for PD with lower propensity to elicit dyskinesia than L-DOPA (Rascol, 1999). The main limitation of this approach is that it does not influence preexisting LID. Moreover, despite the entry of several new DA agonists into the clinical practice, the ideal agonist with long duration of action and efficacy equal to L-DOPA is still lacking. For this reason, the most common approach to alleviate LID, is to act in patients with already established LID, using pharmacological tools aimed at reducing the overactivity of the direct pathway. This can be accomplished by targeting one of the neurotransmitter systems which appear to be dysregulated in LID. Here below a brief summary of the most successful drugs tested for reducing LID.

Dopaminergic drugs

The antidyskinetic effect of D1 and D2 receptor antagonists observed in rats concomitantly decrease the antiparkinsonian effect of L-DOPA and are thus not suitable for treating PD patients. Interestingly the modulation of D3 receptor reduces LID in MPTP-lesioned monkeys without worsening akinesia (Hadj Tahar et al., 2001). Indeed the D3R mRNA levels are increased during repeated L-DOPA treatment in the rat model of LID. In this latter study, nafadotride a preferential D3 receptor antagonist, reduced the enhanced locomotor response to repeated L-DOPA treatment (Bordet et al., 1997). Recently, a novel D3 antagonists (S33084) failed in reducing LID when chronically administered together with L-DOPA but revealed a possible antiparkinsonian synergistic effect when combined with L-DOPA (Mela et al., 2010).

Serotoninergic drugs

An imbalance in serotoninergic transmission has been proposed to play a role in LID (Carta et al., 2007; Rylander et al., 2010). The agonists of $5HT_{1A}$ receptor ($5HT_{1A}R$) reduce LID in MPTP-lesioned monkeys and in PD patients without worsening parkinsonian symptoms (Bonifati et al., 1994; Bibbiani et al., 2001). It is currently unclear whether the antidyskinetic effects of $5HT_{1A}R$ agonists result from an action within the basal ganglia, as the expression of such receptors in this region is low. A putative site of action of $5HT_{1A}$ agonists might be the raphe nucleus, where the receptor is densely expressed (Burnet et al., 1995). Moreover in a pivotal 2007 study using rat model of LID, Carta and collaborators (Carta et al., 2007) demonstrated that administration of $5HT_{1A}$ and $5HT_{1b}R$ agonists abolished established dyskinesia through the inhibition of ectopic DA release from serotoninergic fiber in striatum.

Opioidergic drugs

In the 6-OHDA-lesioned rat, μ receptors were increased in the premotor and motor cortex of dyskinetic animals when compared with L-DOPA-treated non-dyskinetic animals whereas their levels in the basal ganglia were reduced in the parkinsonian state but unaltered by L-DOPA, whether AIMs were present or not (Johansson et al., 2001). In PD patients treated chronically with L-DOPA, μ-receptor binding levels were reduced in both the caudate and putamen compared with non-parkinsonian individuals (Fernandez et al., 1994). Thus, there appears to be variability in μ-receptor levels depending on the area of the brain studied and the time of death, and it is difficult to correlate μ-receptor levels with the dyskinetic phenotype. Pharmacological studies have provided supportive evidence of increased μ-mediated opioid transmission in the dyskinetic state. Thus, the μ-receptor antagonists cyprodine and ADL5510 both alleviated LID in the MPTP-lesioned non-human primates (NHPs) without affecting L-DOPA antiparkinsonian efficacy (Henry et al., 2001; Koprich et al., 2011). In the dyskinetic rats κ-receptor levels were decreased in the striatum and SN, but unaltered in the GP, compared with non-dyskinetic animals. Despite the decreased levels, binding studies suggest an hyperactive κ-mediated signaling in the caudate nucleus and motor cortex of dyskinetic MPTP-lesioned NHPs (Johansson et al., 2001). Paradoxically, despite overactive κ-mediated signaling in LID, antagonizing κ-receptors with norbinaltorphimine did not reduce LID in the MPTP-lesioned NHPs (Henry et al.,

2001), whereas stimulation of ƙ-receptors with U50-488 reduced established AIMs in the 6-OHDA-lesioned rat and dyskinesia in the MPTP lesioned squirrel monkey, although at the expense of impairing L-DOPA antiparkinsonian action (Cox et al., 2007). Perhaps highlighting the importance of ƙ-mediated neurotransmission over μ and δ transmissions, in the acute expression of LID, non-subtype selective stimulation of opioid receptors with morphine alleviated established LID. Only one study examined blockade of the nociceptin/orphanin FQ receptor to alleviate LID. In that study, J-113397 worsened LID in the MPTP-lesioned NHP (Visanji et al., 2008).

Glutamatergic drugs

mGluRs

The unbalanced situation within the basal ganglia in LID, leading to the excitation of striato-nigral neurons, represents a potential target for antidyskinetic drugs. This observation suggests that antagonists of glutamate, might be potential candidate drugs for the treatment of LID. Indeed, the most promising anti-dyskinetic drugs are represented by glutamatergic antagonists. Metabotropic glutamate receptors have a modulatory action on neuronal activity and excitability. The inhibition of metatabotropic glutamate receptors, and in particular of the mGlu5R type has been shown to be effective in attenuating both the priming to L-DOPA and the acute expression of LID (Mela et al., 2007; Dekundy et al., 2011). Recent studies have focused on group III metabotropic glutamate receptors (mGluRIII), including subtypes 4, 7 and 8, that are largely expressed in basal ganglia (Conn et al., 2005). mGlu4R depresses glutamatergic transmission, thus it has been suggested that mGlu4R agonists might represent a valid target for the treatment of LID. Different from mGlu5R antagonist, however, mGlu4R agonists do not reduce LID once it has been established (Beurrier et al., 2009).

AMPARs

The non-competitive AMPA receptor (AMPARs) antagonists reduce LID in the MPTP-lesioned NHPs model of PD (Konitsiotis et al., 2000), suggesting a role for overactive AMPARs transmission in LID. This hypothesis is supported by findings of an increased AMPARs binding in the lateral striatum of dyskinetic MPTP lesioned NHPs (Calon et al., 2002) and parkinsonian

patients (Calon et al., 2003). Enhanced phosphorylation and trafficking of AMPARs subunits in striatal synapses is also described in animal models of LID (Santini et al., 2007).

NMDARs

NMDA receptors (NMDARs) are composed of seven known subunits and in the mature brain they are present as heteromers comprised of NR1 and NR2 subunits, with a possible coexpression of NR3 subunits. The NR1 subunit contains the glycine binding site and forms the receptor channel, while the NR2 (NR2A-D) subunit contains the glutamate binding site and govern the functional properties of NMDARs, such as the voltage-dependence of the Mg^{2+} block, the time course of NMDA currents and the intracellular binding partners for synaptic localization, clustering and signal transduction (Chen and Roche, 2007). NMDARs are abundantly expressed in the basal ganglia (Standaert et al., 1994). While the NR1 subunit is ubiquitously expressed, the relative abundance of NR2A and NR2B varies among the different neuronal populations in the striatum, STN, SNc and SNr (Standaert et al., 1999; Standaert et al., 1994; Clarke and Bolam, 1998; Chatha et al., 2000). For many years, NMDARs have been the most popular target for antidyskinetic drugs. Several studies performed in animal models of PD and LID have pointed to a possible important role of NR2B subunits, and evaluated NMDR NR2B-selective antagonists. High striatal levels of tyrosine phosphorilation of the NR2B subunit on the residue 1472 (Tyr^{1472}) have been observed in several animal models of LID (Dunah et al., 2000, Hurley et al., 2005; Quintana et al., 2010), and it has been demonstrated that the intrastriatal administration of a tyrosine kinase inhibitor shortens the rotational response to L-DOPA in rats with 6-OHDA lesions, while normalizing the levels of NR2B phosphorylation (Oh et al., 1998). The phosphorylation of NR2B on Tyr^{1472} disrupts the interaction of NR2B with AP-2 clathrin endocytic complex and leads to the stabilization of NMDARs on the cell surface, increasing synaptic efficiency (Dunah et al., 2004). In animal models of LID and motor fluctuations, pharmacological blockade of NR2B has however produced inconsistent results. For example CP-101.606 reduces LID in macaque (Blanchet et al., 1999) but exacerbated LID in marmosets (Nash et al., 2004). Moreover in the same animal models the NR2B antagonists Ro256981 and Ro631908 failed to improve LID (Rylander et al., 2009). Dyskinetiogenic L-DOPA treatment was found to normalize the synaptic NR1 and NR2B abundance, while markedly increasing the

abundance of NR2A (Hallett et al., 2005). The results from both rat and primate models of LID have led to the suggestion that a relative enhancement in the NR2A expression plays an important role in LID development and that blockade of NR2A subunit may represent a possible therapeutic target (Gardoni et al., 2012).

Amantadine, a weak non competitive NMDARs antagonist is the only clinical prescribed antidyskinetic drug (Del Dotto et al., 2001). Accordingly amantadine improves motor fluctuation and dyskinesia in MPTP lesioned monkeys and in rats 6-OHDA-lesioned (Bibbiani et al., 2005, Dekundy et al., 2007). These effect of amantadine have been taken as indicator of the role of NMDARs in both parkinsonian motor symptoms and LID (Chase and Oh, 2000), even if amantadine can bind to several other targets beyond NMDARs. Amantadine was developed in 1960 as antiviral agent as it was found to block or slow the penetration of the influenza virus in the host cell (Davies et al., 1964, Cochran et al., 1965). In October 1966, amantadine was approved as a prophylactic agent against the Asian influenza and ten years after also for the treatment of influenza A. However, in 2006, the usage of amantadine in the influenza prophylaxis was discouraged because of the frequent mutation of the virus. Simultaneously with the growing popularity of amantadine in flu treatment, an increasing number of PD patients reported an improvement of rigidity, tremor and akinesia while taking amantadine for flu (Schwab et al., 1969). After several clinical trials, the use of amantadine for alleviating the PD symptoms, either as monotherapy or in combination with L-DOPA and anticholinergic drugs was approved by the Food and Drug Administration in 1973, despite the reported side-effects (jitteriness, insomnia, gastrointestinal dysfunction, confusion, depression, hallucinations) probably due to the high dose utilized to reach the antiparkinsonian effect. The mechanisms underlying the antiparkinsonian effect of amantadine as well as the antidyskinetic properties of the drug are still not clear. The antiparkinsonian effect could be due in part to the stimulating effect exerted on the dopaminergic system by enhancing L-DOPA decarboxylase activity and DA synthesis (Deep et al., 1999). Moreover the non-competitive inhibition of the NMDA-evoked release of acetylcholine in rat striatal tissue could account for its clinical efficacy as anticholinergic treatment (Stoof et al., 1992). The affinity of amantadine for NMDARs has been demonstrated by the displacement of the non-competitive antagonist MK-801 within therapeutic concentration in the human cortex (Kornhuber et al., 1991). Later it has been found

that amantadine exerts its inhibitory effect through the stabilization of the closed state of the channel coupled to NMDARs (Blanpied et al., 2005). The discovery of amantadine as NMDARs inhibitor, prompted to evaluate its antidyskinetic effect in rodent and in NHPs models of LID, approaching the clinical efficacy of the drug in humans. In rats, the administration of amantadine produces a reduction of the total AIMs score by 50% at the most effective dose (Dekundy et al., 2007). A similar effect has been seen also in mice model (Lundblad et al., 2005). In NHPs amantadine nearly suppresses choreic dyskinesia and reduced by 35% dystonic dyskinesia, but at low doses of L-DOPA this effect is mirrored by a 50% of reduction in motor benefit (Blanchet et al., 2003). In humans, amantadine showed the ability to reduce the duration and severity of dyskinesia by 50-60%, when administered either for few weeks (Rajput et al., 1998) or up to one year (Wolf et al., 2010).

RasGRFs

The proteins of the Ras family regulate a wide range of cellular processes including cell proliferation and cell differentiation, and a number of tissue-specific functions. They are the main mediators of cellular transduction, capable of altering the activity of a large number of proteins, and then the whole cell physiology. The status of Ras is influenced mainly by two types of regulatory proteins:

• GEFs (guanine nucleotide exchange factors) that activate Ras GTPases by binding to GTP. There are many families of GEF enabling the activation of Ras. These include proteins Sos (SOS1 and SOS2) which hook the tyrosine kinase protein Ras.

• GAPs (GTPase activating protein) that inactivate Ras, promoting the hydrolysis of bounded GTP to GDP.

Of particular interest for neuronal signaling pathways are the 140-kd protein RasGRF1 (RasGRF1) and 135-kd RasGRF2 (RasGRF2). The RasGRF1 protein is abundantly expressed in mature neurons but also in peripheral tissues such as pancreas and lungs, although to a lesser extent. This protein contains two catalytic domains and multiple regulatory domains; one of the most important is the '"IQ motif", a web calcium/calmodulin dependent protein that activates the protein itself. The N-terminal sequence called "plekstrin homologous domain" (PH) is involved in protein-lipid and protein-protein interaction. The PH domain is followed by the

"coiled coil" (CC) and the Dbl homolog domain (DH), the former involved in the regulation of gene expression and the latter in the activation of Rac GTPase. The C-terminal sequence lodges the cell division cycle domain (Cdc25) which, assisted by the Ras exchange motif domain (REM) is responsible of the activation of Ras and R-Ras facilitating the exchange of GDP with GTP. The neuronal domain (ND), seems to be important for the coupling of RasGRF1 with the NR2B subunit of the NMDARs. This characteristic distinguishes the functions of RasGRF1 from those of RasGRF2, making the RasGRF1 particularly sensitive to the increase of intracellular calcium concentration due to the opening of the NMDA channel (for a review see Feig, 2011).

In order to shed light on the roles of RasGRF1 in neurons, some laboratories generated knockout animals lacking a specific isoform of the protein. To generate the knockout mice, Brambilla ($GRF1^{Brambilla}$), Itier ($GRF1^{Itier}$), Font de Mora ($GRF1^{Font\ de\ Mora}$) and their collaborators decided to delete the domain Cdc25, obtaining the inactivation of isoform 1 and 2 of the protein. Yoon and his collegues ($GRF1^{Yoon}$) have targeted the gene promoter sequence, virtually blocking the expression of all the isoforms of Ras-GRF1. With an another strategy Giese ($GRF1^{Giese}$) has eliminated the DH domain leaving untouched both the isoform 2 and 3.

Later, the phenotypes of the different genetically modified mice have been characterized. $GRF1^{Itier}$, $GRF1^{Giese}$ and $GRF1^{Font\ de\ Mora}$ mice have shown to be significantly smaller than wild type animals, likely due to a reduced levels of the growth hormone in the pituitary gland (Itier et al., 1998). Even in the amygdala, an important structure for the preservation of memory-associated with emotional events, some impairments have been recorded . In fact, $GRF1^{Brambilla}$ mice has shown difficulties in solving tasks that require the re-consolidation of memory associated with emotions (Brambilla et al., 1997). Another type of behavioral experiment was carried out with $GRF1^{Giese}$ mice, which has shown that in different context the decision-making capacity is instead compromised. At the biochemical level, the functions of RasGRF1 have been studied in important regions of the striatum involved in cognitive processes and in movement control. Brambilla and colleagues have demonstrated the correlation between D1R and the activation of ERK using $GRF1^{Brambilla}$ mice after cocaine administration. These experiments established that the block of RasGRF1 induces a reduction of the activity of ERK in the striatum in response to DA stimulation. Moreover, it has been shown that the activation of ERK pathway by NMDAR agonists is also prevented in $GRF1^{Brambilla}$ mice (Fasano et al., 2009). These results

implicate that RasGRF1 is involved in the integration of the two main neurotransmitter inputs to the striatum involved in the appearance of dyskinesia. Indeed the genetic ablation of RasGRF1 is sufficient to determine the reduction of dyskinesia development (Fasano et al., 2010).

RasGRF2 presents the same sequences of RasGFR1 with the exception of the ND domain, virtually providing to the protein a different subcellular distribution (for a review see Feig, 2011). In contrast to that seen in the RasGRF1 knockout, RasGRF2 knockout mice did not display any phenotypic changes compared to wild type littermates (Fernandez-Medarde et al., 2002). With respect to the studies on signaling, two different transgenic models of RasGRF2 mice have been generated. Fernandez-Medarde and collaborators inactivated the CDC25 domain ($GRF2^{Fernandez}$; Fernandez-Medarde et al., 2002) whilst Tian and colleagues targeted the PH sequence ($GRF2^{Tian}$; Tian et al., 2004). $GRF2^{Tian}$ mice allow to disclose the role of RasGRF2 in the regulation of ERK pathway in cortical neurons (Tian et al., 2004). Interestingly, in cortical neurons of neonatal animals NMDARs signal through Sos rather than RasGRF exchange factors, implying that both RasGRFs endow NMDARs with functions unique to mature neurons (Tian et al., 2004).

Aims of the study

The overall purpose of the present thesis is to provide novel insights into the neurochemical pathways underlying the expression of LID, and to dissect out roles of the striatal direct and indirect pathways.

In *part 1* of the thesis, we used microdialysis to investigate the neurochemical and behavioural changes exerted by different antidyskinetic treatments or approaches in basal ganglia. We first found that levodopa evoked AIMs, and simultaneously elevated GABA levels in the substantia nigra reticulata but not globus pallidus of dyskinetic mice and rats, suggesting the involvement of the striato-nigral "direct" GABAergic pathway in both species. Amantadine attenuated AIMs expression and prevented the nigral GABA rise, suggesting nigral GABA as a neurochemical correlate of LID (*part 1*).

To confirm the involvement of the direct pathway in LID, and dissect out the role of striatal and nigral dopamine D1 and D2 receptors we performed regional perfusion (striatum and substantia nigra pars reticulata) of selective D1 and D2 antagonists simultaneously with systemic L-DOPA administration (*part 2*). Intrastriatal blockade of D1 receptor attenuated LID and prevented the accompanying rise of nigral GABA levels whereas blockade of D2 receptor was ineffective. When perfused in the substantia nigra, both the D1 and D2 antagonists attenuated LID expression, although only the D1 antagonist prevented the GABA rise.

To further investigate which pathway is involved in LID and in the antidyskinetic effect of amantadine, we took advantage from recent studies showing the specificity of Ras-guanine nucleotide-releasing factor 1 and 2 to selectively couple NR2B and NR2A NMDA receptor subunits, respectively. We showed (*part 3*) that blockade of striatal expression of Ras-GRF1 using a lentiviral vector carrying a short hairpin RNA (LV Ras-GRF1) caused an attenuation of LID development and expression, which was accompanied by the lack of the increase in nigral GABA. However, in LV Ras-GRF1 mice the antydyskinetic effect of amantadine and its neurochemical correlates were lost, suggesting LV Ras-GRF1 might interfere with the antidyskinetic effect of amantadine by acting on the same target (possibly the NR2B receptor). Conversely, injection of a viral construct expressing a small hairpin directed against RasGRF2 caused only a not significant reduction of LID, and did not prevent the increase of nigral GABA

following L-DOPA. In these mice, also the antidyskinetic effect of amantadine remained unaltered.

Materials and methods

Animals

All animals used in the study were housed with free access to food and water and kept under environmentally controlled conditions (12-h light/dark cycle with light on between 07:00 and 19:00). The experimental protocols were approved by the Italian Ministry of Health (licenses n. 94/2007B and 194/2008B) and Ethical Committee of the University of Ferrara. Adequate measures were taken to minimize animal pain and discomfort. After surgery, the skin was closed using surgical sutures and the wound was cleansed with an antibiotic solution (Rifamicina SV, Lepetit, Milano).

Mice

Young male (20-25 g; 8-9 weeks old) Swiss (utilized in *part 1*) and C57BL/6J mice (utilized in *part 3*) were used in this study. Swiss mice were purchased from Stefano Morini S.a.s. (S.Polo D'enza, Reggio Emilia, Italy), while C57BL/6J mice were purchased from Charles River Laboratories (Calco, Sant'Angelo Lodigiano, Italy).

Rats

Young adult male (120-150 g; 12-13 weeks old; used in *part 1* and *part 2*) Sprague-Dawley were used in this study. Rats were purchased from Harlan Italy (S. Pietro al Natisone, Italy).

Lesion of the DA system

In order to lesion the DAergic neurons in SNc, and consequently deplete the striatum of DA, different protocols were used. All lesion procedures led to achieve an unilateral massive destruction of the nigrostriatal DA projection.

6-OHDA lesion in rats (used as a animal model in part 1 and 2)

Unilateral lesion of nigro-striatal DA neurons was induced in isoflurane-anaesthetised rats (Marti et al., 2005a) by stereotactically injecting 8 ug of 6-hydroxydopamine (6-OHDA; in 4 µl of saline containing 0.02% ascorbic acid) in the right medial forebrain bundle (MFB) according to the following coordinates from bregma: AP= -4.4 mm, ML= -1.2 mm, VD= -7.8 mm below dura (Paxinos and Watson, 1982). Two weeks after surgery, rats were injected with amphetamine (5

mg/kg i.p., dissolved in saline) and only those rats performing > 7 ipsilateral turns/min were enrolled in the study. Indeed such behavior is associated with a DA depletion > 95% (Marti et al., 2007)

6-OHDA lesion in Swiss mice (used as animal model in part 1)

Unilaeral lesion of nigrostriatal DA neurons was performed in isoflurane-anesthetized mice as described by Lundblad and collaborators (Lundblad et al., 2004). Six micrograms of 6-OHDA free-base (in 2 µL of saline containing 0.02% ascorbic acid) were stereotaxically injected into the striatum according to the following coordinates from bregma (in mm); first injection, AP +1.0, ML -2.1, DV -2.9 below dura; second injection, AP +0.3, ML +2.3, DV -2.9 below dura (Paxinos and Franklin 2001). 2 weeks after lesion mice were screened using cylinder test (Schallert et al., 2000). Mice showing a number of wall contacts with contralateral forelimb < 40% of total contacts in 5 min of observation were enrolled in the study. Such behavior is associated with a striatal DA depletion < 90% (Santini et al., 2007).

6-OHDA lesion in C57/6J mice (used as animal model in part 3)

MFB injections of 6-OHDA were performed in isoflurane-anesthetized mice as described by Lundblad and collegues. (Lundblad et al., 2004). One microliter of 6-OHDA (3 µg/µL) was injected into the right ascending MFB according to the following coordinates from bregma (in mm): AP −0.7, L −1.2, DV −4.7 below the dura (Paxinos and Franklin 2001). Mice were evaluated in the open field 2 weeks after lesion to estimate the success rate of lesion. Mice showing < 10 of spontaneous contralateral rotation in 10 min of observation were enrolled in the study, since this behavior was associated with < 90% (Fasano et al., 2010).

LID induction and AIMs ratings

Different protocols of LID induction were used in 6-OHDA lesioned mice and rats. Swiss mice utilized in *part 1* were treated with 15 mg/kg i.p. L-DOPA (plus 12 mg/kg benserazide) once a day for 10 days (Santini et al., 2009), while C57BL/6J mice used in *part 3* were injected with escalating doses of L-DOPA (3, 6, 9 mg/kg i.p. plus 12 mg/kg benserazide i.p.) once a day, for 9 consecutive days (Fasano et al., 2010).

Rats used in *part 1* and *2* received 6 mg/kg i.p. L-DOPA (plus 12 mg/kg benserazide, i.p), once a day for 21 days (Cenci et al., 1998). Quantification of L-DOPA-induced AIMs was carried out as extensively described in several papers of Cenci's group (Lee et al., 2000; Lundblad et al., 2002; Lundblad et al., 2004; Winkler et al., 2002). Rats and mice were observed individually for 1 min every 20 min during the 2–3 h that followed an L-DOPA injection. Dyskinetic movements were classified based on their topographic distribution into three subtypes: (i) axial AIM, that is, twisted posture or choreiform twisting of the neck and upper body toward the side contralateral to the lesion; (ii) forelimb AIM, that is, jerky or dystonic movements of the contralateral forelimb and/or purposeless grabbing movement of the contralateral paw; (iii) orolingual AIM, that is, orofacial muscle twitching, empty masticatory movements and contralateral tongue protrusion. Each AIM subtype was rated on frequency and amplitude scales from 0 to 4 as described in Cenci and Lundblad (Cenci and Lundblad, 2007). Dyskinesia score was calculated as the product of frequency x amplitude and presented either as the sum of total AIMs score in one-day session (cumulative ALO AIMs score, representing AIMs score during the development of dyskinesia) or as the total AIMs score for each time point of observation in one single session (ALO AIMs score, representing AIMs during microdialysis). Axial, forelimb and orolingual (ALO) were presented also as separated items (Carta et al., 2006), either as the sum of separated ALO score in one-day session (cumulative AIMs score, represented during the development of dyskinesia) or as the separates ALO score for each time point of observation in one single session (AIMs score, presented during microdialysis).

Behavioural studies

Motor activity in rodents was evaluated by means of different behavioural tests specific for different motor abilities, as previously described (Marti et al., 2005b). The different tests are useful to evaluate motor functions under static or dynamic conditions, different motor feature such as akinesia and bradykinesia. Akinesia appears as an abnormal absence or poverty of movements, that is associated in hemi-lesioned mice and rats to the loss of the ability to move the forepaw when placed on blocks at different highs. Bradykinesia is refers to slowness of movement and in particular to difficulties to adjust the correct body position, that in rats and mice is associated to difficulties to reach a correct forepaw position when the animals are

dragged. The battery of tests described below, can be use to assess the degree of bradykinesia and akinesia of the animals, representing important behavioral correlates of parkinsonian symptoms. We performed these tests in a fixed sequence (bar test, drag test, and rotarod test). In *part 1* the tests are used to compare the motor performance of lesioned mice/paw with the un-lesioned mice/paw. In part 3 animals were scored the first day of tests, thus they underwent to consecutive 4 days of training and scored the fifth day. Such of protocol serves to highlight differences in motor learning, in terms of adaptation to experimental conditions.

Bar test

This test, also known as the catalepsy test (Sanberg et al., 1988), measures the ability of the animal to respond to an externally imposed static posture. Each rodent was placed gently on a table and the right and left forepaws were placed alternatively on blocks of increasing heights (1.5, 3 and 6 cm for mice and 3, 6 and 9 cm for rats). The immobility time (in sec) of each forepaw on the block was recorded (cut-off time 20 sec per step, 60 sec maximum). Akinesia was calculated as total time spent on the blocks by each forepaw.

Drag test

The test (modification of the ”wheelbarrow” test; (Schallert et al., 1979), measures the ability of the animal to balance its body posture using forelimbs in response to an externally imposed dynamic stimulus (backward dragging; Marti et al., 2005). Each rodent was gently lifted by the tail (allowing the forepaws on the table) and dragged backwards at a constant speed (about 20 cm/sec) for a fixed distance (100 cm). The number of touches made by each forepaw was counted by two separate observers (mean between the two forepaws).

Rotarod test

This test analyzes the ability of the rodents to run on a rotating cylinder (diameter 8 cm) and provides information on different motor parameters such as coordination, gait, balance, muscle tone and motivation to run (Rozas and Labandeira Garcia, 1997). The fixed-speed rotarod 27 test was employed according to a previously described protocol (Marti et al., 2004; Viaro et al., 2010). Briefly, animals were tested at stepwise increasing speeds (180 sec each) and time spent on the rod calculated (in sec).

In vivo microdialysis

In *part 1* and in *part 3* of the present work, microdialysis was used to simultaneously monitor GABA and GLU release in the SNr and GP of freely moving mice (Mabrouk et al., 2010; Volta et al., 2010); and rats (Morari et al., 1996a; Morari et al., 1996b; Marti et al., 2002; Marti et al., 2005a). Briefly, two microdialysis probes of concentric design were stereotaxically implanted under isoflurane anesthesia (1.5% in air) into the lesioned SNr and ipsilateral GP (1 and 2 mm dialyzing membrane, respectively), according to the following coordinates from bregma and the dural surface (mm): mouse GP, AP -0.46, ML -1.8, DV -3.9, mouse SNr, AP -3.3, ML -1.25, DV -4.6; rat GP, AP -1.3, ML -3.3, DV -7.5, rat SNr, AP -5.5, ML -2.2, DV -8. In *part 2* of the present study, rats were stereotaxically implanted with one microdialysis probe into the lesioned SNr (for coordinates see above) and another in the ipsilateral dorsolateral striatum (3mm dialyzing membrane; coordinates from bregma and the dural surface (mm) : AP +1.0, ML -3.5, DV -6).

Twenty-four hours after surgery, probes were perfused with a modified Ringer solution (CaCl2 1.2 mmol/L, KCl 2.7 mmol/L, NaCl 148 mmol/L and MgCl2 0.85 mmol/L) at a flow rate of 2.1 (mouse) and 3 µL/min (rat). After 6 h rinsing, samples were collected (every 15 or 20 min depending on the study) for a total of 3–4 h. At least three baseline samples were collected before i.p. administration of L-DOPA, amantadine (40 mg/kg, i.p.) or saline. In the combination studies, amantadine was administered 1 h before L-DOPA. In *part 2* each rat received L-DOPA (i.p.), a DA receptor antagonist (SCH23390, raclopride) locally-perfused in SNr or dorsolateral striatum, or their combination in a randomized fashion. At the end of experiment, animals were sacrificed and the correct placement of the probes was verified histologically.

Endogenous glutamate and GABA analysis

Glutamate and GABA levels in the dialysate were measured by HPLC coupled with fluorometric detection as previously described (Marti et al., 2007). Thirty microliters of o-phthaldialdehyde/mercaptoethanol reagent were added to aliquots of sample (30 µL collected from rats or 28 µL from mice) and 50 µL of the mixture was automatically injected (Triathlon autosampler; Spark Holland, Emmen, the Netherlands) onto a 5-C18 Chromsep analytical column (3 mm inner diameter, 10 cm length; Chrompack, Middelburg, the Netherlands) perfused at a flow rate of 0.48 mL/min (Jasco quaternary gradient pump PU-2089 PLUS; Jasco,

Tokyo, Japan) with a mobile phase containing 0.1 M sodium acetate, 10% methanol and 2.2% tetrahydrofuran (pH 6.5). Glutamate and GABA were detected by means of a fluorescence spectrophotometer FP- 2020 Plus (Jasco, Tokyo, Japan) with the excitation and the emission wavelengths set at 370 and 450 nm respectively. The limits of detection for glutamate and GABA were ~1 and ~0.5 nM, respectively. Retention times for glutamate and GABA were ~3.5 and ~18.0 min, respectively.

TH immunoreactivity evaluation

Tyrosine hydroxylase (TH) immunostaining was used to verify the degree of DA depletion in striatum. Mice were anaesthetized with ketamine (85 mg/kg; i.p.) and xylazine (15 mg/kg; i.p.), transcardially perfused with 20 mM phosphate buffered saline (PBS) and fixed with 4% paraformaldehyde in PBS at pH 7.4. Brains were removed, post-fixed overnight and cryoprotected in 50% glycerol (solution in PBS). Serial coronal sections of 30 µm thickness were made in the striatum -0.8 to +1.3 from bregma) and every second section processed for TH immunohistochemistry (see below). Free-floating striatal sections were rinsed in Tris-buffered saline (TBS; 0.25 M Tris and 0.5 M NaCl, pH 7.5), incubated for 5 min TBS containing 3% H2O2 and 10% methanol (vol/vol), and then rinsed three times (10 min each) in TBS. After 20 min incubation in 0.2% Triton X- 100 in TBS, sections were rinsed three times in TBS again. Finally, they were incubated overnight at 4°C with the anti-TH mouse monoclonal primary antibody (1 : 40; AbCam, Cambridge, UK). Following incubation, sections were rinsed three times for 10 min in TBS and incubated for 45 min with secondary antibody (1 : 200; Alexa Fluor 680 anti-mouse IgG). In SNc triple staining was needed to distinguish dopaminergic neurons from the rest of cellular population. We used anti-NeuN monoclonal antibody (1:50; Millipore; Alexa Fluor 488 conjugated) for unspecific neuronal staining and DAPI (Sigma) to stain neuronal and non-neuronal cells.

Mouse brain sections were analyzed with a Zeiss LSM 510 (Zeiss, Oberkochem, Germany) and acquired with Plan-Neofluar 10· (Edmund Optics, Barrington, IL, USA) lens. TH-immunoreactive fiber density was analyzed using ImageJ software (Wayne Rasband, National Institute of Health, Bethesda, MD, USA). To quantify TH staining, the optical densities were corrected for non-specific background density, measured in the corpus callosum. TH-positive fiber density and the

number of TH-positive neurons was calculated as the ratio between optical density in the denervated (ipsilateral) and intact (contralateral) side.

Drugs

6-OHDA hydrobromide, D-amphetamine sulphate, L-DOPA methyl ester hydrochloride, benserazide hydrochloride and amantadine hydrochloride were purchased from Sigma-Aldrich (AB, Italy), SCH23390 hydrochloride and raclopride from Tocris Bioscience (Bristol, UK). Except from 6-OHDA, all drugs were dissolved in saline and administered within 1 h at the volume of 1.0 mL/kg body weight. 6-OHDA were dissolved in saline containing 0.02% ascorbic acid, and used within 2 h. SCH23390 and raclopride were dissolved in water to 1 mM, and then diluted to 1 μM with perfusion Ringer.

Data presentation and statistical analysis

Motor performance has been expressed as time (in seconds) on bar or rod (bar and rotarod tests), and number of steps (drag test). AIMs rating has been expressed as ALO score (magnitude x amplitude). In microdialysis studies, GABA and GLU release has been expressed as percentage ± SEM of basal values (calculated as mean of the two samples before the treatment). In Figure legends (and in Results section), basal dialysate levels of amino acids were also given as absolute values (in nM). Statistical analysis has been performed by one way and analysis of variance (ANOVA) and two-way repeated measure (RM ANOVA). In case ANOVA yielded a significant F score, post hoc analysis has been performed by contrast analysis to determine group differences. In case a significant time x treatment interaction was found, the sequentially rejective Bonferroni's test was used (implemented on Excel spreadsheet) to determine specific differences (i.e. at the single time-point level) between groups. Statistical analysis for the data presented in Fig. 8 was performed by the paired Student's t test. Statistical analysis for the data presented in Fig. 9 and Fig. 12 was performed by Mann Whitney U-test. p-values < 0.05 were considered to be statistically significant.

Results

Part 1. Effect of amantadine in reducing LID in mouse and rat with already-established dyskinesia.

In the first part of the present study we investigate the feasibility of the dual probe microdialysis approach in dyskinetic mice. Simultaneously recording dyskinesia and collecting dialysate samples Moreover we compared the mouse model with the already-validated rat model. The antidyskinetic effects of amantadine on the behavioral and neurochemical changes in GP and SNr of 6-OHDA hemi-lesioned dyskinetic mice and rats were also assessed.

1.1 Acute L-DOPA improves bradykinesia and motor deficit in 6-OHDA lesioned mice

Basal motor scores of naive mice (n = 11) were 8.0 ± 1.0 s of immobility (bar test), 15.0 ± 2.0 steps (drag test) and 1253.5 ± 122.7 s of permanence on the rod (rotarod test). Unilateral intrastriatal injections of 6-OHDA caused marked akinesia and bradykinesia mainly affecting the contralateral forepaw, and an overall reduction of motor performance. Immobility time at the contralateral paw increased by about 4-fold compared with the ipsilateral paw (Fig. 1A) whereas the number of steps was reduced by ~70% (Fig. 1B). Finally, rotarod performance was reduced by ~58% after 6-OHDA lesioning (Fig. 1C). To test the dopaminergic nature of this motor deficit, L-DOPA was systemically administered (i.p.) at a dose which was reported to attenuate hypokinesia in MPTP-treated mice (10 mg/kg in combination with 12 mg/kg benserazide; Viaro et al., 2008). L-DOPA normalized the immobility time (Fig. 1A) and stepping activity (Fig. 1B) at the contralateral paw but was unable to attenuate deficit in rotarod performance (Fig. 1C). This behavioral phenotype was associated with a 90.3 ± 2.7% reduction of striatal TH immunopositive fibers in the ipsilateral compared with the contralateral striatum (n = 9, $t = 9.367$, $p < 0.0001$, Student's t-test).

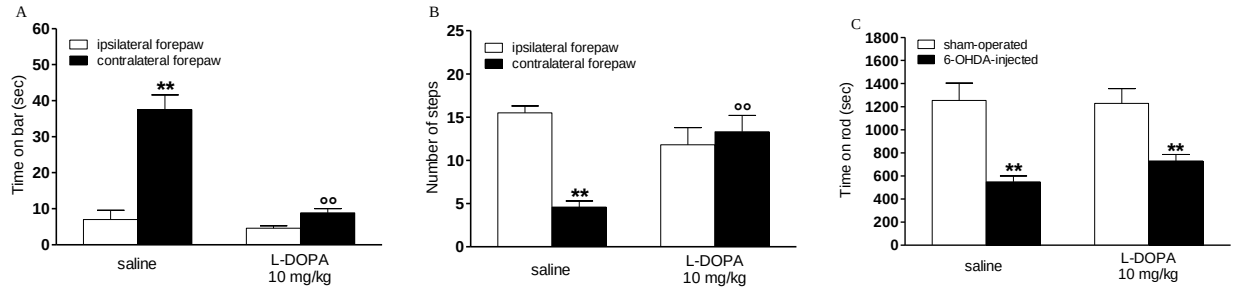

Fig. 1 L-DOPA relieved akinesia/bradykinesia in hemi-parkinsonian mice. Systemic (i.p.) administration of L-DOPA (15 mg/kg plus 12 mg/kg of benserazide) reduced the time spent on the blocks in the bar test (A), increased the number of steps of the contralateral forepaw in the drag test (B), and failed in improving overall motor performance in the rotarod test (C). Behavioral testing was performed 30 min after L-DOPA injection. Motor asymmetry was evaluated separately at the ipsilateral and contralateral (parkinsonian) paw (A, B). Data are expressed as absolute values (s, number of steps) and are mean ± SEM of 8–10 animals. Statistical analysis was performed by one-way ANOVA followed by contrast analysis and the sequentially rejective Bonferroni's test. Panel A: significant effect of treatment ($F_{3,28} = 37.70$, $p < 0.001$). Panel B: significant effect of treatment ($F_{3,28} = 10.16$, $p < 0.001$). Panel C: significant effect of treatment ($F_{3,24} = 20.65$, $p < 0.001$). **p < 0.01 versus the ipsilateral forepaw (A, B) or sham-operated mice (C), °°p < 0.01 versus the contralateral forepaw of saline injected mice (A, B).

1.2 Chronic L-DOPA treatment elicits LID in hemi-lesioned mice

Chronic treatment of hemi-parkinsonian mice with L-DOPA (15 mg/kg plus 12 mg/kg benserazide; i.p., once daily for 10 days) caused the development of axial, limb and orolingual AIMs having a similar temporal profile. AIMs appearance was gradual and progressive, reaching a plateau at the fifth day of treatment (Fig. 2A,B).

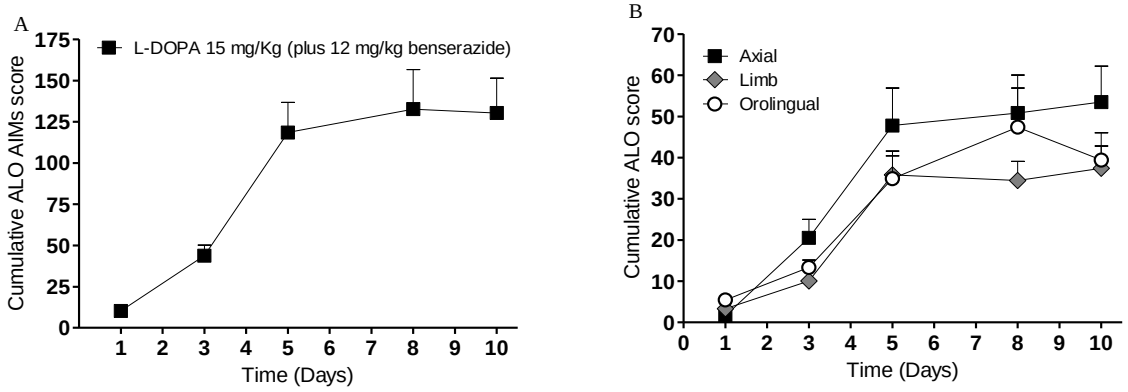

Fig. 2 Development of dyskinesia during chronic L-DOPA administration in 6-OHDA hemi-lesioned mice. Mice were treated for 10 days with L-DOPA 15 mg/kg (plus benserazide 12 mg/kg, i.p., once daily) and AIMs were evaluated at days 1, 3, 5, 8, and 10 after treatment onset. Axial, limb and orolingual (ALO) AIMs were scored every 20 min for 120 min after L-DOPA administration. Data (in arbitrary units; see Results section) have been presented either as the sum of each AIM subtype (cumulative ALO score; A) or as each AIMs subtype separately (B). Each value is the mean ± SEM of 10–11 animals.

1.3 Amantadine attenuates LID expression and its neurochemical correlates in hemi-parkinsonian mice.

To examine whether mouse dyskinesia was accompanied by changes of activity along the striatofugal pathways, GABA and glutamate release was monitored in SNr and GP along with behavior following L-DOPA alone (15 mg/kg plus 12 mg/kg benserazide, i.p.) or in combination with amantadine. A dose of 40 mg/kg amantadine was chosen because it proved effective in reducing ALO AIMs in mice and rats without affecting the locomotive components of AIMs (Lundblad et al., 2002; Dekundy et al., 2007) which is considered a marker of the therapeutic effect of L-DOPA (Cenci, 2002). L-DOPA caused the appearance of dyskinetic movements already at 20 min after injection. The intensity of dyskinesia remained stably at maximal levels up to 80 min after injection (Fig. 3A), after which AIMs tended to decline. Amantadine administration (1 h before L-DOPA) caused an overall (~50%) attenuation of AIMs severity with some preference for orolingual (~66%) over axial (~47%) and limb (~43%) AIMs (Fig. 3B,D).

These behavioral changes were associated with different neurochemical patterns in SNr and GP (Fig. 4). A marked increase of GABA levels was observed in SNr after L-DOPA administration, with a peak (~3-fold over basal) at 80 min (Fig. 4A). Consistent with its anti-dyskinetic effect, amantadine prevented the rise in GABA levels induced by L-DOPA (Fig. 4A) without causing per se any change in basal values. Nigral GLU levels were not significantly affected by L-DOPA although showing a tendency to decline over time (Fig. 4B). Amantadine, alone or in combination with L-DOPA, was also ineffective, although causing a trend for an increase (~30% 1 h after injection, Fig. 4B). Opposite to SNr, L DOPA alone did not cause any significant changes of GABA levels in GP (Fig. 4C). Amantadine alone was also ineffective. However, when co-administered with L-DOPA it caused a marked elevation of GABA levels up to ~217% at the end of collection period. L-DOPA, amantadine or their combination failed to affect pallidal glutamate levels (Fig. 4D).

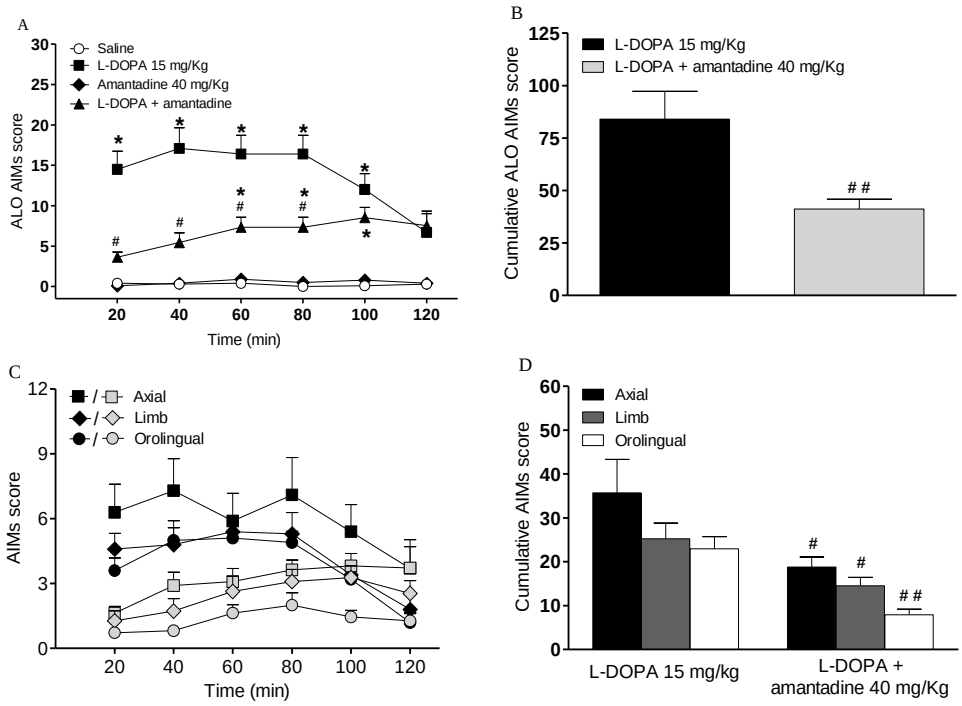

Fig. 3 Behavioral effect of L-DOPA and amantadine in dyskinetic mice undergoing microdialysis. 6-OHDA hemi-lesioned mice were made dyskinetic by chronic L-DOPA administration (15 mg/kg plus 12 mg/kg benserazide, i.p., once a day for 10 days). At the end of treatment, mice underwent surgery for microdialysis probe implantation, and 24 h later were challenged with L-DOPA alone or in combination with amantadine (40 mg/kg; i.p., 1 h in advance). Control mice were treated with either amantadine or saline alone. ALO AIMs were scored every 20 min for 120 min after L-DOPA administration. Temporal profiles of AIMs taken as a whole (ALO AIMs; A) or as separate items (C) are shown. Cumulative dyskinesia score (i.e. the sum of the scores given at each of the six observation sessions) is shown for ALO AIMs as a whole (B) or for each AIM subtype separately (D). Co-administration of amantadine reduced AIMs expression, affecting about to the same extent each AIMs subtype. Data are expressed as arbitrary units (see Results section) and are mean ± SEM of 10–11 animals. Panel A: significant effect of treatment ($F_{3,15} = 111.8$, $p < 0.001$) but not time ($F_{5,198} = 1.68$, $p = 0.14$), and significant time treatment interaction ($F_{15,198} = 2.31$, $p = 0.005$), according to two-way RM ANOVA followed by contrast analysis and the sequentially rejective Bonferroni's test. Panel B: significant effect of amantadine ($t = 3.15$, $df = 19$, $p = 0.005$), according to unpaired Student's t-test. Panel D: significant effect of amantadine; axial ($t = 2.2$, $df = 19$, $p = 0.039$), limb ($t = 2.73$, $df = 19$, $p = 0.013$), orolingual ($t = 5,0$, $df = 19$, $p < 0.001$) AIMs, according to unpaired Student's t -test. *$p < 0.05$ versus saline, #$p < 0.05$, ##$p < 0.01$ versus L-DOPA.

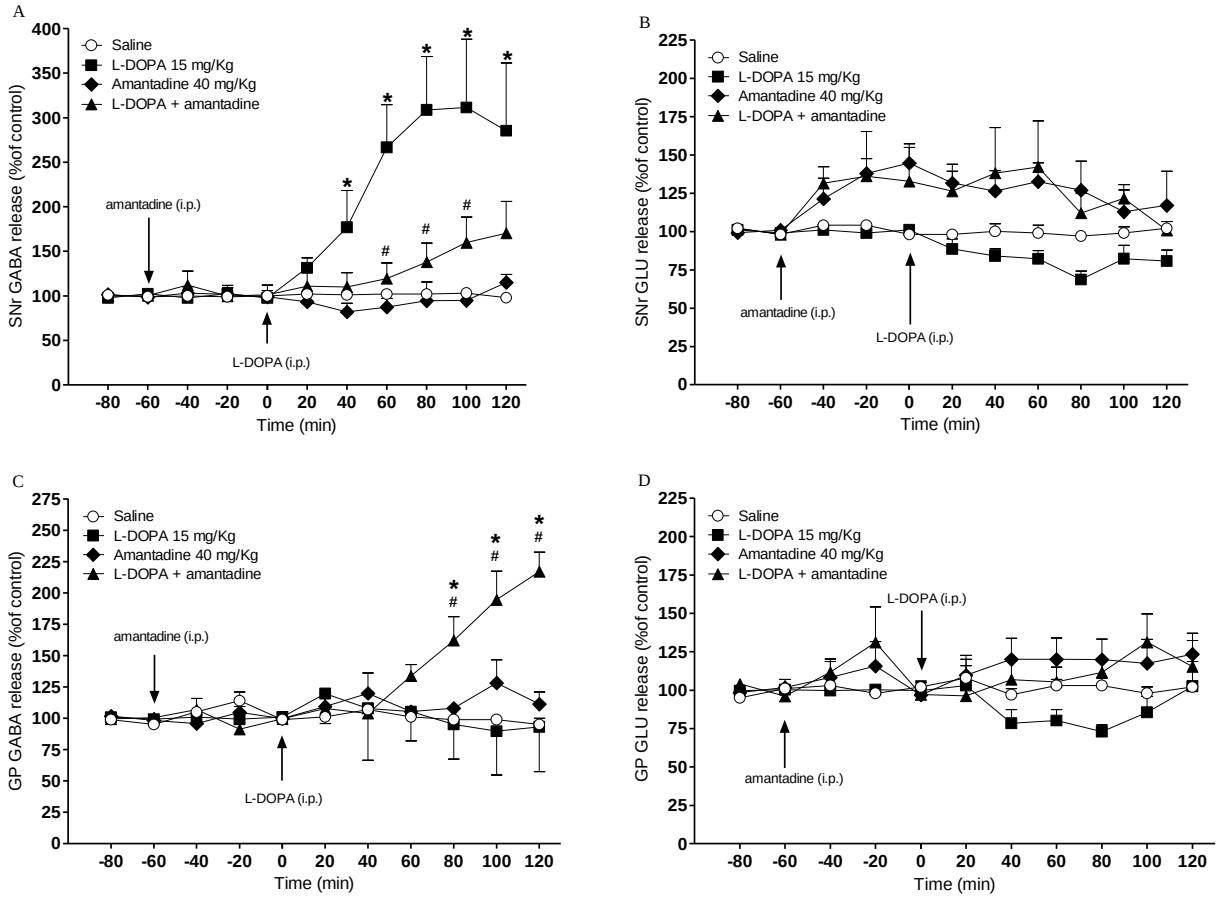

Fig. 4 Neurochemical effects of L-DOPA and amantadine in dyskinetic mice undergoing microdialysis. Dyskinetic mice were implanted with a probe in the lesioned substantia nigra reticulata (SNr; A, B) and another in ipsilateral globus pallidus (GP; C, D). Twenty-four hr later, mice received an acute challenge with L-DOPA alone (15 mg/kg plus 12 mg/kg benserazide, i.p.) or in combination with amantadine (40 mg/kg; i.p., 1 h in advance), and GABA (A, C) and GLU (B, D) levels were monitored for 120 min. Control mice were injected either with amantadine alone or saline. Data are expressed as percentage of basal pre-treatment levels (calculated as the mean of the two samples preceding the treatment) and are mean ± SEM of 7–11 animals. Basal dialysate levels of GABA and GLU were 8.0 ± 0.4 and 73.6 ± 8.0 nM, respectively, in SNr, and 7.7 ± 0.6 and 79.5 ± 8.7 nM, respectively, in GP. Statistical analysis was performed by two-way RM ANOVA followed by contrast analysis and the sequentially rejective Bonferroni's test. Panel A: significant effect of treatment ($F_{3,30} = 24.66$, $p < 0.0001$), time ($F_{10,264} = 1.94$, $p = 0.0398$) but not time x treatment interaction ($F_{30,264} = 1.09$, $p = 0.34$). Panel C: significant effect of treatment ($F_{3,30} = 9.84$, $p < 0.0001$), time ($F_{10,255} = 2.46$, $p = 0.0079$) and time x treatment interaction ($F_{30,255} = 2.75$, $p < 0.0001$). *$p < 0.05$ versus saline; $^{\#}p < 0.05$ versus L-DOPA alone.

1.4 Chronic L-DOPA treatment elicits LID in hemi-lesioned rats

Rats chronically treated with L-DOPA (6 mg/kg plus 12 mg/kg of benserazide) developed a stable degree of dyskinesia already at the ninth day of treatment, scoring the maximal values at the

17th day. Axial and limb AIMs showed a similar temporal profile, reaching a similar level of intensity over the 21-day treatment. Conversely, the development of orolingual AIMs was less appreciable, and this AIM subtype was poorly represented in this group of animals (Fig. 5A,B).

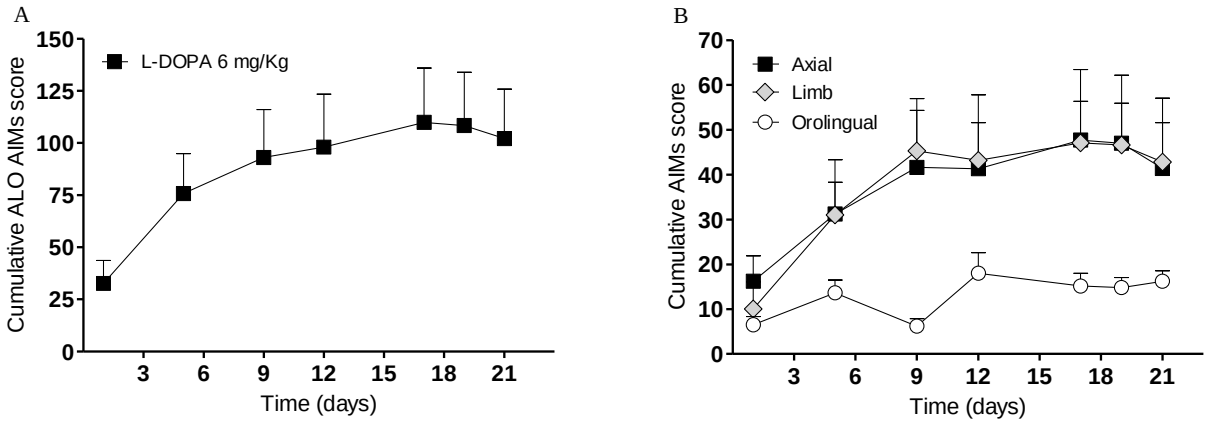

Fig. 5 Development of dyskinesia during chronic L-DOPA administration in 6-OHDA hemi-lesioned rats. Rats were treated for 21 days with L-DOPA 6 mg/kg (plus benserazide 12 mg/kg, one injection per day). AIMs were evaluated at days 1, 5, 9, 12, 17, 19, 21 after L-DOPA injection. ALO AIMs were scored every 20 min over a period of 120 min after L-DOPA administration. Data have been presented either as the sum of each AIM subtype (cumulative ALO AIMs; a) or as each AIM subtype separately (b). Data are mean ± SEM of 10–11 animals.

1.5 Amantadine attenuates LID expression and its neurochemical correlates in hemi-parkinsonian mice and rats.

L-DOPA (6 mg/kg plus 12 mg/kg benserazide) induced AIMs appearance already at 20 min after injection, the maximal intensity (15.5 ± 2.1) being reached after 60 min. Amantadine reduced AIMs expression by ~53% (Fig 6A) being more effective on the axial and limb components (~55% both) than the orolingual one (~44%, Fig. 6C,D). As previously reported (Mela et al., 2007), an increase of GABA levels was observed in the SNr of dyskinetic rats after L-DOPA challenge (6 mg/kg plus 12 mg/kg benserazide, i.p.) which reached the maximum value (~2-fold over basal) at 60 min (Fig. 7A). Different from that observed in mice, the increase of GABA was accompanied by a quantitatively similar increase of glutamate levels (Fig. 7B). Amantadine, ineffective alone, prevented the rise of both amino acids associated with AIMs. Conversely, no changes of GABA or glutamate levels were observed in GP following administration of L-DOPA, amantadine or their combination (Fig. 7C,D).

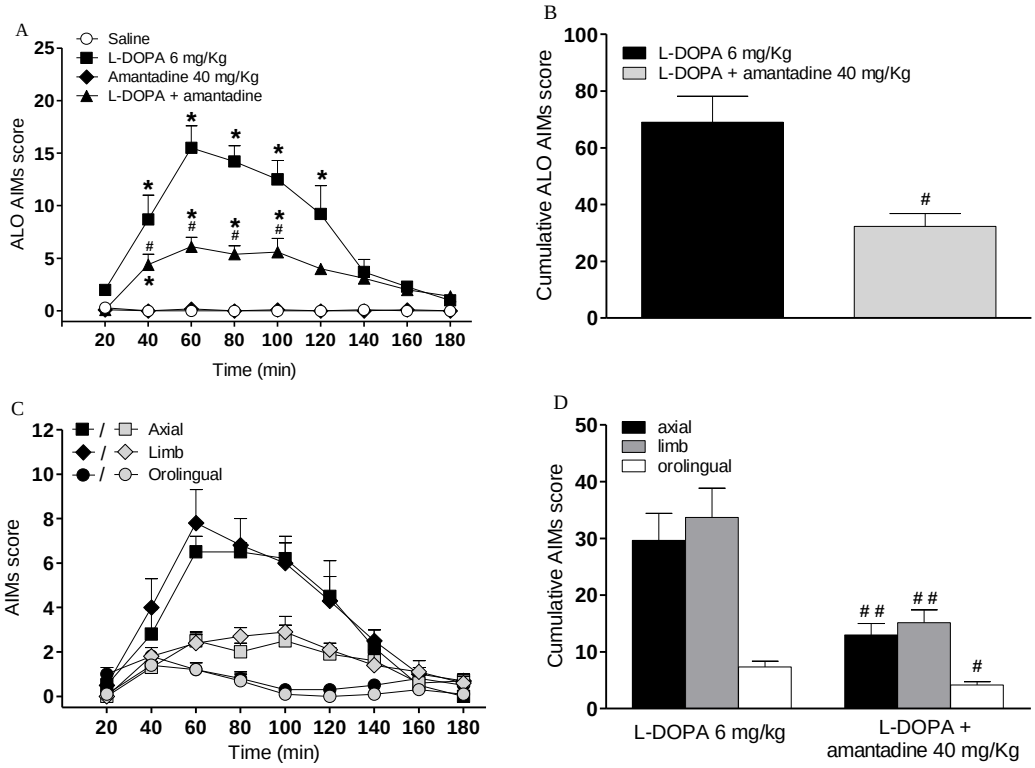

Fig. 6 Behavioral effect of L-DOPA and amantadine in dyskinetic rats undergoing microdialysis. 6-OHDA hemi-lesioned rats were made dyskinetic by chronic L-DOPA administration (6 mg/kg plus 12 mg/kg benserazide, i.p., once a day for 21 days). At the end of treatment, rats underwent surgery for microdialysis probe implantation, and were challenged with L-DOPA alone or in combination with amantadine (40 mg/kg; i.p., 1 h in advance) 24 h later. Control rats were treated with either amantadine or saline alone. ALO AIMs were scored every 20 min over 180 min after L-DOPA administration. Temporal profiles of AIMs taken as a whole (ALO AIMs; A) or as separate items (C) are shown. Cumulative dyskinesia score (i.e. the sum of the scores given at each of the nine observation sessions) is shown for ALO AIMs as a whole (B) or for each AIM subtype separately (D). Data are expressed as arbitrary units (see Results section) and are mean ± SEM of 5–7 animals. Panel A: significant effect of treatment ($F_{3,24} = 117.9$, $p < 0.001$), time ($F_{8,171} = 14.22$, $p < 0.001$) and time treatment interaction ($F_{24,171} = 7.13$, $p < 0.001$), according to two-way RM ANOVA followed by contrast analysis and the sequentially rejective Bonferroni's test. Panel B: significant effect of amantadine ($t = 3.35$, $df = 5$, $p = 0.020$), according to unpaired Student's t-test. Panel D: significant effect of amantadine; axial ($t = 3.40$, $df = 11$, $p = 0.005$), limb ($t = 3.46$, $df = 11$, $p = 0.005$), orolingual ($t = 2.79$, $df = 11$, $p = 0.017$) AIMs, according to unpaired Student's t-test. $^{*}p < 0.05$ versus saline, $^{\#}p < 0.05$, $^{\#\#}p < 0.01$ versus L-DOPA.

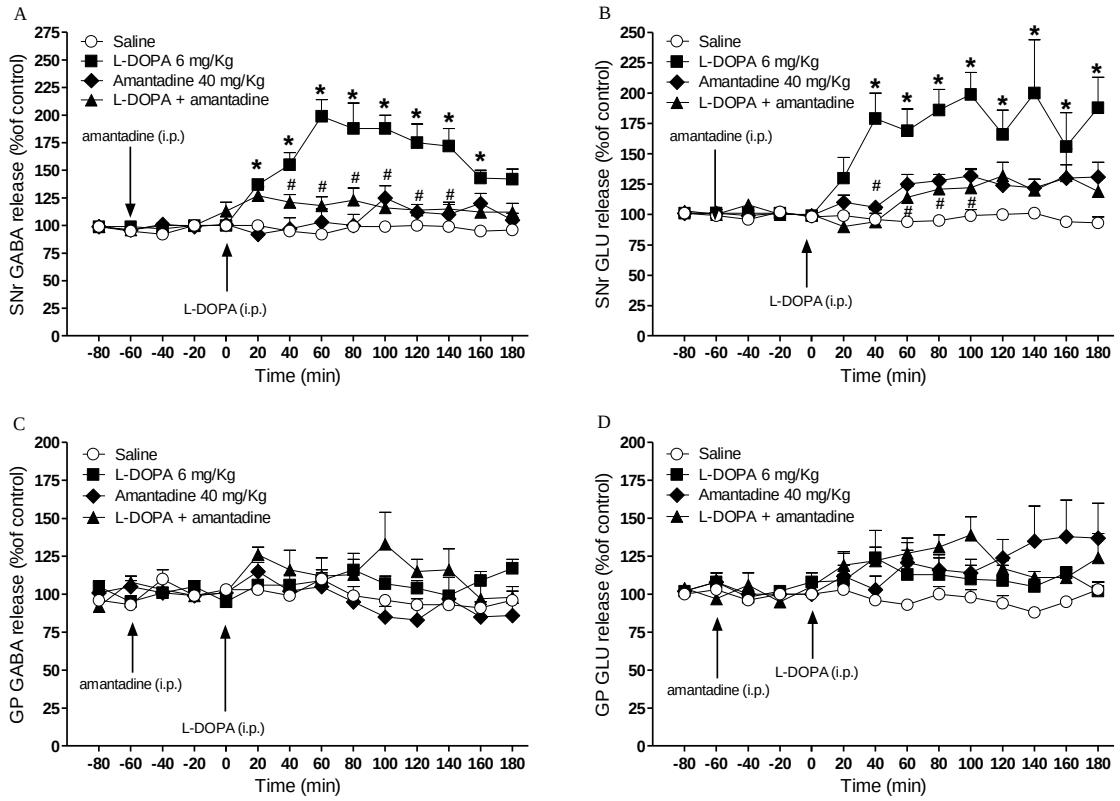

Fig. 7 Neurochemical effects of L-DOPA and amantadine in dyskinetic rats undergoing microdialysis. Dyskinetic rats were implanted with one probe in the lesioned SNr (A, B) and another in ipsilateral GP (C, D). Twenty-four hours later, rats received an acute challenge with L-DOPA alone (6 mg/kg plus 12 mg/kg benserazide, i.p.) or in combination with amantadine (40 mg/kg; i.p., 1 h in advance), and GABA (A, C) and GLU (B, D) levels were monitored for 180 min. Data are expressed as percentage of basal pre-treatment levels (calculated as the mean of the two samples preceding the treatment) and are mean ± SEM of 5–7 animals. Basal dialysate levels of GABA and GLU were 10.5 ± 0.5 and 98.3 ± 5.6 nM, respectively, in SNr, and 11.9 ± 0.5 and 79.6 ± 5.3, respectively, in GP. Panel A: significant effect of treatment ($F_{3,39} = 90.23$, $p < 0.001$), time ($F_{13,280} = 10.34$, $p < 0.001$) and time x treatment interaction ($F_{39,280} = 5.46$, $p < 0.001$). Panel B: significant effect of treatment ($F_{3,39} = 43.74$, $p < 0.001$), time ($F_{13,280} = 6.43$, $p < 0.001$) and time x treatment interaction ($F_{39,280} = 2.46$, $p < 0.001$), according to two-way RM ANOVA followed by contrast analysis and the sequentially rejective Bonferroni's test. *$p < 0.05$ versus saline; $^{\#}p < 0.05$ versus L-DOPA.

1.6 Microdialysis setting have no effect on dyskinesia score and does not influence the antidyskinetic effect of amantadine.

Dyskinetic freely moving animals were challenged with dyskinesiogenic dose of L-DOPA (6 and 15 mg/kg, for rats and mice, respectively plus 12 mg/kg benserazide) and scored for LID magnitude. Rats were also scored when co-administrated with amantadine (40 mg/kg,i.p.). Subsequently the same animals were submitted to surgery procedures for probe implantation. The day after surgery, the animals were placed in the microdialysis setting and challenged with the dyskinesiogenic dose of L-DOPA. Wired rats were also scored when co-administrated with amantadine. Dialysis setting did not significantly alter LID magnitude. Amantadine exerted its antidyskinetic effect in rats with the same extent when tested in the two different conditions (causing a reduction by ~60% of LID).

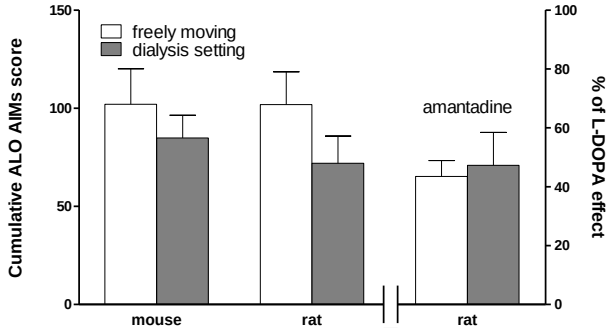

Fig. 8 Impact of microdialysis setting on the behavioral response to L-DOPA and amantadine in dyskinetic animals. AIMs were evaluated in the same animal before and after dialysis probe implantation (i.e. during microdialysis). The anti-dyskinetic effect of amantadine was evaluated in rats only. Data have been presented as cumulative ALO AIMs score or, in the case of amantadine, as percentage of L-DOPA response. Data are mean ± SEM of n = 8 (mice) or n = 5 (rats) experiments. Statistical analysis was performed by the paired Student's t-test.

Part 2. Differential role of nigral and striatal D1 and D2 receptors in LID expression

The second part of the thesis was undertaken to dissect the role of striatal and nigral D1 and D2 receptors in LID, together with the changes in amino acids level in these structures. Using reverse microdialysis in awake rats, we perfused D1R/D5R and D2R/D3R antagonists (SCH23390 and raclopride, respectively, 1 μM) in dorsolateral striatum or SNr simultaneously with LID monitoring.

2.1 Effects of DLS perfusion with SCH23390 and raclopride

Monitoring the behavioral effects of L-DOPA during intrastriatal perfusion with selective DA receptor antagonists (Fig. 9A) revealed that SCH23390 markedly attenuated (~47%) AIMs expression whereas raclopride was without effect (Fig. 9B). Stratification of behavioral analysis for dyskinesia typology showed that SCH23390 prevented approximately to the same extent both limb and axial AIMs whereas orolingual AIMs remained unchanged (Fig. 9C).

To investigate whether striatal D1 and D2 receptors were involved in LID expression, the D1/D5 selective antagonist SCH23390 or D2/D3 selective antagonist raclopride were perfused through a microdialysis probe in dorsolateral striatum, alone or in combination with a systemic dose of L-DOPA. GABA and glutamate levels were monitored in both dorsolateral striatum and SNr simultaneously with AIMs rating. Systemic administration of L-DOPA, alone or in combination with intrastriatal SCH23390, did not affect GABA levels in striatum (Fig. 10A,B). Unlike amino acid levels in dorsolateral striatum, nigral GABA and glutamate concentrations showed a large and sustained increase following the administration of L-DOPA (Fig. 10C,D), an effect that was consistent across all experiments presented in the thesis. GABA levels were significantly elevated above control levels 30 min after L-DOPA treatment (i.e. in the 90 min perfusate fraction; $p<0.05$). reaching maximal values (~86%) in the next sample (105 min). The increase remained significant for at least 90 min following the injection of L-DOPA (150 min perfusate fraction), although it tended to decline by the end of the observation period (180 min fraction, corresponding to 2 hours post L-DOPA administration). Intrastriatal SCH23390 prevented the surge in GABA levels following L-DOPA. Nigral glutamate levels (Fig. 10D) showed a similar temporal course, starting to be significantly elevated above control values in the 90 min perfusate fraction, and reaching a peak (~80%) at 105–120 min. Glutamate levels showed a

steady increase until the end of the observation period (panels D in Figs. 10–11). Local perfusion of SCH23390 in dorsolateral striatum completely blocked the effect of L-DOPA (Fig. 10D). Intrastriatal perfusion of raclopride did not affect striatal amino acid levels when given alone, nor did it disclose any effect of LDOPA in dorsolateral striatum (Figs. 11A–B). Likewise, raclopride did not modulate basal GABA and glutamate levels in SNr (Figs. 11C–D) or their responses to L-DOPA.

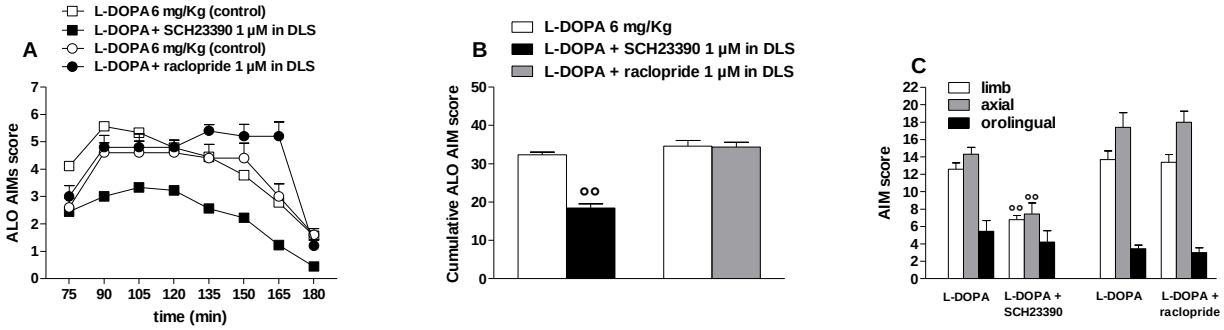

Fig. 9 Reverse dialysis of the D1R selective antagonist SCH23390 but not the D2R selective antagonist raclopride in the DA-depleted dorsolateral striatum (DLS) of unilateral 6-OHDA lesioned dyskinetic rats modulates L-DOPA induced abnormal involuntary movements (AIMs). SCH23390 and raclopride (1 µM) were perfused through the probe implanted in DLS starting 1 h before systemic administration of L-DOPA (6 mg/kg+12 mg/kg benserazide, i.p.). Axial, limb and orolingual (ALO) AIMs were scored every 15 min (for 120 min after L-DOPA administration) according to the scale described in Methods. Data were presented as time-course (A), cumulative ALO scores (B) or separate scores for each subtype (C). Data are means ± SEM of 5– 9 determinations. Statistical analysis was performed by the Mann Whitney U-test. Significant results: panel B, U=0.5; panel C Limb AIMs, U=1.5, axial AIMs U=5.0. °°p<0.01 different from L-DOPA alone.

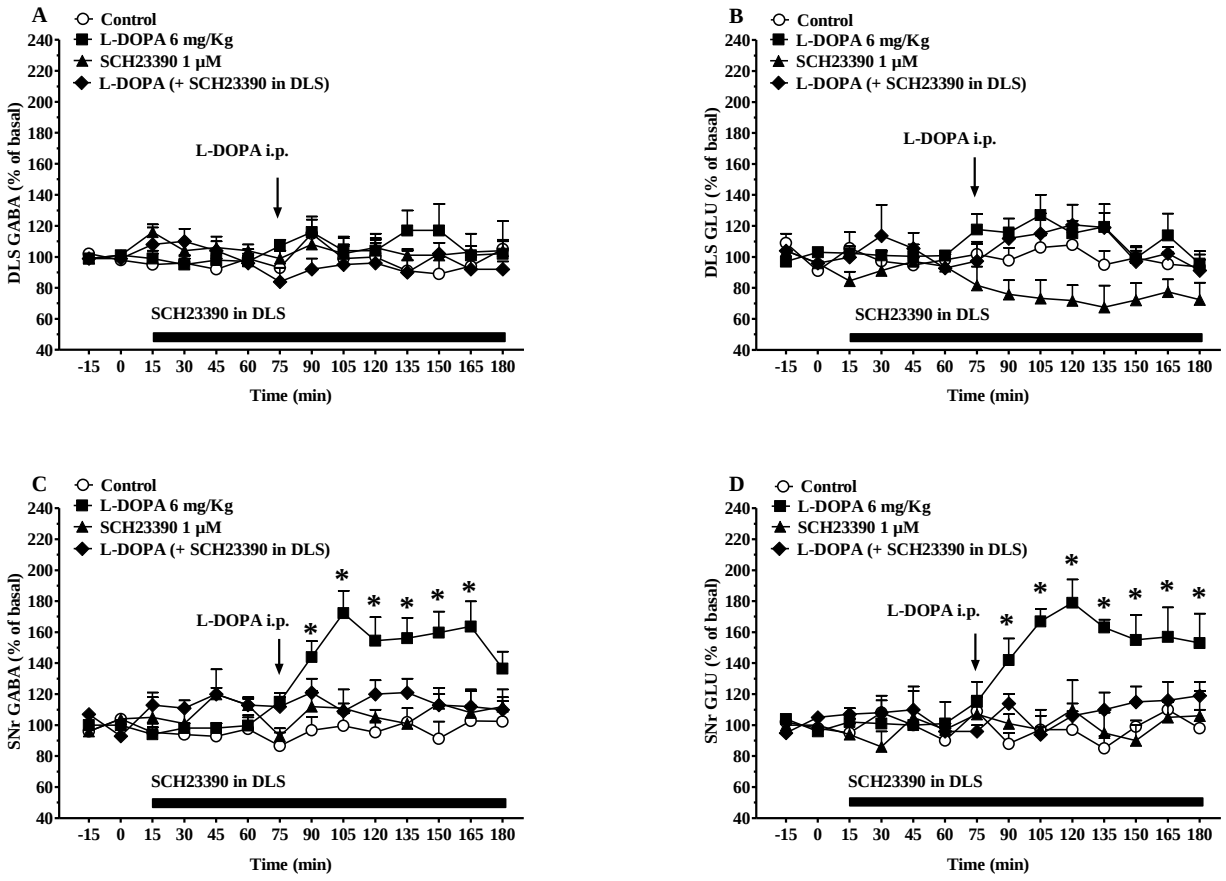

Fig. 10 Reverse dialysis of the D1 receptor selective antagonist SCH23390 in the DA-depleted dorsolateral striatum (DLS) of unilateral 6-OHDA lesioned dyskinetic rats modulates L-DOPA induced amino acid levels. SCH23390 (1 µM) was perfused through the probe implanted in DLS, and GABA and GLU levels monitored in DLS (A–B) and SNr (C–D). SCH23390 was perfused (black bar) starting 1 h before systemic administration of L-DOPA (6 mg/kg+12 mg/kg benserazide, i.p.; arrow). Data are expressed as percentages of basal pre-treatment values, and are means ± SEM of 5–7 determinations. Basal GABA and GLU levels (nM) were 10.6 ± 0.6 and 179.3 ± 14.7 (DLS), and 9.7 ± 0.5 and 161.3±15.6 (SNr), respectively. Statistical analysis was performed by Two-way RM ANOVA followed by the sequentially rejective Bonferroni's test. Significant interactions: panel B, L-DOPA X time ($F_{11,188}=2.17$, $p=0.0175$); panel C, L-DOPA x time ($F_{11,220} = 2.91$, $p = 0.001$), SCH23390 x time ($F_{11,220} = 4.29$, $p < 0.001$) or L-DOPA x SCH23390 x time ($F_{11,220} = 3.89$, $p < 0.001$); panel D, L-DOPA x time ($F_{11,212} = 3.40$, $p < 0.001$), SCH23390 × time ($F_{11,212} = 2.52$, $p = 0.005$) or L-DOPA x SCH23390 x time ($F_{11,212} = 3.23$, $p < 0.001$). *p<0.01 different from control.

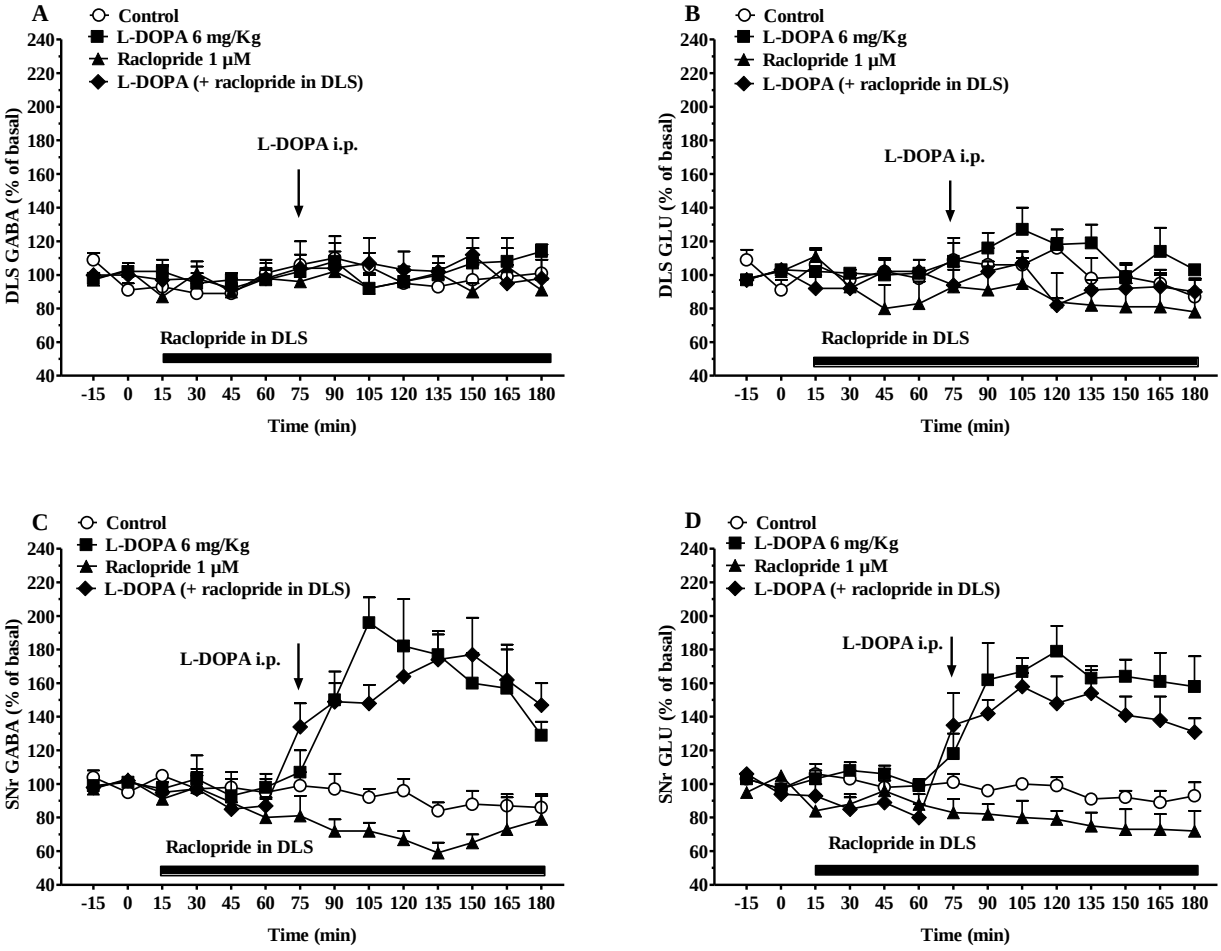

Fig. 11 Reverse dialysis of the D2R selective antagonist raclopride in the DA-depleted dorsolateral striatum (DLS) of unilateral 6-OHDA lesioned dyskinetic rats modulates L-DOPA induced amino acid levels. Raclopride (1 µM) was perfused through the probe implanted in DLS, and GABA and GLU levels monitored in DLS (A–B) and SNr (C–D). Raclopride was perfused (black bar) starting 1 h before systemic administration of L-DOPA (6mg/kg + 12mg/kg benserazide, i.p.; arrow). Data are expressed as percentages of basal pre-treatment values, and are means ± SEM of 5–6 determinations. Basal GABA and GLU levels (nM) were, respectively, 20.4 ± 3.1 and 128.7.3 ± 25.8 (DLS), and 13.1 ± 1.9 and 132.5 ± 23.1 (SNr). Statistical analysis was performed by Two-way RM ANOVA followed by the sequentially rejective Bonferroni's test. Significant interactions: panel C, L-DOPA x time ($F_{11,200} = 13.50$, $p < 0.001$); panel D, L-DOPA x time ($F_{11,200} = 13.56$, $p < 0.001$).

2.2 Effects of SNr perfusion with SCH23390 and raclopride

Monitoring the effect of L-DOPA on AIMs expression during intranigral perfusion with selective DA receptor antagonists (Fig. 12A) revealed that both SCH23390 and raclopride significantly attenuated AIMs expression (~21% and ~40%, respectively; Fig. 12B), causing a reduction of limb AIMs (Fig. 12C).

To investigate the role of nigral D1R and D2R in LID, perfusions of SCH23390 or raclopride through the probe implanted in SNr were combined with systemic L-DOPA administration (Figs. 13–14). Intranigral perfusion with SCH23390 did not affect amino acid levels in striatum when given alone or in combination with L-DOPA (Figs. 13A–B). However, intranigral SCH23390 alone transiently elevated GABA levels in SNr and attenuated the GABA response to L-DOPA (Fig. 13C). Conversely, SCH23390 did not affect basal glutamate levels nor did it attenuate the rise in nigral glutamate following L-DOPA (Fig. 13D) Differently from SCH23390, intranigral perfusion with raclopride caused marked changes in amino acid levels in striatum. Intranigral raclopride caused a slow increase in striatal GABA levels which was unaffected by L-DOPA (Fig. 14A). In contrast, raclopride caused a prompt elevation of striatal glutamate levels which was overall enhanced by L-DOPA (Fig. 14B). However, at any time point the effect of L-DOPA was different from that of raclopride. Perfusion of raclopride in SNr significantly decreased GABA levels (~40%) although it did not change the facilitatory effect of L-DOPA (Fig. 14C). Intranigral raclopride did not change basal glutamate levels in this area nor did it alter the surge in nigral glutamate in response to L-DOPA (Fig. 14D).

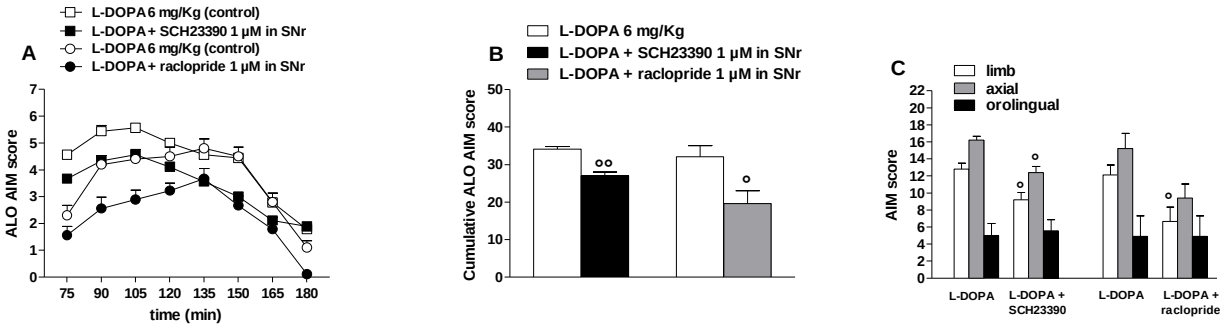

Fig. 12. Reverse dialysis of the D1R selective antagonist SCH23390 and the D2R selective antagonist raclopride in the lesioned substantia nigra reticulata (SNr) of unilateral 6 OHDA lesioned dyskinetic rats modulates L-DOPA induced abnormal involuntary movements (AIMs). SCH23390 and raclopride (1 µM) were perfused through the probe implanted in SNr starting 1 h before systemic administration of L-DOPA (6 mg/kg + 12 mg/kg benserazide, i.p.). Axial, limb and orolingual (ALO) AIMs were scored every 15 min (for 135 min after L-DOPA administration) according to the scale described in methods. Data were presented as time-course (A), cumulative ALO scores (B) or separate scores for each subtype (C). Data are means ± SEM of 7–9 determinations. Statistical analysis was performed by the Mann–Whitney U-test. Significant results: panel B, SCH23390, U = 10.0, raclopride U = 7.50; panel C Limb AIMs, SCH23390 U = 10.5, raclopride U = 8.0; axial AIMs, SCH23390 U = 7.0, raclopride U = 10.0. °p < 0.05, °°p < 0.01, different from L-DOPA alone.

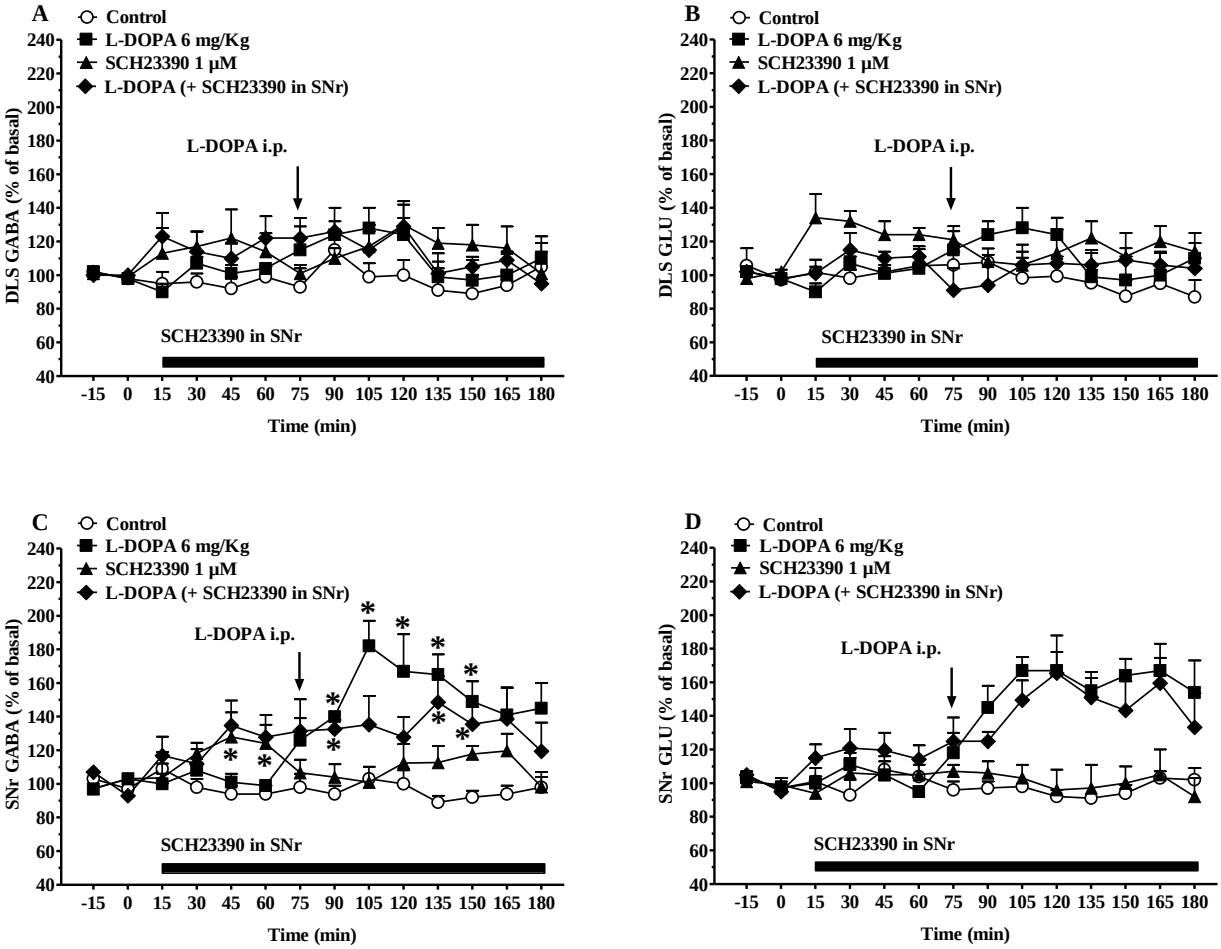

Fig. 13. Reverse dialysis of the D1R selective antagonist SCH23390 in the lesioned substantia nigra pars reticulata (SNr) of unilateral 6-OHDA lesioned dyskinetic rats modulates L-DOPA-induced amino acid levels. SCH23390 (1 µM) was perfused through the probe implanted in SNr, and GABA and GLU levels monitored in ipsilateral dorsolateral striatum (DLS; A–B) and SNr (C–D). SCH23390 was perfused (black bar) 1 h before systemic administration of L-DOPA (6 mg/kg + 12 mg/kg benserazide, i.p.; arrow). Data are expressed as percentages of basal pre-treatment values, and are means ± SEM of 5–7 determinations. Basal GABA and GLU levels (nM) were 10.8 ± 0.7 and 147.7 ± 8.3 (DLS), and 9.6 ± 0.7 and 166.7 ± 16.3 (SNr), respectively. Statistical analysis was performed by Two-way RM ANOVA followed by the sequentially rejective Bonferroni's test. Significant interactions: panel C, SCH23390 x time ($F_{11,252} = 20.21$, $p<0.001$), L-DOPA x time ($F_{11,252} = 9.59$, $p < 0.001$) and L-DOPA x SCH23390 x time ($F_{11,252}=10.52$, $p < 0.001$). *$p < 0.01$ different from control

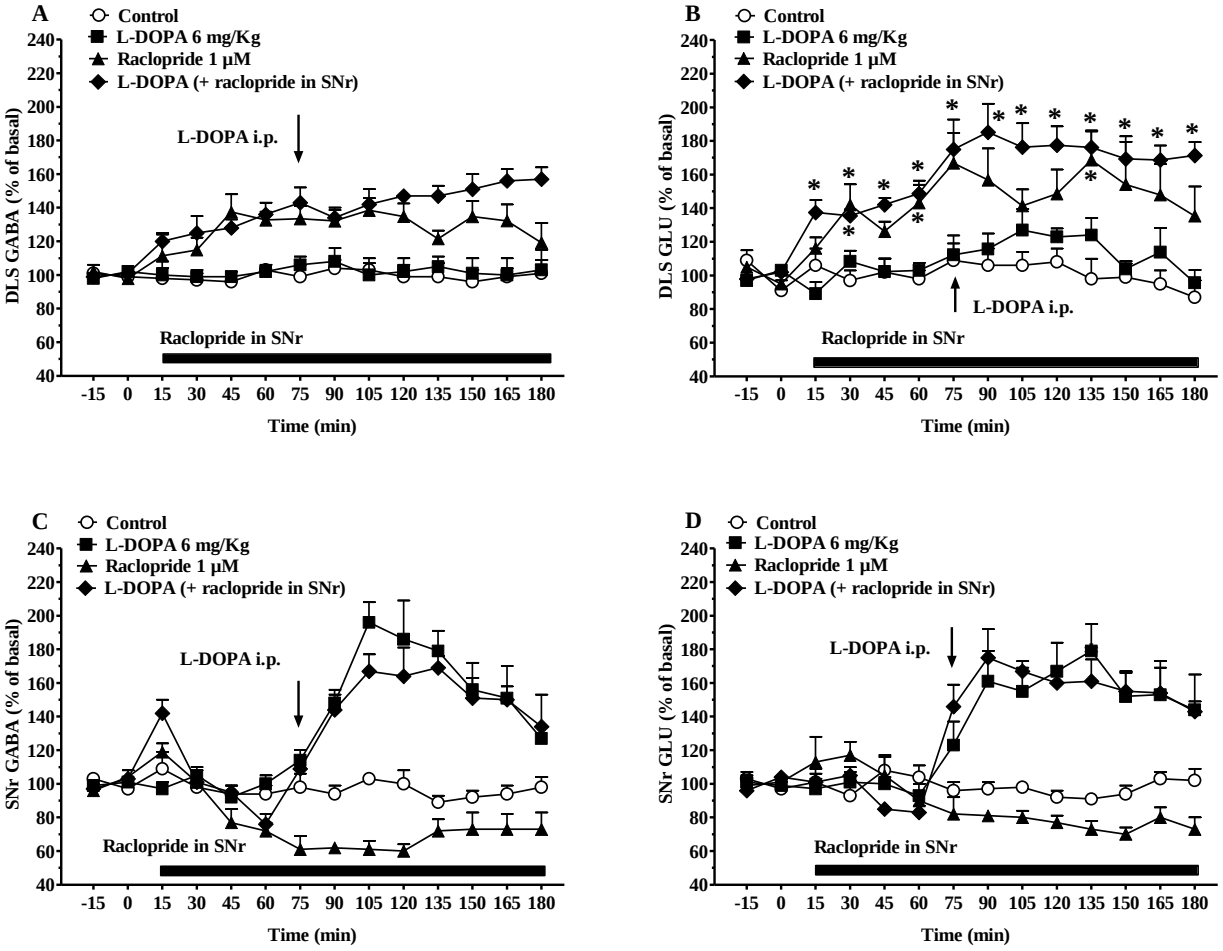

Fig.14 Reverse dialysis of the D2R selective antagonist raclopride in the lesioned substantia nigra pars reticulata (SNr) of unilateral 6-OHDA lesioned dyskinetic rats modulates L-DOPA-induced amino acid release. Raclopride (1 µM) was perfused through the probe implanted in SNr, and GABA and GLU levels monitored in ipsilateral dorsolateral striatum (DLS; A B) and SNr (C–D). Raclopride was perfused (black bar) 1 h before systemic administration of L-DOPA (6 mg/kg + 12 mg/kg benserazide, i.p.; arrow). Data are expressed as percentages of basal pre-treatment values, and are means ± SEM of 5–6 determinations. Basal GABA and GLU levels (nM) were 11.3 ± 1.3 and 87.2 ± 23.1 (DLS), and 10.6 ± 1.4 and 77.7 ± 18.8 (SNr), respectively. Statistical analysis was performed by two-way RM ANOVA followed by the sequentially rejective Bonferroni's test. Significant interactions: panel A, raclopride X time ($F_{11,220} = 2.35$, $p = 0.009$); panel B, L-DOPA x time ($F_{11,176} = 10.57$, $p < 0.001$), raclopride x time ($F_{11,17}$ 6= 5.61, $p < 0.001$) and L-DOPA x raclopride x time ($F_{11,176} = 4.62$, $p < 0.001$); panel C, raclopride x time ($F_{11,208} = 2.78$, $p = 0.002$) and L-DOPA x time ($F_{11,208} = 17.22$, $p < 0.001$).

*$p < 0.01$ different from control.

Part 3. Targeting striatal RasGRFs as possible approach to reduce LID

In the third part of the study, we investigated whether the selective striatal blockade of RasGRF1 or RasGRF2 is able to reduce the expression of dyskinesia, and if such effect could be accompanied by changes in neurochemical correlates. Moreover, we investigated whether RasGRF1 or RasGRF2 inhibition could synergize with amantadine in reducing LID expression. In order to achieve a striatal-selective inhibition of RasGRF1 and RasGRF2 we used lentiviral vectors (LVs) carrying small hairpin (sh) RNA targeted towards RasGRF1 (sh-RasGRF1) and RasGRF2 (sh-RasGRF2). Control mice are represented by 6-OHDA hemi-lesioned mice injected with LV expressing only the green fluorescent gene as report gene (LV-CTR). The data presented for the motor activity are referred to the forepaw contralateral to the lesion side.

3.1 Sh-RasGRF1 expression has no effects on basal motor activity and motor learning

At the first day of training, the motor scores of LV-CTR animals (n=10) were 32.0 ± 4.3 seconds of immobility (bar test), 3.6 ± 0.7 steps (drag test) and 429.7 ± 51.9 s of permanence on the rod (rotarod test). Mice injected with sh-RasGRF1 (n=9) showed similar values: 28.1 ± 4.7 seconds of immobility, 4.6 ± 0.9 steps and 408.3 ± 55.2 seconds of permanence on the rod (Fig. 15). After five days of training both group of animals displayed the same extent of motor improvement (in terms of adaptation to experimental conditions) without any differences among the two experimental groups. LV-CTR and sh-RasGRF1 increased immobility time in the bar test by ~30% and ~40% respectively (Fig. 15A), as well as motor performance on the rotarod by ~50% and ~65% respectively (Fig. 15C). In the drag test both groups of mice showed a tendency to increase in the number of steps (Fig 15B).

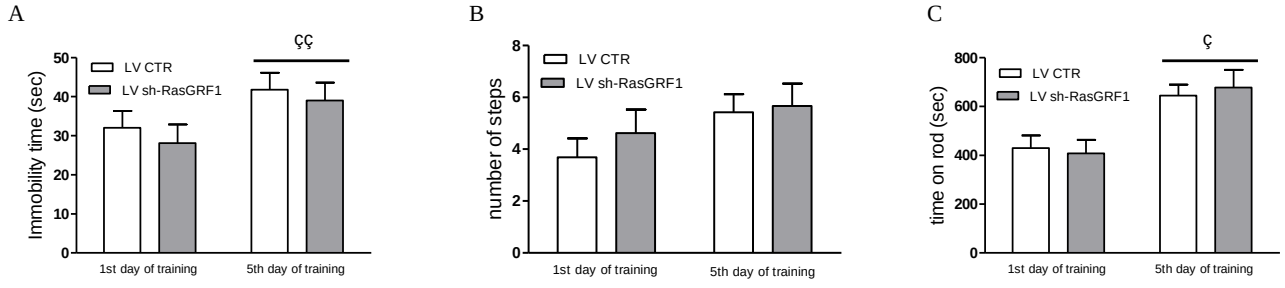

Fig. 15 LVs injection does not affect the motor performance in 6-OHDA hemi-lesioned mice. Repeated testing (5 days training) increased the time spent on the blocks in the bar test (A), improved the overall motor performance in the rotarod test (C) and

had no effect on the number of steps in drag test (B). Motor performance in the bar and drag test refers to the contralateral separately (parkinsonian) paw (A, B). Data are expressed as absolute values (s, number of steps) and are mean ± SEM of 9–10 animals. Statistical analysis was performed by two-way ANOVA followed by contrast analysis and the sequentially rejective Bonferroni's test. Panel A: significant effect of time ($F_{1,34} = 5.21$, $p = 0.028$). Panel C: significant effect of time ($F_{1,34} = 34.78$, $p < 0.001$). $^{\S\S}p < 0.01$ versus the first day of training (A), $^{\S}p < 0.05$ versus the first day of training (C).

3.2 Sh-RasGRF1 expression attenuates LID development in 6-OHDA hemi-lesioned mice

Chronic treatment with escalating doses of L-DOPA (3, 6, 9 mg/kg plus 12 mg/kg benserazide; i.p., once daily for 9 days) caused the development of LID in both LV-CTR and sh-RasGRF1. AIMs appearance resulted constantly reduced in sh-RasGRF1 compared to LV-CTR mice (Fig. 16A) and such difference was maximal at the ninth day of treatment (Fig. 16A). Cumulative ALO AIMs score emphasizes the difference in LID over the entire period of treatment, and revealed that sh-RasGRF1 mice had ~60% less severe dyskinesia (36.4 ± 9.7) than the controls (103.0 ± 19.7; Fig. 16A,B).

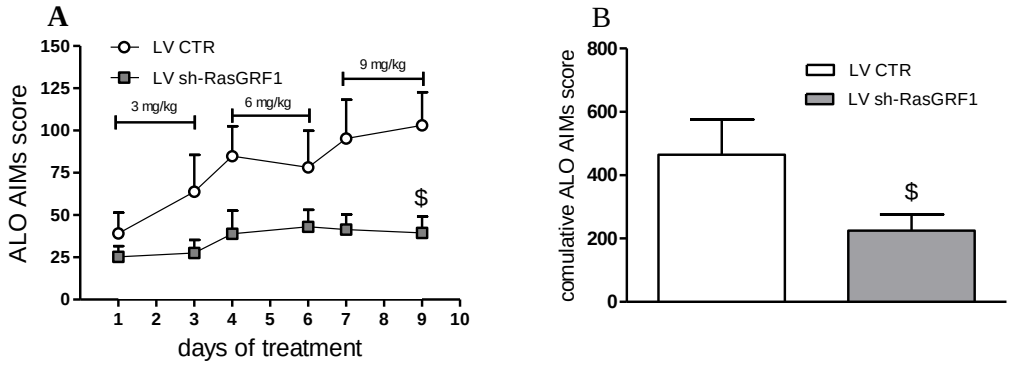

Fig. 16 Development of dyskinesia during chronic L-DOPA administration in LV-CTR and sh-RasGRF1 6-OHDA hemi-lesioned mice. Mice were treated for 9 days with escalating doses of L-DOPA (3, 6, 9 mg/kg plus benserazide 12 mg/kg, i.p., once daily) and AIMs were evaluated at days 1, 3, 4, 6, 7 and 9 after treatment onset. Axial, limb and orolingual (ALO) AIMs were scored every 20 min for 120 min after L-DOPA administration (A). The sum of AIMs for overall the time period of observation (cumulative ALO AIMs) are also represented (B). Data are expressed as arbitrary units (see Results section) and are mean ± SEM of 8–9 animals. Panel A: significant effect of sh-RasGRF1 according to two-way RM ANOVA followed by contrast analysis and the sequentially rejective Bonferroni's test ($F_{1,90} = 22.88$, $p < 0.001$). Panel B: significant effect of sh-RasGRF1 according to unpaired Student's t-test ($t = 2.02$, $df = 15$, $p = 0.030$). $^{\$}p < 0.05$ versus LV-CTR.

3.3 Amantadine improves LID in LV-CTR animal but its anti-dyskinetic effect is occluded in sh-RasGRF1 mice.

In LV-CTR and sh-RasGRF1 mice undergoing microdialysis, L-DOPA (9 mg/kg plus 12 mg/kg benserazide) induced AIMs appearance already at 20 min after injection, the maximal intensity

(16.8 ± 1.4 and 8.7 ± 3.0 respectively) being observed within the 40-80 min time window (Fig 17A,B). Amantadine co-administration reduced AIMs expression by ~50% (Fig 17A) in LV-CTR mice but failed to further reduce LID severity in sh-RasGRF1 animals (Fig. 17B) As previously reported (*part 1,2*), GABA levels increased in the SNr of dyskinetic LV-CTR mice after L-DOPA challenge (9 mg/kg plus 12 mg/kg benserazide, i.p.), reaching the maximum value (~2.5-fold over basal) at 100 min and prevented the rise of GABA in SNr when co-administered with L-DOPA (Fig. 18A). L-DOPA and amantadine, did not affect glutamate levels in SNr when administered alone or in combination (Fig. 18B). Conversely, LID expression followed by L-DOPA injection did not coincide with the increase of GABA levels in SNr (Fig. 19A).

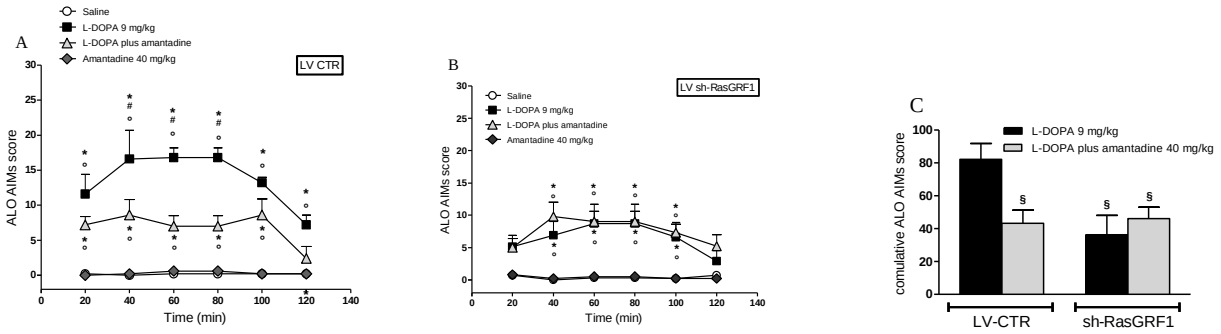

Fig. 17 Behavioral effect of L-DOPA and amantadine in dyskinetic mice undergoing microdialysis. Dyskinetic mice underwent surgery for microdialysis probe implantation, and were challenged with L-DOPA alone or in combination with amantadine (40 mg/kg; i.p., 1 h in advance) 24 h later. Control mice were treated with either amantadine or saline alone. ALO AIMs were scored every 20 min over 120 min after L-DOPA administration. Temporal profiles of AIMs taken as a whole (ALO AIMs; A,B) or as sum of AIMs for overall the time period of observation (cumulative ALO AIMs; C) are shown. Data are expressed as arbitrary units (see Results section) and are mean ± SEM of 5–7 animals. Panel A: significant effect of treatment ($F_{5,96} = 4.07$, $p = 0.002$), time ($F_{3,96} = 117.90$, $p < 0.001$) and time x treatment interaction ($F_{15,93} = 1.83$, $p < 0.040$), according to two-way RM ANOVA followed by contrast analysis and the sequentially rejective Bonferroni's test. Panel B: significant effect of time ($F_{3,126} = 36.21$, $p < 0.001$), time ($F_{3,96} = 117.90$, $p < 0.001$) and time x treatment interaction ($F_{15,93} = 1.83$, $p = 0.040$), according to two-way RM ANOVA followed by contrast analysis and the sequentially rejective Bonferroni's test. Panel C: significant effect of treatment ($F_{3,20} = 4.08$, $p = 0.020$), according to one-way ANOVA followed Newman-Keuls multiple comparison test . *$p < 0.05$ versus saline, °$p < 0.05$ versus amantadine, $^{\#}p < 0.05$ versus L-DOPA plus amantadine, $^{\S}p<0.05$ versus L-DOPA-injected LV-CTR mice.

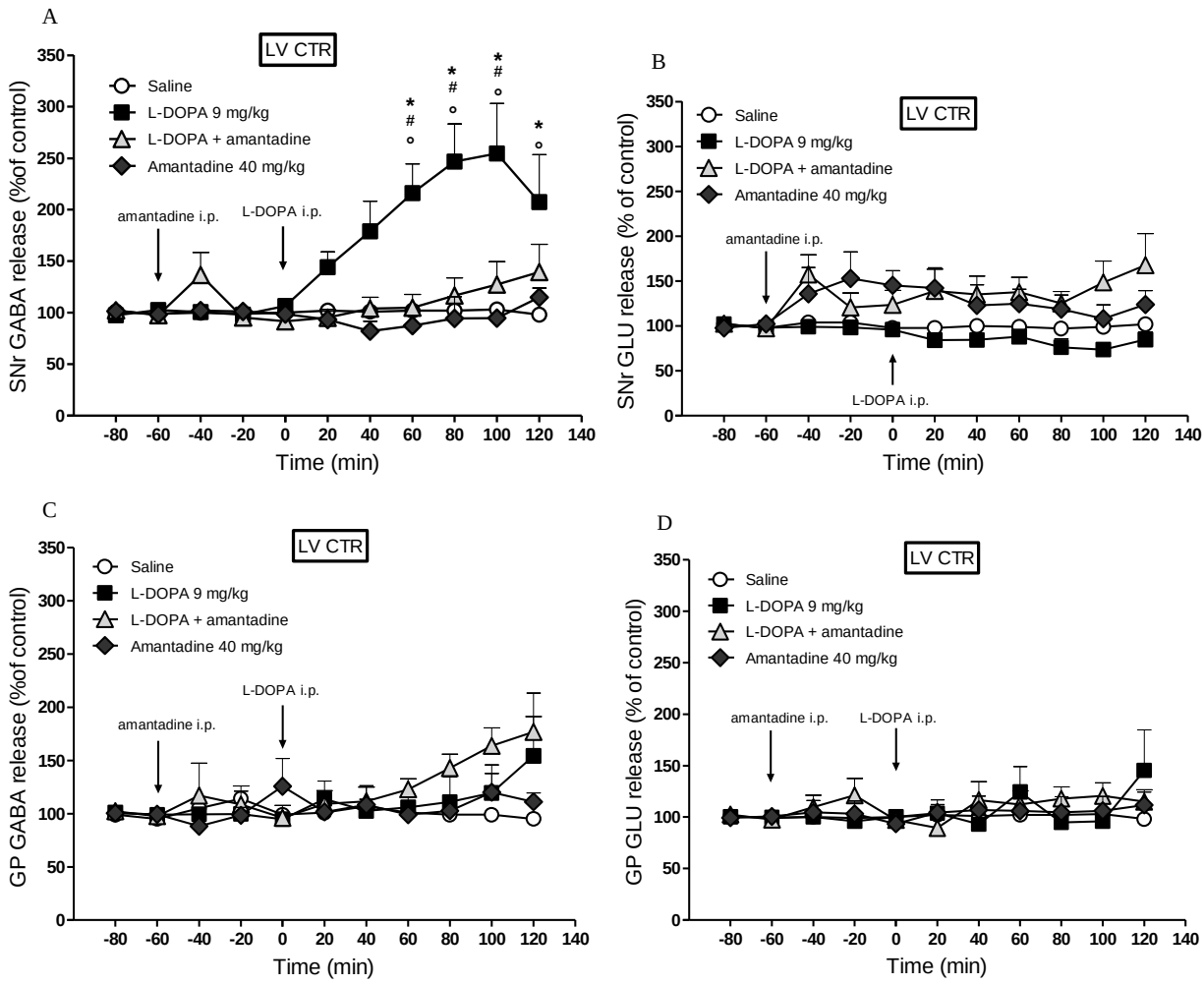

Fig. 18 Neurochemical effects of L-DOPA and amantadine in dyskinetic LV-CTR mice undergoing microdialysis. Dyskinetic mice were implanted with one probe in the lesioned SNr (A, B) and another in ipsilateral GP (C, D). Twenty-four hours later, rats received an acute challenge with L-DOPA alone (9 mg/kg plus 12 mg/kg benserazide, i.p.) or in combination with amantadine (40 mg/kg; i.p., 1 h in advance), and GABA (A, C) and GLU (B, D) levels were monitored for 120 min. Data are expressed as percentage of basal pre-treatment levels (calculated as the mean of the two samples preceding the treatment) and are mean ± SEM of 4–8 animals. Basal dialysate levels of GABA and GLU were 9.8 ± 0.8 and 102.1 ± 16.2 nM, respectively, in SNr, and 10.1 ± 0.8 and 103.4 ± 13.1, respectively, in GP. Panel A: significant effect of treatment ($F_{3,319} = 15.94$, $p < 0.001$), time ($F_{10,319} = 2.29$, $p = 0.012$) and time x treatment interaction ($F_{30,319} = 1.75$, $p = 0.01$) according to two-way RM ANOVA followed by contrast analysis and the sequentially rejective Bonferroni's test. $^{*}p < 0.05$ versus saline, °$p < 0.05$ versus amantadine, $^{\#}p < 0.05$ versus L-DOPA plus amantadine.

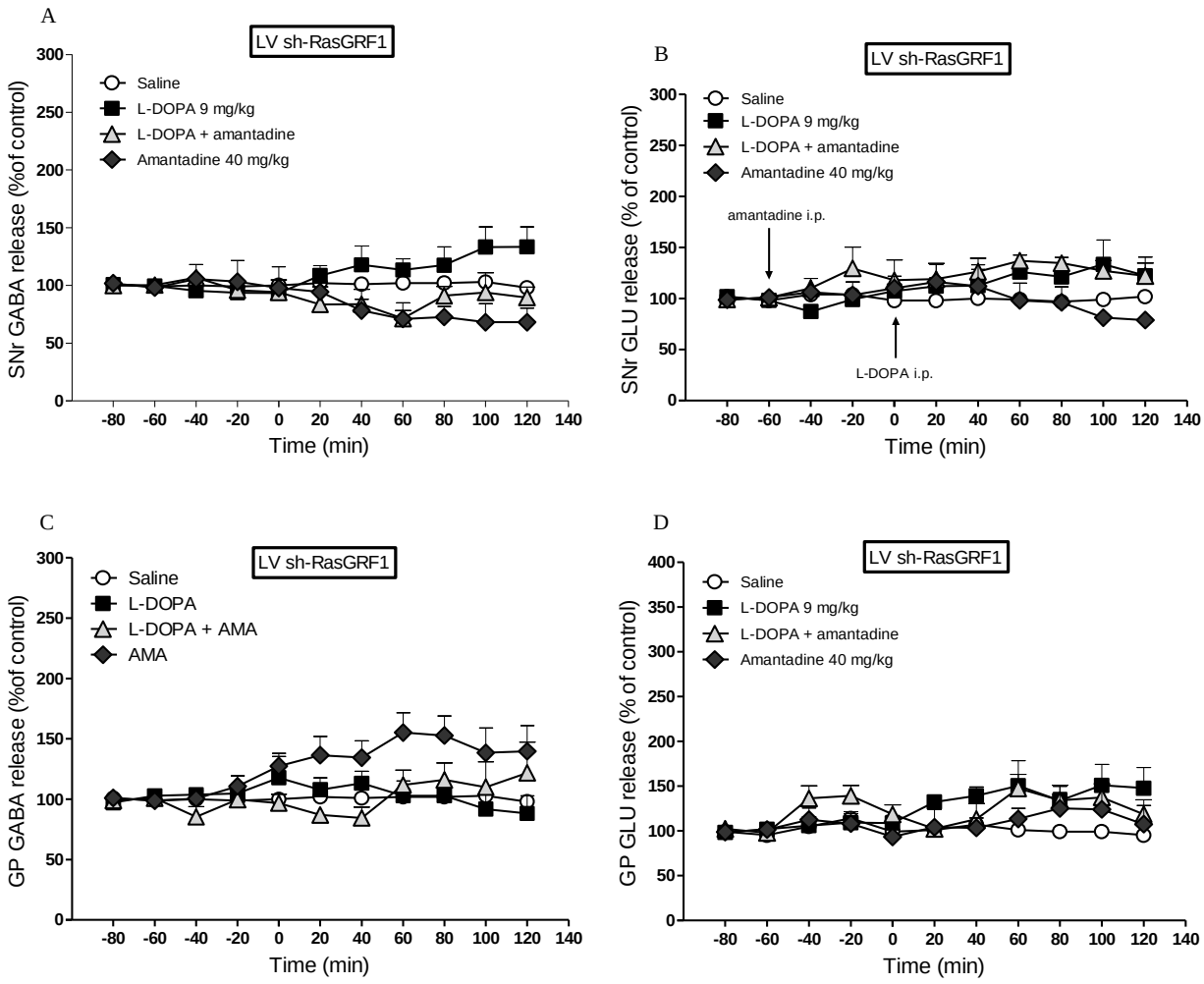

Fig. 19 Neurochemical effects of L-DOPA and amantadine in dyskinetic sh-RasGRF1 mice undergoing microdialysis. Dyskinetic mice were implanted with one probe in the lesioned SNr (A, B) and another in ipsilateral GP (C, D). Twenty-four hours later, rats received an acute challenge with L-DOPA alone (9 mg/kg plus 12 mg/kg benserazide, i.p.) or in combination with amantadine (40 mg/kg; i.p., 1 h in advance), and GABA (A, C) and GLU (B, D) levels were monitored for 120 min. Data are expressed as percentage of basal pre-treatment levels (calculated as the mean of the two samples preceding the treatment) and are mean ± SEM of 4–8 animals. Basal dialysate levels of GABA and GLU were 9.98 ± 0.7 and 115.3 ± 16.2 nM, respectively, in SNr, and 13.0 ± 1.1 and 97.2 ± 6.8, respectively, in GP.

3.4 Sh-RasGRF2 expression has no effect on basal motor activity and motor learning

At the first day of training, the motor scores of LV-CTR animals (n=15) were 15.8 ± 2.1 s of immobility (bar test), 5.7 ± 1.0 steps (drag test) and 377.2 ± 37.7 s of permanence on the rod (rotarod test). Mice injected with sh-RasGRF2 (n=19) did not show significantly different performance compared to controls: 19.8 ± 2.4 s of immobility, 5.3 ± 1.0 steps and 455.3 ± 43.8

seconds of permanence on the rod (Fig. 20). After five days of training both groups of animals displayed the same extent of motor improvement showing a similar increase in immobility time (Fig. 20A) and in stepping activity (Fig. 20B). Conversely, the rotarod performance not show any improvement in both groups of mice (Fig. 20C).

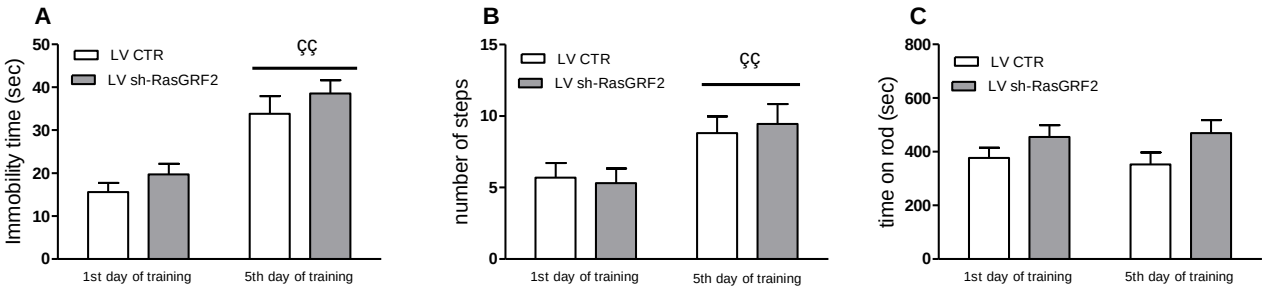

Fig. 20 LVs unilateral injection does not affect the motor performance adaptation in 6-OHDA mice. 5 days of training to the experimental conditions increased the time spent on the blocks in the bar test (A), improved the overall motor performance in the rotarod test (C) and had no effect on the number of steps in drag test (B). Behavioral testing was performed the first day of animals manipulation and at the fifth day, after 3 days of daily training. Motor skills were evaluated for the contralateral separately (parkinsonian) paw (A, B). Data are expressed as absolute values (s, number of steps) and are mean ± SEM of 15–19 animals. Statistical analysis was performed by two-way ANOVA followed by contrast analysis and the sequentially rejective Bonferroni's test. Panel A: significant effect of time ($F_{1,64} = 38.34$, $p < 0.001$). Panel B: significant effect of time ($F_{1,64} = 9.21$, $p = 0.003$). $^{çç}p < 0.01$ versus the first day of training (A).

3.5 Sh-RasGRF2 expression has no effect on LID development in 6-OHDA lesioned mice

Chronic treatment of hemi-parkinsonian mice with escalating doses of L-DOPA (3, 6, 9 mg/kg plus 12 mg/kg benserazide; i.p., once daily for 9 days) caused the development of LID in both LV-CTR and sh-RasGRF2. Although, sh-RasGRF2 mice showed less severe dyskinesia compared to controls, the difference did not reach statistical significance. AIMs were maximal at the ninth day of treatment, reaching the value of 119.7 ± 16.3 in LV-CTR (n=8) and 78.1 ± 13.8 in sh-RasGRF1 animals (n=11; Fig. 21A).

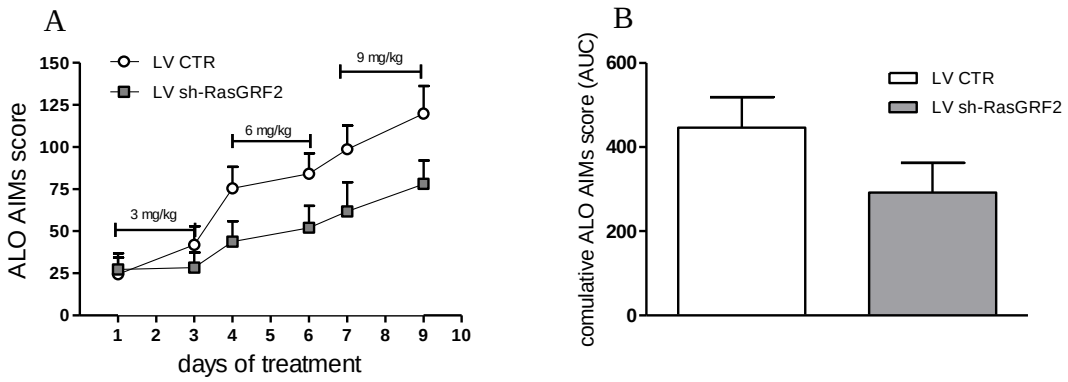

Fig. 21 Development of dyskinesia during chronic L-DOPA administration in LV-CTR and sh-RasGRF2 6-OHDA hemi-lesioned mice. Mice were treated for 9 days with escalating doses of L-DOPA (3, 6, 9 mg/kg plus benserazide 12 mg/kg, i.p., once daily) and AIMs were evaluated at days 1, 3, 4, 6, 7 and 9 after treatment onset. Axial, limb and orolingual (ALO) AIMs were scored every 20 min for 120 min after L-DOPA administration (A). The sum of AIMs for overall the time period of observation (cumulative ALO AIMs) are also represented (B). Data are expressed as arbitrary units (see Results section) and are mean ± SEM of 8–11 animals.

3.6 Amantadine improves LID to the same extent in LV-CTR and in sh-RasGRF2 mice

In LV-CTR and sh-RasGRF2 mice undergoing microdialysis, L-DOPA (9 mg/kg plus 12 mg/kg benserazide) induced AIMs appearance already at 20 min after injection, the maximal intensity (21.1 ± 1.8 and 16.7 ± 0.8) being observed within the 40-80 min time window (Fig 22A,B). Amantadine reduced AIMs expression by ~50% in both LV-CTR and sh-RasGRF2 (Fig 22). As previously reported, the levels of GABA are increased in the SNr of dyskinetic LV-CTR mice after L-DOPA challenge (9 mg/kg plus 12 mg/kg benserazide, i.p.) reaching the maximum value (~3-fold over basal) at 100 min (Fig. 23A) and prevented the rise of GABA in SNr when co-administered with L-DOPA (Fig. 23A). L-DOPA and amantadine, did not affect GLU levels in SNr when administered alone or in combination (Fig. 23B). L-DOPA, amantadine and their combination did not cause changes in amino acid levels in GP (Fig. 23C,D). Similarly, in sh-RasGRF2 mice LID expression followed by L-DOPA injection coincided with the increase of GABA levels in SNr (~3-fold over basal) at 80min (Fig. 24A). The co-administration of amantadine prevented the rise of GABA in SNr when co-administered with L-DOPA (Fig. 24A). L-DOPA and amantadine, did not affect glutamate levels in SNr when administered alone or in combination (Fig. 24B). L-DOPA, amantadine and their combination did not cause changes in amino acid levels in GP (Fig. 24 C,D).

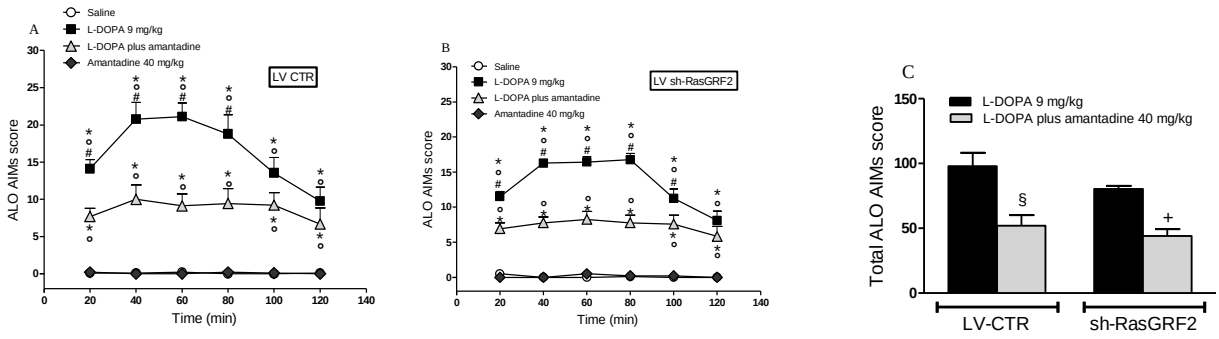

Fig. 22 Behavioral effect of L-DOPA and amantadine in dyskinetic mice undergoing microdialysis. Dyskinetic mice underwent surgery for microdialysis probe implantation, and were challenged with L-DOPA alone or in combination with amantadine (40 mg/kg; i.p., 1 h in advance) 24 h later. Control mice were treated with either amantadine or saline alone. ALO AIMs were scored every 20 min over 120 min after L-DOPA administration. Temporal profiles of AIMs taken as a whole (ALO AIMs; A,B) or as sum of AIMs for overall the time period of observation (cumulative ALO AIMs; C) are shown. Data are expressed as arbitrary units (see Results section) and are mean ± SEM of 5–8 animals. Panel A: significant effect of treatment ($F_{3,192} = 202.8$, $p < 0.001$), time ($F_{5,192} = 4.40$, $p < 0.001$) and time x treatment interaction ($F_{15,192} = 2.65$, $p = 0.001$), according to two-way RM ANOVA followed by contrast analysis and the sequentially rejective Bonferroni's test. Panel B: significant effect of treatment ($F_{3,264} = 425.60$, $p < 0.001$), time ($F_{5,264} = 8.58$, $p < 0.001$) and time x treatment interaction ($F_{15,264} = 5.10$, $p < 0.001$), according to two-way RM ANOVA followed by contrast analysis and the sequentially rejective Bonferroni's test. Panel C: significant effect of amantadine treatment ($F_{3,38} = 14.45$, $p < 0.001$), according to one-way ANOVA followed by contrast analysis and the sequentially rejective Bonferroni's test. *$p < 0.05$ versus saline, °$p < 0.05$ versus amantadine, $^{\#}p < 0.05$ versus L-DOPA plus amantadine, $^{\S}p<0.05$ versus L-DOPA-injected LV-CTR mice, $^{+}p<0.05$ versus L-DOPA-injected sh-RasGRF2 mice

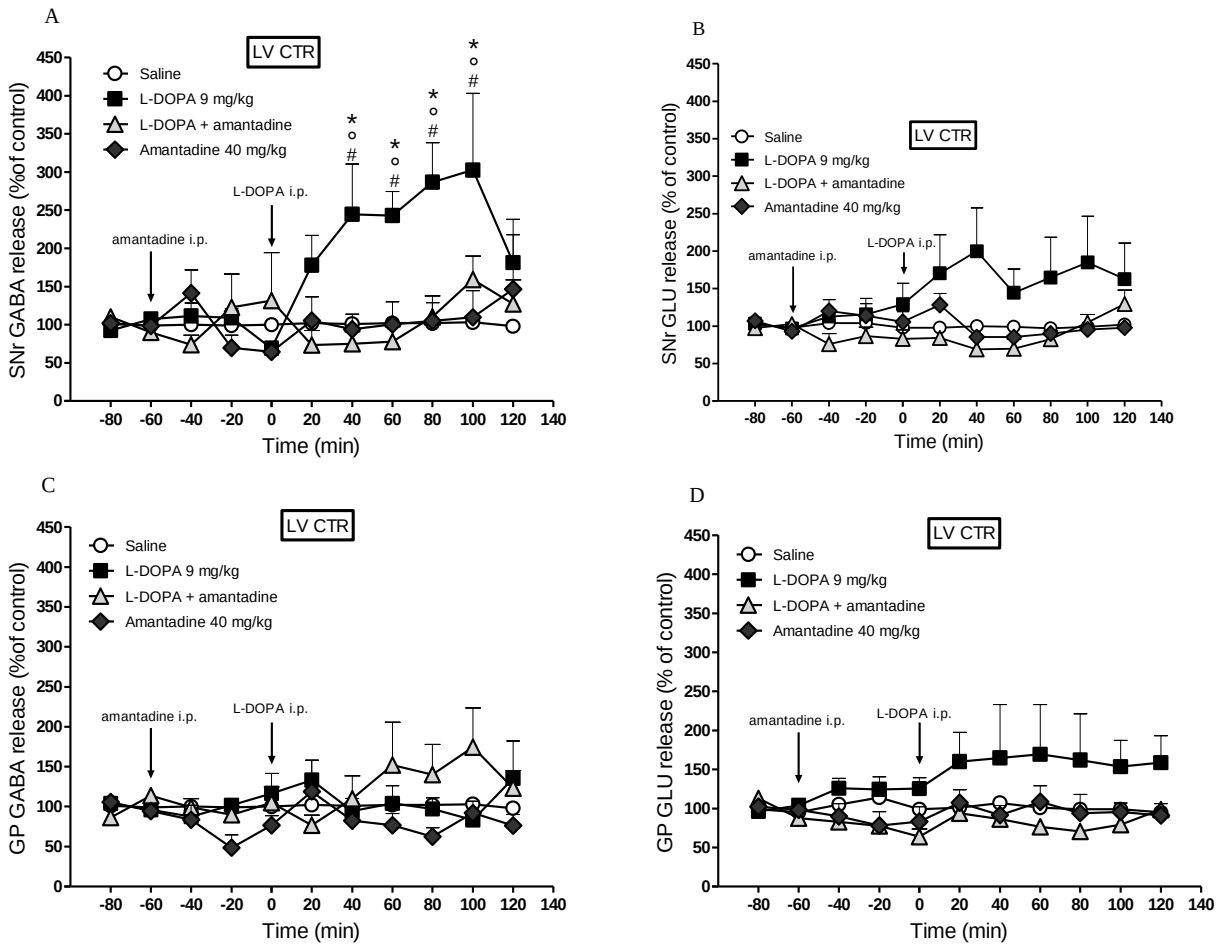

Fig. 23 Neurochemical effects of L-DOPA and amantadine in dyskinetic LV-CTR mice undergoing microdialysis. Dyskinetic mice were implanted with one probe in the lesioned SNr (A, B) and another in ipsilateral GP (C, D). Twenty-four hours later, rats received an acute challenge with L-DOPA alone (9 mg/kg plus 12 mg/kg benserazide, i.p.) or in combination with amantadine (40 mg/kg; i.p., 1 h in advance), and GABA (A, C) and GLU (B, D) levels were monitored for 120 min. Data are expressed as percentage of basal pre-treatment levels (calculated as the mean of the two samples preceding the treatment) and are mean ± SEM of 4–10 animals. Basal dialysate levels of GABA and GLU were 4.4 ± 0.7 and 25.7 ± 5.4 nM, respectively, in SNr, and 5.9 ± 0.8 and 23.0 ± 3.2, respectively, in GP. Panel A: significant effect of treatment ($F_{3,187} = 11.27$, $p < 0.001$), time ($F_{10,187} = 1.90$, $p = 0.046$) and time x treatment interaction ($F_{30,187} = 1.55$, $p = 0.041$) according to two-way RM ANOVA followed by contrast analysis and the sequentially rejective Bonferroni's test. *$p < 0.05$ versus saline, °$p < 0.05$ versus amantadine, $^{\#}p < 0.05$ versus L-DOPA plus amantadine.

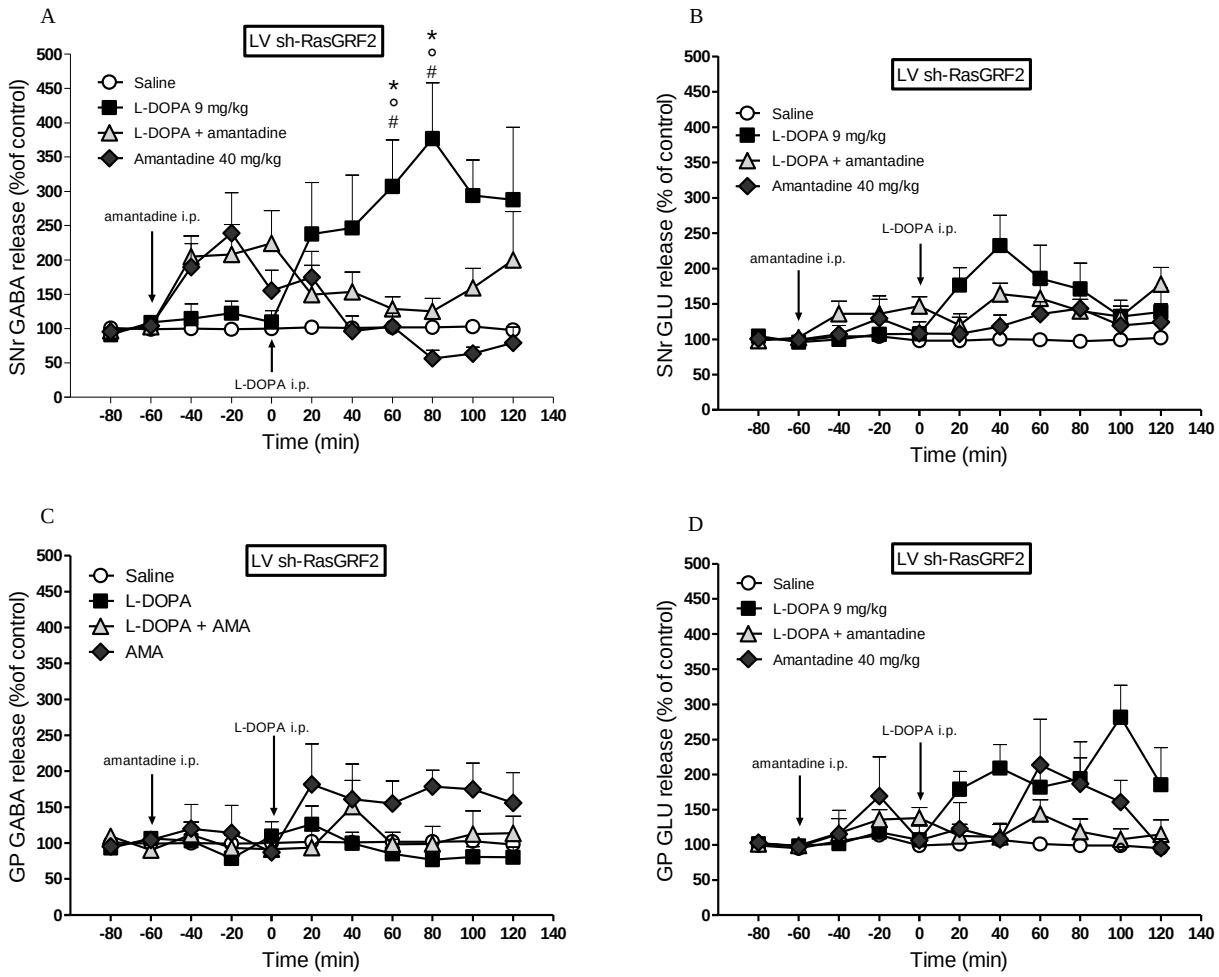

Fig. 24 Neurochemical effects of L-DOPA and amantadine in dyskinetic sh-RasGRF2 mice undergoing microdialysis. Dyskinetic mice were implanted with one probe in the lesioned SNr (A, B) and another in ipsilateral GP (C, D). Twenty-four hours later, rats received an acute challenge with L-DOPA alone (9 mg/kg plus 12 mg/kg benserazide, i.p.) or in combination with amantadine (40 mg/kg; i.p., 1 h in advance), and GABA (A, C) and GLU (B, D) levels were monitored for 120 min. Data are expressed as percentage of basal pre-treatment levels (calculated as the mean of the two samples preceding the treatment) and are mean ± SEM of 4–10 animals. Basal dialysate levels of GABA and GLU were 2.9 ± 0.2 and 14.5 ± 1.3 nM, respectively, in SNr, and 4.2 ± 0.4 and 26.6 ± 8.4, respectively, in GP. Panel A: significant effect of treatment ($F_{3,286} = 12.46$, $p < 0.001$) and time X treatment interaction ($F_{30,286} = 2.24$, $p < 0.001$) according to two-way RM ANOVA followed by contrast analysis and the sequentially rejective Bonferroni's test. *$p < 0.05$ versus saline, °$p < 0.05$ versus amantadine, $^{\#}p < 0.05$ versus L-DOPA plus amantadine.

Discussion

Part 1

Validation of the hemi-parkinsonian mouse model of LID provided a unique tool in dyskinesia research because it allows for the comparison of different species to antidyskinetic treatments. Moreover the mouse model is suitable to genetic manipulation, a strategic tool for target validation. The motor impairments observed in striatally lesioned hemi-parkinsonian mice had a dopaminergic origin because these mice showed a marked reduction of striatal TH terminals associated with motor recovery in response to L-DOPA (Lundblad et al., 2004). In our hands, recovery from akinesia and bradykinesia (Fig. 1A,B) was obtained at the same dose effective in MPTP-treated mice (10 mg/kg; Viaro et al., 2008), although at variance with this model, L-DOPA could not rescue rotarod performance (Fig. 1C). However, the rotarod test is a test for gross motor ability, which integrates motor and non-motor parameters (Rozas et al., 1997), and therefore involves not only the dorsal motor but also the limbic striatum and other structures outside the basal ganglia (e.g. peduncolo pontine nucleus and brainstem; Nauta et al., 1978; Christoph et al. 1986; Braak et al., 2000). The lack of response of the rotarod performance to L-DOPA may thus be related to the recruitment of dopaminergic areas less or not affected by intrastriatal 6-OHDA, in which post-synaptic DA receptor up-regulation has not fully developed.

Axial, limb and orolingual AIMs gradually developed during chronic treatment with L-DOPA, showing maximal expression after 5 days of treatment (Fig. 2A,B). This may reflect the homogeneity of the lesion within the dorsolateral striatum, because this region receives somatotopic cortical projections representing trunk, forepaw and orofacial muscles (McGeorge and Faull, 1989).

Microdialysis setting did not influence the acute response to L-DOPA because, in line with previous studies (Lundblad et al., 2004; Santini et al., 2007), AIMs were already maximal 20 min after L DOPA administration and tended to disappear after 120 min (Fig 3A-D) Moreover, the overall response to L-DOPA recorded in the dialysis setting (i.e. after probe implantation) was not different from that observed in the same animal before surgery (Fig. 8). The anti-dyskinetic effect of amantadine was also quantitatively similar in rats under the two different conditions (Fig. 8).

In keeping with that found in the rat (see also Mela et al., 2007), L-DOPA caused a rise in GABA levels in the mouse SNr (Fig.4A). Major sources of neuronal GABA levels in SNr are the striato-nigral and the pallido nigral projections as well as GABA interneurons and collaterals of nigrofugal GABAergic neurons. Therefore, elevation of GABA levels might be related to activation of the direct striato-nigral pathway, leading to GABA receptor-mediated overinhibition of nigro-thalamic neurons and thalamic disinhibition (Deniau and Chevalier, 1985). The concomitant lack of significant changes of GABA (and glutamate) levels in GP seems to exclude a contribution of the indirect pathway (Fig. 4C,D). This is in line with a study showing that DARPP-32 knockdown in striato-nigral neurons abolished dyskinesia whereas the same procedure in striato-pallidal neurons was ineffective (Bateup et al., 2010). The increase in nigral GABA has been completely replicable in mouse and rat, and in different experimental groups of animal (see also *part 2/3*) suggesting it can be used as a neurochemical marker of LID. A temporal mismatch was found between the behavioral and neurochemical responses in mice, the rise in nigral GABA being more gradual and prolonged compared with AIMs expression. As no such mismatch was observed in the rat, the lower perfusion rate through the mouse probe might be the cause for the delay of the neurochemical response. In contrast, however, we found that under the same microdialysis conditions nigral glutamate levels closely matched the rapid (20 min) reduction of immobility time induced by administration of a nociceptin/orphanin FQ receptor antagonist in mice (Mabrouk et al., 2010; Volta et al., 2010). Interestingly enough, in the same studies changes in GABA levels were delayed compared with those of glutamate. Therefore, the temporal dissociation observed in the mouse may reflect differences in intrinsic (e.g. uptake efficiency) mechanisms regulating extracellular GABA concentrations. Alternatively, we have to consider the possibility that elevation of nigral GABA may not be the only trigger for dyskinesia. In support of this view, reverse dialysis of GABA alone in SNr failed to evoke AIMs (Buck et al., 2010). The mechanisms underlying the dual effect of amantadine, used both as anti-parkinsonian and anti-dyskinetic in combination with L-DOPA are not completely understood, also because amantadine has a complex pharmacodynamic profile. It inhibits DA reuptake (Heikkila and Cohen, 1972; Mizoguchi et al., 1994) and increases DOPA decarboxyalase activity (Fisher et al. 1998; Deep et al. 1999). Amantadine also behaves as an antagonist at NMDA receptors (Kornhuber et al., 1991; Parsons et al., 1996), where it acts by stabilizing the

"closed" state of the channel (Blanpied et al., 2005). Finally, it inhibits K^+ channels in the atria in a similar way to 4-aminopyridine, an action resulting in an increase of membrane excitability (Northover, 1994). The mild antiparkinsonian effect of amantadine has been related to its dopaminergic actions, in particular to the ability to potentiate the L-DOPA-induced elevation of striatal DA release (Arai et al., 2003). However, this effect is difficult to reconcile with its anti-dyskinetic action because a potentiation of the L-DOPA- induced DA release would also lead to stimulation of D1R on the striatal cell bodies and nigral terminals of striato-nigral GABA neurons, thereby promoting LID. Interestingly, the potentiation of the L-DOPA-induced striatal DA release (Sarre et al., 2008) and the mild anti-parkinsonian effect (Loschmann et al., 2004) of amantadine are shared by NR2B receptor antagonists. In addition, we showed that the NR2B antagonist Ro25–6981 slightly reduced AIMs expression (maximally of ~25% at 5 mg/kg) in 6-OHDA hemi-lesioned dyskinetic rats (Mela et al., 2010). However, given the mild and inconsistent (see Rylander et al., 2009) effect of Ro25–6981 in dyskinetic rats, it is unlikely that NR2B blockade represents the only mechanism underlying the anti-dyskinetic effect of amantadine. This might suggest that the amantadine profile is different from that of a selective NR2B antagonist. Indeed, amantadine does not display NMDA subtype receptor selectivity (Danysz et al., 1997). As dysfunction of glutamate transmission is associated with LID (Calabresi et al., 2000; Oh and Chase, 2002), reduction of striatal glutamatergic signal may result in an anti-dyskinetic effect. The data provided in this part of the study support the view that peak-dose dyskinesia involves activation of the striato-nigral GABA pathway in both dyskinetic rats and mice, and that amantadine opposes this effect likely via interaction with striatal NMDA receptors. Minor neurochemical differences in the response to L-DOPA and amantadine were observed between the two models, which do not appear to shape the behavioral response. Overall, this study proves the feasibility of a combined behavioral and neurochemical analysis of the dyskinetic mouse, and the consistency of the neurochemical and behavioral response to L-DOPA and amantadine among species.

One of the most intriguing evidences findings from this part of the study is that, even if amantadine prevented the rise in nigral GABA it could not completely block AIMs appearance. Larger increases in extracellular DA levels have been demonstrated in the SNr (and striatum) of dyskinetic compared with non-dyskinetic rats following L-DOPA administration (Lindgren et al.,

2010). This suggests that nigral DA might play a role in triggering dyskinesia, via direct modulation of different DA receptor expressed by nigro-thalamic neurons (Zhou et al., 2009) or through the release of other neurotransmitters acting on the nigral output. To dissect the role of different DA receptors in striatum and SNr in LID expression, we planned the experiments described in *Part 2.*

Part 2

The contribution of DA receptor subtypes to LID and the underlying mechanisms have been evaluated performing reverse dialysis of DA selective antagonists in striatum and SNr of dyskinetic rats.

Striatal perfusion of D1R or D2R antagonists provided neuroanatomical information about the site from which D1R mediate the dyskinetic behaviors, showing that both LID manifestation and the accompanying rise in nigral GABA and glutamate release are significantly attenuated by intrastriatal perfusion with SCH23390 (Fig. 10C,D). The possibility that the action of SCH23390 extends beyond D1R should also be considered. Indeed, SCH23390 binds to D1-like receptors (0.3–1.3 nM; Hyttel, 1983; Millan et al., 2001) and with lower affinity to 5-HT2c (previously known as 5- HT1c; 15–30 nM; Hyttel, 1983; Millan et al., 2001), 5-HT4 (270 nM; Schiavi et al., 1994) receptors as well as to the 5-HT transporter (1,400 nM; Zarrindast et al., 2011). Assuming a ~10% in vivo recovery under the present experimental conditions, the perfusion of 1 µM SCH23390 through the microdialysis probe is expected to generate striatal extracellular levels of ~100 nM, for which significant binding to 5-HT2c receptors in addition to D1R may occur. However, a contribution of 5-HT2c receptors in the antidyskinetic effect of intrastriatal SCH23390 is unlikely since striatal 5-HT2c receptors do not interfere with the hyperlocomotion induced by injection of a D1R agonists in the DA-depleted striatum of 6-OHDA lesioned rats (Bishop et al., 2005). Moreover, SCH23390 activates 5-HT2c receptors (Millan et al., 2001), which would result in a worsening rather than attenuation of dyskinesia, indeed, 5-HT2c receptor stimulation induced orofacial dyskinesia (Beyeler et al., 2010) whereas 5-HT2c receptor blockade attenuated neuroleptic-induced dyskinesia (Creed-Carson et al., 2011). Therefore, although binding to striatal 5-HT2c receptors may occur during intrastriatal perfusion with SCH23390, these receptors are not likely to contribute to the antidyskinetic effect of SCH23390. In addition The concomitant lack of significant changes in GABA (and glutamate) levels in GP

during the expression of LID (Mela et al., 2007) rules out a contribution of the indirect pathway to the neurochemical alterations measured in the SNr. As seen in *part 1*, the surge of nigral glutamate levels exclusive in rat model (absent in the mouse model) of LID is likely to reflect an increased glutamatergic input from a cortically-activated subthalamic nucleus and/or may depend on the overactivation of the direct pathway.

Different from SCH23390, intrastriatal raclopride failed to affect LID (Fig. 9) and the accompanying nigral amino acid response (Fig. 11). Raclopride affinity for D2 and D3 receptors is 1.8 and 3.5 nM respectively (Seeman and Van Tol, 1994). Therefore the 1 μM raclopride concentration in the perfusate is expected to generate extracellular concentrations (~100 nM) which largely cover D2-like receptors without unspecifically interfering with other receptors (Kohler et al., 1985). This data rules out a major role for striatal D2R in dyskinesia, and is consistent with the findings that systemic D2R agonists do not activate the ERK pathway in striatal neurons, a molecular marker of LID (Westin et al., 2007) and that genetic deletion of the D2R gene does not affect LID in mice (Darmopil et al., 2009). Despite the existence of a well-documented opposite D1–D2 receptor modulation of striatal GABAergic function (Cepeda and Levine, 1998; Harsing and Zigmond, 1997; Hernandez-Lopez et al., 1997; Morari et al., 1994), the inconsistent effects of striatal raclopride infusion in this study may indicate that striatal D2R do not significantly affect the L-DOPA-induced activation of already primed striato-nigral neurons, possibly confirming the morphological and functional segregation of D1 and D2 receptors along striatal output pathways (Gerfen et al., 1990).

This study showed also that both D1R and D2R blockade in SNr is able to attenuate LID expression. This confirms the role of this brain area in generating dyskinesia as emerged from previous studies. Indeed, L-DOPA is converted to DA in SNr (Sarre et al., 1998), and L-DOPA administration results in abnormal elevations of extracellular DA levels in both the SNr and striatum of dyskinetic rats (Lindgren et al., 2010). Moreover, dyskinesia is associated with abnormal oscillatory activity in the theta/alpha band of nigral neurons (Meissner et al., 2006) as well as with angiogenesis in nigral microvasculature (Westin et al., 2006). In keeping with the finding that nigral D1R mediate the contralateral turning induced by L-DOPA in hemi-lesioned rats (Robertson et al., 1989), intranigral SCH23390 attenuated LID (Fig. 12) and the accompanying rise of nigral GABA levels (Fig. 13C). D1R are largely expressed on striato-nigral

GABAergic afferents, their activation resulting in an increase of GABA release, overinhibition of nigro-thalamic neurons and motor initiation. Interestingly, similar to the situation in the striatum, D1 receptor signaling appears to be up-regulated in the SNr, leading to an enhancement of agonist stimulated [3H]-GABA release in nigral slices (Rangel-Barajas et al., 2011). Therefore, by opposing a phasic D1R activation by L-DOPA, nigral SCH23390 infusion attenuates both the GABAergic inhibition of nigro-thalamic neurons and dyskinesia. In addition, SCH23390 also elevated basal GABA levels in SNr. This finding can be differently interpreted since microdialysis samples different GABA pools, which can be differentially affected by local treatment. Therefore, the increase in basal GABA levels may indicate the existence of a DA inhibitory tone on GABA release mediated by D1R located on GABA interneurons or reflect disinhibition of nigro-thalamic GABA neurons, which have extensive axon collaterals ramifying in SNr (Grofova et al., 1982). This latter possibility is further substantiated by the findings that SCH23390 application in vitro attenuates GABA-mediated IPSP in nigro-thalamic neurons (Aceves et al., 2011; Radnikow and Misgeld, 1998) and systemic SCH23390 administration increases the discharge rate of nigro-thalamic neurons in vivo (Windels and Kiyatkin, 2006). Alternatively, SCH23390 may impact on 5-HT2c receptors.

Indeed, stimulation of nigral 5-HT2c receptors elevated GABA release and excited nigral GABA neurons in vivo (Di Giovanni et al., 2001; Invernizzi et al., 2007) an action that may be consistent with motor inhibition (Kennett and Curzon, 1988). Consistently, intranigral infusion of 5-HT2c receptor antagonists induced contralateral rotations and potentiated the turning behavior induced by DA agonists in unilateral 6-OHDA lesioned rats (Fox et al., 1998). Similar to SCH23390, intranigral raclopride attenuated expression of limb and axial dyskinesia. This suggests that nigral D2R contribute to LID, and that nigral but not striatal D2R may mediate the antidyskinetic effect of D2 antagonists when given systemically. Differently from SCH23390, the antidyskinetic effect of intranigral raclopride was not accompanied by changes of the GABA surge induced by L-DOPA, possibly suggesting it did not involve modulation of the striato-nigral pathway. This is in line with the finding that D2R ligands modulate GABA release from pallido-nigral but not striato-nigral terminals, in keeping with the view of a segregation of D2/D3/D4 and D1R on afferent projections from GP and striatum, respectively (Aceves et al., 2011). It should be emphasized that intranigral raclopride produced dramatic preconditioning effect on

basal ganglia circuitry, reducing nigral GABA and elevating striatal GABA and glutamate levels (Fig. 14A,B). It is not clear how these changes impact on the striatal output. However, it seems unlikely that changes in striatal amino acids contribute to the antidyskinetic effect of raclopride since the nigral amino acid response to L-DOPA was not altered (Fig. 14C,D). Instead, raclopride might act through setting the responsiveness of nigro-thalamic neurons to L-DOPA (Volta et al., 2011). Blockade of an inhibitory D2-mediated tone on pallido-nigral terminals would alter the activity of nigro-thalamic neurons (Aceves et al., 2011). This would lead to disinhibition of thalamo-striatal and/or thalamo-cortical glutamate projections, which is in line with the observed elevation of amino acid release in striatum(see also Morari et al., 1996b). Activation of the cortico- and/or thalamo- striatal glutamate inputs may enrich the otherwise negligible neuronal component of basal extracellular glutamate levels (Baker et al., 2002; Morari et al., 1993; Morari et al., 1996b) and allow a facilitatory action of L-DOPA to be unraveled.

AIMs expression appears to be mediated by intrastriatal and to a lesser extent, intranigral D1R, likely through activation of the striato-nigral pathway and stimulation of GABA release from striato-nigral terminals. A contribution of nigral D2R was also demonstrated, although the mechanisms remain elusive. In line with these evidences in the *part 3* we try to disclose the possible neurochemical mechanism underlying the anti-dyskinetic effect of amantadine using specific inhibitors carried by lentiviral vectors.

Part 3

The contribution of striatal MAP kinases cascade in the development of LID has been documented (Matamales and Girault, 2011). As this pathway is deeply involved in learning process, we focused our attention on enzymes belonging to the family of RasGEF, RasGRF1 and RasGRF2, both implicated in synaptic plasticity (Brambilla et al., 1997; Orban et al., 1999).

Previous studies have determined the location of RasGRF1 in the striatum (Brambilla et al., 1997; Giese et al., 2001; Fasano and Brambilla, 2002) and its regulation by dopaminergic stimuli (Zhang et al., 2007; Fasano et al., 2009; Parelkar et al., 2009). In particular, cocaine and amphetamine are capable of increasing the expression of the RasGRF1 protein in striatum, indicating that it contributes to the modifications of long-term synaptic plasticity, which requires the de novo synthesis of proteins (Zhang et al., 2007; Parelkar et al., 2009).

Subsequently, Fasano and collaborators demonstrated that RasGRF1 controls the activation of ERK (Fasano et al., 2009), and that animals lacking the isoform 1 of RasGRF1 develop less severe LID compared to control animals chronically treated with L-DOPA (Fasano et al., 2010). It is likely that RasGRF1 exerts its effects on the MAP kinase cascade through the physical interaction with NR2B subunit containing NMDARs. This interaction leads to NMDAR activation which is followed by Ca^{++} influx through the channel and activation of ERK pathway (Krapivinsky et al., 2003). Conversely there are no published data on the role of RasGRF2 in striatum. A possible role is envisaged since RasGRF2 is known to be involved in learning process taking place in hippocampus through NR2A signal (Jin and Feig, 2010). This evidence prompted us to verify whether the specific inhibition of striatal RasGRF1 or RasGRF2 was the determining factor in reducing LID. Moreover we took advantage of the selective inhibition of striatal RasGRF1 or RasGRF2 to disclose a novel mechanism of action of amantadine. Due to the lack of selective pharmacological tools, we used lentiviral vectors (provided by Dr. Brambilla's research group) carrying a short hairpin RNA, to achieve the selective inhibition of striatal RasGRF1 and RasGRF2. LVs expressing sh-RasGRF1, sh-RasGRF2 or LV-CTR (as control group) were microinjected (at the laboratories of Dr Brambilla) in the dorsolateral striatum of hemi-parkinsonian mice.

To verify whether Sh-RasGRF1 and sh-RasGRF2 blockade could affect the motor function in 6-OHDA hemi-lesioned mice, we investigated the motor phenotypes of Sh-RasGRF1 and sh-RasGRF2 injected mice two weeks after lesion. Moreover, since the RasGEFs are involved in the learning process we evaluated whether could affect motor performance over repeated testing. No differences in motor performance were observed among the different experimental groups either the first or the fifth day of repeated testing (training; Fig. 15, 20). Therefore we can conclude that the selective inhibition of striatal RasGRF1 and RasGRF2 do not affect the motor component of parkinsonism and preserve the ability of the animal to adapt to experimental tasks.

Sh-RasGRF1 mice treated with escalating doses of L-DOPA (3, 6, 9 mg/kg i.p.) for 9 days, showed a ~50% attenuation of LID throughout the period of treatment (Fig. 16). The antidyskinetic effect is consistent with that observed by Fasano and colleagues in the RasGRF1 knockout mouse (Fasano et al., 2010). Such reduction can be ascribed to the inhibitory effect on the MAP

kinase pathway, interfering with the priming process underlying LID expression (Fasano et al., 2010; Santini et al., 2010). To determine how blockade of RasGRF1 is able to reduce LID development, electrophysiological studies on cortico-striatal synaptic plasticity are needed, along with biochemical experiments to study of the expression of LID related genes (Cenci et al., 1998; Cenci, 2002; Lundblad et al., 2004). Different from sh-RasGRF1, Sh-RasGRF2 injected mice did not show significant differences from LV-CTR in LID severity. This rules out the role of this GEF in LID development.

Another important difference between sh-RasGRF1 and sh-RasGRF2 mice was the response to amantadine. Indeed, we investigated whether sh-RasGRF1 and sh-RasGRF2 blockade could produced additive attenuation of LID. Surprisingly, amantadine was ineffective in sh-RasGRF1 mice (Fig. 17B) but maintained its efficacy in sh-RasGRF2 mice. The lack of an additive effect with RasGRF1 blockade could indicate a possible common pathway between the two approaches. A possible site of action is represented by the NMDAR. Indeed, amantadine is able to block NMDA receptors (Blanpied et al., 2005) while RasGRF1 is physically linked to the NR2B subunit (Krapivinsky et al., 2003; Fasano et al., 2009). Therefore, we might speculate that both amantadine and rasGRF1 blockade act on the NMDA-NR2B receptor.

The results obtained from the analysis of GABA levels in SNr correlate well with the behavioral analysis, also supporting the existence of an interaction between amantadine and sh-RasGRF1 blockade. In LV CTR mice, the expression of LID is accompanied by a strong increase of GABA levels in SNr (Fig. 18A), while the antidyskinetic effect of amantadine (~50% reduction of LID) was associated with the lack of the GABA rise in SNr (Fig. 18A). Likewise, no increase of nigral GABA was observed in sh-RasGRF1 injected mice after L-DOPA challenge (Fig. 19A). The results suggest that both amantadine and sh-RasGRF1 exert their anti-dyskinetic effect through inhibition of the striato-nigral GABA neurons (i.e the direct pathway), which are activated by L-DOPA through D1 receptors, an event that requires endogenous glutamate.

Sh-RasGRF2 mice did not show any significant attenuation in LID development compared to LV-CTR (Fig. 21), and maintained their responsiveness to amantadine (Fig. 22). Sh-RasGRF2 mice subjected to microdialysis also displayed the same degree of LID in response to L-DOPA with respect to control animals (Fig 22). Consistently, the neurochemical pattern of sh-RasGRF2

animals was similar to LV-CTR (Fig. 23, 24), and amantadine was able to prevent the GABA rise in SNr (Fig. 24A).

There is no evidence that RasGRF2 controls striatal function, but it is well known that it plays important roles in long-lasting increase in synaptic efficiency (LTP) in hippocampus (Li et al., 2006). Studies on RasGRF2 KO mice demonstrated that NR2A receptors induce LTP through RasGRF2 in hippocampus (Jin and Feig, 2010). These studies also suggest that NR2B-containing receptors induce LTD through RasGRF1 (Li et al., 2006). We could therefore speculate that the different effect of RasGRF1 and RasGRF2 blockade on LID is due to a preferential interference with the NR2B and NR2A receptors. Microdialysis studies conducted by Fantin and colleagues have shown a possible functional segregation of NR2A and NR2B subunits along the striato-pallidal and striato-nigral, respectively (Fantin et al., 2008). According to these data, the failure of RasGRF2 blockade to prevent dyskinesia might be in line with the lack of involvement of the indirect pathway in LID expression (see part 1). This hypothesis is however might be contradicted by a recent paper of Gardoni and collaborators showing that chronic administration of a synthetic peptide targeted to NR2A (TAT2A) attenuates the priming to L-DOPA in rats, being however ineffective once dyskinesia has been established (Gardoni et al., 2012).

Concluding Remarks

The results obtained can be summarized as follows:

i) A comparative neurochemical and behavioral study in the mouse and rat models of dyskinesia revealed that AIMs appearance in response to L-DOPA challenge is accompanied by an increase of GABA release in SNr but not GP. Amantadine attenuated about to the same extent the severity of dyskinesia in dyskinetic rats and mice, preventing the accompanying surge in nigral GABA. These data provide strong neurochemical support to the view that peak-dose dyskinesia involves activation of the striato-nigral GABA pathway, and that amantadine opposes this effect likely by modulating this pathway. However, amantadine only attenuated by 50% the severity of LID in face of a suppression of the increase of nigral GABA, suggesting that other neurotransmitters/circuits are involved. This study also demonstrates the feasibility of a combined behavioral and neurochemical analysis of the dyskinetic mouse, and the consistency of the neurochemical and behavioral response to L-DOPA and amantadine among species.

ii) Regional perfusion with selective D1 and D2 receptor antagonists allowed to demonstrate that AIMs expression is differentially mediated by intrastriatal and to a lesser extent, intranigral, D1R and D2R. These data confirm the role of the striato-nigral direct pathway in LID, showing at the same time the role of extrastriatal areas.

iii) Blockade of Ras-GRF1 but not Ras-GRF2 reduced dyskinesia and its neurochemical correlate (increase in nigral GABA) in mice. Ras-GRF1 blockade interferes with the antidyskinetic effect of amantadine as this drug is ineffective in sh-Ras-GRF1 injected mice (but not sh-Ras-GRF2 mice). The data suggest that blockade of Ras-GRF1 and amantadine act on a common pathway, possibly the NR2B receptor, and point to rasGRF1 as a novel target in LID therapy.

References

Aceves JJ, Rueda-Orozco PE, Hernandez-Martinez R, Galarraga E, Bargas J (Bidirectional plasticity in striatonigral synapses: a switch to balance direct and indirect basal ganglia pathways. Learn Mem 18:764-773.2011).

Albin RL, Young AB, Penney JB (The functional anatomy of basal ganglia disorders. Trends Neurosci 12:366-375.1989).

Alexander GE, Crutcher MD, DeLong MR (Basal ganglia-thalamocortical circuits: parallel substrates for motor, oculomotor, "prefrontal" and "limbic" functions. Prog Brain Res 85:119-146.1990).

Alexander GE, DeLong MR, Strick PL (Parallel organization of functionally segregated circuits linking basal ganglia and cortex. Annu Rev Neurosci 9:357-381.1986).

Andersson M, Hilbertson A, Cenci MA (Striatal fosB expression is causally linked with l-DOPA-induced abnormal involuntary movements and the associated upregulation of striatal prodynorphin mRNA in a rat model of Parkinson's disease. Neurobiol Dis 6:461-474.1999).

Andersson M, Westin JE, Cenci MA (Time course of striatal DeltaFosB-like immunoreactivity and prodynorphin mRNA levels after discontinuation of chronic dopaminomimetic treatment. Eur J Neurosci 17:661-666.2003).

Arai A, Kannari K, Shen H, Maeda T, Suda T, Matsunaga M (Amantadine increases L-DOPA-derived extracellular dopamine in the striatum of 6-hydroxydopamine-lesioned rats. Brain Res 972:229-234.2003).

Aubert I, Ghorayeb I, Normand E, Bloch B (Phenotypical characterization of the neurons expressing the D1 and D2 dopamine receptors in the monkey striatum. J Comp Neurol 418:22-32.2000).

Baker DA, Xi ZX, Shen H, Swanson CJ, Kalivas PW (The origin and neuronal function of in vivo nonsynaptic glutamate. J Neurosci 22:9134-9141.2002).

Bateup HS, Santini E, Shen W, Birnbaum S, Valjent E, Surmeier DJ, Fisone G, Nestler EJ, Greengard P (Distinct subclasses of medium spiny neurons differentially regulate striatal motor behaviors. Proc Natl Acad Sci U S A 107:14845-14850.2010).

Beaulieu JM, Del'guidice T, Sotnikova TD, Lemasson M, Gainetdinov RR (Beyond cAMP: The Regulation of Akt and GSK3 by Dopamine Receptors. Front Mol Neurosci 4:38.2011).

Berthet A, Porras G, Doudnikoff E, Stark H, Cador M, Bezard E, Bloch B (Pharmacological analysis demonstrates dramatic alteration of D1 dopamine receptor neuronal distribution in the rat analog of L-DOPA-induced dyskinesia. J Neurosci 29:4829-4835.2009).

Beurrier C, Lopez S, Revy D, Selvam C, Goudet C, Lherondel M, Gubellini P, Kerkerian-LeGoff L, Acher F, Pin JP, Amalric M (Electrophysiological and behavioral evidence that modulation of metabotropic glutamate receptor 4 with a new agonist reverses experimental parkinsonism. FASEB J 23:3619-3628.2009).

Bevan MD, Atherton JF, Baufreton J (Cellular principles underlying normal and pathological activity in the subthalamic nucleus. Curr Opin Neurobiol 16:621-628.2006).

Beyeler A, Kadiri N, Navailles S, Boujema MB, Gonon F, Moine CL, Gross C, De Deurwaerdere P (Stimulation of serotonin2C receptors elicits abnormal oral movements by acting on pathways other than the sensorimotor one in the rat basal ganglia. Neuroscience 169:158-170.2010).

Bezard E, Gross CE, Qin L, Gurevich VV, Benovic JL, Gurevich EV (L-DOPA reverses the MPTP-induced elevation of the arrestin2 and GRK6 expression and enhanced ERK activation in monkey brain. Neurobiol Dis 18:323-335.2005).

Bibbiani F, Oh JD, Chase TN (Serotonin 5-HT1A agonist improves motor complications in rodent and primate parkinsonian models. Neurology 57:1829-1834.2001).

Bibbiani F, Oh JD, Kielaite A, Collins MA, Smith C, Chase TN (Combined blockade of AMPA and NMDA glutamate receptors reduces levodopa-induced motor complications in animal models of PD. Exp Neurol 196:422-429.2005).

Bishop C, Daut GS, Walker PD (Serotonin 5-HT2A but not 5-HT2C receptor antagonism reduces hyperlocomotor activity induced in dopamine-depleted rats by striatal administration of the D1 agonist SKF 82958. Neuropharmacology 49:350-358.2005).

Blanchet PJ, Konitsiotis S, Whittemore ER, Zhou ZL, Woodward RM, Chase TN (Differing effects of N-methyl-D-aspartate receptor subtype selective antagonists on dyskinesias in levodopa-treated 1-methyl-4-phenyl-tetrahydropyridine monkeys. J Pharmacol Exp Ther 290:1034-1040.1999).

Blanchet PJ, Metman LV, Chase TN (Renaissance of amantadine in the treatment of Parkinson's disease. Adv Neurol 91:251-257.2003).

Blanpied TA, Clarke RJ, Johnson JW (Amantadine inhibits NMDA receptors by accelerating channel closure during channel block. J Neurosci 25:3312-3322.2005).

Bonifati V, Fabrizio E, Cipriani R, Vanacore N, Meco G (Buspirone in levodopa-induced dyskinesias. Clin Neuropharmacol 17:73-82.1994).

Bordet R, Ridray S, Carboni S, Diaz J, Sokoloff P, Schwartz JC (Induction of dopamine D3 receptor expression as a mechanism of behavioral sensitization to levodopa. Proc Natl Acad Sci U S A 94:3363-3367.1997).

Braak H, Rub U, Sandmann-Keil D, Gai WP, de Vos RA, Jansen Steur EN, Arai K, Braak E (Parkinson's disease: affection of brain stem nuclei controlling premotor and motor neurons of the somatomotor system. Acta Neuropathol 99:489-495.2000).

Brambilla R, Gnesutta N, Minichiello L, White G, Roylance AJ, Herron CE, Ramsey M, Wolfer DP, Cestari V, Rossi-Arnaud C, Grant SG, Chapman PF, Lipp HP, Sturani E, Klein R (A role for the Ras signalling pathway in synaptic transmission and long-term memory. Nature 390:281-286.1997).

Buck K, Voehringer P, Ferger B (The alpha(2) adrenoceptor antagonist idazoxan alleviates L-DOPA-induced dyskinesia by reduction of striatal dopamine levels: an in vivo microdialysis study in 6-hydroxydopamine-lesioned rats. J Neurochem 112:444-452.2010).

Burnet PW, Eastwood SL, Lacey K, Harrison PJ (The distribution of 5-HT1A and 5-HT2A receptor mRNA in human brain. Brain Res 676:157-168.1995).

Calabresi P, Giacomini P, Centonze D, Bernardi G (Levodopa-induced dyskinesia: a pathological form of striatal synaptic plasticity? Ann Neurol 47:S60-68; discussion S68-69.2000).

Calabresi P, Pisani A, Mercuri NB, Bernardi G (Long-term Potentiation in the Striatum is Unmasked by Removing the Voltage-dependent Magnesium Block of NMDA Receptor Channels. Eur J Neurosci 4:929-935.1992).

Calon F, Morissette M, Ghribi O, Goulet M, Grondin R, Blanchet PJ, Bedard PJ, Di Paolo T (Alteration of glutamate receptors in the striatum of dyskinetic 1-methyl-4-phenyl-

1,2,3,6-tetrahydropyridine-treated monkeys following dopamine agonist treatment. Prog Neuropsychopharmacol Biol Psychiatry 26:127-138.2002).

Calon F, Rajput AH, Hornykiewicz O, Bedard PJ, Di Paolo T (Levodopa-induced motor complications are associated with alterations of glutamate receptors in Parkinson's disease. Neurobiol Dis 14:404-416.2003).

Carta M, Carlsson T, Kirik D, Bjorklund A (Dopamine released from 5-HT terminals is the cause of L-DOPA-induced dyskinesia in parkinsonian rats. Brain 130:1819-1833.2007).

Carta M, Lindgren HS, Lundblad M, Stancampiano R, Fadda F, Cenci MA (Role of striatal L-DOPA in the production of dyskinesia in 6-hydroxydopamine lesioned rats. J Neurochem 96:1718-1727.2006).

Castle M, Aymerich MS, Sanchez-Escobar C, Gonzalo N, Obeso JA, Lanciego JL (Thalamic innervation of the direct and indirect basal ganglia pathways in the rat: Ipsi- and contralateral projections. J Comp Neurol 483:143-153.2005).

Cenci MA (Transcription factors involved in the pathogenesis of L-DOPA-induced dyskinesia in a rat model of Parkinson's disease. Amino Acids 23:105-109.2002).

Cenci MA, Konradi C (Maladaptive striatal plasticity in L-DOPA-induced dyskinesia. Prog Brain Res 183:209-233.2010).

Cenci MA, Lee CS, Bjorklund A (L-DOPA-induced dyskinesia in the rat is associated with striatal overexpression of prodynorphin- and glutamic acid decarboxylase mRNA. Eur J Neurosci 10:2694-2706.1998).

Cenci MA, Lundblad M (Ratings of L-DOPA-induced dyskinesia in the unilateral 6-OHDA lesion model of Parkinson's disease in rats and mice. Curr Protoc Neurosci Chapter 9:Unit 9 25.2007).

Centonze D, Gubellini P, Picconi B, Calabresi P, Giacomini P, Bernardi G (Unilateral dopamine denervation blocks corticostriatal LTP. J Neurophysiol 82:3575-3579.1999).

Cepeda C, Levine MS (Dopamine and N-methyl-D-aspartate receptor interactions in the neostriatum. Dev Neurosci 20:1-18.1998).

Chase TN (Levodopa therapy: consequences of the nonphysiologic replacement of dopamine. Neurology 50:S17-25.1998).

Chase TN, Oh JD (Striatal dopamine- and glutamate-mediated dysregulation in experimental parkinsonism. Trends Neurosci 23:S86-91.2000).

Chatha BT, Bernard V, Streit P, Bolam JP (Synaptic localization of ionotropic glutamate receptors in the rat substantia nigra. Neuroscience 101:1037-1051.2000).

Chen BS, Roche KW (Regulation of NMDA receptors by phosphorylation. Neuropharmacology 53:362-368.2007).

Christoph GR, Leonzio RJ, Wilcox KS (Stimulation of the lateral habenula inhibits dopamine-containing neurons in the substantia nigra and ventral tegmental area of the rat. J Neurosci 6:613-619.1986).

Clarke NP, Bolam JP (Distribution of glutamate receptor subunits at neurochemically characterized synapses in the entopeduncular nucleus and subthalamic nucleus of the rat. J Comp Neurol 397:403-420.1998).

Cochran KW, Maassab HF, Tsunoda A, Berlin BS (Studies on the antiviral activity of amantadine hydrochloride. Ann N Y Acad Sci 130:432-439.1965).

Colzi A, Turner K, Lees AJ (Continuous subcutaneous waking day apomorphine in the long term treatment of levodopa induced interdose dyskinesias in Parkinson's disease. J Neurol Neurosurg Psychiatry 64:573-576.1998).

Conn PJ, Battaglia G, Marino MJ, Nicoletti F (Metabotropic glutamate receptors in the basal ganglia motor circuit. Nat Rev Neurosci 6:787-798.2005).

Corvol JC, Muriel MP, Valjent E, Feger J, Hanoun N, Girault JA, Hirsch EC, Herve D (Persistent increase in olfactory type G-protein alpha subunit levels may underlie D1 receptor functional hypersensitivity in Parkinson disease. J Neurosci 24:7007-7014.2004).

Cox H, Togasaki DM, Chen L, Langston JW, Di Monte DA, Quik M (The selective kappa-opioid receptor agonist U50,488 reduces L-dopa-induced dyskinesias but worsens parkinsonism in MPTP-treated primates. Exp Neurol 205:101-107.2007).

Creed-Carson M, Oraha A, Nobrega JN (Effects of 5-HT(2A) and 5-HT(2C) receptor antagonists on acute and chronic dyskinetic effects induced by haloperidol in rats. Behav Brain Res 219:273-279.2011).

Danysz W, Parsons CG, Kornhuber J, Schmidt WJ, Quack G (Aminoadamantanes as NMDA receptor antagonists and antiparkinsonian agents--preclinical studies. Neurosci Biobehav Rev 21:455-468.1997).

Darmopil S, Martin AB, De Diego IR, Ares S, Moratalla R (Genetic inactivation of dopamine D1 but not D2 receptors inhibits L-DOPA-induced dyskinesia and histone activation. Biol Psychiatry 66:603-613.2009).

Davies WL, Grunert RR, Haff RF, McGahen JW, Neumayer EM, Paulshock M, Watts JC, Wood TR, Hermann EC, Hoffmann CE (Antiviral Activity of 1-Adamantanamine (Amantadine). Science 144:862-863.1964).

Deep P, Dagher A, Sadikot A, Gjedde A, Cumming P (Stimulation of dopa decarboxylase activity in striatum of healthy human brain secondary to NMDA receptor antagonism with a low dose of amantadine. Synapse 34:313-318.1999).

Dekundy A, Gravius A, Hechenberger M, Pietraszek M, Nagel J, Tober C, van der Elst M, Mela F, Parsons CG, Danysz W (Pharmacological characterization of MRZ-8676, a novel negative allosteric modulator of subtype 5 metabotropic glutamate receptors (mGluR5): focus on L: -DOPA-induced dyskinesia. J Neural Transm 118:1703-1716.2011).

Dekundy A, Lundblad M, Danysz W, Cenci MA (Modulation of L-DOPA-induced abnormal involuntary movements by clinically tested compounds: further validation of the rat dyskinesia model. Behav Brain Res 179:76-89.2007).

Del Dotto P, Pavese N, Gambaccini G, Bernardini S, Metman LV, Chase TN, Bonuccelli U (Intravenous amantadine improves levadopa-induced dyskinesias: an acute double-blind placebo-controlled study. Mov Disord 16:515-520.2001).

DeLong MR (Primate models of movement disorders of basal ganglia origin. Trends Neurosci 13:281-285.1990).

Delwaide PJ, Sabbatino M, Delwaide C (Some pathophysiological aspects of the parkinsonian rigidity. J Neural Transm Suppl 22:129-139.1986).

Deniau JM, Chevalier G (Disinhibition as a basic process in the expression of striatal functions. II. The striato-nigral influence on thalamocortical cells of the ventromedial thalamic nucleus. Brain Res 334:227-233.1985).

Di Giovanni G, Di Matteo V, La Grutta V, Esposito E (m-Chlorophenylpiperazine excites non-dopaminergic neurons in the rat substantia nigra and ventral tegmental area by activating serotonin-2C receptors. Neuroscience 103:111-116.2001).

Dunah AW, Sirianni AC, Fienberg AA, Bastia E, Schwarzschild MA, Standaert DG (Dopamine D1-dependent trafficking of striatal N-methyl-D-aspartate glutamate receptors requires Fyn protein tyrosine kinase but not DARPP-32. Mol Pharmacol 65:121-129.2004).

Dunah AW, Wang Y, Yasuda RP, Kameyama K, Huganir RL, Wolfe BB, Standaert DG (Alterations in subunit expression, composition, and phosphorylation of striatal N-methyl-D-aspartate glutamate receptors in a rat 6-hydroxydopamine model of Parkinson's disease. Mol Pharmacol 57:342-352.2000).

Elble RJ (Origins of tremor. Lancet 355:1113-1114.2000).

Fahn S (Pathophysiological mechanisms of adverse effects from levodopa therapy. Rinsho Shinkeigaku 22:1088-1091.1982).

Fantin M, Auberson YP, Morari M (Differential effect of NR2A and NR2B subunit selective NMDA receptor antagonists on striato-pallidal neurons: relationship to motor response in the 6-hydroxydopamine model of parkinsonism. J Neurochem 106:957-968.2008).

Fasano S, Bezard E, D'Antoni A, Francardo V, Indrigo M, Qin L, Dovero S, Cerovic M, Cenci MA, Brambilla R (Inhibition of Ras-guanine nucleotide-releasing factor 1 (Ras-GRF1) signaling in the striatum reverts motor symptoms associated with L-dopa-induced dyskinesia. Proc Natl Acad Sci U S A 107:21824-21829.2010).

Fasano S, Brambilla R (Cellular mechanisms of striatum-dependent behavioral plasticity and drug addiction. Curr Mol Med 2:649-665.2002).

Fasano S, D'Antoni A, Orban PC, Valjent E, Putignano E, Vara H, Pizzorusso T, Giustetto M, Yoon B, Soloway P, Maldonado R, Caboche J, Brambilla R (Ras-guanine nucleotide-releasing factor 1 (Ras-GRF1) controls activation of extracellular signal-regulated kinase (ERK) signaling in the striatum and long-term behavioral responses to cocaine. Biol Psychiatry 66:758-768.2009).

Feig LA (Regulation of Neuronal Function by Ras-GRF Exchange Factors. Genes Cancer 2:306-319.2011).

Fenelon G, Mahieux F, Huon R, Ziegler M (Hallucinations in Parkinson's disease: prevalence, phenomenology and risk factors. Brain 123 (Pt 4):733-745.2000).

Fernandez-Medarde A, Esteban LM, Nunez A, Porteros A, Tessarollo L, Santos E (Targeted disruption of Ras-Grf2 shows its dispensability for mouse growth and development. Mol Cell Biol 22:2498-2504.2002).

Fernandez A, de Ceballos ML, Jenner P, Marsden CD (Neurotensin, substance P, delta and mu opioid receptors are decreased in basal ganglia of Parkinson's disease patients. Neuroscience 61:73-79.1994).

Fox SH, Moser B, Brotchie JM (Behavioral effects of 5-HT2C receptor antagonism in the substantia nigra zona reticulata of the 6-hydroxydopamine-lesioned rat model of Parkinson's disease. Exp Neurol 151:35-49.1998).

Francardo V, Recchia A, Popovic N, Andersson D, Nissbrandt H, Cenci MA (Impact of the lesion procedure on the profiles of motor impairment and molecular responsiveness to L-DOPA in the 6-hydroxydopamine mouse model of Parkinson's disease. Neurobiol Dis 42:327-340.2011).

Gardoni F, Picconi B, Ghiglieri V, Polli F, Bagetta V, Bernardi G, Cattabeni F, Di Luca M, Calabresi P (A critical interaction between NR2B and MAGUK in L-DOPA induced dyskinesia. J Neurosci 26:2914-2922.2006).

Gardoni F, Sgobio C, Pendolino V, Calabresi P, Di Luca M, Picconi B (Targeting NR2A-containing NMDA receptors reduces L-DOPA-induced dyskinesias. Neurobiol Aging 33:2138-2144.2012).

Gerfen CR, Engber TM, Mahan LC, Susel Z, Chase TN, Monsma FJ, Jr., Sibley DR (D1 and D2 dopamine receptor-regulated gene expression of striatonigral and striatopallidal neurons. Science 250:1429-1432.1990).

Gerfen CR, Miyachi S, Paletzki R, Brown P (D1 dopamine receptor supersensitivity in the dopamine-depleted striatum results from a switch in the regulation of ERK1/2/MAP kinase. J Neurosci 22:5042-5054.2002).

Giese KP, Friedman E, Telliez JB, Fedorov NB, Wines M, Feig LA, Silva AJ (Hippocampus-dependent learning and memory is impaired in mice lacking the Ras-guanine-nucleotide releasing factor 1 (Ras-GRF1). Neuropharmacology 41:791-800.2001).

Grafton ST, Turner RS, Desmurget M, Bakay R, Delong M, Vitek J, Crutcher M (Normalizing motor-related brain activity: subthalamic nucleus stimulation in Parkinson disease. Neurology 66:1192-1199.2006).

Greengard P (The neurobiology of dopamine signaling. Biosci Rep 21:247-269.2001).

Grofova I, Deniau JM, Kitai ST (Morphology of the substantia nigra pars reticulata projection neurons intracellularly labeled with HRP. J Comp Neurol 208:352-368.1982).

Grofova I, Zhou M (Nigral innervation of cholinergic and glutamatergic cells in the rat mesopontine tegmentum: light and electron microscopic anterograde tracing and immunohistochemical studies. J Comp Neurol 395:359-379.1998).

Guigoni C, Doudnikoff E, Li Q, Bloch B, Bezard E (Altered D(1) dopamine receptor trafficking in parkinsonian and dyskinetic non-human primates. Neurobiol Dis 26:452-463.2007).

Hadj Tahar A, Ekesbo A, Gregoire L, Bangassoro E, Svensson KA, Tedroff J, Bedard PJ (Effects of acute and repeated treatment with a novel dopamine D2 receptor ligand on L-DOPA-induced dyskinesias in MPTP monkeys. Eur J Pharmacol 412:247-254.2001).

Hallett PJ, Dunah AW, Ravenscroft P, Zhou S, Bezard E, Crossman AR, Brotchie JM, Standaert DG (Alterations of striatal NMDA receptor subunits associated with the development of dyskinesia in the MPTP-lesioned primate model of Parkinson's disease. Neuropharmacology 48:503-516.2005).

Harsing LG, Jr., Zigmond MJ (Influence of dopamine on GABA release in striatum: evidence for D1-D2 interactions and non-synaptic influences. Neuroscience 77:419-429.1997).

Heikkila RE, Cohen G (Evaluation of amantadine as a releasing agent or uptake blocker for H 3 -dopamine in rat brain slices. Eur J Pharmacol 20:156-160.1972).

Hemmings HC, Jr., Greengard P, Tung HY, Cohen P (DARPP-32, a dopamine-regulated neuronal phosphoprotein, is a potent inhibitor of protein phosphatase-1. Nature 310:503-505.1984).

Henry B, Fox SH, Crossman AR, Brotchie JM (Mu- and delta-opioid receptor antagonists reduce levodopa-induced dyskinesia in the MPTP-lesioned primate model of Parkinson's disease. Exp Neurol 171:139-146.2001).

Hernandez-Lopez S, Bargas J, Surmeier DJ, Reyes A, Galarraga E (D1 receptor activation enhances evoked discharge in neostriatal medium spiny neurons by modulating an L-type Ca2+ conductance. J Neurosci 17:3334-3342.1997).

Hope BT, Nye HE, Kelz MB, Self DW, Iadarola MJ, Nakabeppu Y, Duman RS, Nestler EJ (Induction of a long-lasting AP-1 complex composed of altered Fos-like proteins in brain by chronic cocaine and other chronic treatments. Neuron 13:1235-1244.1994).

Hurley MJ, Jackson MJ, Smith LA, Rose S, Jenner P (Immunoautoradiographic analysis of NMDA receptor subunits and associated postsynaptic density proteins in the brain of dyskinetic MPTP-treated common marmosets. Eur J Neurosci 21:3240-3250.2005).

Hyttel J (SCH 23390 - the first selective dopamine D-1 antagonist. Eur J Pharmacol 91:153-154.1983).

Invernizzi RW, Pierucci M, Calcagno E, Di Giovanni G, Di Matteo V, Benigno A, Esposito E (Selective activation of 5-HT(2C) receptors stimulates GABA-ergic function in the rat substantia nigra pars reticulata: a combined in vivo electrophysiological and neurochemical study. Neuroscience 144:1523-1535.2007).

Itier JM, Tremp GL, Leonard JF, Multon MC, Ret G, Schweighoffer F, Tocque B, Bluet-Pajot MT, Cormier V, Dautry F (Imprinted gene in postnatal growth role. Nature 393:125-126.1998).

Jellinger K (Overview of morphological changes in Parkinson's disease. Adv Neurol 45:1-18.1987).

Jin SX, Feig LA (Long-term potentiation in the CA1 hippocampus induced by NR2A subunit-containing NMDA glutamate receptors is mediated by Ras-GRF2/Erk map kinase signaling. PLoS One 5:e11732.2010).

Johansson PA, Andersson M, Andersson KE, Cenci MA (Alterations in cortical and basal ganglia levels of opioid receptor binding in a rat model of l-DOPA-induced dyskinesia. Neurobiol Dis 8:220-239.2001).

Joyce JN (Differential response of striatal dopamine and muscarinic cholinergic receptor subtypes to the loss of dopamine. I. Effects of intranigral or intracerebroventricular 6-hydroxydopamine lesions of the mesostriatal dopamine system. Exp Neurol 113:261-276.1991).

Kennett GA, Curzon G (Evidence that mCPP may have behavioural effects mediated by central 5-HT1C receptors. Br J Pharmacol 94:137-147.1988).

Kohler C, Hall H, Ogren SO, Gawell L (Specific in vitro and in vivo binding of 3H-raclopride. A potent substituted benzamide drug with high affinity for dopamine D-2 receptors in the rat brain. Biochem Pharmacol 34:2251-2259.1985).

Koller WC, Hutton JT, Tolosa E, Capilldeo R (Immediate-release and controlled-release carbidopa/levodopa in PD: a 5-year randomized multicenter study. Carbidopa/Levodopa Study Group. Neurology 53:1012-1019.1999).

Konitsiotis S, Blanchet PJ, Verhagen L, Lamers E, Chase TN (AMPA receptor blockade improves levodopa-induced dyskinesia in MPTP monkeys. Neurology 54:1589-1595.2000).

Koprich JB, Fox SH, Johnston TH, Goodman A, Le Bourdonnec B, Dolle RE, DeHaven RN, DeHaven-Hudkins DL, Little PJ, Brotchie JM (The selective mu-opioid receptor antagonist ADL5510 reduces levodopa-induced dyskinesia without affecting antiparkinsonian action in MPTP-lesioned macaque model of Parkinson's disease. Mov Disord 26:1225-1233.2011).

Kornhuber J, Bormann J, Hubers M, Rusche K, Riederer P (Effects of the 1-amino-adamantanes at the MK-801-binding site of the NMDA-receptor-gated ion channel: a human postmortem brain study. Eur J Pharmacol 206:297-300.1991).

Krapivinsky G, Krapivinsky L, Manasian Y, Ivanov A, Tyzio R, Pellegrino C, Ben-Ari Y, Clapham DE, Medina I (The NMDA receptor is coupled to the ERK pathway by a direct interaction between NR2B and RasGRF1. Neuron 40:775-784.2003).

Kravitz AV, Freeze BS, Parker PR, Kay K, Thwin MT, Deisseroth K, Kreitzer AC (Regulation of parkinsonian motor behaviours by optogenetic control of basal ganglia circuitry. Nature 466:622-626.2010).

Kreitzer AC, Malenka RC (Striatal plasticity and basal ganglia circuit function. Neuron 60:543-554.2008).

Le Moine C, Bloch B (D1 and D2 dopamine receptor gene expression in the rat striatum: sensitive cRNA probes demonstrate prominent segregation of D1 and D2 mRNAs in distinct neuronal populations of the dorsal and ventral striatum. J Comp Neurol 355:418-426.1995).

Lee CS, Cenci MA, Schulzer M, Bjorklund A (Embryonic ventral mesencephalic grafts improve levodopa-induced dyskinesia in a rat model of Parkinson's disease. Brain 123 (Pt 7):1365-1379.2000).

Li S, Tian X, Hartley DM, Feig LA (Distinct roles for Ras-guanine nucleotide-releasing factor 1 (Ras-GRF1) and Ras-GRF2 in the induction of long-term potentiation and long-term depression. J Neurosci 26:1721-1729.2006).

Lindgren HS, Andersson DR, Lagerkvist S, Nissbrandt H, Cenci MA (L-DOPA-induced dopamine efflux in the striatum and the substantia nigra in a rat model of Parkinson's disease: temporal and quantitative relationship to the expression of dyskinesia. J Neurochem 112:1465-1476.2010).

Loschmann PA, De Groote C, Smith L, Wullner U, Fischer G, Kemp JA, Jenner P, Klockgether T (Antiparkinsonian activity of Ro 25-6981, a NR2B subunit specific NMDA receptor antagonist, in animal models of Parkinson's disease. Exp Neurol 187:86-93.2004).

Lundblad M, Andersson M, Winkler C, Kirik D, Wierup N, Cenci MA (Pharmacological validation of behavioural measures of akinesia and dyskinesia in a rat model of Parkinson's disease. Eur J Neurosci 15:120-132.2002).

Lundblad M, Picconi B, Lindgren H, Cenci MA (A model of L-DOPA-induced dyskinesia in 6-hydroxydopamine lesioned mice: relation to motor and cellular parameters of nigrostriatal function. Neurobiol Dis 16:110-123.2004).

Lundblad M, Usiello A, Carta M, Hakansson K, Fisone G, Cenci MA (Pharmacological validation of a mouse model of l-DOPA-induced dyskinesia. Exp Neurol 194:66-75.2005).

Luquin MR, Scipioni O, Vaamonde J, Gershanik O, Obeso JA (Levodopa-induced dyskinesias in Parkinson's disease: clinical and pharmacological classification. Mov Disord 7:117-124.1992).

Mabrouk OS, Marti M, Morari M (Endogenous nociceptin/orphanin FQ (N/OFQ) contributes to haloperidol-induced changes of nigral amino acid transmission and parkinsonism: a combined microdialysis and behavioral study in naive and nociceptin/orphanin FQ receptor knockout mice. Neuroscience 166:40-48.2010).

Marsden CD, Merton PA, Morton HB (Human postural responses. Brain 104:513-534.1981).

Marti M, Guerrini R, Beani L, Bianchi C, Morari M (Nociceptin/orphanin FQ receptors modulate glutamate extracellular levels in the substantia nigra pars reticulata. A microdialysis study in the awake freely moving rat. Neuroscience 112:153-160.2002).

Marti M, Manzalini M, Fantin M, Bianchi C, Della Corte L, Morari M (Striatal glutamate release evoked in vivo by NMDA is dependent upon ongoing neuronal activity in the substantia nigra, endogenous striatal substance P and dopamine. J Neurochem 93:195-205.2005a).

Marti M, Mela F, Fantin M, Zucchini S, Brown JM, Witta J, Di Benedetto M, Buzas B, Reinscheid RK, Salvadori S, Guerrini R, Romualdi P, Candeletti S, Simonato M, Cox BM, Morari M (Blockade of nociceptin/orphanin FQ transmission attenuates symptoms and neurodegeneration associated with Parkinson's disease. J Neurosci 25:9591-9601.2005b).

Marti M, Mela F, Veronesi C, Guerrini R, Salvadori S, Federici M, Mercuri NB, Rizzi A, Franchi G, Beani L, Bianchi C, Morari M (Blockade of nociceptin/orphanin FQ receptor signaling in rat substantia nigra pars reticulata stimulates nigrostriatal dopaminergic transmission and motor behavior. J Neurosci 24:6659-6666.2004).

Marti M, Rodi D, Li Q, Guerrini R, Fasano S, Morella I, Tozzi A, Brambilla R, Calabresi P, Simonato M, Bezard E, Morari M (Nociceptin/Orphanin FQ Receptor Agonists Attenuate L-DOPA-Induced Dyskinesias. J Neurosci 32:16106-16119.2012).

Marti M, Trapella C, Viaro R, Morari M (The nociceptin/orphanin FQ receptor antagonist J-113397 and L-DOPA additively attenuate experimental parkinsonism through overinhibition of the nigrothalamic pathway. J Neurosci 27:1297-1307.2007).

Matamales M, Girault JA (Signaling from the cytoplasm to the nucleus in striatal medium-sized spiny neurons. Front Neuroanat 5:37.2011).

McGeorge AJ, Faull RL (The organization of the projection from the cerebral cortex to the striatum in the rat. Neuroscience 29:503-537.1989).

McIntyre CC, Savasta M, Walter BL, Vitek JL (How does deep brain stimulation work? Present understanding and future questions. J Clin Neurophysiol 21:40-50.2004).

Meissner W, Ravenscroft P, Reese R, Harnack D, Morgenstern R, Kupsch A, Klitgaard H, Bioulac B, Gross CE, Bezard E, Boraud T (Increased slow oscillatory activity in substantia nigra pars reticulata triggers abnormal involuntary movements in the 6-OHDA-lesioned rat in the presence of excessive extracellular striatal dopamine. Neurobiol Dis 22:586-598.2006).

Mela F, Marti M, Dekundy A, Danysz W, Morari M, Cenci MA (Antagonism of metabotropic glutamate receptor type 5 attenuates l-DOPA-induced dyskinesia and its molecular and neurochemical correlates in a rat model of Parkinson's disease. J Neurochem 101:483-497.2007).

Mela F, Millan MJ, Brocco M, Morari M (The selective D(3) receptor antagonist, S33084, improves parkinsonian-like motor dysfunction but does not affect L-DOPA-induced dyskinesia in 6-hydroxydopamine hemi-lesioned rats. Neuropharmacology 58:528-536.2010).

Millan MJ, Newman-Tancredi A, Quentric Y, Cussac D (The "selective" dopamine D1 receptor antagonist, SCH23390, is a potent and high efficacy agonist at cloned human serotonin2C receptors. Psychopharmacology (Berl) 156:58-62.2001).

Mink JW, Thach WT (Basal ganglia motor control. III. Pallidal ablation: normal reaction time, muscle cocontraction, and slow movement. J Neurophysiol 65:330-351.1991).

Mizoguchi K, Yokoo H, Yoshida M, Tanaka T, Tanaka M (Amantadine increases the extracellular dopamine levels in the striatum by re-uptake inhibition and by N-methyl-D-aspartate antagonism. Brain Res 662:255-258.1994).

Morari M, O'Connor WT, Darvelid M, Ungerstedt U, Bianchi C, Fuxe K (Functional neuroanatomy of the nigrostriatal and striatonigral pathways as studied with dual probe microdialysis in the awake rat--I. Effects of perfusion with tetrodotoxin and low-calcium medium. Neuroscience 72:79-87.1996a).

Morari M, O'Connor WT, Ungerstedt U, Bianchi C, Fuxe K (Functional neuroanatomy of the nigrostriatal and striatonigral pathways as studied with dual probe microdialysis in the awake rat--II. Evidence for striatal N-methyl-D-aspartate receptor regulation of striatonigral GABAergic transmission and motor function. Neuroscience 72:89-97.1996b).

Morari M, O'Connor WT, Ungerstedt U, Fuxe K (N-methyl-D-aspartic acid differentially regulates extracellular dopamine, GABA, and glutamate levels in the dorsolateral neostriatum of the halothane-anesthetized rat: an in vivo microdialysis study. J Neurochem 60:1884-1893.1993).

Morari M, O'Connor WT, Ungerstedt U, Fuxe K (Dopamine D1 and D2 receptor antagonism differentially modulates stimulation of striatal neurotransmitter levels by N-methyl-D-aspartic acid. Eur J Pharmacol 256:23-30.1994).

Nadjar A, Brotchie JM, Guigoni C, Li Q, Zhou SB, Wang GJ, Ravenscroft P, Georges F, Crossman AR, Bezard E (Phenotype of striatofugal medium spiny neurons in parkinsonian and dyskinetic nonhuman primates: a call for a reappraisal of the functional organization of the basal ganglia. J Neurosci 26:8653-8661.2006).

Nash JE, Ravenscroft P, McGuire S, Crossman AR, Menniti FS, Brotchie JM (The NR2B-selective NMDA receptor antagonist CP-101,606 exacerbates L-DOPA-induced dyskinesia and provides mild potentiation of anti-parkinsonian effects of L-DOPA in the MPTP-lesioned marmoset model of Parkinson's disease. Exp Neurol 188:471-479.2004).

Nauta WJ, Smith GP, Faull RL, Domesick VB (Efferent connections and nigral afferents of the nucleus accumbens septi in the rat. Neuroscience 3:385-401.1978).

Nicholas AP, Lubin FD, Hallett PJ, Vattem P, Ravenscroft P, Bezard E, Zhou S, Fox SH, Brotchie JM, Sweatt JD, Standaert DG (Striatal histone modifications in models of levodopa-induced dyskinesia. J Neurochem 106:486-494.2008).

Northover BJ (Effect of pre-treating rat atria with potassium channel blocking drugs on the electrical and mechanical responses to phenylephrine. Biochem Pharmacol 47:2163-2169.1994).

Noyce AJ, Bestwick JP, Silveira-Moriyama L, Hawkes CH, Giovannoni G, Lees AJ, Schrag A (Meta-analysis of early nonmotor features and risk factors for Parkinson disease. Ann Neurol.2012).

Obeso JA, Rodriguez-Oroz MC, Rodriguez M, Lanciego JL, Artieda J, Gonzalo N, Olanow CW (Pathophysiology of the basal ganglia in Parkinson's disease. Trends Neurosci 23:S8-19.2000).

Oh JD, Chartisathian K, Ahmed SM, Chase TN (Cyclic AMP responsive element binding protein phosphorylation and persistent expression of levodopa-induced response alterations in unilateral nigrostriatal 6-OHDA lesioned rats. J Neurosci Res 72:768-780.2003).

Oh JD, Chase TN (Glutamate-mediated striatal dysregulation and the pathogenesis of motor response complications in Parkinson's disease. Amino Acids 23:133-139.2002).

Oh JD, Russell DS, Vaughan CL, Chase TN (Enhanced tyrosine phosphorylation of striatal NMDA receptor subunits: effect of dopaminergic denervation and L-DOPA administration. Brain Res 813:150-159.1998).

Orban PC, Chapman PF, Brambilla R (Is the Ras-MAPK signalling pathway necessary for long-term memory formation? Trends Neurosci 22:38-44.1999).

Parelkar NK, Jiang Q, Chu XP, Guo ML, Mao LM, Wang JQ (Amphetamine alters Ras-guanine nucleotide-releasing factor expression in the rat striatum in vivo. Eur J Pharmacol 619:50-56.2009).

Parent A, Hazrati LN (Functional anatomy of the basal ganglia. I. The cortico-basal ganglia-thalamo-cortical loop. Brain Res Brain Res Rev 20:91-127.1995a).

Parent A, Hazrati LN (Functional anatomy of the basal ganglia. II. The place of subthalamic nucleus and external pallidum in basal ganglia circuitry. Brain Res Brain Res Rev 20:128-154.1995b).

Parent A, Sato F, Wu Y, Gauthier J, Levesque M, Parent M (Organization of the basal ganglia: the importance of axonal collateralization. Trends Neurosci 23:S20-27.2000).

Parsons CG, Panchenko VA, Pinchenko VO, Tsyndrenko AY, Krishtal OA (Comparative patch-clamp studies with freshly dissociated rat hippocampal and striatal neurons on the NMDA receptor antagonistic effects of amantadine and memantine. Eur J Neurosci 8:446-454.1996).

Paxinos G. and Watson C. (The Rat Brain in Stereotaxic Coordinates. Academic Press. Sydney.1982).

Paxinos G. and Franklin K. B. J. (The Mouse Brain in StereotaxicCoordinates, 2nd edn. Academic Press. San Diego. 2001)

Picconi B, Centonze D, Hakansson K, Bernardi G, Greengard P, Fisone G, Cenci MA, Calabresi P (Loss of bidirectional striatal synaptic plasticity in L-DOPA-induced dyskinesia. Nat Neurosci 6:501-506.2003).

Pifl C, Reither H, Hornykiewicz O (Functional sensitization of striatal dopamine D1 receptors in the 6-hydroxydopamine-lesioned rat. Brain Res 572:87-93.1992).

Porras G, Berthet A, Dehay B, Li Q, Ladepeche L, Normand E, Dovero S, Martinez A, Doudnikoff E, Martin-Negrier ML, Chuan Q, Bloch B, Choquet D, Boue-Grabot E, Groc L, Bezard E (PSD-95 expression controls l-DOPA dyskinesia through dopamine D1 receptor trafficking. J Clin Invest 122:3977-3989.2012).

Quinn N, Critchley P, Marsden CD (Young onset Parkinson's disease. Mov Disord 2:73-91.1987).

Quintana A, Melon C, Kerkerian-Le Goff L, Salin P, Savasta M, Sgambato-Faure V (Forelimb dyskinesia mediated by high-frequency stimulation of the subthalamic nucleus is linked to rapid activation of the NR2B subunit of N-methyl-D-aspartate receptors. Eur J Neurosci 32:423-434.2010).

Radnikow G, Misgeld U (Dopamine D1 receptors facilitate GABAA synaptic currents in the rat substantia nigra pars reticulata. J Neurosci 18:2009-2016.1998).

Rajput AH, Rajput A, Lang AE, Kumar R, Uitti RJ, Galvez-Jimenez N (New use for an old drug: amantadine benefits levodopa-induced dyskinesia. Mov Disord 13:851.1998).

Rangel-Barajas C, Silva I, Lopez-Santiago LM, Aceves J, Erlij D, Floran B (L-DOPA-induced dyskinesia in hemiparkinsonian rats is associated with up-regulation of adenylyl cyclase

type V/VI and increased GABA release in the substantia nigra reticulata. Neurobiol Dis 41:51-61.2011).

Rascol O (L-dopa-induced peak-dose dyskinesias in patients with Parkinson's disease: a clinical pharmacologic approach. Mov Disord 14 Suppl 1:19-32.1999).

Robertson HA, Peterson MR, Murphy K, Robertson GS (D1-dopamine receptor agonists selectively activate striatal c-fos independent of rotational behaviour. Brain Res 503:346-349.1989).

Rozas G, Guerra MJ, Labandeira-Garcia JL (An automated rotarod method for quantitative drug-free evaluation of overall motor deficits in rat models of parkinsonism. Brain Res Brain Res Protoc 2:75-84.1997).

Rozas G, Labandeira Garcia JL (Drug-free evaluation of rat models of parkinsonism and nigral grafts using a new automated rotarod test. Brain Res 749:188-199.1997).

Rylander D, Parent M, O'Sullivan SS, Dovero S, Lees AJ, Bezard E, Descarries L, Cenci MA (Maladaptive plasticity of serotonin axon terminals in levodopa-induced dyskinesia. Ann Neurol 68:619-628.2010).

Rylander D, Recchia A, Mela F, Dekundy A, Danysz W, Cenci MA (Pharmacological modulation of glutamate transmission in a rat model of L-DOPA-induced dyskinesia: effects on motor behavior and striatal nuclear signaling. J Pharmacol Exp Ther 330:227-235.2009).

Sanberg PR, Bunsey MD, Giordano M, Norman AB (The catalepsy test: its ups and downs. Behav Neurosci 102:748-759.1988).

Santini E, Heiman M, Greengard P, Valjent E, Fisone G (Inhibition of mTOR signaling in Parkinson's disease prevents L-DOPA-induced dyskinesia. Sci Signal 2:ra36.2009).

Santini E, Sgambato-Faure V, Li Q, Savasta M, Dovero S, Fisone G, Bezard E (Distinct changes in cAMP and extracellular signal-regulated protein kinase signalling in L-DOPA-induced dyskinesia. PLoS One 5:e12322.2010).

Santini E, Valjent E, Usiello A, Carta M, Borgkvist A, Girault JA, Herve D, Greengard P, Fisone G (Critical involvement of cAMP/DARPP-32 and extracellular signal-regulated protein kinase signaling in L-DOPA-induced dyskinesia. J Neurosci 27:6995-7005.2007).

Sarre S, Lanza M, Makovec F, Artusi R, Caselli G, Michotte Y (In vivo neurochemical effects of the NR2B selective NMDA receptor antagonist CR 3394 in 6-hydroxydopamine lesioned rats. Eur J Pharmacol 584:297-305.2008).

Sarre S, Vandeneede D, Ebinger G, Michotte Y (Biotransformation of L-DOPA to dopamine in the substantia nigra of freely moving rats: effect of dopamine receptor agonists and antagonists. J Neurochem 70:1730-1739.1998).

Savasta M, Dubois A, Benavides J, Scatton B (Different plasticity changes in D1 and D2 receptors in rat striatal subregions following impairment of dopaminergic transmission. Neurosci Lett 85:119-124.1988).

Schallert T, De Ryck M, Whishaw IQ, Ramirez VD, Teitelbaum P (Excessive bracing reactions and their control by atropine and L-DOPA in an animal analog of Parkinsonism. Exp Neurol 64:33-43.1979).

Schallert T, Fleming SM, Leasure JL, Tillerson JL, Bland ST (CNS plasticity and assessment of forelimb sensorimotor outcome in unilateral rat models of stroke, cortical ablation, parkinsonism and spinal cord injury. Neuropharmacology 39:777-787.2000).

Schiavi GB, Brunet S, Rizzi CA, Ladinsky H (Identification of serotonin 5-HT4 recognition sites in the porcine caudate nucleus by radioligand binding. Neuropharmacology 33:543-549.1994).

Schwab RS, England AC, Jr., Poskanzer DC, Young RR (Amantadine in the treatment of Parkinson's disease. JAMA 208:1168-1170.1969).

Seeman P, Van Tol HH (Dopamine receptor pharmacology. Trends Pharmacol Sci 15:264-270.1994).

Sgambato V, Pages C, Rogard M, Besson MJ, Caboche J (Extracellular signal-regulated kinase (ERK) controls immediate early gene induction on corticostriatal stimulation. J Neurosci 18:8814-8825.1998).

Sidibe M, Pare JF, Smith Y (Nigral and pallidal inputs to functionally segregated thalamostriatal neurons in the centromedian/parafascicular intralaminar nuclear complex in monkey. J Comp Neurol 447:286-299.2002).

Standaert DG, Friberg IK, Landwehrmeyer GB, Young AB, Penney JB, Jr. (Expression of NMDA glutamate receptor subunit mRNAs in neurochemically identified projection and interneurons in the striatum of the rat. Brain Res Mol Brain Res 64:11-23.1999).

Standaert DG, Testa CM, Young AB, Penney JB, Jr. (Organization of N-methyl-D-aspartate glutamate receptor gene expression in the basal ganglia of the rat. J Comp Neurol 343:1-16.1994).

Stoof JC, Booij J, Drukarch B, Wolters EC (The anti-parkinsonian drug amantadine inhibits the N-methyl-D-aspartic acid-evoked release of acetylcholine from rat neostriatum in a non-competitive way. Eur J Pharmacol 213:439-443.1992).

Tian X, Gotoh T, Tsuji K, Lo EH, Huang S, Feig LA (Developmentally regulated role for Ras-GRFs in coupling NMDA glutamate receptors to Ras, Erk and CREB. EMBO J 23:1567-1575.2004).

Tong J, Fitzmaurice PS, Ang LC, Furukawa Y, Guttman M, Kish SJ (Brain dopamine-stimulated adenylyl cyclase activity in Parkinson's disease, multiple system atrophy, and progressive supranuclear palsy. Ann Neurol 55:125-129.2004).

Viaro R, Marti M, Morari M (Dual motor response to l-dopa and nociceptin/orphanin FQ receptor antagonists in 1-methyl-4-phenyl-1,2,5,6-tetrahydropyridine (MPTP) treated mice: Paradoxical inhibition is relieved by D(2)/D(3) receptor blockade. Exp Neurol 223:473-484.2010).

Viaro R, Sanchez-Pernaute R, Marti M, Trapella C, Isacson O, Morari M (Nociceptin/orphanin FQ receptor blockade attenuates MPTP-induced parkinsonism. Neurobiol Dis 30:430-438.2008).

Visanji NP, de Bie RM, Johnston TH, McCreary AC, Brotchie JM, Fox SH (The nociceptin/orphanin FQ (NOP) receptor antagonist J-113397 enhances the effects of levodopa in the MPTP-lesioned nonhuman primate model of Parkinson's disease. Mov Disord 23:1922-1925.2008).

Volta M, Mabrouk OS, Bido S, Marti M, Morari M (Further evidence for an involvement of nociceptin/orphanin FQ in the pathophysiology of Parkinson's disease: a behavioral and neurochemical study in reserpinized mice. J Neurochem 115:1543-1555.2010).

Volta M, Viaro R, Trapella C, Marti M, Morari M (Dopamine-nociceptin/orphanin FQ interactions in the substantia nigra reticulata of hemiparkinsonian rats: involvement of D2/D3 receptors and impact on nigro-thalamic neurons and motor activity. Exp Neurol 228:126-137.2011).

Walaas SI, Greengard P (DARPP-32, a dopamine- and adenosine 3':5'-monophosphate-regulated phosphoprotein enriched in dopamine-innervated brain regions. I. Regional and cellular distribution in the rat brain. J Neurosci 4:84-98.1984).

Westin JE, Lindgren HS, Gardi J, Nyengaard JR, Brundin P, Mohapel P, Cenci MA (Endothelial proliferation and increased blood-brain barrier permeability in the basal ganglia in a rat model of 3,4-dihydroxyphenyl-L-alanine-induced dyskinesia. J Neurosci 26:9448-9461.2006).

Westin JE, Vercammen L, Strome EM, Konradi C, Cenci MA (Spatiotemporal pattern of striatal ERK1/2 phosphorylation in a rat model of L-DOPA-induced dyskinesia and the role of dopamine D1 receptors. Biol Psychiatry 62:800-810.2007).

Windels F, Kiyatkin EA (Dopamine action in the substantia nigra pars reticulata: iontophoretic studies in awake, unrestrained rats. Eur J Neurosci 24:1385-1394.2006).

Winkler C, Kirik D, Bjorklund A, Cenci MA (L-DOPA-induced dyskinesia in the intrastriatal 6-hydroxydopamine model of parkinson's disease: relation to motor and cellular parameters of nigrostriatal function. Neurobiol Dis 10:165-186.2002).

Wolf E, Seppi K, Katzenschlager R, Hochschorner G, Ransmayr G, Schwingenschuh P, Ott E, Kloiber I, Haubenberger D, Auff E, Poewe W (Long-term antidyskinetic efficacy of amantadine in Parkinson's disease. Mov Disord 25:1357-1363.2010).

Zarrindast MR, Honardar Z, Sanea F, Owji AA (SKF 38393 and SCH 23390 inhibit reuptake of serotonin by rat hypothalamic synaptosomes. Pharmacology 87:85-89.2011).

Zhang GC, Hoffmann J, Parelkar NK, Liu XY, Mao LM, Fibuch EE, Wang JQ (Cocaine increases Ras-guanine nucleotide-releasing factor 1 protein expression in the rat striatum in vivo. Neurosci Lett 427:117-121.2007).

Zhou ZD, Kerk SY, Xiong GG, Lim TM (Dopamine auto-oxidation aggravates non-apoptotic cell death induced by over-expression of human A53T mutant alpha-synuclein in dopaminergic PC12 cells. J Neurochem 108:601-610.2009).

Originals papers

I) Esposito E, Mariani P, Ravani L, Contado C, Volta M, **Bido S**, Drechsler M, Mazzoni S, Menegatti E, Morari M, Cortesi R. Nanoparticulate lipid dispersions for bromocriptine delivery: Characterization and in vivo study. Eur J Pharm Biopharm. 2012 Feb; 80:306-14

II) Mela F, Marti M, **Bido S**, Cenci MA, Morari M. In vivo evidence for a differential contribution of striatal and nigral D1 and D2 receptors to l-DOPA induced dyskinesia and the accompanying surge of nigral amino acid levels. Neurobiol. Dis. 2012 Jan; 45:573-82

III) **Bido S**, Marti M, Morari M. Amantadine attenuates levodopa-induced dyskinesia in mice and rats preventing the accompanying rise in nigral GABA levels. J Neurochem. 2011 Sep;118: 1043-55

IV) Volta M, Mabrouk OS, **Bido S**, Marti M, Morari M. Further evidence for an involvement of nociceptin/orphanin FQ in the pathophysiology of Parkinson's disease: a behavioral and neurochemical study in reserpinized mice. J Neurochem. 2010 Dec;115:1543-55.

European Journal of Pharmaceutics and Biopharmaceutics 80 (2012) 306–314

Contents lists available at SciVerse ScienceDirect

European Journal of Pharmaceutics and Biopharmaceutics

journal homepage: www.elsevier.com/locate/ejpb

Research paper

Nanoparticulate lipid dispersions for bromocriptine delivery: Characterization and in vivo study

Elisabetta Esposito [a,*], Paolo Mariani [b], Laura Ravani [a], Catia Contado [c], Mattia Volta [d], Simone Bido [d], Markus Drechsler [e], Serena Mazzoni [b], Enea Menegatti [a], Michele Morari [d], Rita Cortesi [a]

[a] Department of Pharmaceutical Sciences, University of Ferrara, Ferrara, Italy
[b] SAIFET Department, Università Politecnica delle Marche, Ancona, Italy
[c] Department of Chemistry, University of Ferrara, Ferrara, Italy
[d] Department of Experimental and Clinical Medicine, University of Ferrara, Ferrara, Italy
[e] Macromolecular Chemistry II, University of Bayreuth, Germany

ARTICLE INFO

Article history:
Received 10 December 2010
Accepted in revised form 22 October 2011
Available online 28 October 2011

Keywords:
Solid Lipid Nanoparticles (SLNs)
Nanostructured Lipid Carrier (NLC)
Bromocriptine (BC)
X-ray
Drag test
Bar test

ABSTRACT

The physico-chemical properties and in vivo efficacies of two nanoparticulate systems delivering the antiparkinsonian drug bromocriptine (BC) were compared in the present study. Monoolein Aqueous Dispersions (MADs) and Nanostructured Lipid Carriers (NLCs) were produced and characterized. Cryogenic transmission electron microscopy (cryo-TEM) and X-ray diffraction revealed the morphology of MAD and NLC. Dimensional distribution was determined by Photon Correlation Spectroscopy (PCS) and Sedimentation Field Flow Fractionation (SdFFF). In particular, BC was shown to be encapsulated with high entrapment efficiency both in MAD and in NLC, according to SdFFF combined with HPLC. Two behavioral tests specific for akinesia (bar test) or akinesia/bradykinesia (drag test) were used to compare the effects of the different BC formulations on motor disabilities in 6-hydroxydopamine hemilesioned rats in vivo, a model of Parkinson's disease. Both free BC and BC–NLC reduced the immobility time in the bar test and enhanced the number of steps in the drag test, although the effects of encapsulated BC were longer lasting (5 h). Conversely, BC–MAD was ineffective in the bar test and improved stepping activity in the drag test to a much lower degree than those achieved with the other preparations. We conclude that MAD and NLC can encapsulate BC, although only NLC provide long-lasting therapeutic effects possibly extending BC half-life in vivo.

© 2011 Elsevier B.V. All rights reserved.

1. Introduction

Lipid dispersions have attracted significant attention due to their potential use as matrixes able to dissolve and deliver active molecules in a controlled fashion, thereby improving their bioavailability and reducing side-effects [1,2].

Solid Lipid Nanoparticles (SLNs) are delivery systems in which the nanodispersed phase has a solid matrix of crystalline solid lipids. SLN are able to protect encapsulated molecules from degradation and modulate their release [3]. The second generation of SLN is represented by Nanostructured Lipid Carriers (NLCs), which are composed of a solid lipid matrix with a certain content of a liquid lipid phase [4]. For instance, the mixture of caprylic/capric triglycerides (liquid at room temperature) with a solid lipid such as tristearin leads to the formation of solid carriers with homogenous lipid nanocompartments [5].

Another type of lipid dispersion that can provide matrices for the sustained release of drugs is represented by Monoolein Aqueous Dispersions (MADs).

The self-assembly of amphiphilic lipids such as monoglycerides in water gives rise to complex lyotropic liquid crystalline nanostructures like micellar, lamellar, hexagonal, and cubic phases [1,6]. The predominance of one species over the other mainly depends on temperature and water content of the system [7].

Cubosomes can be defined as stable reverse bicontinuous structures with two distinct regions of water separated by a contorted bilayer [8]. The methods of preparation [9,10] and the inner structure [11,12] of cubosomes have been widely studied. Nevertheless, drug release from these systems has been poorly investigated [13].

The use of lipid nanosystems for the therapy of brain diseases has been recently proposed [14,15]. Indeed, the pharmacological

Abbreviations: MADs, Monoolein aqueous dispersions; PSD, particle size distribution.

* Corresponding author. Dipartimento di Scienze Farmaceutiche, Via Fossato di Mortara, 19, I-44100 Ferrara, Italy. Tel.: +39 532 455259; fax: +39 532 291296.
E-mail address: ese@unife.it (E. Esposito).

0939-6411/$ - see front matter © 2011 Elsevier B.V. All rights reserved.
doi:10.1016/j.ejpb.2011.10.015

treatment of brain tumors, as well as neurological and psychiatric disorders, is often hindered by the inability of potent drugs to pass the blood brain barrier (BBB) [16]. BBB significantly restricts water-soluble, charged and high molecular weight therapeutics to the vascular space, while allowing brain penetration of small and/or lipophilic molecules. Multiple strategies have been employed to circumvent BBB. An emerging approach is the use of colloidal carriers, which allow brain penetration of non-transportable drugs by masking their physico-chemical characteristics [17,18]. In fact, colloidal carriers represent a non-invasive mean of administration, which offers clinical advantages such as the reduction in drug dosage and side-effects, the increase in drug viability, and the improvement of patient quality of life [19].

In a recent study, we demonstrated the potential application of NLC as a delivery system of the dopamine receptor agonist bromocriptine (BC) for Parkinson's disease (PD) therapy [20]. This follow-up study was aimed at investigating the use of MAD as formulations for controlled delivery of BC. An in-depth characterization of morphology, size, inner structure, and drug distribution of NLC and MAD was made. In addition, the ability of both BC preparations to attenuate motor deficits in 6-hydroxydopamine (6-OHDA) hemilesioned rats, a model of PD, was determined in vivo and compared to that of free BC.

2. Materials and methods

2.1. Materials

RYLO MG 19, glyceryl monooleate (MO) was a gift from Danisco Cultor (Grindsted, Denmark). Pluronic F127 (PEO_{98}–POP_{67}–PEO_{98}) (poloxamer 407) was obtained from BASF (Ludwigshafen, Germany).

Lutrol F 68, oxirane, methyl-, polymer with oxirane (75;30) (poloxamer 188) was a gift of BASF ChemTrade GmbH (Burgbernheim, Germany). FL-70 is a detergent (water 88.8%, triethanolamine oleate 3.8%, sodium carbonate 2.7%, alcohols, C12-14-secondary, ethoxylated 1.8%, tetrasodium ethylenediaminetetraacetate 1.4%, Polyethylene glycol 0.9%, sodium oleate 0.5%, sodium bicarbonate 0.1%) and was obtained from Fisher Scientific (Fair Lawn, NJ, USA) [21].

Tristearin, stearic triglyceride (tristearin), was provided by Fluka (Buchs, Switzerland). Miglyol 812, caprylic/capric triglycerides (Miglyol), was purchased from Eigenmann & Veronelli (Rho, Milano, Italy).

Bromocriptine mesylate, 2-Bromo-α-ergocriptine methansulfonate salt (BC), amphetamine, and 6-hydroxydopamine (6-OHDA) were purchased from Sigma Chemical Company (St Louis, MO, USA).

2.2. MAD preparation

Production of dispersions was based on the emulsification of MO (4.5% w/w) and poloxamer 407 (0.5% w/w) in water (95% w/w), as described by Esposito et al. [22]. After emulsification, the dispersion was subjected to homogenization (15,000 rev min^{-1}, Ultra Turrax, Janke & Kunkel, Ika-Werk, Sardo, Italy) at 60 °C for 1 min, then cooled and maintained at room temperature in glass vials.

Twelve point five (12.5) milligrams of BC (0.55% w/w with respect to the monoolein, 0.025% w/w with respect to the dispersion) was added to the molten MO/poloxamer solution and dissolved before addition to the aqueous solution.

A representative amount of dispersion was analyzed by cryo-TEM. The dispersion was then filtered through a mixed esters cellulose membrane (1.2 μm pore size) to separate large MO/poloxamer aggregates. Dimensional characterization of MO dispersions as well as in vivo experiments was performed after filtration.

The density of MAD (0.0133 g/ml) was calculated as reported in Supplementary data.

2.3. NLC preparation

NLC were prepared by stirring followed by ultrasonication [20]. Briefly, 1 g of lipid mixture was melted at 75 °C. The lipid mixture was constituted of tristearin/Miglyol 2:1 w/w. The fused lipid phase was dispersed in 19 ml of an aqueous poloxamer 188 solution (2.5% w/w). The emulsion was subjected to ultrasonication (Microson™, Ultrasonic cell Disruptor) at 6.75 kHz for 15 min and then cooled down to room temperature by placing it in a water bath at 22 °C. NLC dispersions were stored at room temperature.

Five milligrams of BC (0.025% w/w with respect to the total dispersions, 0.5% w/w with respect to the lipid phase) was added to the molten lipid mixture and dissolved before addition to the aqueous solution. The density of NLC (0.0283 g/ml) was obtained as described for MAD in Supplementary data.

2.4. Characterization of lipid dispersions

Water and disperse phase loss after dispersion production were determined as reported in Supplementary data.

2.4.1. Photon Correlation Spectroscopy (PCS)

Submicron particle size analysis was performed using a Zetasizer 3000 PCS (Malvern Instr., Malvern, England) equipped with a 5 mW helium neon laser with a wavelength output of 633 nm. The dispersant refractive index was 1.33 and the absorbance was 0.00. Glassware was cleaned of dust by washing with detergent and rinsing twice with sterile water. Measurements were made at 25 °C at an angle of 90° with a run time of at least 180 s. Samples were diluted with bidistilled water in a 1:10 V:V ratio. Data were analyzed using the "CONTIN" method [23].

2.4.2. Sedimentation Field Flow Fractionation Analysis

A Sedimentation Field Flow Fractionation (SdFFF) system (Model S101, FFFractionation, Inc., Salt Lake City, UT, USA), described elsewhere [24], was employed to determine the size distribution of particles (PSD) by converting the fractograms, i.e., the graphical results, assuming the particle density is known [25]. The mobile phase was a 0.01% v/v solution of FL-70 in Milli-Q water (Millipore S.p.A., Vimodrone, Milan, Italy) pumped at 2.0 ml/min and monitored in each run. Fifty microliter samples were injected as they were through a 50 μl Rheodyne loop valve.

The fractions were automatically collected by a Model 2110 fraction collector positioned at the end of the SdFFF system (Bio Rad laboratories, UK) after setting a collecting time of 90 s. The volume of each fraction was 3 ml.

2.4.3. Cryogenic Transmission Electron Microscopy (Cryo-TEM)

Samples were vitrified as described in a previous study by Esposito et al. [9]. The vitrified specimen was transferred to a Zeiss EM922Omega (Zeiss SMT, Oberkochen, Germany) transmission electron microscope using a cryoholder (CT3500, Gatan, Munich, Germany). Sample temperature was kept below 100 K throughout the examination. Specimens were examined with doses of about 1000–2000 e/nm^2 at 200 kV. Images were recorded by a CCD digital camera (Ultrascan 1000, Gatan) and analyzed using a GMS 1.8 software (Gatan).

2.4.4. X-ray diffraction measurements

Low-angle X-ray scattering experiments were performed at the DESY synchrotron facility on the A2 beamline in Hamburg, Germany. The investigated Q-range ($Q = 4\pi \sin\theta/\lambda$, where 2θ is the scattering angle and $\lambda = 1.50$ Å the X-ray wavelength) was

0.02–0.35 $Å^{-1}$. Experiments were performed in the 20–40 °C range. Scattering data were recorded on a bidimensional CCD camera of 1024 × 1024 pixels, radially averaged and corrected for the dark, detector efficiency and sample transmission [26]. A few wide-angle X-ray diffraction experiments were performed using a laboratory 3.5 kW Philips PW 1830 X-ray generator equipped with a Guinier-type focusing camera operating with a bent quartz crystal monochromator (λ = 1.54 Å). Diffraction patterns were recorded on GNR Analytical Instruments Imaging Plate system. Samples were held in a tight vacuum cylindrical cell provided with thin Mylar windows. Diffraction data were collected at 20 °C.

In each experiment, a number of Bragg peaks were detected in the low-angle X-ray diffraction region. The peak indexing was performed considering the different symmetries commonly observed in lipid phases [27]. From the averaged spacing of the observed peaks, the unit cell dimension, *a*, was calculated using the Bragg law. The nature of the short-range lipid conformation was derived analyzing the high-angle X-ray diffraction profiles [28].

2.5. Drug content of dispersions

The method used to determine BC content in the dispersion is reported in Supplementary data. BC associated with particles was quantified by HPLC analyses of several fractions collected after the separation by SdFFF.

2.6. HPLC procedure

HPLC determinations were performed using a two-plungers alternative pump (Jasco, Japan), an UV-detector operating at 305 nm, and a 7125 Rheodyne injection valve with a 50 µl loop. Samples were loaded on a stainless steel C-18 reverse-phase column (15 × 0.46 cm) packed with 5 µm particles (Hypersil BDS, Alltech, USA).

Elution was performed with a mobile phase containing 0.1 M ammonium formate (pH 3) and acetonitrile 55:45 v/v at a flow rate of 0.8 ml/min. Retention time of BC was 5.8 min [20].

2.7. In vivo tests

Male Sprague-Dawley rats were kept under regular lighting conditions (12 h light/dark cycle) and given food and water ad libitum. The experimental protocols used in the present study were approved by the Italian Ministry of Health (license n. 194/2008-B) and by the Ethical Committee of the University of Ferrara. Adequate measures were taken to minimize animal pain and discomfort and to limit the number of animals employed in the study.

2.7.1. 6-Hydroxydopamine lesion

Unilateral lesion of dopamine (DA) neurons was induced in isoflurane-anaesthetized male Sprague-Dawley rats (150 g; Harlan Italy; S. Pietro al Natisone, Italy) as previously described [29]. Eight micrograms of 6-OHDA, dissolved in 4 µl of saline (NaCl 0.9% w/v) containing 0.02% ascorbic acid, was stereotaxically injected according to the following coordinates from bregma: antero-posterior – 4.4 mm, medio-lateral – 1.2 mm, dorso-ventral – 7.8 mm below dura [30]. In order to select the rats that had been successfully lesioned, the rotational model was employed. Two weeks after 6-OHDA injection, rats were tested for denervation with a dose of amphetamine (5 mg/kg i.p., dissolved in saline). Forty-nine rats showing a turning behavior >7 turns/min in a direction ipsilateral to the lesion side were enrolled in the study. Experiments were usually performed 6–8 weeks after lesion. Marked (>95%) reduction in striatal DA levels and tyrosine hydroxylase-positive DA terminals have been detected at this stage [31,32].

2.7.2. Behavioral studies in hemiparkinsonian rats

The 6-OHDA hemilesioned rat is a well-established model of experimental parkinsonism, in which hypokinetic motor disturbance primarily affects the side of the body contralateral to the denervated hemisphere (i.e., the toxin injection side). Parkinsonian-like disabilities were investigated in rats by using two previously validated behavioral tests [30,32]. The "bar test" measures the ability of the rat to respond to an externally imposed static posture and provides information on the time to initiate a movement (akinesia) [33]. The "drag test" measures the ability of the forepaws to adapt to an external dynamic stimulus (i.e., dragging backwards) and provides information on the time to initiate and execute (bradykinesia) a movement [29,34].

In the bar test, the contralateral and ipsilateral forepaws of each rat were alternatively placed on blocks of increasing heights (3, 6, and 9 cm). The immobility time (in seconds) of each paw on the blocks was recorded (cut-off time at each step of 20 s) and summed. In the drag test, the animal was gently lifted from the tail, allowing the forepaws to rest on the table, and dragged backwards at a constant speed (20 cm/s) for 100 cm. The adjusting steps made with the forepaws were counted by two distinct observers. Rats were trained on both motor tasks until their performance was reproducible. On the day of experiment, motor performance in the bar and drag test was evaluated before (control session) and at different time-points after drug administration (30, 90, 180, 300, 480 min). Drug effect has been expressed as a percent of pre-treatment values. BC preparations (free BC, BC–MAD, and BC–NLC) were given intraperitoneally (i.p.) at a dose of 0.3 mg/Kg (9–13 animals each group). Free BC was administered in a saline solution (0.9 mg/ml). The effect of vehicle (empty MAD and empty NLC) was also investigated (7–9 animals each group). The dose of the lipid given to each rat was calculated to be 70 mg/Kg and 67 mg/Kg for NLC and MAD, respectively.

2.7.3. Statistical analysis

Statistical analysis was performed on percent data by one-way repeated measures (RM) analysis of variance (ANOVA). In case ANOVA yielded to a significant *F* score, post hoc analysis was performed by contrast analysis to determine group differences. In case a significant time × treatment interaction was found, the sequentially rejective Bonferroni's test was used (implemented on excel spreadsheet) to determine specific differences (i.e., at the single time point level) between groups. p-Values < 0.05 were considered to be statistically significant.

3. Results and discussion

For several years, we have been trying to develop an approach to deliver BC in a controlled fashion [35,36]. Our interest in this molecule arises from its wide therapeutic potential. BC is a dopamine receptor agonist used for the treatment of pituitary tumors, PD, hyperprolactinaemia, neuroleptic malignant syndrome, and recently approved for the treatment of type 2 diabetes [37].

We previously produced and characterized SLN to deliver BC, demonstrating that NLC constituted of tristearin/Miglyol mixture can prolong BC antiparkinsonian action in vivo [20]. In the present study, we investigated MAD as an alternative nanotechnology system to deliver BC. MAD are biocompatible nanosystems able to incorporate lipid molecules in a molecular sponge consisting of interpenetrating nanochannels filled with water and coated by lipid bilayers [38]. Much interest grew around cubic phases because of their unique biologically compatible microstructure, which is capable to control the release of soluble molecules such as drugs and proteins [39]. Like NLC, MAD represents an interesting alterna-

tive to liposomes, being characterized by a higher viscous resistance to rupture and a consequent greater stability.

3.1. Characterization of dispersions

Table 1 summarizes the results of PCS studies conducted to determine the dimensional distribution of MAD and NLC dispersions, in the absence and in the presence of BC.

Both MAD and NLC had mean intensity diameters of ~200 nm. Empty MAD had a mean diameter of 198.2 nm, expressed as Z Average. The analysis by volume revealed a mean diameter of 121.0 nm. BC incorporation slightly increased the mean diameter of nanostructures to 204.8 nm. In-depth analysis of the distribution by volume revealed a huge peak with a mean diameter of 109.1 nm (84.3% of Peak Area) and a smaller one with a mean diameter of 286.3 nm (15.7%). After filtration, the mean size of the larger particles measured by laser diffraction was 28 ± 2.7 μm (mean ± SD of three runs), ranging between 25 and 30 μm (data not shown).

NLC dispersions were not filtered since they did not display aggregates or large microparticles. Empty NLC showed a mean diameter of 196.2 nm, which was not affected by BC incorporation, even if the amount of larger nanoparticles increased, conferring the distribution a bimodal profile. Dimensional analysis by volume revealed a mean diameter of 131.4 nm for the more conspicuous population and a mean diameter of 392.4 nm for the other. On the other hand both populations displayed low polydispersity indexes (0.18 and 0.19), indicating a narrow dimensional distribution [22].

Size distribution was also determined by SdFFF. The fractograms obtained under the same separation conditions (to allow a direct comparison) were converted into PSD plots, i.e., the amount of material per unit change of diameter, according to well-proven equations, by transforming the retention time in the diameter of the equivalent sphere (d), and the UV signal into a mass frequency function (dd) [24,40]. Fig. 1 shows the PSD plots of a diluted amount of BC–MAD (panel A) and BC–NLC (panel B) dispersions. The conversion was performed by assuming an average density of 0.0133 g/ml for MAD and 0.0283 g/ml for NLC. In panel A, the main peak had a maximum at ~130 nm and showed a small shoulder, possibly masking a minor population of particles of ~160 nm size, as also evidenced in the original fractogram reported in the inset of panel A. These size distributions partly differed from PCS data reported in Table 1. However, the cryo-TEM image reported below (Fig. 2) confirms the presence of particles of different size, structure, and possibly density, which generates particle masses difficult to be efficiently separated under these experimental conditions.

As shown in a previous study [20], NLC particles had instead a quite regular and reproducible shape, independent of their size, thus also their density might be considered constant, guaranteeing a better reliability to the SdFFF results presented in panel B. The graph shows a thin peak centered at ~100 nm and another one, smaller and broader, with a maximum at ~275 nm. These data are in good agreement with the PCS analysis. The apparent

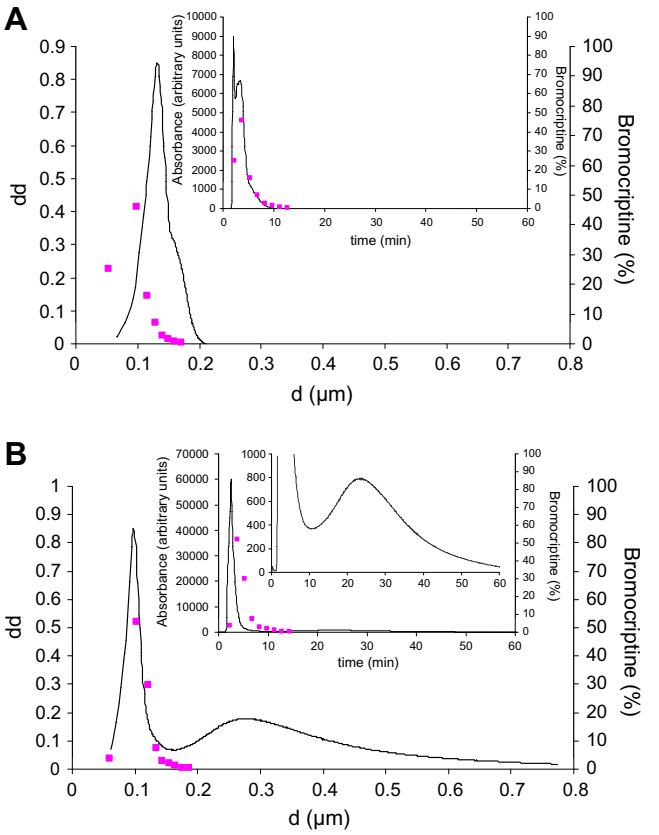

Fig. 1. PSDs elaborated from the SdFFF fractograms. (A) MAD particles were assumed to have a density of 0.0133 g/ml (d = diameter of nanoparticles; dd = dimensional distribution; the dots indicate BC content, as determined by HPLC). (B) NLC particles: assumed density 0.0283 g/ml. (For interpretation of the references to color in this figure legend, the reader is referred to the web version of this article.)

discrepancy in the relative proportions between the two peaks is an artifact introduced by the conversion into PSD, as it can be verified by observing the original fractogram reported on the top of panel B, where the larger peak is scarcely visible from the baseline, unless to zoom in the graph.

Cryo-TEM analyses were conducted in order to investigate the internal structures of MAD and NLC. Fig. 2 reports cryo-TEM images of a sample of non-filtered BC–MAD. Well-shaped particles with a homogeneous, ordered inner structure can be observed. Upon closer inspection, images reveal two different internal patterns (labeled C and H), with a predominance of the C over the H structural motif (panel A). The H motif also appears in some larger particles (panel B) with poly-"crystalline" nature, whereas smaller particles show a single internal structure. Finally, particles with ordered inner structure and vesicular structures attached on their surface can be observed, as previously found by other authors [7].

Fast Fourier transform (FFT) analysis was used to characterize the internal morphology of the particles, since FFT easily allows

Table 1
Mean diameters of MAD and NLC determined by PCS.

Parameter	MAD dispersion	BC–MAD dispersion[a]	NLC dispersion	BC–NLC dispersion[a]
Z Average mean diameter (nm)	198.2 ± 1.2	204.8 ± 1.2	196.2 ± 2.4	195.1 ± 3.3
Analysis by volume mean diameter (nm)	121 ± 2.5 (Peak Area 100%)	109.1 ± 2.4 (Peak Area 84.3 ± 3.2%) 286.3 ± 3.3 (Peak Area 15.7 ± 4.1%)	135.9 ± 3.2 (Peak Area 100%)	101.4 ± 1.8 (Peak Area 85.5 ± 3.1%) 272.4 ± 2.2 (Peak Area 14.5 ± 2.3%)
Polydispersity index	0.18 ± 0.02	0.19 ± 0.01	0.18 ± 0.02	0.19 ± 0.03

PCS data are means of five determinations on different batches of the same type of dispersion.
[a] Produced in the presence of bromocriptine.

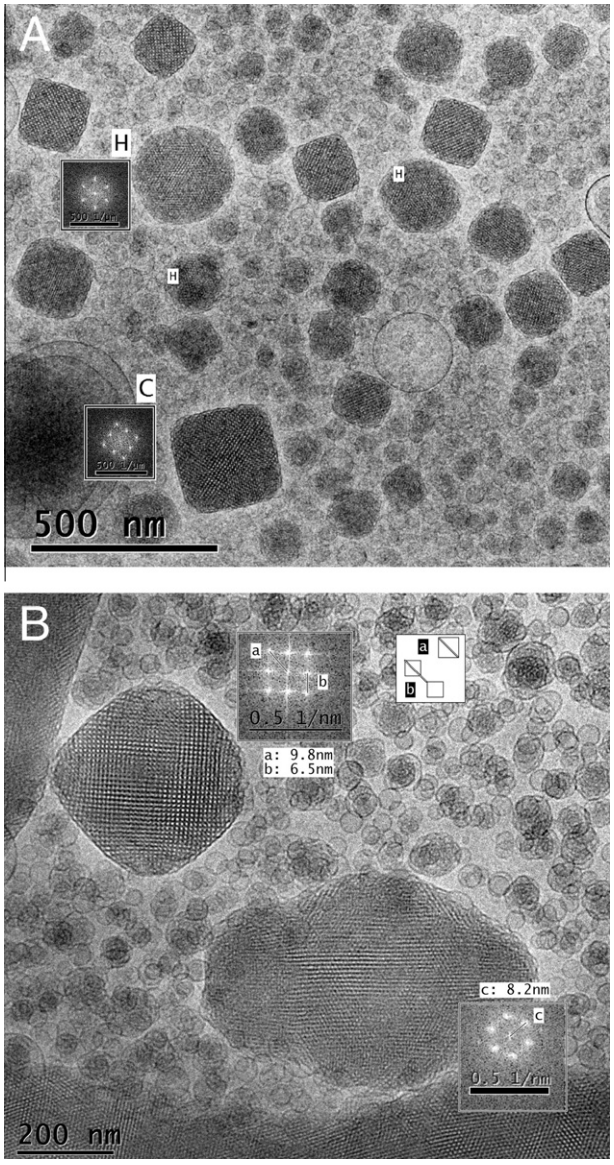

Fig. 2. Cryo-TEM images of BC–MAD. The insets show Fast Fourier transforms of some particles.

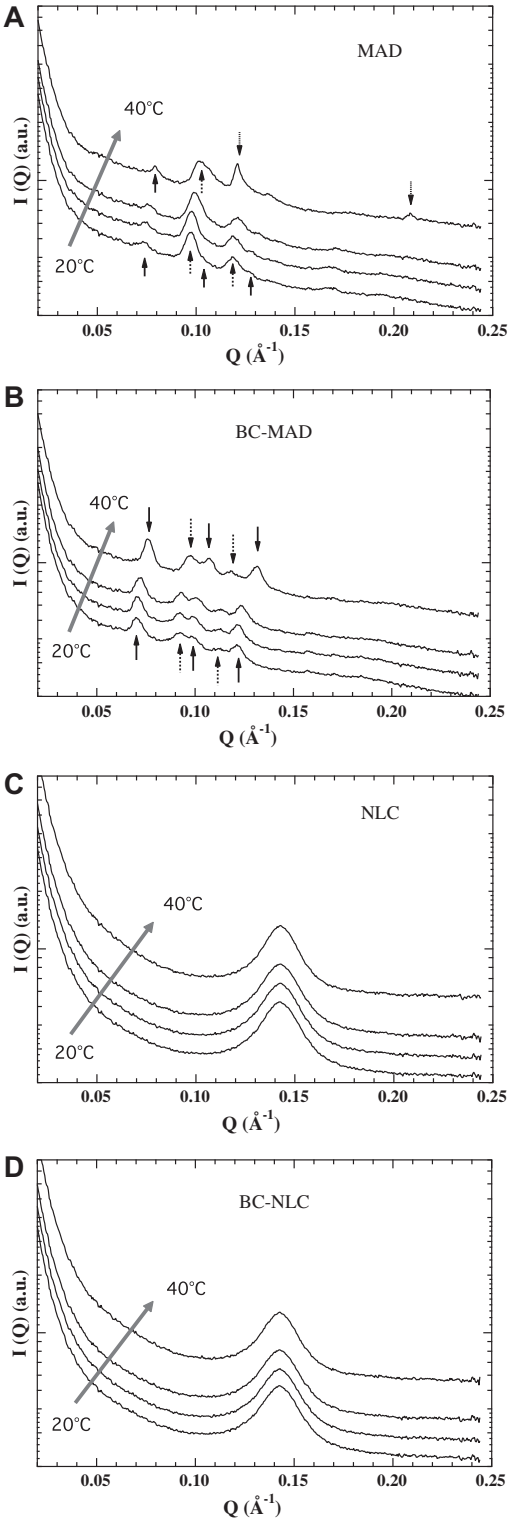

Fig. 3. Low-angle X-ray diffraction profiles observed from MAD and NLC samples at different temperatures. Measurements have been performed at 20, 25, 30, and 40 °C, scattering curves are stacked consistently, following the direction of the gray arrows. In panels A and B, small arrows indicate the peak indexing: upward, continuous arrow, *Im3m* phase (the indicated peak sequence is [110], [200], [211]); upward, dashed arrow, *Pn3m* phase ([110] and [111]); downward, pointed arrow, *H* phase ([10] and [21]).

to obtain an optical diffractogram similar to an electron diffraction pattern. In this way, periodic or repeatable distances in the mesophase structure could be detected, together with the symmetry of the motif. According to the different internal morphologies shown in Fig. 2, FFT evidenced two different patterns. The first, observed in the particles with the H structural motif, corresponds to a two dimensional (2D) hexagonal symmetry with 2D lattice parameters $v = w = 8.2$ nm (labeled c in panel B) and $\gamma = 120°$. The second, observed in the particles with the C structural motif, corresponds to a rectangular symmetry with 2D lattice parameters $v = 6.5$ nm (labeled a), $w = 9.8$ nm (labeled b), and $\gamma = 90°$.

The presence of particles with two different inner structures was also indicated by X-ray diffraction results. However, since both structures are cubic, data definitely prove that MAD dispersions are cubosomes. Fig. 3 (panels A and B) shows the low-angle X-ray diffraction profiles of empty and BC–MAD obtained as a function of temperature. At room temperature, diffraction profiles are characterized by two series of peaks, consistent with the presence of dispersed cubic phase particles of *Pn3m* and *Im3m* symmetry. In other words, in the presence and in the absence of BC, MAD dispersions can exhibit D-type or P-type structures. Phase coexistence in the MO/poloxamer 407/water disperse system has already been

Table 2
Structure identifications and unit cell dimensions observed in the different samples at various temperatures.

Sample	Temp. (°C)	Phase and unit cell (nm)						Hydrocarbon chain conformation
MAD	20	Im3m	12.11	**Pn3m**	9.16			α
	25	Im3m	12.01	**Pn3m**	9.11			α
	30	Im3m	11.77	**Pn3m**	8.99			α
	40	Im3m	11.25	**Pn3m**	8.71	H	6.01	α
BC-MAD	20	**Im3m**	12.69	Pn3m	9.66			α
	25	**Im3m**	12.64	Pn3m	9.65			α
	30	**Im3m**	12.41	Pn3m	9.58			α
	40	**Im3m**	11.72	Pn3m	9.14			α
NLC	20–40[a]	L	4.42					β
BC-NLC	20–40[a]	L	4.42					β

When samples show more than one structure, the one characterized by the higher X-ray diffraction profile is shown in bold. Error in unit cells is ±0.02 nm.
[a] From 20 to 40° C, i.e., 20, 25, 30, and 40 °C.

observed [11], even if in the same conditions the presence of a pure *Im3m* phase was also reported [8]. As previously discussed [41], the different structural behaviors of MAD may be related to differences in composition (e.g., MO quality, buffer, ionic force of the aqueous solution) and production procedures (e.g., ultrasonication, homogenization, temperature and pressure parameters). However, the present results confirmed that at this poloxamer 407 concentration, the cubic and not the vesicular structure is the equilibrium state, even in the presence of BC. It should be noticed that both types of cubic structures detected in our preparation are bicontinuous, but the P-surface structure only occurs in the MO–water system when a third component is added [42]. Moreover, the lattice constants, which have been derived from peak positions (Table 2), are very similar to those reported by Nakano et al. [11]. More interestingly, lattice constants are slightly sensitive to the presence of BC, probably due to an increased hydration of the lipid phases induced by BC.

Cryo-TEM and X-ray diffraction results are in perfect agreement. Indeed, the FFT patterns suggest that the H and C structural motifs correspond to planes normal to the crystallographic directions [1 1 1] and [1 1 0] of a cubic lattice, respectively (Fig. 2). Concerning the H motif, it should be recalled that the projection of a 3D cubic array on 2D is hexagonal when visualized along the [1 1 1] direction and that the corresponding 2D lattice parameters are related to the cubic unit cell dimension a by $v = w = a/\sqrt{2}$. This does neither allow to identify the space group of the particle internal structure nor to differentiate between a hexagonal and a cubic structure. However, the comparison of 2D lattice values with the unit cell dimensions determined by X-ray diffraction (Table 2) strongly suggests that the H particles are cubosomes with an inner cubic structure belonging to the *Im3m* space group. It is worthy of mention that only the *Pn3m* and *Im3m* space groups are allowed in cubosome dispersions because those are the only two space groups established in reversed bicontinuous cubic phases in excess water [43] or in reversed bicontinuous cubic phase dispersions [12]. Concerning the C-motif, the observed 2D lattice parameters are consistent with the ideal values for a cubic array ($v = w/\sqrt{2}$) and correspond to a cubic unit cell dimension a of 9.8 nm. This value compares well with the unit cell of the *Pn3m* cubic phase determined in the same system by X-ray diffraction (Table 2), indicating that C particles are cubosomes with an inner cubic structure belonging to the *Pn3m* space group. Overall, cryo-TEM images of BC–MAD dispersed particles gave strong and direct evidence for the coexistence of cubosomes with two different internal structures: one with a *Pn3m* space group and a lattice parameter of 9.8 nm and another with *Im3m* space group and a lattice parameter of 11.6 nm.

X-ray diffraction experiments also reveal the thermal stability of MAD. As shown in Fig. 3, both D- and P-type cubosomes exist at all the investigated temperatures. However, in empty MAD samples, two other peaks, characteristic of a 2D hexagonal space group, appeared at 40 °C. Since at this temperature, the peaks of the *Pn3m* cubic structure broadened, it appears that temperature induces a D-type cubosome-to-hexasome phase transition [12,44]. Therefore, even if the inner structure of MAD can be highly dependent on manufacturing parameters and then be relevant for the properties of the dispersions, X-ray diffraction demonstrates that the presence of D-type cubosomes does not cause the complete loss of the cubic state of the particles at relatively high temperatures.

Empty and BC–NLC dispersions have been already characterized [20]. In addition, low-angle X-ray diffraction obtained as a function of temperature is now reported (see Fig. 3, panels C and D). In agreement with previous observation [20], both in the absence and in the presence of BC, the diffraction profile is characterized by a large peak, whose position is unaffected by temperature and BC addition (Table 2). The inner lamellar order and the strong structural stability of NLC, even in the presence of BC, appear also confirmed.

3.2. BC encapsulation

HPLC analyses revealed that BC recovery after the production process in the filtered dispersion was 70 ± 0.75% (MAD) and 84 ± 0.58% (NLC) of the total amount of drug used for the preparation. The values of drug loss were taken in consideration to determine BC encapsulation.

SdFFF was employed to obtain information about the drug distribution in the dispersions. During the fractionation, some fractions were collected and analyzed by HPLC to quantify the amount of drug contained in the different particle populations of the disperse phase. In Fig. 1, the concentration of BC determined by HPLC is reported. BC was found to be entirely associated with particles in both MAD and NLC dispersions.

The fraction corresponding to a mean diameter of about 54 nm contains 25% of the total drug, as shown in panel A. The highest amount of BC (46%) is contained in the most representative portion of nanoparticles/vesicles, having a diameter of 98 nm. The remaining 29% of BC is associated with the least representative population of particles, having larger diameters. In fact, cryo-TEM and PCS analyses showed that MAD are mainly characterized by vesicles and cubosomes with 90–100 nm mean diameter, and few structures with larger dimensions.

Also for NLC, whose PSD is reported in panel B, the highest amount of BC (52%) is contained in the most representative fraction, characterized by particles with a mean diameter of ~103 nm. The fraction corresponding to a mean diameter of ~59 nm contains only 3.5% of the total drug, the remaining 44.5% of BC being found into a less representative population of larger particles.

3.3. In vivo tests

In 6-OHDA hemilesioned rats, motor impairment mainly affects the side of the body contralateral to the denervated hemisphere (i.e., the toxin injection side). Consistently, the immobility time of the ipsilateral paw (35.7 ± 1.9 s; $n = 42$) was lower compared to that of the contralateral (parkinsonian) one (47.4 ± 1.9, $n = 42$). Moreover, the number of steps made by the ipsilateral paw was higher (11.1 ± 0.4; $n = 46$) than that made by the contralateral one (1.9 ± 0.1; $n = 46$).

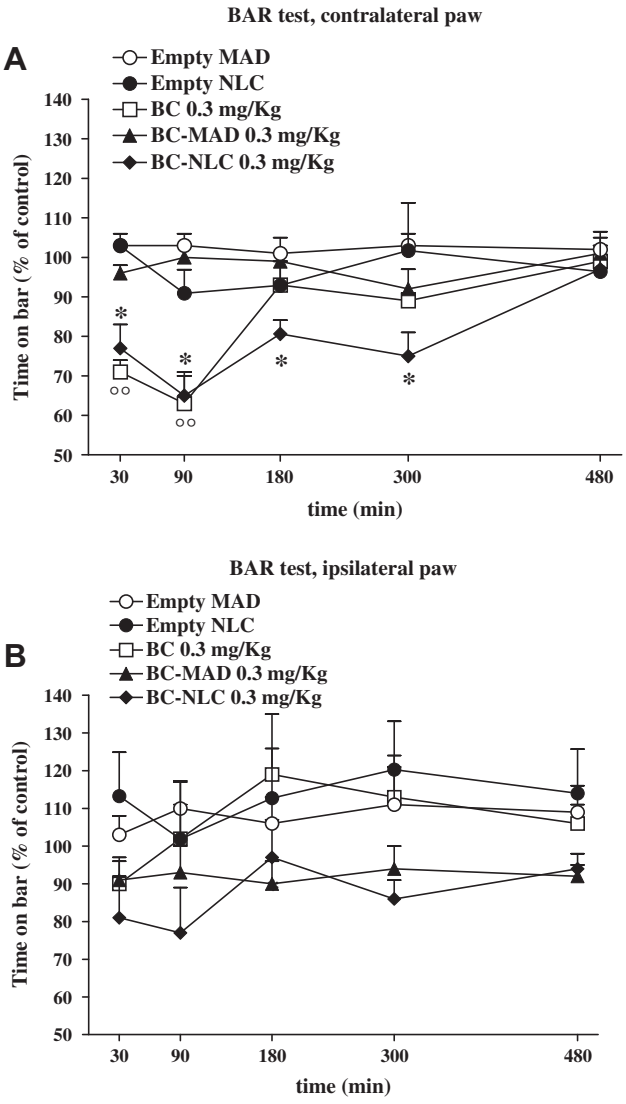

Fig. 4. Systemic administration via i.p. of free bromocriptine (BC) and bromocriptine encapsulated in MAD (BC–MAD) or nanoparticles (BC–NLC) in hemiparkinsonian rats attenuated akinesia in the bar test. The administered dose of BC was always 0.3 mg/Kg. Rats injected with vehicles (empty MAD or NLC) are also shown. Immobility time was calculated at different time-points (30, 90, 180, 300, and 480 min from injection) both at the contralateral (panel A) and at ipsilateral (panel B) forepaw (in sec), and expressed as percent of pre-treatment values. Data are means ± SEM of 7–11 animals per group. $^{**}p < 0.01$ different from empty NLC. $^{\circ\circ}p < 0.01$ different from empty MAD and NLC.

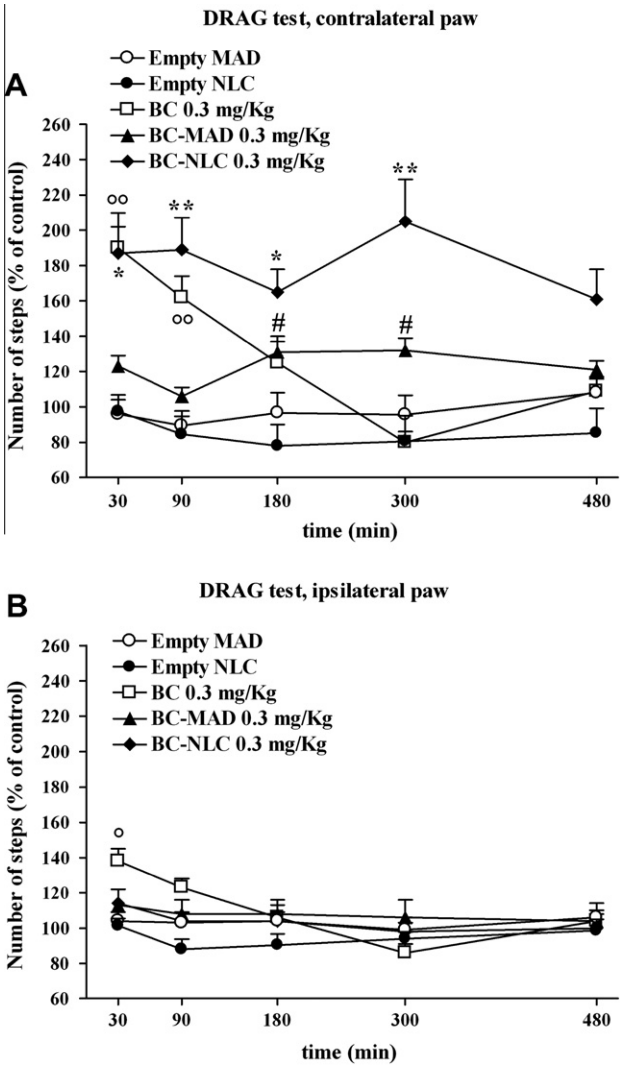

Fig. 5. Systemic administration via i.p. of free bromocriptine (BC) and bromocriptine encapsulated in MAD (BC–MAD) or nanoparticles (BC–NLC) in hemiparkinsonian rats attenuated akinesia/bradykinesia in the drag test. The administered dose of BC was always 0.3 mg/Kg. Rats injected with vehicles (empty MAD or NLC) are also shown. The number of steps was calculated at different time-points (30, 90, 180, 300, and 480 min from injection) both at the contralateral (panel A) and at the ipsilateral (panel B) forepaw, and expressed as percent of pre-treatment values. Data are means ± SEM of 7–13 animals per group. $^{*}p < 0.05$; $^{**}p < 0.01$ different from empty NLC. $^{\circ\circ}p < 0.01$ different from empty MAD and NLC. $^{\#}p < 0.05$ different from empty MAD.

Repeated measure ANOVA on the immobility time at the contralateral paw in the bar test (Fig 4A) revealed main effects of treatment ($F_{4,36} = 15.83$, $p < 0.0001$) and time ($F_{4,155} = 7.51$, $p < 0.0001$), and a time × treatment interaction ($F_{16,155} = 3.58$, $p < 0.0001$). Post hoc analysis showed that both free BC and BC–NLC reduced the time spent on bar (i.e., attenuated akinesia) compared to vehicle-treated animals, although the action of BC–NLC was more prolonged (Fig. 4A). Indeed, both free BC and BC–NLC produced a significant reduction in akinesia 30 min after administration (∼77% and ∼71% of control, respectively) and were maximally effective after 90 min (∼63% and ∼65% of control, respectively). However, the effect of free BC was not significant after 3 h (∼93%) whereas that of BC–NLC was still detectable up to 3 h after administration (∼80%). No significant changes of the immobility time at the ipsilateral paw were induced by any BC formulations (Fig 4B).

Repeated measure ANOVA on the number of steps at the contralateral paw in the drag test (Fig 5A) revealed main effects of treatment ($F_{4,36} = 41.31$, $p < 0.0001$) and time ($F_{4,185} = 3.38$, $p = 0.0106$) and a significant time × treatment interaction ($F_{16,185} = 3.80$, $p < 0.0001$). Post hoc analysis revealed that the three BC preparations improved stepping activity at the contralateral paw although with different efficacies and time-courses. As shown in the bar test, both free BC and BC–NLC elevated stepping activity at 30 min after administration (both ∼190% of control). However, the effect of free BC vanished after 3 h (∼125%) whereas that of BC–NLC was significant both at 3 h (∼165%) and 5 h (∼205%) after administration. At 8 h after administration, rats treated with BC–NLC still showed an elevated stepping activity (∼160%), although this value did not reach the level of statistical significance. At variance with the bar test, BC–MAD was able to attenuate motor disability in the drag test, causing a mild elevation at 3 h (∼131%) and 5 h (∼132%) from administration.

Also stepping activity at the ipsilateral paw was affected by BC treatment (Fig 5B). Repeated measure ANOVA on the number of

steps at the ipsilateral paw did not reveal main effect of treatment ($F_{4,36} = 0.96$, $p = 0.44$) but a significant effect of time ($F_{4,185} = 9.82$, $p < 0.0001$) and a time × treatment interaction ($F_{16,185} = 3.43$, $p < 0.0001$). Post hoc analysis showed that among the different BC formulations, only free BC improved stepping activity at the ipsilateral paw, specifically at 30 min after administration (~139%).

Among the various therapeutic applications of BC, we chose to focus on the antiparkinsonian activity since great therapeutic value has been attributed to formulations capable to provide continuous DA receptor stimulation [45,46]. Indeed, it has been demonstrated that long-term side-effects of L-DOPA (mainly dyskinesia) arise from non-physiological "pulsatile" stimulation of DA receptors, which parallels plasmatic drug levels [47]. Thus, continuous delivery or sustained release formulations of L-DOPA have been proved to be less dyskinesiogenic than conventional formulations. Consistently, DA receptor agonists (the most effective alternative to L-DOPA) are less dyskinesiogenic than L-DOPA, probably due to the longer half-life. Achieving a stable and prolonged DA receptor stimulation may also be advantageous in the case of DA agonists, as it allows for a reduction in the frequency of administration and occurrence of side-effects at peak levels. In the present study, we employed two different behavioral tests providing complementary information on motor function: the bar and the drag tests. The responses to BC and its NLC formulation were consistent in both tests. Thus, BC caused a reduction in immobility time (i.e., reduced akinesia) and improvement of stepping activity (i.e., reduced akinesia/bradykinesia), which lasted for at least 90 min and disappeared after 3 h from administration. BC encapsulated in NLC essentially mimicked these effects providing a more prolonged attenuation of motor disability which lasted for at least 5 h and vanished within 8 h. The obtained results extend our previous finding [20] and confirm the ability of BC–NLC to provide longer lasting therapeutic benefit compared to conventional BC formulations. The finding that free BC caused a rapid and transient (30 min) elevation of stepping also at the ipsilateral paw may reflect differences in drugs kinetics since it was not replicated by BC–NLC. In fact, in keeping with the view that conventional BC preparations result in higher peak levels, BC might also improve motility at the ipsilateral paw, which is controlled by the undenervated striatum.

Quite remarkably, BC–MAD was ineffective in the bar test and caused only a mild and delayed elevation of stepping activity in the drag test.

The different in vivo efficacies of BC–MAD and BC–NLC could be attributed to differences in nanoparticulate morphology. In fact, the former are characterized by the coexistence of cubosomes and vesicles while the latter are solid matrix systems.

It has been demonstrated that the intraperitoneal administration prolongs the blood circulation of colloidal drug carriers with respect to the intravenous administration, due to slow absorption of the carrier from the abdominal cavity [48]. On the other hand, it is known that colloidal drug carriers are rapidly opsonized and cleared by the macrophages of the reticulo-endothelial system (RES). Thus, as a general rule, nanosystems are mostly taken up by the liver and the spleen within minutes after systemic administration [49]. In the case of BC–MAD, it can be hypothesized that cubosomes are mainly sequestered by the peritoneal and RES macrophages, as shown for liposomes and nanoparticles [50,51]. Therefore, the mild and sustained effect of BC–MAD may be due to the smaller vesicular liquid-like component of MAD that is responsible for prolonging the half-life of the incorporated drug, having a long circulating time.

Conversely, the NLC structure allows to provide therapeutic BC concentrations to the brain for a long period of time [20]. This might be related to the ability of NLC to pass the BBB [14,18] and/or to a longer stability of NLC in the blood. In fact, previous studies [52] demonstrated that after intraperitoneal administration, nanoparticles show a biphasic absorption: an initial rapid distribution into blood, followed by a slow disposition from peritoneum, resulting in sustained drug release.

Moreover, NLC produced in the presence of poloxamer 188 in the aqueous phase may behave as "stealth carriers," thus being somewhat protected by opsonization [19].

4. Conclusions

This study indicates that both MAD and NLC are able to encapsulate BC, the drug being fully dissolved in nanoparticles. X-ray diffraction and cryo-TEM studies consistently revealed the presence of dispersed cubic phase of *Pn3m* and *Im3m* symmetry in MAD and a gel state with an inner lamellar order in NLC. In vivo studies showed that only BC–NLC were able to markedly attenuate motor deficit in 6-OHDA hemilesioned rats, suggesting that NLC represent a more effective carrier to prolong the half-life of BC in vivo.

Appendix A. Supplementary data

Supplementary data associated with this article can be found, in the online version, at doi:10.1016/j.ejpb.2011.10.015.

References

[1] A. Yaghmur, O. Glatter, Characterization and potential applications of nanostructured aqueous dispersions, Adv. Coll. Interf. Sci. 148 (2009) 333–342.
[2] K. Westesen, B. Siekmann, Biodegradable colloidal drug carrier systems based on solid lipids, in: S. Benita (Ed.), Microencapsulation, Marcel Dekker, New York, 1996, pp. 213–258.
[3] R.H. Muller, K. Mader, S. Gohla, Solid lipid nanoparticles (SLN) for controlled delivery – a review of the state of the art, Eur. J. Pharm. Biopharm. 50 (2000) 161–177.
[4] J. Pardeike, A. Hommoss, R.H. Müller, Lipid nanoparticles (SLN,NLC) in cosmetic and pharmaceutical dermal products, Int. J. Pharm. 366 (2009) 170–184.
[5] R.H. Muller, M. Radtke, S.A. Wissing, Solid lipid nanoparticles (SLN) and nanostructured lipid carriers (NLC) in cosmetic and dermatological preparations, Adv. Drug Del. Rev. 54 (2002) S131s–S155.
[6] J. Gustafsson, H. Ljusberg-Wharen, M. Almgrem, K. Larsson, Cubic lipid/water phase dispersed into submicron particles, Langmuir 12 (1996) 4611–4613.
[7] L. de campo, A. Yaghmur, L. Sagalowicz, M.E. Leser, H. Watzke, O. Gattler, Reversible phase transitions in emulsified nanostructured lipid systems, Langmuir 20 (2004) 5254–5261.
[8] J. Gustafsson, H. Ljusberg-Wharen, M. Almgrem, K. Larsson, Submicron particles of reversed lipid phases in water stabilized by a nonionic amphiphilic polymer, Langmuir 13 (1997) 6964–6971.
[9] E. Esposito, N. Eblovi, S. Rasi, M. Drechsler, G.M. Di Gregorio, E. Menegatti, R. Cortesi, Lipid based supramolecular systems for topical application: a preformulatory study, AAPS Pharm. Sci. 5 (2003) 4 (article 30).
[10] P.T. Spicer, K.L. Hayden, Novel process for producing cubic liquid crystalline nanoparticles (cubosomes), Langmuir 17 (2001) 5748–5756.
[11] M. Nakano, A. Sugita, H. Matsuoka, T. Handa, Small angle X-ray scattering and 13C NMR investigation on the internal structure of cubosome, Langmuir 17 (2001) 3917–3922.
[12] L. Sagalowicz, R. Mezzenga, M.E. Leser, Investigating reversed liquid crystalline mesophases, Curr. Opin. Colloid Interf. Sci. 11 (2006) 224–229.
[13] J. Lai, J. Chen, Y. Lu, J. Sun, F. Hu, Z. Yin, W. Wu, Glyceryl monooleate/Poloxamer 407 cubic nanoparticles as oral drug delivery systems: I. In vitro evaluation and enhanced oral bioavailability of the poorly water-soluble drug simvastatin, AAPS Pharm. Sci. Technol. 10 (2009) 960–966.
[14] E. Barbu, É. Molnàr, J. Tsibouklis, D.C. Górecki, The potential for nanoparticle-based drug delivery to the brain: overcoming the blood–brain barrier, Expert Opin. Drug Del. 6 (2009) 553–565.
[15] S. Pasha, K. Gupta, Various drug delivery approaches to the central nervous system, Expert Opin. Drug Del. 7 (2010) 113–135.
[16] V. Kabanov, E.V. Batrakova, New technologies for drug delivery across the blood brain barrier, Curr. Pharm. Des. 10 (2004) 1355–1363.
[17] K. Andrieux, P. Couvreur, Polyalkylcyanoacrylate nanoparticles for delivery of drugs across the blood–brain barrier, Nanomed. Nanobiotechnol. 1 (2009) 463–474.
[18] I.P. Kaur, R. Bhandari, S. Bhandari, V. Kakkar, Potential of solid lipid nanoparticles in brain targeting, J. Control. Rel. 127 (2008) 97–109.
[19] M.D. Joshi, R.H. Müller, Lipid nanoparticles for parenteral delivery of actives, Eur. J. Pharm. Biopharm. 71 (2009) 161–172.
[20] E. Esposito, M. Fantin, M. Marti, M. Drechsler, L. Paccamiccio, P. Mariani, E. Sivieri, F. Lain, E. Menegatti, M. Morari, R. Cortesi, Solid lipid nanoparticles as delivery systems for bromocriptine, Pharm. Res. 25 (2008) 1521–1530.

[21] http://www.fscimage.fishersci.com/msds/06352.html.
[22] E. Esposito, R. Cortesi, M. Drechsler, L. Paccamiccio, P. Mariani, C. Contado, E. Stellin, E. Menegatti, F. Bonina, C. Puglia, Cubosome dispersions as delivery systems for percutaneous administration of indomethacin, Pharm. Res. 22 (2005) 2163–2173.
[23] R. Pecora, Dynamic light scattering measurement of nanometer particles in liquids, J. Nanoparticle Res. 2 (2000) 123–131.
[24] C. Contado, A. Dalpiaz, E. Leo, M. Zborowski, P.S. Williams, Complementary use of flow and sedimentation field-flow fractionation techniques for size characterizing biodegradable poly(lactic acid) nanospheres, J. Chromatogr. A 1157 (2007) 321–335.
[25] C. Contado, G. Blo, F. Fagioli, F. Dondi, R. Beckett, Characterisation of River Po particles by sedimentation field-flow fractionation coupled to GFAAS and ICP-MS, Colloid Surf. A – Physicochem. Eng. Asp. 120 (1997) 47–59.
[26] P. Andreozzi, S.S. Funari, C. La Mesa, P. Mariani, M.G. Ortore, R. Sinibaldi, F. Spinozzi, Multi- to unilamellar transitions in catanionic vesicles, J. Phys. Chem. B 114 (2010) 8056–8060.
[27] P. Mariani, V. Luzzati, H. Delacroix, Cubic phases of lipid containing systems. Structure analysis and biological implications, J. Mol. Biol. 204 (1988) 165–189.
[28] F. Spinozzi, L. Paccamiccio, P. Mariani, L.Q. Amaral, Melting regime of the anionic phospholipid DMPG: new lamellar phase and porous bilayer model, Langmuir 26 (2010) 6484–6493.
[29] M. Marti, F. Mela, M. Fantin, S. Zucchini, J. M Brown, J. Witta, M. Di Benedetto, B. Buzas, R.K. Reinscheid, S. Salvadori, R. Guerrini, P. Romualdi, S. Candeletti, M. Simonato, B.M. Cox, M. Morari, Blockade of nociceptin/orphanin FQ transmission attenuates symptoms and neurodegeneration associated with Parkinson's disease, J. Neurosci. 95 (2005) 9591–9601.
[30] G. Paxinos, C. Watson, The rat brain in stereotaxic coordinates, Academic, Sydney, 1982.
[31] M. Marti, C. Trapella, R. Viaro, M. Morari, The nociceptin/orphanin FQ receptor antagonist J-113397 and L-DOPA additively attenuate experimental parkinsonism through overinhibition of the nigrothalamic pathway, J. Neurosci. 27 (2007) 1297–1307.
[32] M. Marti, F. Mela, C. Bianchi, L. Beani, M. Morari, Striatal dopamine-NMDA receptor interactions in the modulation of glutamate release in the substantia nigra pars reticulata in vivo. Opposite role for D1 and D2 receptors, J. Neurochem. 83 (2002) 635–644.
[33] P.R. Sanberg, M.D. Bunsey, M. Giordano, A.B. Norman, The catalepsy test: its ups and downs, Behav. Neurosci. 102 (1988) 748–759.
[34] T. Schallert, M. De Rick, I.Q. Whishaw, V.D. Ramirez, P. Teitelbaum, Excessive bracing reactions and their control by atropine and L-DOPA in an animal analog of Parkinsonism, Exp. Neurol. 64 (1979) 33–43.
[35] C. Nastruzzi, C. Pastesini, R. Cortesi, E. Esposito, R. Gambari, E. Menegatti, Kinetic of bromocriptine release from microspheres: comparative analysis between different in vitro models, J. Microencapsul. 11 (1993) 565–574.
[36] E. Esposito, R. Cortesi, E. Menegatti, C. Nastruzzi, Preformed gelatin microspheres as a delivery system for bromocriptine, Pharm. Sci. Comm. 4 (1994) 239–246.
[37] R. Mahajan, Bromocriptine mesylate: FDA-approved novel treatment for type-2 diabetes, Indian J. Pharmacol. 41 (2009) 197–198.
[38] G. Garg, S. Saraf, S. Saraf, Cubosomes: an overview, Biol. Pharm. Bull. 30 (2007) 350–353.
[39] J.C. Shah, Y. Sadhale, D.M. Chilukuri, Cubic phase gels as drug delivery systems, Adv. Drug Deliv. Rev. 47 (2001) 229–250.
[40] K. Jores, W. Mehnert, M. Drechsler, H. Bunjes, C. Johann, K. Maeder, Investigations on the structure of solid lipid nanoparticles (SLN) and oil-loaded solid lipid nanoparticles by photon correlation spectroscopy, field-flow fractionation and transmission electron microscopy, J. Control. Rel. 95 (2004) 217–227.
[41] G. Worle, M. Drechsler, M.H.J. Koch, B. Siekmann, K. Westesen, H. Bunjes, Influence of composition and preparation parameters on the properties of aqueous Monoolein dispersions, Int. J. Pharm. 329 (2007) 150–157.
[42] V. Luzzati, H. Delacroix, A. Gulik, T. Gulik-Krzywicki, P. Mariani, R. Vargas, The cubic phases of lipids, Curr. Top. Membr. 44 (1997) 3–24.
[43] M. Pisani, S. Bernstorff, C. Ferrero, P. Mariani, Pressure induced cubic-to-cubic phase transition in Monoolein hydrated system, J. Phys. Chem. B 105 (2001) 3109–3119.
[44] A. Yaghmur, L. de Campo, S. Salentinig, L. Sagalowicz, M.E. Leser, O. Glatter, Oil-loaded monolinolein-based particles with confined inverse discontinuous cubic structure (Fd3m), Langmuir 22 (2006) 517–521.
[45] A. Di Stefano, P. Sozio, A. Iannitelli, L.S. Cerasa, New drug delivery strategies for improved Parkinson's disease therapy, Expert Opin. Drug Del. 6 (2009) 389–404.
[46] G. Modi, V. Pillay, Y.E. Choonara, V.M. Ndesendo, L.C. du Toit, D. Naidoo, Nanotechnological applications for the treatment of neurodegenerative disorders, Prog. Neurobiol. 88 (2009) 272–285.
[47] J.A. Obeso, F. Grandas, M.T. Herrero, R. Horowski, The role of pulsatile versus continuous dopamine receptor stimulation for functional recovery in Parkinson's disease, Eur. J. Neurosci. 6 (1994) 889–897.
[48] Y. Sadzuka, R. Hirama, T. Sonobe, Effects of intraperitoneal administration of liposomes and methods of preparing liposomes for local therapy, Toxicol. Lett. 126 (2002) 83–90.
[49] J.K. Vasir, M.K. Reddy, V.D. Labhasetwar, Nanosystems in drug targeting: opportunities and challenges, Curr. Nanosci. 1 (2005) 47–64.
[50] T.M. Allen, C.B. Hansen, L.S.S. Guo, Subcutaneous administration of liposomes: a comparison with the intravenous and intraperitoneal routes of injection, Biochim. Biophys. Acta 1150 (1993) 9–169.
[51] L.H. Reddy, R.K. Sharma, K. Chuttani, A.K. Mishra, R.S.R. Murthy, Influence of administration route on tumour uptake and biodistribution of etoposide loaded solid lipid nanoparticles in Dalton's lymphoma tumour bearing mice, J. Control. Rel. 105 (2005) 185–198.
[52] L.H. Reddy, R.S.R. Murthy, Pharmacokinetics and biodistribution studies of doxorubicin loaded poly(butyl cyanoacrilate) nanoparticles synthesized by two different techniques, Biomed. Papers 148 (2) (2004) 161–166.

Neurobiology of Disease 45 (2012) 573–582

Contents lists available at SciVerse ScienceDirect

Neurobiology of Disease

journal homepage: www.elsevier.com/locate/ynbdi

In vivo evidence for a differential contribution of striatal and nigral D1 and D2 receptors to l-DOPA induced dyskinesia and the accompanying surge of nigral amino acid levels

Flora Mela [a], Matteo Marti [a], Simone Bido [a], M. Angela Cenci [b], Michele Morari [a,*]

[a] Department of Experimental and Clinical Medicine, Section of Pharmacology, Center for Neuroscience and National Institute of Neuroscience, University of Ferrara, Ferrara, Italy
[b] Basal Ganglia Pathophysiology, Department of Experimental Medical Science, Lund University, Lund, Sweden

ARTICLE INFO

Article history:
Received 1 June 2011
Revised 14 September 2011
Accepted 29 September 2011
Available online 7 October 2011

Keywords:
Dyskinesia
D1 receptor
D2 receptor
GABA
Glutamate
L-DOPA
Raclopride
SCH23390
Striatum
Substantia nigra reticulata

ABSTRACT

Evidence for an involvement of striatal D1 receptors in levodopa-induced dyskinesia has been presented whereas the contribution of striatal D2 receptors remains controversial. In addition, whether D1 and D2 receptors located in the substantia nigra reticulata shape the response to levodopa remains unknown. We therefore used dual probe microdialysis to unravel the impact of striatal and nigral D1 or D2 receptor blockade on abnormal involuntary movements (AIMs) and striatal output pathways in unilaterally 6-hydroxydopamine lesioned dyskinetic rats. Regional perfusion of D1/D5 (SCH23390) and D2/D3 (raclopride) receptor antagonists was combined with systemic administration of levodopa. Levodopa-induced AIMs coincided with a prolonged surge of GABA and glutamate levels in the substantia nigra reticulata. Intrastriatal SCH23390 attenuated the levodopa-induced AIM scores (~50%) and prevented the accompanying neurochemical response whereas raclopride was ineffective. When perfused in the substantia nigra, both antagonists attenuated AIM expression (~21–40%). However, only intranigral SCH23390 attenuated levodopa-induced nigral GABA efflux, whereas raclopride reduced basal GABA levels without affecting the response to levodopa. In addition, intranigral raclopride elevated amino acid release in the striatum and revealed a (mild) facilitatory effect of levodopa on striatal glutamate. We conclude that both striatal and nigral D1 receptors play an important role in dyskinesia possibly via modulation of the striato-nigral direct pathway. In addition, the stimulation of nigral D2 receptors contributes to dyskinesia while modulating glutamate and GABA efflux both locally and in the striatum.

© 2011 Elsevier Inc. All rights reserved.

Introduction

L-DOPA still represents the most effective treatment for Parkinson's disease (PD), although long-term therapy with L-DOPA is burdened by side-effects such as motor fluctuations and abnormal involuntary movements (dyskinesia; Fabbrini et al., 2007; Nutt, 1990). L-DOPA-induced dyskinesia (LID) results from maladaptive pre- and postsynaptic changes in dopamine (DA) transmission (Cenci, 2007). DA activates 5 receptor subtypes which are classified in the D1-like (D1 and D5) and D2-like (D2, D3 and D4) classes (henceforth D1 and D2), based on structural and pharmacological analogies (Seeman and Van Tol, 1994; Sibley and Monsma, 1992). A wealth of studies has demonstrated a major role for D1 receptors in LID. In particular, unregulated DA release from DA and non-DA neurons causes up-regulation and abnormal trafficking of D1 receptors in striatal neurons (Aubert et al., 2005; Berthet et al., 2009; Konradi et al., 2004), along with abnormal downstream signaling responses (reviewed in Cenci and Konradi, 2010). Altered D1 receptor trafficking leads to a relative enrichment of D1, but not D2 receptors at the plasma membrane in dyskinetic rats (Berthet et al., 2009). These changes are likely to alter the functions of D1-expressing striato-nigral GABAergic neurons (the so-called direct pathway), which monosynaptically inhibit nigro-thalamic output neurons causing thalamic disinhibition and movement initiation (Deniau and Chevalier, 1985). Supporting a pivotal role for D1 receptors in LID, D1 receptor agonists have strong dyskinesiogenic properties, whereas D1 receptor antagonists prevent LID in both nonhuman primate (Grondin et al., 1999) and rat (Lindgren et al., 2009; Monville et al., 2005; Taylor et al., 2005; Westin et al., 2007) models of PD. Consistently, D1 receptor knockout mice are poorly susceptible to LID, while D2 receptor knockout mice do not differ from wild-type controls in this regard (Darmopil et al., 2009). These findings do not however exclude a role of D2 receptors in LID. In fact, D2 receptor agonists precipitate dyskinesia in L-DOPA primed animals, whereas D2 receptor antagonists can attenuate LID (Grondin et al., 1999; Lindgren et al., 2009; Monville et al., 2005; Taylor

Abbreviations: AIMs, abnormal involuntary movements; ALO, axial, limb and orolingual; DA, dopamine; DLS, dorsolateral striatum; GLU, glutamate; GP, globus pallidus; LID, L-DOPA-induced dyskinesia; 6-OHDA, 6-hydroxydopamine; SNr, substantia nigra reticulata.

* Corresponding author at: Department of Experimental and Clinical Medicine, Section of Pharmacology, University of Ferrara, via Fossato di Mortara 17–19, 44100 Ferrara, Italy. Fax: +39 0532 455205.
E-mail address: m.morari@unife.it (M. Morari).
Available online on ScienceDirect (www.sciencedirect.com).

0969-9961/$ – see front matter © 2011 Elsevier Inc. All rights reserved.
doi:10.1016/j.nbd.2011.09.015

et al., 2005). Furthermore, striatal overexpression of RGS-9, a GTPase accelerating protein that terminates signaling at D2 receptors, improves LID in macaques and rodent models of PD (Gold et al., 2007). Although most studies thus far have focused on the striatum, it will be important to also consider changes occurring in other areas were D1 and D2 receptors are highly expressed, such as the substantia nigra. Indeed, contralateral turning induced by L-DOPA in unilateral 6-OHDA lesioned rats correlates with the dynamics of DA release in the substantia nigra reticulata (SNr), and can be blocked by local infusion of the D1/D5 receptor antagonist SCH23390 in this brain area (Robertson and Robertson, 1989). Moreover, L-DOPA-treated dyskinetic rats show abnormally large elevations in extracellular DA levels not only in the striatum but also in the SNr (Lindgren et al., 2010). Finally, abnormal oscillatory activity in the theta/alpha band (Meissner et al., 2006) and pronounced microvascular plasticity (Westin et al., 2006) have been detected in the SNr of dyskinetic rats. Further strengthening the contribution of the SNr to LID, we found a temporal correlation between the expression of abnormal involuntary movements (AIMs) and a large elevation of extracellular GABA levels within the SNr of dyskinetic rats (Mela et al., 2007), suggesting that GABA release from striato-nigral neurons is involved in generating LID. This previous study did not however clarify whether the surge in extracellular GABA depended on a stimulation of D1 or D2 receptors by L-DOPA-derived DA, nor did it address the anatomical location from which the effect was generated. In addition, it did not examine whether changes of nigral glutamate (GLU) levels were associated with LID. Indeed, the role of GLU in dyskinesia has long been established (Calabresi et al., 2000; Chase and Oh, 2000) and elevated in vivo GLU levels have been documented in the striatum and SNr of dyskinetic rats under basal conditions but not following L-DOPA (Robelet et al., 2004). Conversely, other studies have reported increased (Dupre et al., 2011) or reduced (Morgese et al., 2009) striatal GLU levels in response to L-DOPA in dyskinetic rats.

The present study was undertaken to investigate the role of striatal and nigral D1 and D2 receptors in LID and the associated changes in GABA and GLU release within the basal ganglia network. This was accomplished using a reverse microdialysis approach in awake rats, whereby D1/D5 and D2/D3 antagonists (SCH23390 and raclopride, respectively) were infused in the dorsolateral striatum (DLS) or SNr while L-DOPA-induced AIMs were monitored.

Experimental procedures

Male Sprague–Dawley rats (150 g; Harlan Italy; S. Pietro al Natisone, Italy) were housed under regular lighting conditions (12 h light/dark cycle) and given food and water ad libitum. The experimental protocols performed in the present study were in accordance with the European Communities Council Directive of 24 November 1986 (86/609/EEC) and were approved by Italian Ministry of Health (license n. 194/2008-B) and Ethical Committee of the University of Ferrara. Adequate measures were taken to minimize the number of animals used and animal pain and discomfort.

Drugs

6-OHDA hydrobromide, D-amphetamine sulfate, L-DOPA methylester hydrochloride, and benserazide hydrochloride were purchased from Sigma (St. Louis, MO, USA), SCH23390 hydrochloride and raclopride from Tocris Bioscience (Bristol, UK). 6-OHDA were dissolved in saline containing 0.02% ascorbic acid, and used within 2 h. D-amphetamine, L-DOPA and benserazide were dissolved in saline immediately prior to use. SCH23390 and raclopride were dissolved in water to 1 mM and then diluted to 1 μM with perfusion Ringer.

Unilateral lesion with 6-hydroxydopamine

Unilateral lesion of dopaminergic neurons was induced in isoflurane-anesthetized Sprague–Dawley male rats according to standard procedures (Marti et al., 2005). Eight micrograms of 6-OHDA (dissolved in 4 μl) were stereotaxically injected into the medial forebrain bundle according to the following coordinates from bregma: antero-posterior (AP) −4.4 mm, medio-lateral (ML) −1.2 mm, dorso-ventral (DV) −7.8 mm below dura (Paxinos and Watson, 1982). Two weeks after 6-OHDA injection, successfully lesioned rats were selected using a test of amphetamine-induced rotation (5 mg/kg i.p. D-amphetamine, 90 min recordings) (Ungerstedt and Arbuthnott, 1970). Forty-five out of 53 6-OHDA lesioned rats showed >7 turns/min in the direction ipsilateral to the lesion, and were enrolled in the study. This behavior is associated with >95% loss of striatal DA terminals (Marti et al., 2007) and extracellular DA levels (Marti et al., 2002).

L-DOPA treatment and AIMs rating

Two weeks after amphetamine testing, DA-depleted rats underwent a 21 day course of L-DOPA treatment (6 mg/kg + benserazide 12 mg/kg, i.p., once daily) for induction of AIMs (Cenci et al., 1998). Quantification of L-DOPA-induced AIMs was carried out as extensively described in previous papers (Lundblad et al., 2002; Winkler et al., 2002). Briefly, rats were observed individually for 1 min every 15 min during the 3 h that followed L-DOPA injection. Dyskinetic movements were classified based on their topographic distribution into three subtypes: (i) axial AIMs, i.e. twisted posture or choreiform twisting of the neck and upper body toward the side contralateral to the lesion; (ii) forelimb AIMs, i.e. jerky or dystonic movements of the contralateral forelimb and/or purposeless grabbing movement of the contralateral paw; (iii) orolingual AIMs, i.e. orofacial muscle twitching, empty masticatory movements and contralateral tongue protrusion. Each AIM subtype was rated on a severity scale from 0 to 4 (1 = occasional; 2 = frequent; 3 = continuous but interrupted by sensory distraction; 4 = continuous, severe and not interrupted by sensory distraction) on each monitoring period. In order to select rats exhibiting stable and reproducible dyskinesias, AIM scoring was performed 5 times during the L-DOPA treatment period. All rats included in the microdialysis experiment had developed moderate-severe AIMs (severity grade ≥ 2 on each of the 3 AIM subtypes).

Microdialysis experiments

Dual probe microdialysis was performed as previously described (Marti et al., 2002). Two probes of concentric design were stereotaxically implanted under isoflurane anesthesia in the DA-depleted DLS (3 mm dialysing membrane, AN69, Hospal, Bologna, Italy) and ipsilateral SNr (1 mm) of dyskinetic rats according to the following coordinates from bregma and the dural surface (Paxinos and Watson, 1982): DLS, AP + 1.0, ML −3.5, DV −6; SNr, AP −5.5, ML −2.2, VD −8.3. Forty-eight hours after surgery, probes were perfused with a modified Ringer solution ($CaCl_2$ 1.2 mM; KCl 2.7 mM; NaCl 148 mM; $MgCl_2$ 0.85 mM) at a 3 μl/min flow rate and, after 6 h rinsing, samples were collected every 15 min. At least three baseline samples were collected before drug treatment. L-DOPA was administered i.p. at the standard dose of 6 mg/kg (in combination with benserazide 12 mg/kg), whereas SCH23390 and raclopride were perfused locally in DLS or SNr at a concentration (1 μM) expected to generate tissue levels in the nanomolar range based on a ~10% in vitro recovery (~100 nM, or lower for the smaller probe). When systemic and local treatments were combined, perfusion with DA receptor antagonists started 1 h before L-DOPA administration and continued until the end of experiment. AIM monitoring was performed every 15 min (for 1 min) according to the scale described above. Microdialysis experiments usually lasted for 3 days. Each rat received L-DOPA, a DA receptor antagonist, or their combination in a randomized fashion according to the following group allocations: L-DOPA, L-DOPA/D1 antagonist in DLS, D1 antagonist in DLS only (group 1); L-DOPA, L-DOPA/D2 antagonist in DLS, D2 antagonist in DLS only (group 2); L-DOPA, L-DOPA/D1 antagonist in SNr, D1 antagonist in SNr only (group 3); L-DOPA, L-DOPA/D2 antagonist in SNr, D2 antagonist in

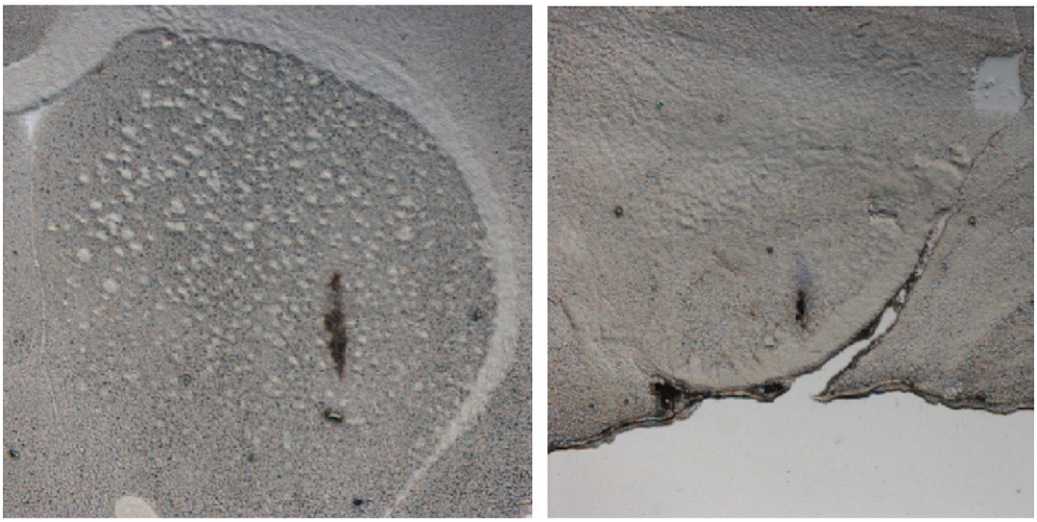

Fig. 1. Representative photographs of striatum (left) and substantia nigra reticulata (right) showing microdialysis probe tracks.

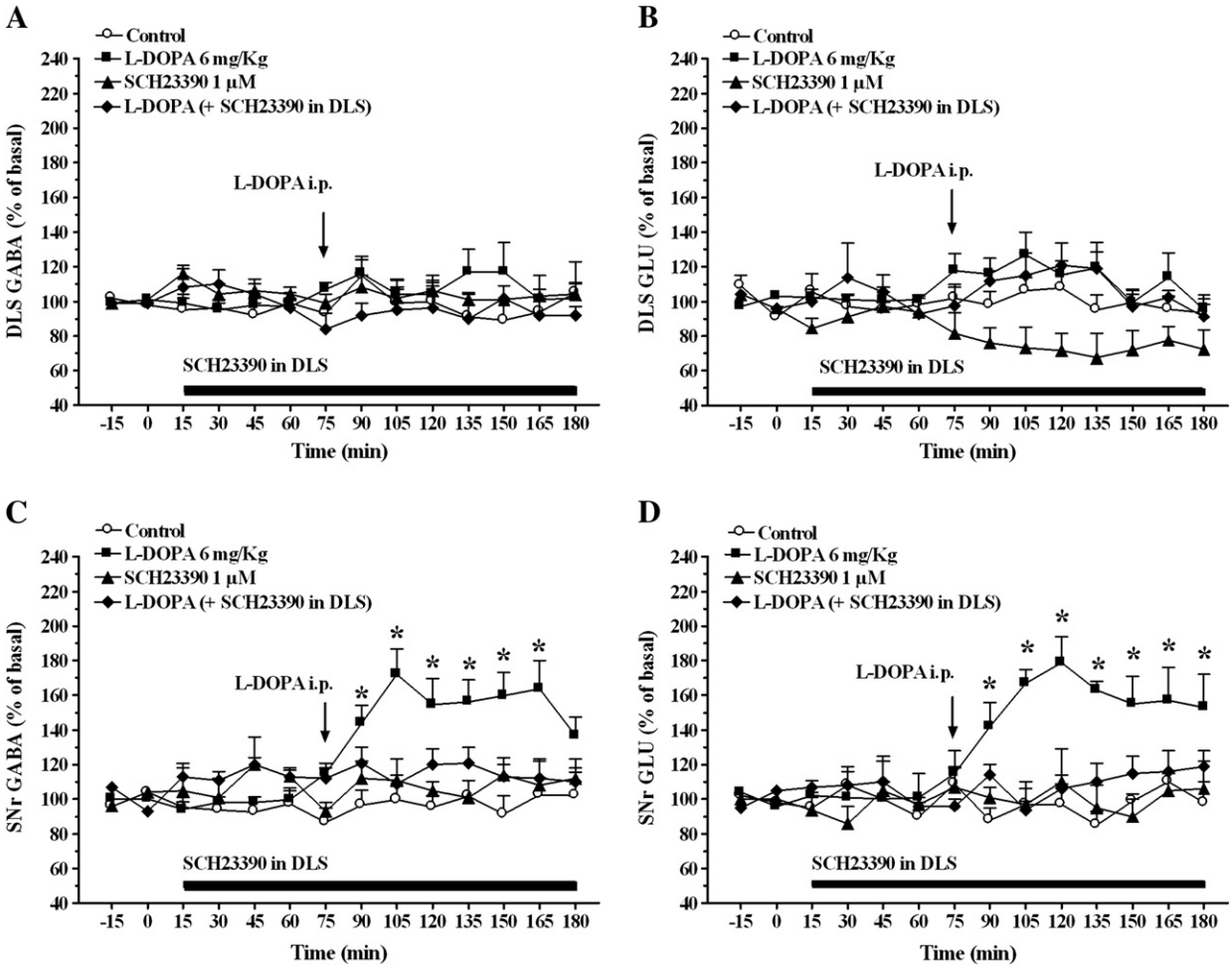

Fig. 2. Reverse dialysis of the D1 receptor selective antagonist SCH23390 in the DA-depleted dorsolateral striatum (DLS) of unilateral 6-OHDA lesioned dyskinetic rats modulates L-DOPA induced amino acid levels. SCH23390 (1 μM) was perfused through the probe implanted in DLS, and GABA and GLU levels monitored in DLS (A–B) and SNr (C–D). SCH23390 was perfused (black bar) starting 1 h before systemic administration of L-DOPA (6 mg/kg + 12 mg/kg benserazide, i.p.; arrow). Data are expressed as percentages of basal pre-treatment values, and are means ± SEM of 5–7 determinations. Basal GABA and GLU levels (nM) were 10.6 ± 0.6 and 179.3 ± 14.7 (DLS), and 9.7 ± 0.5 and 161.3 ± 15.6 (SNr), respectively. Statistical analysis was performed by 2-way RM ANOVA followed by the sequentially rejective Bonferroni's test. Significant interactions: panel B, L-DOPA × time ($F_{11,188} = 2.17$, $p = 0.0175$); panel C, L-DOPA × time ($F_{11,220} = 2.91$, $p = 0.0013$), SCH23390 × time ($F_{11,220} = 4.29$, $p < 0.0001$) or L-DOPA × SCH23390 x time ($F_{11,220} = 3.89$, $p < 0.0001$); panel D, L-DOPA × time ($F_{11,212} = 3.40$, $p = 0.0002$), SCH23390 × time ($F_{11,212} = 2.52$, $p = 0.0053$) or L-DOPA × SCH23390 × time ($F_{11,212} = 3.23$, $p = 0.0004$). *$p < 0.01$ different from control.

SNr only (group 4). The microdialysis experiments continued so as to reach the predetermined number of animals per group (n = 5–9). Control experiments were occasionally run at day 4 or during the 3-days dialysis course in a counter-balanced order. At the end of the experiments, animals were sacrificed and the correct placement of the probes was verified histologically (Fig. 1).

Endogenous GLU and GABA analysis

GLU and GABA were measured by HPLC coupled with fluorometric detection as previously described (Marti et al., 2007). Thirty microliters of o-phthaldialdehyde/mercaptoethanol reagent were added to 30 µl aliquots of sample, and 50 µl of the mixture was automatically injected (Triathlon autosampler; Spark Holland, Emmen, Netherlands) onto a 5-C18 Chromsep analytical column (3 mm inner diameter, 10 cm length; Chrompack, Middelburg, Netherlands) perfused at a flow rate of 0.48 ml/min (Beckman 125 pump; Beckman Instruments, Fullerton, CA, USA) with a mobile phase containing 0.1 M sodium acetate, 10% methanol and 2.2% tetrahydrofuran (pH 6.5). GLU and GABA were detected by means of a fluorescence spectrophotometer FP-2020 Plus (Jasco, Tokyo, Japan) with the excitation and the emission wavelengths set at 370 and 450 nm respectively. The limits of detection for GLU and GABA were ~1 and ~0.5 nM, respectively. Retention times for GLU and GABA were 3.5 ± 0.2 min and 18.0 ± 0.5 min respectively.

Data presentation and statistical analysis

Treatment effects on GABA and GLU levels have been expressed as percentage ± SEM of basal values (calculated as mean of the two samples before treatment). Absolute basal values are detailed in the Figure legends. Statistical analysis was performed on neurochemical data (Figs. 2–3, 5–6) by two-way repeated measure (RM) analysis of variance (ANOVA), Factor 1 being the DA antagonist (SCH23390 or raclopride) and Factor 2 L-DOPA. The interactions of Factor 1, Factor 2 and Factor 1 × Factor 2 with time were analyzed, and only in the case ANOVA yielded to a significant interaction of Factor 1 × Factor 2 with time, the sequentially rejective Bonferroni's post hoc test analysis was performed to study group differences at each time-point. The Mann–Whitney U-test was used to compare AIM score in each rat following L-DOPA in the presence or in the absence of a DA receptor antagonist (Figs. 4, 7). Only relevant statistical results have been given in figure legends. P values <0.05 were considered to be statistically significant.

Results

Effects of DLS perfusion with SCH23390 and raclopride

To investigate whether striatal D1 and D2 receptors were involved in LID expression, the D1/D5 selective antagonist SCH23390 or the

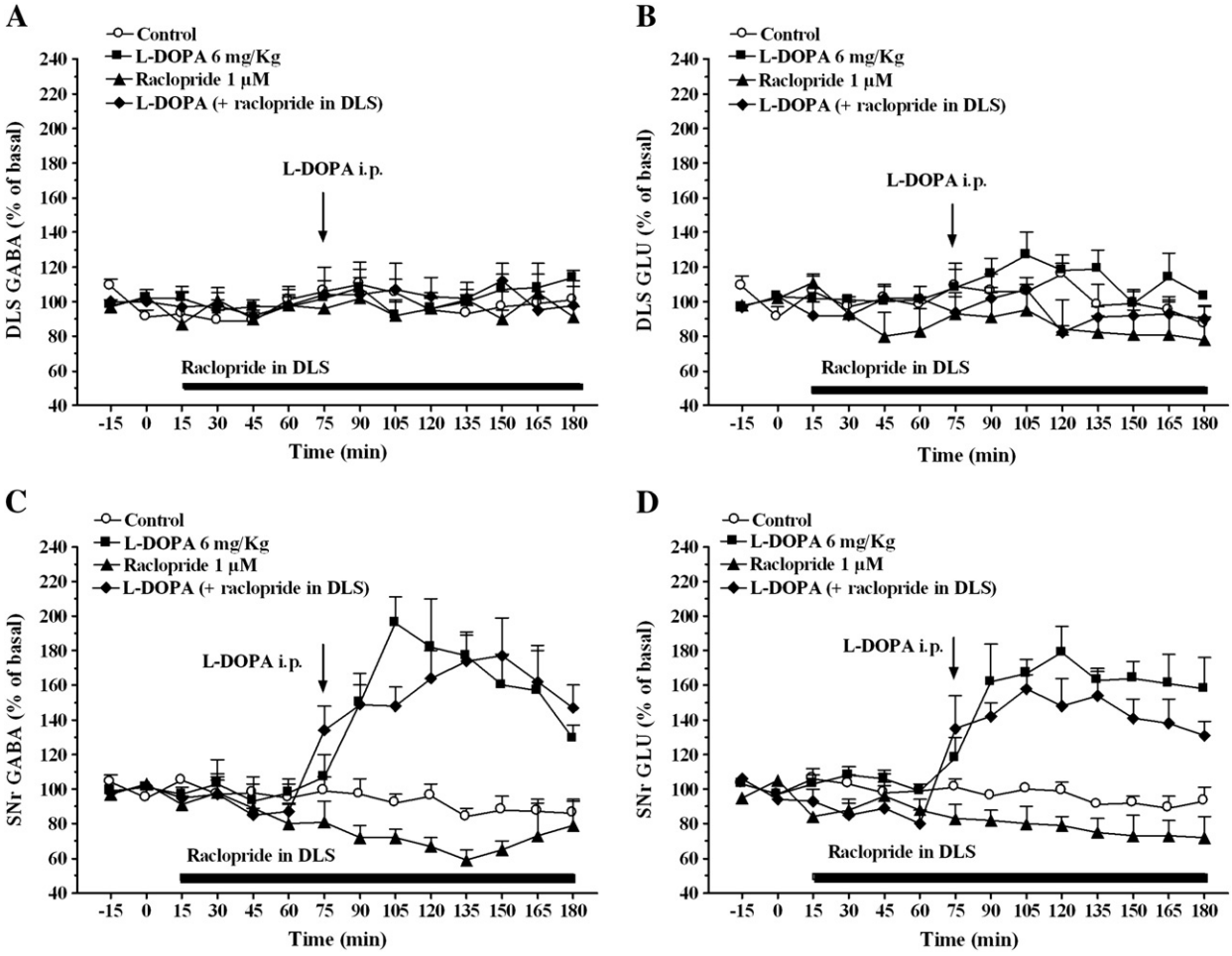

Fig. 3. Reverse dialysis of the D2 receptor selective antagonist raclopride in the DA-depleted dorsolateral striatum (DLS) of unilateral 6-OHDA lesioned dyskinetic rats modulates L-DOPA induced amino acid levels. Raclopride (1 µM) was perfused through the probe implanted in DLS, and GABA and GLU levels monitored in DLS (A–B) and SNr (C–D). Raclopride was perfused (black bar) starting 1 h before systemic administration of L-DOPA (6 mg/kg + 12 mg/kg benserazide, i.p.; arrow). Data are expressed as percentages of basal pre-treatment values, and are means ± SEM of 5–6 determinations. Basal GABA and GLU levels (nM) were, respectively, 20.4 ± 3.1 and 128.7.3 ± 25.8 (DLS), and 13.1 ± 1.9 and 132.5 ± 23.1 (SNr). Statistical analysis was performed by 2-way RM ANOVA followed by the sequentially rejective Bonferroni's test. Significant interactions: panel C, L-DOPA × time ($F_{11,200} = 13.50$, $p < 0.0001$); panel D, L-DOPA × time ($F_{11,200} = 13.56$, $p < 0.0001$).

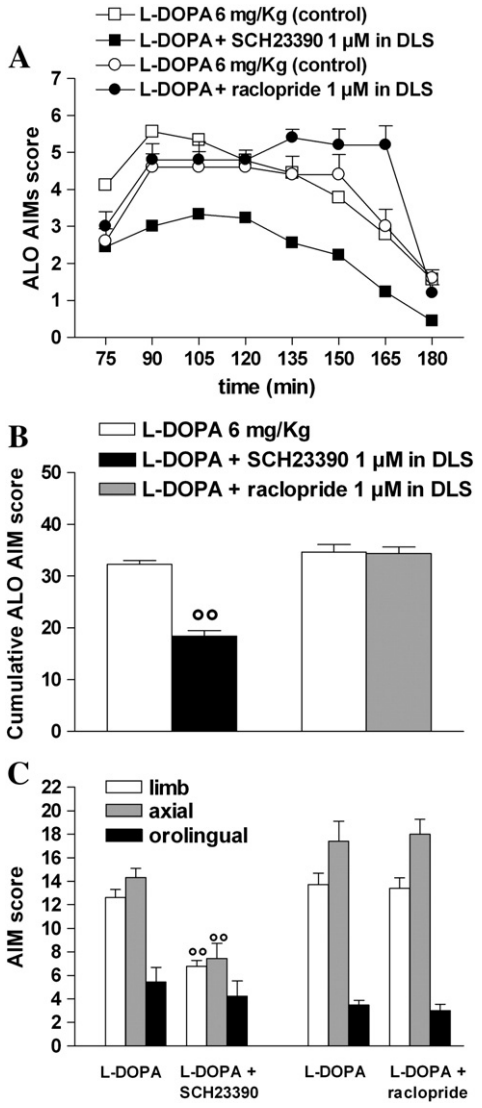

Fig. 4. Reverse dialysis of the D1 receptor selective antagonist SCH23390 but not the D2 receptor selective antagonist raclopride in the DA-depleted dorsolateral striatum (DLS) of unilateral 6-OHDA lesioned dyskinetic rats modulates L-DOPA induced abnormal involuntary movements (AIMs). SCH23390 and raclopride (1 μM) were perfused through the probe implanted in DLS starting 1 h before systemic administration of L-DOPA (6 mg/kg + 12 mg/kg benserazide, i.p.). Axial, limb and orolingual (ALO) AIMs were scored every 15 min (for 120 min after L-DOPA administration) according to the scale described in Methods. Data were presented as time-course (A), cumulative ALO scores (B) or separate scores for each subtype (C). Changes in amino acid levels in DLS and SNr were recorded in parallel and are shown in Figs. 2–3. Data are mens ± SEM of 5–9 determinations. Statistical analysis was performed by the Mann–Whitney U-test. Significant results: panel B, U = 0.5; panel C Limb AIMs, U = 1.5, axial AIMs U = 5.0. °°$p<0.01$ different from L-DOPA alone.

D2/D3 selective antagonist raclopride were perfused through a microdialysis probe in DLS, alone or in combination with a systemic dose of L-DOPA. GABA and GLU levels were monitored in both DLS and SNr simultaneously with AIMs rating (Figs. 2–4).

Systemic administration of L-DOPA, alone or in combination with intrastriatal SCH23390, did not affect GABA levels in striatum (Fig. 2A). Conversely, RM ANOVA on striatal GLU levels (Fig. 2B) revealed a significant L-DOPA × time interaction, possibly suggesting that L-DOPA elevated GLU levels.

Unlike amino acid levels in DLS, nigral GABA and GLU concentrations showed a large and sustained increase following the administration of L-DOPA (Figs. 2C–D), an effect that was consistent across all experiments (cf. panels C in Figs. 2–3 and 5–6). GABA levels were significantly elevated above control levels 30 min after L-DOPA administration (i.e. in the 90 min perfusate fraction; $p<0.05$) reaching maximal values (~86%) in the next sample (105 min). The increase remained significant for at least 90 min following the injection of L-DOPA (150 min perfusate fraction), although it tended to decline by the end of the observation period (180 min fraction, corresponding to 2 hours post L-DOPA administration). Intrastriatal SCH23390 prevented the surge in GABA levels following L-DOPA. Nigral GLU levels (Fig. 2D) showed a similar temporal course, starting to be significantly elevated above control values in the 90 min perfusate fraction, and reaching a peak (~80%) at 105–120 min. GLU levels showed a steady increase until the end of the observation period ($p<0.05$ at 180 min; cf. panels D in Figs. 2–3 and 5–6). Local perfusion of SCH23390 in DLS completely blocked the effect of L-DOPA (Fig. 2D).

Intrastriatal perfusion of raclopride did not affect striatal amino acid levels when given alone, nor did it disclose any effect of L-DOPA in DLS (Figs. 3A–B). Likewise, raclopride did not modulate basal GABA and GLU levels in SNr (Figs. 3C–D) or their responses to L-DOPA.

Monitoring the behavioral effects of L-DOPA during intrastriatal perfusion with selective DA receptor antagonists (Fig. 4A) revealed that SCH23390 markedly attenuated (~47%) AIMs expression whereas raclopride was without effect (Fig. 4B). Stratification of behavioral analysis for dyskinesia typology showed that SCH23390 prevented approximately to the same extent both limb and axial AIMs whereas orolingual AIMs remained unchanged (Fig. 4C).

Effects of SNr perfusion with SCH23390 and raclopride

To investigate the role of nigral D1 and D2 receptors in LID, perfusions of SCH23390 or raclopride through the probe implanted in SNr were combined with systemic L-DOPA administration (Figs. 5–7).

Intranigral perfusion with SCH23390 did not affect amino acid levels in striatum when given alone or in combination with L-DOPA (Figs. 5A–B). However, intranigral SCH23390 alone transiently elevated GABA levels in SNr and attenuated the GABA response to L-DOPA (Fig. 5C). Conversely, SCH23390 did not affect basal GLU levels nor did it attenuate the rise in nigral GLU following L-DOPA (Fig. 5D).

Differently from SCH23390, intranigral perfusion with raclopride caused marked changes in amino acid levels in striatum. Intranigral raclopride caused a slow increase in striatal GABA levels which was unaffected by L-DOPA (Fig. 6A). In contrast, raclopride caused a prompt elevation of striatal GLU levels which was overall enhanced by L-DOPA (Fig. 6B). However, at any time point the effect of L-DOPA was different from that of raclopride.

Perfusion of raclopride in SNr significantly decreased GABA levels (~40%) although it did not change the facilitatory effect of L-DOPA (Fig. 6C). Intranigral raclopride did not change basal GLU levels in this area nor did it alter the surge in nigral GLU in response to L-DOPA (Fig. 6D).

Monitoring the effect of L-DOPA on AIMs expression during intranigral perfusion with selective DA receptor antagonists (Fig. 7A) revealed that both SCH23390 and raclopride significantly attenuated AIMs expression (~21% and ~40%, respectively; Fig. 7B), causing a reduction of limb AIMs (Fig. 7C). Also axial AIMs were attenuated by SCH23390 whereas the reduction observed with raclopride was just above the limit of significance ($p = 0.072$).

Discussion

This study provides the first demonstration that concomitant elevations in GABA and GLU extracellular levels occur in SNr during the expression of LID, and that both striatal and nigral DA receptors contribute to shape the response to L-DOPA. The intrastriatal infusion of a D1 receptor antagonist prevented the surge of nigral amino acids and simultaneously reduced dyskinesia, whereas a D2 antagonist was ineffective. D1 and D2 receptor antagonists achieved a very different

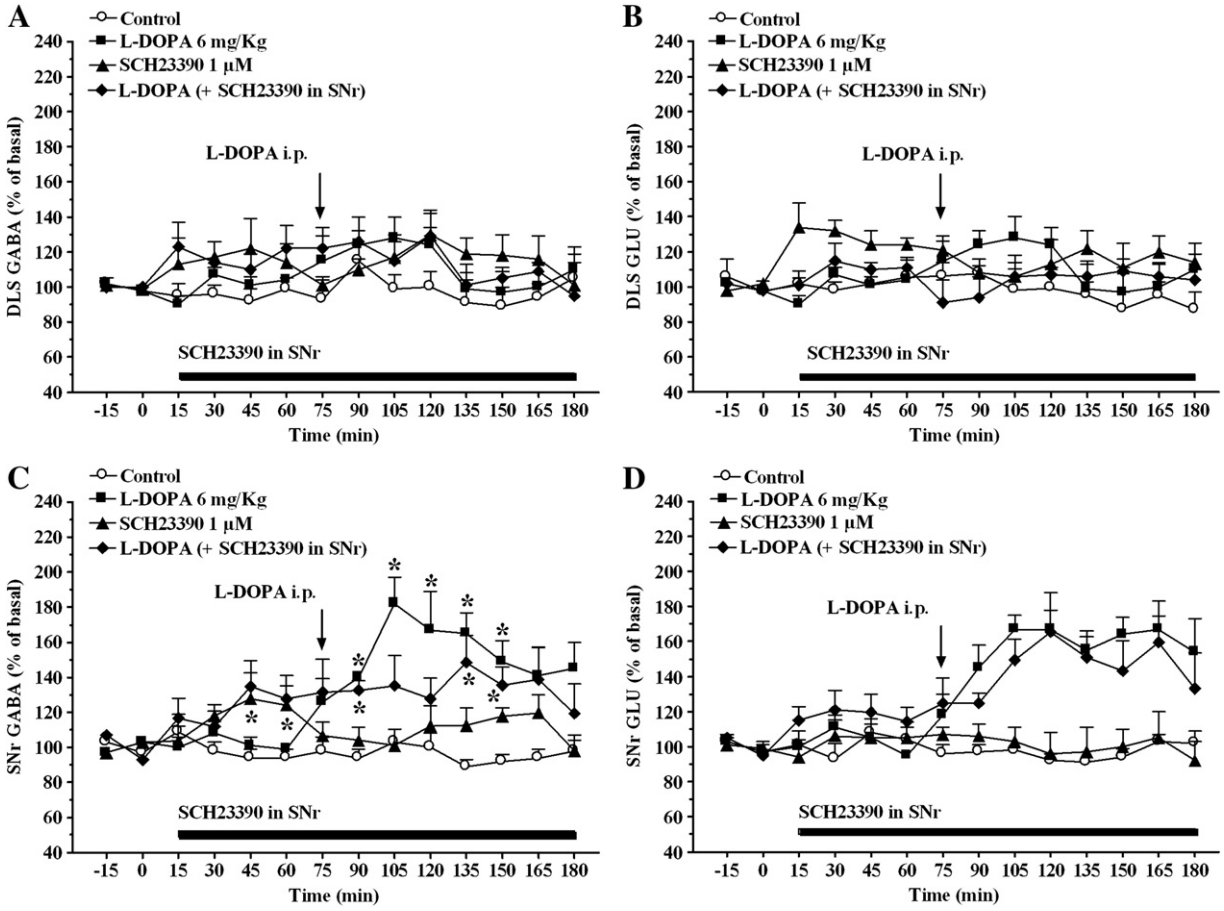

Fig. 5. Reverse dialysis of the D1 receptor selective antagonist SCH23390 in the lesioned substantia nigra pars reticulata (SNr) of unilateral 6-OHDA lesioned dyskinetic rats modulates L-DOPA-induced amino acid levels. SCH23390 (1 μM) was perfused through the probe implanted in SNr, and GABA and GLU levels monitored in ipsilateral dorsolateral striatum (DLS; A–B) and SNr (C–D). SCH23390 was perfused (black bar) 1 h before systemic administration of L-DOPA (6 mg/kg + 12 mg/kg benserazide, i.p.; arrow). Data are expressed as percentages of basal pre-treatment values, and are means ± SEM of 5–7 determinations. Basal GABA and GLU levels (nM) were 10.8 ± 0.7 and 147.7 ± 8.3 (DLS), and 9.6 ± 0.7 and 166.7 ± 16.3 (SNr), respectively. Statistical analysis was performed by 2-way RM ANOVA followed by the sequentially rejective Bonferroni's test. Significant interactions: panel C, SCH23390 × time ($F_{11,252} = 20.21$, $p < 0.0001$), L-DOPA × time ($F_{11,252} = 29.59$, $p < 0.0001$) and L-DOPA × SCH23390 × time ($F_{11,252} = 10.52$, $p < 0.0001$). *$p < 0.01$ different from control.

pattern of effects when perfused into SNr. Although both antagonists mildly attenuated dyskinesia, the D1 antagonist elevated basal GABA output but dampened the L-DOPA-evoked surge in nigral GABA levels, whereas the D2 antagonist reduced basal nigral GABA without altering the response to L-DOPA. In addition, raclopride alone increased basal amino acid levels in DLS, facilitating the effects of L-DOPA on striatal GLU. Taken together these results provide novel and important information on the role of striatal and nigral dopamine D1 and D2 receptors in regulating GABA and GLU overflow in the parkinsonian brain both under baseline conditions and following the administration of L-DOPA.

Striatal D1 and D2 receptors and LID

Dopamine denervation is accompanied by up-regulation of D1 signaling in the striatum (Aubert et al., 2005; Berke et al., 1998; Gerfen et al., 2002) as well as by changes in receptor trafficking leading to enrichment of D1 receptors at the membrane of striatal GABAergic neurons (Berthet et al., 2009). Treatment with L-DOPA does not normalize these changes in animals that develop dyskinesia (reviewed in Cenci and Konradi, 2010). Consistent with a pathogenic role of up-regulated striatal D1 transmission in LID, systemic administration of D1 antagonists prevents AIM expression in different models of dyskinesia (Grondin et al., 1999; Lindgren et al., 2009; Monville et al., 2005; Taylor et al., 2005; Westin et al., 2007). The present study provides neuroanatomical information about the site from which D1 receptors mediate the dyskinetic behaviors, showing that both LID manifestation and the accompanying rise in nigral GABA and GLU release are significantly attenuated by intrastriatal perfusion with SCH23390. The possibility that the action of SCH23390 extends beyond D1 receptors should also be considered. Indeed, SCH23390 binds to D1-like receptors (0.3–1.3 nM; Hyttel, 1983; Millan et al., 2001) and with lower affinity to 5-HT2c (previously known as 5-HT1c; 15–30 nM; Hyttel, 1983; Millan et al., 2001; Taylor et al., 1991), 5-HT4 (270 nM; Schiavi et al., 1994) receptors as well as to the 5-HT transporter (1,400 nM; Zarrindast et al., 2011). Assuming a ~10% in vivo recovery under the present experimental conditions, the perfusion of 1 μM SCH23390 through the microdialysis probe is expected to generate striatal extracellular levels of ~100 nM, for which significant binding to 5-HT2c receptors in addition to D1 receptors may occur. However, a contribution of 5-HT2c receptors in the antidyskinetic effect of intrastriatal SCH23390 is unlikely since striatal 5-HT2c receptors do not interfere with the hyperlocomotion induced by injection of a D1 receptor agonists in the DA-depleted striatum of 6-OHDA lesioned rats (Bishop et al., 2005). Moreover, SCH23390 activates 5-HT2c receptors (Millan et al., 2001; Ramos et al., 2005; Woodward et al., 1992), which would result in a worsening rather than attenuation of dyskinesia (Beyeler et al., 2010; Nicholson and Brotchie, 2002). Indeed, 5-HT2c receptor stimulation induced orofacial dyskinesia (Beyeler et al., 2010) whereas 5-HT2c receptor blockade attenuated neuroleptic-induced dyskinesia (Creed-Carson et al., 2011). Therefore, although binding to striatal 5-HT2c receptors

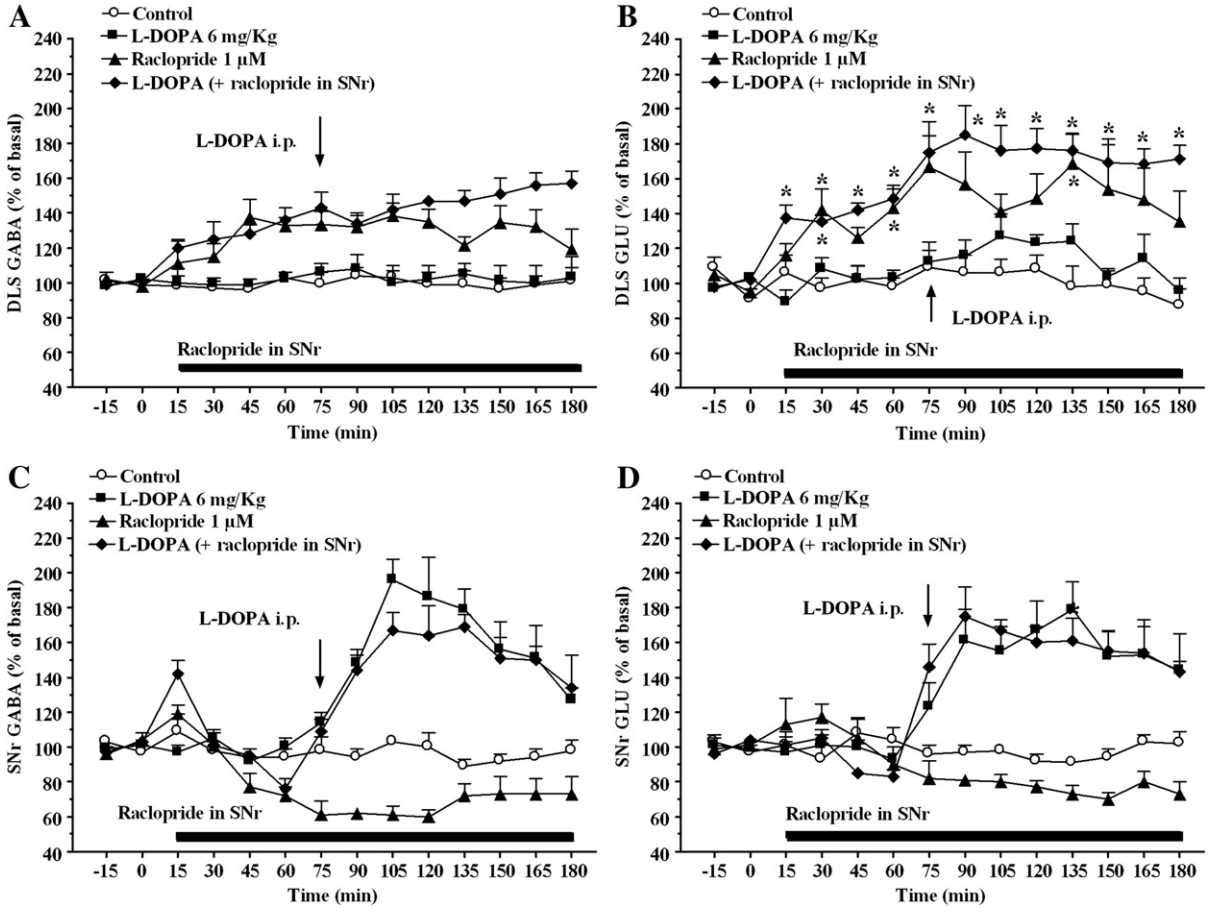

Fig. 6. Reverse dialysis of the D2 receptor selective antagonist raclopride in the lesioned substantia nigra pars reticulata (SNr) of unilateral 6-OHDA lesioned dyskinetic rats modulates L-DOPA-induced amino acid release. Raclopride (1 μM) was perfused through the probe implanted in SNr, and GABA and GLU levels monitored in ipsilateral dorsolateral striatum (DLS; A–B) and SNr (C–D). Raclopride was perfused (black bar) 1 h before systemic administration of L-DOPA (6 mg/kg + 12 mg/kg benserazide, i.p.; arrow). Data are expressed as percentages of basal pre-treatment values, and are means ± SEM of 5–6 determinations. Basal GABA and GLU levels (nM) were 11.3 ± 1.3 and 87.2 ± 23.1 (DLS), and 10.6 ± 1.4 and 77.7 ± 18.8 (SNr), respectively. Statistical analysis was performed by 2-way RM ANOVA followed by the sequentially rejective Bonferroni's test. Significant interactions: panel A, raclopride × time ($F_{11,220} = 2.35$, $p = 0.0092$); panel B, L-DOPA × time ($F_{11,176} = 10.57$, $p < 0.0001$), raclopride × time ($F_{11,176} = 5.61$, $p < 0.0001$) and L-DOPA × raclopride × time ($F_{11,176} = 4.62$, $p < 0.0001$); panel C, raclopride × time ($F_{11,208} = 2.78$, $p = 0.0022$) and L-DOPA × time ($F_{11,208} = 17.22$, $p < 0.0001$). *$p < 0.01$ different from control.

may occur during intrastriatal perfusion with SCH23390, these receptors are not likely to contribute to the antidyskinetic effect of SCH23390.

In addition to the axon terminals of striato-nigral neurons, sources of neuronal GABA outflow in the SNr are the GP-nigral projections, as well as GABA interneurons and collaterals of nigrofugal GABAergic neurons. We therefore conclude that increases in nigral GABA release induced by L-DOPA reflect a hyperactivity in the direct striato-nigral pathway, confirming that such hyperactivity plays a crucial role in LID (reviewed in Cenci, 2007). The concomitant lack of significant changes in GABA (and GLU) levels in GP during the expression of LID (Mela et al., 2007) rules out a contribution of the indirect pathway to the neurochemical alterations measured in the SNr. The surge of nigral GLU levels in this LID model is likely to reflect an increased glutamatergic input from a cortically-activated subthalamic nucleus and/or may depend on the overactivation of the direct pathway. Indeed, also reverse dialysis of NMDA in striatum evokes an increase in GLU levels in SNr, which is attenuated by DA depletion or intrastriatal SCH23390 (Marti et al., 2002). Striato-nigral GABA neurons co-release Substance P which might elevate GLU release acting on facilitatory NK1 receptors located on subthalamo-nigral terminals. Such presynaptic facilitatory control has been demonstrated in various brain areas (Bailey et al., 2004; Liu et al., 2002; Stacey et al., 2002), although not yet in the SNr.

Different from SCH23390, intrastriatal raclopride failed to affect LID and the accompanying nigral amino acid response. Raclopride affinity for D2 and D3 receptors is 1.8 and 3.5 nM respectively (Seeman and Van Tol, 1994). Therefore the 1 μM raclopride concentration in the perfusate is expected to generate extracellular concentrations (~100 nM) which largely cover D2-like receptors without unspecifically interfering with other receptors (Köhler et al., 1985). This data rules out a major role for striatal D2 receptors in dyskinesia, and is consistent with the findings that systemic D2 receptor agonists do not activate the ERK pathway in striatal neurons, a molecular marker of LID (Westin et al., 2007) and that genetic deletion of the D2 receptor gene does not affect LID in mice (Darmopil et al., 2009). Despite the existence of a well-documented opposite D1–D2 receptor modulation of striatal GABAergic function (Cepeda and Levine, 1998; Harsing and Zigmond, 1997; Hernandez-Lopez et al., 1997; Morari et al., 1994; Nicola et al., 2000), the inconsistent effects of striatal raclopride infusion in this study may indicate that striatal D2 receptors do not significantly affect the L-DOPA-induced activation of already primed striato-nigral neurons, possibly confirming the morphological and functional segregation of D1 and D2 receptors along striatal output pathways (Gerfen et al., 1990).

Nigral D1 and D2 receptors and LID

Different from the striatum, both D1 and D2 receptor blockade in SNr attenuated LID expression. This confirms the role of this brain area in generating dyskinesia as emerged from previous studies. Indeed,

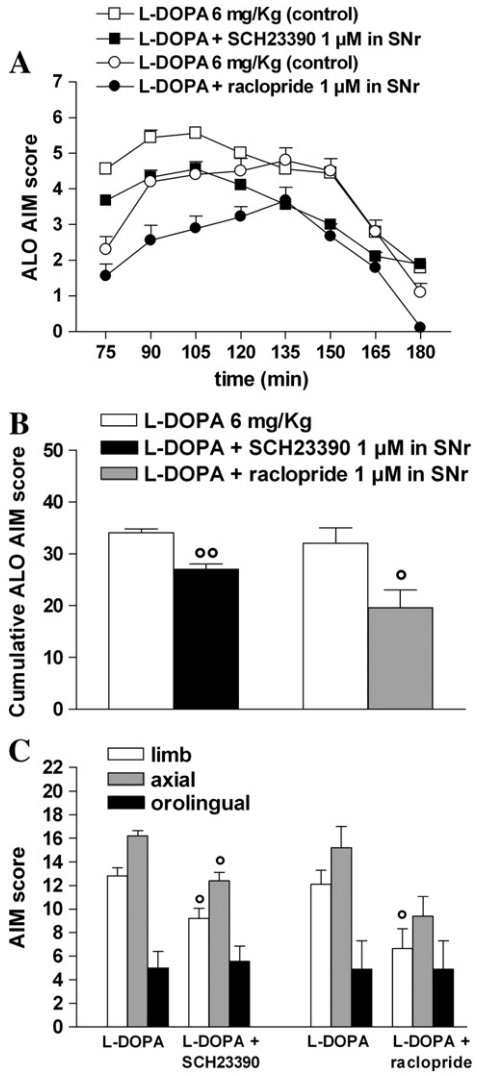

Fig. 7. Reverse dialysis of the D1 receptor selective antagonist SCH23390 and the D2 receptor selective antagonist raclopride in the lesioned substantia nigra reticulata (SNr) of unilateral 6-OHDA lesioned dyskinetic rats modulates L-DOPA induced abnormal involuntary movements (AIMs). SCH23390 and raclopride (1 μM) were perfused through the probe implanted in SNr starting 1 h before systemic administration of L-DOPA (6 mg/kg + 12 mg/kg benserazide, i.p.). Axial, limb and orolingual (ALO) AIMs were scored every 15 min (for 135 min after L-DOPA administration) according to the scale described in Methods. Data were presented as time-course (A), cumulative ALO scores (B) or separate scores for each subtype (C). Changes in amino acid levels in DLS and SNr were recorded in parallel and are shown in Figs. 5–6. Data are means ± SEM of 7–9 determinations. Statistical analysis was performed by the Mann–Whitney U-test. Significant results: panel B, SCH23390, U = 10.0, raclopride U = 7.50; panel C Limb AIMs, SCH23390 U = 10.5, raclopride U = 8.0; axial AIMs, SCH23390 U = 7.0, raclopride U = 10.0. °p<0.05, °°p<0.01, different from L-DOPA alone.

L-DOPA is converted to DA in SNr (Sarre et al., 1998), and L-DOPA administration results in abnormal elevations of extracellular DA levels in both the SNr and striatum of dyskinetic rats (Lindgren et al., 2010). Moreover, dyskinesia is associated with abnormal oscillatory activity in the theta/alpha band of nigral neurons (Meissner et al., 2006) as well as with angiogenesis in nigral microvasculature (Westin et al., 2006).

In keeping with the finding that nigral D1 receptors mediate the contralateral turning induced by L-DOPA in unilateral 6-OHDA lesioned rats (Robertson and Robertson, 1989), intranigral SCH23390 attenuated LID and the accompanying rise of nigral GABA levels. D1 receptors are largely expressed on striato-nigral GABAergic afferents, their activation resulting in an increase of GABA release, overinhibition of nigro-thalamic neurons and motor initiation. Interestingly, similar to the situation in the striatum, D1 receptor signaling appears to be up-regulated in the SNr, leading to an enhancement of agonist-stimulated [^{3}H]-GABA release in nigral slices (Rangel-Barajas et al., 2011). Therefore, by opposing a phasic D1 receptor activation by L-DOPA, nigral SCH23390 infusion attenuates both the GABAergic inhibition of nigro-thalamic neurons and dyskinesia. In addition, SCH23390 also elevated basal GABA levels in SNr. This finding can be differently interpreted since microdialysis samples different GABA pools, which can be differentially affected by local treatment. Therefore, the increase in basal GABA levels may indicate the existence of a DA inhibitory tone on GABA release mediated by D1 receptors located on GABA interneurons or reflect disinhibition of nigro-thalamic GABA neurons, which have extensive axon collaterals ramifying in SNr (Grofova et al., 1982). This latter possibility is further substantiated by the findings that SCH23390 application in vitro attenuates GABA-mediated IPSP in nigro-thalamic neurons (Aceves et al., 2011; Radnikow and Misgeld, 1998) and systemic SCH23390 administration increases the discharge rate of nigro-thalamic neurons in vivo (Windels and Kiyatkin, 2006). Alternatively, SCH23390 may impact on 5-HT2c receptors, as discussed above. Indeed, stimulation of nigral 5-HT2c receptors elevated GABA release and excited nigral GABA neurons in vivo (Di Giovanni et al., 2001; Invernizzi et al., 2007) an action that may be consistent with motor inhibition (Kennett and Curzon, 1988). Consistently, intranigral infusion of 5-HT2c receptor antagonists induced contralateral rotations and potentiated the turning behavior induced by DA agonists in unilateral 6-OHDA lesioned rats (Fox et al., 1998).

Similar to SCH23390, intranigral raclopride attenuated expression of limb and axial dyskinesia. This suggests that nigral D2 receptors contribute to LID, and that nigral but not striatal D2 receptors may mediate the antidyskinetic effect of D2 antagonists when given systemically (see Introduction). Differently from SCH23390, the antidyskinetic effect of intranigral raclopride was not accompanied by changes of the GABA surge induced by L-DOPA, possibly suggesting it did not involve modulation of the striato-nigral pathway. This is in line with the finding that D2 receptor ligands modulate GABA release from pallido-nigral but not striato-nigral terminals, in keeping with the view of a segregation of D2/D3/D4 and D1 receptors on afferent projections from GP and striatum, respectively (Aceves et al., 2011). It should be emphasized that intranigral raclopride produced dramatic preconditioning effect on basal ganglia circuitry, reducing nigral GABA and elevating striatal GABA and GLU levels. It is not clear how these changes impact on the striatal output. However, it seems unlikely that changes in striatal amino acids contribute to the antidyskinetic effect of raclopride since the nigral amino acid response to L-DOPA was not altered. Instead, raclopride might act through setting the responsiveness of nigro-thalamic neurons to L-DOPA (Volta et al., 2011). Blockade of an inhibitory D2-mediated tone on pallido-nigral terminals would alter the activity of nigro-thalamic neurons (Aceves et al., 2011). This would lead to disinhibition of thalamo-striatal and/or thalamo-cortical GLU projections, which is in line with the observed elevation of amino acid release in striatum (see also Morari et al., 1996). Activation of the cortico- and/or thalamo-striatal GLU inputs may enrich the otherwise negligible neuronal component of basal extracellular GLU levels (Baker et al., 2002; Morari et al., 1993, 1996) and allow a facilitatory action of L-DOPA to be unraveled. These data confirm that low therapeutic doses of L-DOPA exert only mild facilitatory effects on striatal GLU levels in dyskinetic rats (Dupre et al., 2011).

Concluding remarks

The contribution of DA receptor subtypes to LID and the underlying mechanisms have been evaluated performing reverse dialysis of DA selective antagonists in striatum and SNr of dyskinetic rats. AIMs expression appears to be mediated by intrastriatal and to a lesser extent, intranigral D1 receptors, likely through activation of the striato-nigral pathway and stimulation of GABA release from striato-nigral

terminals. A contribution of nigral D2 receptors was also demonstrated, although the mechanisms remain elusive. These data indicate that L-DOPA act on both receptor subtypes to trigger AIMs expression, suggesting the existence of an additive or synergistic cooperative interaction between these signals. An improved understanding of the role of different basal ganglia nuclei and DA receptor subtypes in generating LID will help developing novel, targeted treatment interventions for this disabling complication of PD therapy.

Acknowledgments

Supported by the Italian Ministry of University (PRIN 2008) grant to M Morari.

References

Aceves, J., Rueda-Orozco, P.E., Hernández, R., Plata, V., Ibañez-Sandoval, O., Galarraga, E., Bargas, J., 2011. Dopaminergic presynaptic modulation of nigral afferents: its role in the generation of recurrent bursting in substantia nigra pars reticulata neurons. Front. Syst. Neurosci. 5, 1–10.

Aubert, I., Guigoni, C., Hakansson, K., Li, Q., Dovero, S., Barthe, N., Bioulac, B.H., Gross, C.E., Fisone, G., Bloch, B., Bezard, E., 2005. Increased D1 dopamine receptor signaling in levodopa-induced dyskinesia. Ann. Neurol. 57, 17–26.

Bailey, C.P., Maubach, K.A., Jones, R.S., 2004. Neurokinin-1 receptors in the rat nucleus tractus solitarius: pre- and postsynaptic modulation of glutamate and GABA release. Neuroscience 127, 467–479.

Baker, D.A., Xi, Z.X., Shen, H., Swanson, C.J., Kalivas, P.W., 2002. The origin and neuronal function of in vivo nonsynaptic glutamate. J. Neurosci. 22, 9134–9141.

Berke, J.D., Paletzki, R.F., Aronson, G.J., Hyman, S.E., Gerfen, C.R., 1998. A complex program of striatal gene expression induced by dopaminergic stimulation. J. Neurosci. 18, 5301–5310.

Berthet, A., Porras, G., Doudnikoff, E., Stark, H., Cador, M., Bezard, E., Bloch, B., 2009. Pharmacological analysis demonstrates dramatic alteration of D1 dopamine receptor neuronal distribution in the rat analog of L-DOPA-induced dyskinesia. J. Neurosci. 29, 4829–4835.

Beyeler, A., Kadiri, N., Navailles, S., Boujema, M.B., Gonon, F., Moine, C.L., Gross, C., De Deurwaerdère, P., 2010. Stimulation of serotonin2C receptors elicits abnormal oral movements by acting on pathways other than the sensorimotor one in the rat basal ganglia. Neuroscience 169, 158–170.

Bishop, C., Daut, G.S., Walker, P.D., 2005. Serotonin 5-HT2A but not 5-HT2C receptor antagonism reduces hyperlocomotor activity induced in dopamine-depleted rats by striatal administration of the D1 agonist SKF 82958. Neuropharmacology 49, 350–358.

Calabresi, P., Giacomini, P., Centonze, D., Bernardi, G., 2000. Levodopa-induced dyskinesia: a pathological form of striatal synaptic plasticity? Ann. Neurol. 47, S60–S68.

Cenci, M.A., 2007. L-DOPA-induced dyskinesia: cellular mechanisms and approaches to treatment. Parkinsonism Relat. Disord. 13, S263–S267.

Cenci, M.A., Konradi, C., 2010. Maladaptive striatal plasticity in L-DOPA-induced dyskinesia. Prog. Brain Res. 183, 209–233.

Cenci, M.A., Lee, C.S., Bjorklund, A., 1998. L-DOPA-induced dyskinesia in the rat is associated with striatal overexpression of prodynorphin- and glutamic acid decarboxylase mRNA. Eur. J. Neurosci. 10, 2694–2706.

Cepeda, C., Levine, M.S., 1998. Dopamine and N-methyl-D-aspartate receptor interactions in the neostriatum. Dev. Neurosci. 20, 1–18.

Chase, T.N., Oh, J.D., 2000. Striatal mechanisms and pathogenesis of parkinsonian signs and motor complications. Ann. Neurol. 47, S122–S129.

Creed-Carson, M., Oraha, A., Nobrega, J.N., 2011. Effects of 5-HT(2A) and 5-HT(2C) receptor antagonists on acute and chronic dyskinetic effects induced by haloperidol in rats. Behav. Brain Res. 219, 273–279.

Darmopil, S., Martin, A.B., De Diego, I.R., Ares, S., Moratalla, R., 2009. Genetic inactivation of dopamine D1 but not D2 receptors inhibits L-DOPA-induced dyskinesia and histone activation. Biol. Psychiatry 66, 603–613.

Deniau, J.M., Chevalier, G., 1985. Disinhibition as a basic process in the expression of striatal functions. II. The striato-nigral influence on thalamocortical cells of the ventromedial thalamic nucleus. Brain Res. 334, 227–233.

Di Giovanni, G., Di Matteo, V., La Grutta, V., Esposito, E., 2001. m-Chlorophenylpiperazine excites non-dopaminergic neurons in the rat substantia nigra and ventral tegmental area by activating serotonin-2C receptors. Neuroscience 103, 111–116.

Dupre, K.B., Ostock, C.Y., Eskow Jaunarajs, K.L., Button, T., Savage, L.M., Wolf, W., Bishop, C., 2011. Local modulation of striatal glutamate efflux by serotonin 1A receptor stimulation in dyskinetic, hemiparkinsonian rats. Exp. Neurol. 229, 288–299.

Fabbrini, G., Brotchie, J.M., Grandas, F., Nomoto, M., Goetz, C.G., 2007. Levodopa-induced dyskinesias. Mov. Disord. 22, 1379–1389.

Fox, S.H., Moser, B., Brotchie, J.M., 1998. Behavioral effects of 5-HT2C receptor antagonism in the substantia nigra zona reticulata of the 6-hydroxydopamine-lesioned rat model of Parkinson's disease. Exp. Neurol. 151, 35–49.

Gerfen, C.R., Engber, T.M., Mahan, L.C., Susel, Z., Chase, T.N., Monsma Jr., F.J., Sibley, D.R., 1990. D1 and D2 dopamine receptor-regulated gene expression of striatonigral and striatopallidal neurons. Science 250, 1429–1432.

Gerfen, C.R., Miyachi, S., Paletzki, R., Brown, P., 2002. D1 dopamine receptor supersensitivity in the dopamine-depleted striatum results from a switch in the regulation of ERK1/2/MAP kinase. J. Neurosci. 22, 5042–5054.

Gold, S.J., Hoang, C.V., Potts, B.W., Porras, G., Pioli, E., Kim, K.W., Nadjar, A., Qin, C., LaHoste, G.J., Li, Q., Bioulac, B.H., Waugh, J.L., Gurevich, E., Neve, R.L., Bezard, E., 2007. RGS9-2 negatively modulates L-3,4-dihydroxyphenylalanine-induced dyskinesia in experimental Parkinson's disease. J. Neurosci. 27, 14338–14348.

Grofova, I., Deniau, J.M., Kitai, S.T., 1982. Morphology of the substantia nigra pars reticulata projection neurons intracellularly labeled with HRP. J. Comp. Neurol. 208, 352–368.

Grondin, R., Goulet, M., Morissette, M., Bedard, P.J., Di Paolo, T., 1999. Dopamine D1 receptor mRNA and receptor levels in the striatum of MPTP monkeys chronically treated with SKF-82958. Eur. J. Pharmacol. 378, 259–263.

Harsing Jr., L.G., Zigmond, M.J., 1997. Influence of dopamine on GABA release in striatum: evidence for D1–D2 interactions and non-synaptic influences. Neuroscience 77, 419–429.

Hernandez-Lopez, S., Bargas, J., Surmeier, D.J., Reyes, A., Galarraga, E., 1997. D1 receptor activation enhances evoked discharge in neostriatal medium spiny neurons by modulating an L-type Ca2+ conductance. J. Neurosci. 17, 3334–3342.

Hyttel, J., 1983. SCH 23390 — the first selective dopamine D-1 antagonist. Eur. J. Pharmacol. 91, 153–154.

Invernizzi, R.W., Pierucci, M., Calcagno, E., Di Giovanni, G., Di Matteo, V., Benigno, A., Esposito, E., 2007. Selective activation of 5-HT(2C) receptors stimulates GABA-ergic function in the rat substantia nigra pars reticulata: a combined in vivo electrophysiological and neurochemical study. Neuroscience 144, 1523–1535.

Kennett, G.A., Curzon, G., 1988. Evidence that mCPP may have behavioural effects mediated by central 5-HT1C receptors. Br. J. Pharmacol. 94, 137–147.

Köhler, C., Hall, H., Ogren, S.O., Gawell, L., 1985. Specific in vitro and in vivo binding of 3H-raclopride. A potent substituted benzamide drug with high affinity for dopamine D-2 receptors in the rat brain. Biochem. Pharmacol. 34, 2251–2259.

Konradi, C., Westin, J.E., Carta, M., Eaton, M.E., Kuter, K., Dekundy, A., et al., 2004. Transcriptome analysis in a rat model of L-DOPA-induced dyskinesia. Neurobiol. Dis. 17, 219–236.

Lindgren, H.S., Ohlin, K.E., Cenci, M.A., 2009. Differential involvement of D1 and D2 dopamine receptors in L-DOPA-induced angiogenic activity in a rat model of Parkinson's disease. Neuropsychopharmacology 34, 2477–2488.

Lindgren, H.S., Andersson, D.R., Lagerkvist, S., Nissbrandt, H., Cenci, M.A., 2010. L-DOPA-induced dopamine efflux in the striatum and the substantia nigra in a rat model of Parkinson's disease: temporal and quantitative relationship to the expression of dyskinesia. J. Neurochem. 112, 1465–1476.

Liu, R., Ding, Y., Aghajanian, G.K., 2002. Neurokinins activate local glutamatergic inputs to serotonergic neurons of the dorsal raphe nucleus. Neuropsychopharmacology 27, 329–340.

Lundblad, M., Andersson, M., Winkler, C., Kirik, D., Wierup, N., Cenci, M.A., 2002. Pharmacological validation of behavioural measures of akinesia and dyskinesia in a rat model of Parkinson's disease. Eur. J. Neurosci. 15, 120–132.

Marti, M., Mela, F., Bianchi, C., Beani, L., Morari, M., 2002. Striatal dopamine-NMDA receptor interactions in the modulation of glutamate release in the substantia nigra pars reticulata in vivo: opposite role for D1 and D2 receptors. J. Neurochem. 83, 635–644.

Marti, M., Mela, F., Fantin, M., Zucchini, S., Brown, J.M., Witta, J., Di Benedetto, M., Buzas, B., Reinscheid, R.K., Salvadori, S., Guerrini, R., Romualdi, P., Candeletti, S., Simonato, M., Cox, B.M., Morari, M., 2005. Blockade of nociceptin/orphanin FQ transmission attenuates symptoms and neurodegeneration associated with Parkinson's disease. J. Neurosci. 25, 9591–9601.

Marti, M., Trapella, C., Viaro, R., Morari, M., 2007. The nociceptin/orphanin FQ receptor antagonist J-113397 and L-DOPA additively attenuate experimental parkinsonism through overinhibition of the nigrothalamic pathway. J. Neurosci. 27, 1297–1307.

Meissner, W., Ravenscroft, P., Reese, R., Harnack, D., Morgenstern, R., Kupsch, A., Klitgaard, H., Bioulac, B., Gross, C.E., Bezard, E., Boraud, T., 2006. Increased slow oscillatory activity in substantia nigra pars reticulata triggers abnormal involuntary movements in the 6-OHDA-lesioned rat in the presence of excessive extracellular striatal dopamine. Neurobiol. Dis. 22, 586–598.

Mela, F., Marti, M., Dekundy, A., Danysz, W., Morari, M., Cenci, M.A., 2007. Antagonism of metabotropic glutamate receptor type 5 attenuates L-DOPA-induced dyskinesia and its molecular and neurochemical correlates in a rat model of Parkinson's disease. J. Neurochem. 101, 483–497.

Millan, M.J., Newman-Tancredi, A., Quentric, Y., Cussac, D., 2001. The "selective" dopamine D1 receptor antagonist, SCH23390, is a potent and high efficacy agonist at cloned human serotonin2C receptors. Psychopharmacology (Berl) 156, 58–62.

Monville, C., Torres, E.M., Dunnett, S.B., 2005. Validation of the L-dopa-induced dyskinesia in the 6-OHDA model and evaluation of the effects of selective dopamine receptor agonists and antagonists. Brain Res. Bull. 68, 16–23.

Morari, M., O'Connor, W.T., Ungerstedt, U., Fuxe, K., 1993. N-methyl-D-aspartic acid differentially regulates extracellular dopamine, GABA, and glutamate levels in the dorsolateral neostriatum of the halothane-anesthetized rat: an in vivo microdialysis study. J. Neurochem. 60, 1884–1893.

Morari, M., O'Connor, W.T., Ungerstedt, U., Fuxe, K., 1994. Dopamine D1 and D2 receptor antagonism differentially modulates stimulation of striatal neurotransmitter levels by N-methyl-D-aspartic acid. Eur. J. Pharmacol. 256, 23–30.

Morari, M., O'Connor, W.T., Darvelid, M., Ungerstedt, U., Bianchi, C., Fuxe, K., 1996. Functional neuroanatomy of the nigrostriatal and striatonigral pathways as studied with dual probe microdialysis in the awake rat-I. Effects of perfusion with tetrodotoxin and low-calcium medium. Neuroscience 72, 79–87.

Morgese, M.G., Cassano, T., Gaetani, S., Macheda, T., Laconca, L., Dipasquale, P., Ferraro, L., Antonelli, T., Cuomo, V., Giuffrida, A., 2009. Neurochemical changes in the striatum of dyskinetic rats after administration of the cannabinoid agonist WIN55,212-2. Neurochem. Int. 54, 56–64.

Nicholson, S.L., Brotchie, J.M., 2002. 5-hydroxytryptamine (5-HT, serotonin) and Parkinson's disease — opportunities for novel therapeutics to reduce the problems of levodopa therapy. Eur. J. Neurol. 9 (Suppl. 3), 1–6.
Nicola, S.M., Surmeier, J., Malenka, R.C., 2000. Dopaminergic modulation of neuronal excitability in the striatum and nucleus accumbens. Annu. Rev. Neurosci. 23, 185–215.
Nutt, J.G., 1990. Levodopa-induced dyskinesia: review, observations, and speculations. Neurology 40, 340–345.
Paxinos, G., Watson, C., 1982. The Rat Brain in Stereotaxic Coordinates. Academic Press, Sydney.
Radnikow, G., Misgeld, U., 1998. Dopamine D1 receptors facilitate GABAA synaptic currents in the rat substantia nigra pars reticulata. J. Neurosci. 18, 2009–2016.
Ramos, M., Goñi-Allo, B., Aguirre, N., 2005. Administration of SCH 23390 into the medial prefrontal cortex blocks the expression of MDMA-induced behavioral sensitization in rats: an effect mediated by 5-HT2C receptor stimulation and not by D1 receptor blockade. Neuropsychopharmacology 30, 2180–2191.
Rangel-Barajas, C., Silva, I., Lopéz-Santiago, L.M., Aceves, J., Erlij, D., Florán, B., 2011. L-DOPA-induced dyskinesia in hemiparkinsonian rats is associated with up-regulation of adenylyl cyclase type V/VI and increased GABA release in the substantia nigra reticulata. Neurobiol. Dis. 41, 51–61.
Robelet, S., Melon, C., Guillet, B., Salin, P., 2004. Kerkerian-Le Goff L. Chronic L-DOPA treatment increases extracellular glutamate levels and GLT1 expression in the basal ganglia in a rat model of Parkinson's disease. Eur. J. Neurosci. 20, 1255–1266.
Robertson, G.S., Robertson, H.A., 1989. Evidence that L-dopa-induced rotational behavior is dependent on both striatal and nigral mechanisms. J. Neurosci. 9, 3326–3331.
Sarre, S., Vandeneede, D., Ebinger, G., Michotte, Y., 1998. Biotransformation of L-DOPA to dopamine in the substantia nigra of freely moving rats: effect of dopamine receptor agonists and antagonists. J. Neurochem. 70, 1730–1739.
Schiavi, G.B., Brunet, S., Rizzi, C.A., Ladinsky, H., 1994. Identification of serotonin 5-HT4 recognition sites in the porcine caudate nucleus by radioligand binding. Neuropharmacology 33, 543–549.
Seeman, P., Van Tol, H.H., 1994. Dopamine receptor pharmacology. Trends Pharmacol. Sci. 15, 264–270.
Sibley, D.R., Monsma Jr., F.J., 1992. Molecular biology of dopamine receptors. Trends Pharmacol. Sci. 13, 61–69.
Stacey, A.E., Woodhall, G.L., Jones, R.S., 2002. Neurokinin-receptor-mediated depolarization of cortical neurons elicits an increase in glutamate release at excitatory synapses. Eur. J. Neurosci. 16, 1896–1906.
Taylor, L.A., Tedford, C.E., McQuade, R.D., 1991. The binding of SCH 39166 and SCH 23390 to 5-HT1C receptors in porcine choroid plexus. Life Sci. 49, 1505–1511.
Taylor, J.L., Bishop, C., Walker, P.D., 2005. Dopamine D1 and D2 receptor contributions to L-DOPA-induced dyskinesia in the dopamine-depleted rat. Pharmacol. Biochem. Behav. 81, 887–893.
Ungerstedt, U., Arbuthnott, G.W., 1970. Quantitative recording of rotational behavior in rats after 6-hydroxy-dopamine lesions of the nigrostriatal dopamine system. Brain Res. 24, 485–493.
Volta, M., Viaro, R., Trapella, C., Marti, M., Morari, M., 2011. Dopamine-nociceptin/orphanin FQ interactions in the substantia nigra reticulata of hemiparkinsonian rats: Involvement of D(2)/D(3) receptors and impact on nigro-thalamic neurons and motor activity. Exp. Neurol. 228, 126–137.
Westin, J.E., Lindgren, H.S., Gardi, J., Nyengaard, J.R., Brundin, P., Mohapel, P., Cenci, M.A., 2006. Endothelial proliferation and increased blood–brain barrier permeability in the basal ganglia in a rat model of 3,4-dihydroxyphenyl-L-alanine-induced dyskinesia. J. Neurosci. 26, 9448–9461.
Westin, J.E., Vercammen, L., Strome, E.M., Konradi, C., Cenci, M.A., 2007. Spatiotemporal pattern of striatal ERK1/2 phosphorylation in a rat model of L-DOPA-induced dyskinesia and the role of dopamine D1 receptors. Biol. Psychiatry 62, 800–810.
Windels, F., Kiyatkin, E.A., 2006. Dopamine action in the substantia nigra pars reticulata: iontophoretic studies in awake, unrestrained rats. Eur. J. Neurosci. 24, 1385–1394.
Winkler, C., Kirik, D., Bjorklund, A., Cenci, M.A., 2002. L-DOPA-induced dyskinesia in the intrastriatal 6-hydroxydopamine model of parkinson's disease: relation to motor and cellular parameters of nigrostriatal function. Neurobiol. Dis. 10, 165–186.
Woodward, R.M., Panicker, M.M., Miledi, R., 1992. Actions of dopamine and dopaminergic drugs on cloned serotonin receptors expressed in Xenopus oocytes. Proc. Natl. Acad. Sci. U. S. A. 89, 4708–4712.
Zarrindast, M.R., Honardar, Z., Sanea, F., Owji, A.A., 2011. SKF 38393 and SCH 23390 inhibit reuptake of serotonin by rat hypothalamic synaptosomes. Pharmacology 87, 85–89.

Journal of Neurochemistry

JOURNAL OF NEUROCHEMISTRY | 2011 | 118 | 1043–1055 doi: 10.1111/j.1471-4159.2011.07376.x

ORIGINAL ARTICLE

Amantadine attenuates levodopa-induced dyskinesia in mice and rats preventing the accompanying rise in nigral GABA levels

Simone Bido,*,† Matteo Marti*,† and Michele Morari*,†

*Department of Experimental and Clinical Medicine, Section of Pharmacology, University of Ferrara, Ferrara, Italy

†Center for Neuroscience and National Institute of Neuroscience, University of Ferrara, Ferrara, Italy

Abstract

Amantadine is the only drug marketed for treating levodopa-induced dyskinesia. However, its impact on basal ganglia circuitry in the dyskinetic brain, particularly on the activity of striatofugal pathways, has not been evaluated. We therefore used dual probe microdialysis to investigate the effect of amantadine on behavioral and neurochemical changes in the globus pallidus and substantia nigra reticulata of 6-hydroxydopamine hemi-lesioned dyskinetic mice and rats. Levodopa evoked abnormal involuntary movements (AIMs) in dyskinetic mice, and simultaneously elevated GABA release in substantia nigra reticulata (~3-fold) but not globus pallidus. Glutamate levels were unaffected in both areas. Amantadine (40 mg/kg, i.p.), ineffective alone, attenuated (~50%) AIMs expression and prevented the GABA rise. Moreover, it unraveled a facilitatory effect of levodopa on pallidal glutamate levels. Levodopa also evoked AIMs expression and a GABA surge (~2-fold) selectively in the substantia nigra of dyskinetic rats. However, different from mice, glutamate levels rose simultaneously. Amantadine, ineffective alone, attenuated (~50%) AIMs expression preventing amino acid increase and leaving unaffected pallidal glutamate. Overall, the data provide neurochemical evidence that levodopa-induced dyskinesia is accompanied by activation of the striato-nigral pathway in both mice and rats, and that the anti-dyskinetic effect of amantadine partly relies on the modulation of this pathway.

Keywords: 6-OHDA, amantadine, dyskinesia, levodopa, microdialysis, substantia nigra.

J. Neurochem. (2011) **118**, 1043–1055.

Levodopa (L-DOPA) is the most effective medication for the treatment of Parkinson's disease. However, chronic treatment with L-DOPA is associated with the development of debilitating choreo-dystonic movements (dyskinesia) in two-third of patients after 6 years of treatment (Fahn 2000; Obeso *et al.* 2000, 2004). Changes at striatal dopamine (DA) D_1 receptor transmission underlie L-DOPA-induced dyskinesia (LID). Indeed, chronic and 'pulsatile' stimulation of up-regulated D_1 receptors leads to a pathological enhancement of cAMP levels (Corvol *et al.* 2004), protein phosphorylation (Santini *et al.* 2007) and expression of specific classes of immediate early genes (Andersson *et al.* 1999) and neuropeptide precursors (Cenci *et al.* 1998; Henry *et al.* 1999; Calon *et al.* 2002) which trigger pathological modifications of membrane excitability and synaptic plasticity in striatal medium spiny neurons (Picconi *et al.* 2003; Carta *et al.* 2006). Two populations of medium spiny neurons are enriched in the striatum. Those projecting monosynaptically to the substantia nigra pars reticulata (SNr)/globus pallidus (GP) internalis, which predominantly express D_1 receptors and are known as the 'direct pathway', and those projecting to the globus pallidus externalis, which predominantly express D_2 receptors and represent the first step of the 'indirect pathway' (Parent and Hazrati 1995a,b). According to the heuristic model of

Received March 2, 2011; revised manuscript received July 4, 2011; accepted July 4, 2011.

Address correspondence and reprint requests to Michele Morari, Department of Experimental and Clinical Medicine, Section of Pharmacology, University of Ferrara via Fossato di Mortara 17-19, 44100 Ferrara, Italy. E-mail: m.morari@unife.it

Abbreviations used: 6-OHDA, 6-hydroxydopamine; AIMs, abnormal involuntary movements; ALO, axial, limb, orolingual; DA, dopamine; GLU, glutamate; GP, globus pallidus; L-DOPA, levodopa; LID, L-DOPA-induced dyskinesia; MFB, medial forebrain bundle; PBS, phosphate buffer saline; SNr, substantia nigra pars reticulata; STN, subthalamic nucleus; TBS, tris buffer saline; TH, tyrosine hydroxylase.

© 2011 The Authors
Journal of Neurochemistry © 2011 International Society for Neurochemistry,

basal ganglia functioning (Albin *et al.* 1989; DeLong 1990), unbalance between the activity of these two pathways underlies the hyperkinetic motions associated with LID. However, although different lines of evidence suggested that dyskinesia appearance is accompanied by over-activation of the direct pathway (Cenci *et al.* 1998; Picconi *et al.* 2003) a parallel over-inhibition of the indirect pathway has not been documented (Calon *et al.* 2002; Carta *et al.* 2008; Bateup *et al.* 2010), although the involvement of GP has been proposed (Mehta *et al.* 2001). Most of these findings have been obtained in non-human primate and rat models of LID (Bezard *et al.* 2003; Cenci and Lundblad 2007). More recently, a mouse model has also been validated (Lundblad *et al.* 2004, 2005) which essentially reproduces peak-dose dyskinesia observed in the rat. Although scoring of abnormal involuntary movements (AIMs, a behavioral correlate of dyskinesia) affecting axial, limb and orolingual muscles appears more challenging in mice than in rats (Cenci and Ohlin 2009), modelling dyskinesia in mice offered a new tool for target validation based on genetic approaches (Xiao *et al.* 2006; Santini *et al.* 2007; Darmopil *et al.* 2009; Bateup *et al.* 2010). Biochemical and behavioral studies have revealed strong similarities between the rat and mouse models of dyskinesia in terms of cellular adaptation mechanisms and responsiveness to anti-dyskinetic drugs (Cenci and Lundblad 2007). However, no neurochemical study has been undertaken to study the correlation between AIMs appearance following L-DOPA and changes in striatofugal pathways in mice. Moreover, the impact of amantadine, the reference drug in LID therapy, on basal ganglia circuitry and, specifically, the striatofugal pathways in dyskinesia has never been investigated. We therefore used dual probe microdialysis to investigate the effect of L-DOPA on GABA and glutamate (GLU) release in the SNr and GP of awake dyskinetic mice as well as the modulation operated by amantadine. The neurochemical pattern of response to amantadine was also measured in dyskinetic rats for a comparison. AIMs were scored simultaneously with sample collection.

Materials and methods

Experimental design

Forty mice were lesioned by intrastriatal injections of 6-hydroxydopamine (6-OHDA) and, 2 weeks later, screened using a battery of behavioral tests. An additional group of mice ($n = 8$) was sham-lesioned for a comparison of motor performance on the rotarod. Thirty-three 6-OHDA-lesioned mice (see selection criteria below) were made dyskinetic by chronic L-DOPA administration (15 mg/kg plus 12 mg/kg benserazide, i.p., once daily for 10 days). During this period, AIMs were scored five times. Mice showing total AIMs score > 100 in the last session were enrolled for the microdialysis study and underwent probe implantation (24 h after the last L-DOPA injection). The theoretical maximal total AIM score for each animal is 288 (48 for each of the six 20-min sessions). After surgery, mice were allotted into three groups receiving L-DOPA (15 mg/kg, i.p.; $n = 11$), amantadine (40 mg/kg, i.p.; $n = 10$) or their combination ($n = 10$). Each animal underwent two microdialysis sessions (24 and 48 h after probe implantation), and received saline or drugs in a randomized fashion.

Rats

Thirty rats were lesioned by medial forebrain bundle (MFB) injection of 6-OHDA and, 2 weeks later, screened using amphetamine testing. Twenty-five 6-OHDA-lesioned rats (see selection criteria below) were made dyskinetic by chronic L-DOPA administration (6 mg/kg plus 12 mg/kg benserazide, i.p., once daily for 21 days). During this period, AIMs were scored seven times. Twenty rats showing total AIMs score > 100 in the last session were enrolled for the microdialysis study and underwent probe implantation (24 h after the last L-DOPA injection). Five rats underwent acute amantadine challenge for a comparison of the response between pre- and post-surgery conditions (Fig. 8). The theoretical maximal total AIMs score for each animal is 432 (48 each of the nine 20-min sessions). After surgery, rats were allotted into three groups receiving L-DOPA (6 mg/kg; i.p., $n = 7$), amantadine (40 mg/kg, i.p.; $n = 6$) or their combination ($n = 6$). Each animal underwent two microdialysis sessions (24 and 48 h after probe implantation), and received saline or drugs in a randomized fashion.

Subjects

Male Sprague–Dawley rats (150 g Harlan Italy; S. Giorgio al Natisone, Italy) and Swiss mice (24–25 g Stefano Morini, Modena, Italy) were used. The animals were housed under a 12-h light/dark cycle and given water and food *ad libitum*. Drug treatments and animal housing conditions had been approved by the Ethical Committee of the University of Ferrara and the Italian Ministry of Health (licenses 94–2007-B and 194–2008-B). Adequate measures were taken to minimize animal pain and discomfort.

Surgery and behavioral screening

Rats

Unilateral lesion of DA neurons was induced in isoflurane-anesthetized rats according to standard procedures (Marti *et al.* 2002, 2005, 2007). Eight micrograms of 6-OHDA (in 4 μL of saline containing 0.02% ascorbic acid) were stereotaxically injected into MFB according to the following coordinates from bregma (in mm): antero-posterior AP −4.4, medio-lateral ML −1.2, dorso-ventral DV −7.8 below dura (Paxinos and Watson 1982). Two weeks after surgery, rats were injected with amphetamine (5 mg/kg i.p., dissolved in saline) and only those rats performing > 7 ipsilateral turns/min were enrolled in the study.

Mice

Striatal injections of 6-OHDA were performed in isoflurane-anesthetized mice as described by Lundblad *et al.* (2004). Six micrograms of 6-OHDA free-base (in 2 μL of saline containing 0.02% ascorbic acid) were stereotaxically injected into the striatum according to the following coordinates from bregma (in mm); first injection, AP +1.0, ML −2.1, DV −2.9 below dura; second injection, AP +0.3, ML −2.3, DV −2.9 below dura (Paxinos and Franklin 2001). Mice were screened with the cylinder test (Schallert *et al.* 2000) 2 weeks after lesion; mice showing a number of wall

© 2011 The Authors

contacts with contralateral forelimb < 40% of total contacts in 5 min of observation were enrolled in the study. This behavioral score was associated with > 90% depletion of DA terminals (Schallert *et al.* 2000; Lundblad *et al.* 2004) and > 95% depletion of striatal DA (Carta *et al.* 2006). In mice, the dopaminergic nature of the motor deficit was confirmed by testing the responsiveness to L-DOPA using the bar, drag and rotarod tests, as previously described (Marti *et al.* 2005, 2007).

LID induction and AIMs ratings

A different protocol of LID induction was used in mice and rats according to the literature: 15 mg/kg L-DOPA (+12 mg/kg benserazide, i.p., once a day for 10 days) in the mouse (Santini *et al.* 2009), and 6 mg/kg L-DOPA (+ 12 mg/kg benserazide, i.p., once a day for 21 days) in the rat (Cenci *et al.* 1998). Quantification of L-DOPA-induced AIMs was carried out as described in previous papers (Lee *et al.* 2000; Lundblad *et al.* 2002, 2004; Winkler *et al.* 2002). Briefly, rats and mice were observed individually for 1 min every 20 min during the 2–3 h that followed an L-DOPA injection. Dyskinetic movements were classified based on their topographic distribution into three subtypes: (i) axial AIM, that is, twisted posture or choreiform twisting of the neck and upper body toward the side contralateral to the lesion; (ii) forelimb AIM, that is, jerky or dystonic movements of the contralateral forelimb and/or purposeless grabbing movement of the contralateral paw; (iii) orolingual AIM, that is, orofacial muscle twitching, empty masticatory movements and contralateral tongue protrusion. Each AIM subtype was rated on frequency and amplitude scales from 0 to 4 as described in Cenci and Lundblad (2007). Axial, forelimb and orolingual (ALO) AIMs were presented together as a global AIMs score and also as separated items per session (sum of the products of amplitude and frequency scores from all monitoring periods (Carta *et al.* 2006).

In vivo microdialysis

Microdialysis was used to simultaneously monitor GABA and GLU release in the SNr and GP of freely moving mice (Mabrouk *et al.* 2010; Volta *et al.* 2010) and rats (Morari *et al.* 1996a,b; Marti *et al.* 2002, 2005). Briefly, two microdialysis probes of concentric design were stereotaxically implanted under isoflurane anesthesia (1.5% in air) into the lesioned SNr and ipsilateral GP (1 and 2 mm dialyzing membrane, respectively), according to the following coordinates from bregma and the dural surface (mm): mouse GP, AP −0.46, ML −1.8, DV −3.9, mouse SNr, AP −3.3, ML −1.25, DV −4.6; rat GP, AP −1.3, ML −3.3, DV −7.5, rat SNr, AP −5.5, ML −2.2, DV −8. Twenty-four hours after surgery, probes were perfused with a modified Ringer solution ($CaCl_2$ 1.2 mmol/L, KCl 2.7 mmol/L, NaCl 148 mmol/L and $MgCl_2$ 0.85 mmol/L) at a flow rate of 2.1 (mouse) and 3 μL/min (rat). After 6 h rinsing, samples were collected every 20 min for a total of 3–4 h. At least three baseline samples were collected before i.p. administration of L-DOPA, amantadine (40 mg/kg, i.p.) or saline. In the combination studies, amantadine was administered 1 h before L-DOPA. At the end of experiment, animals were sacrificed and the correct placement of the probes was verified histologically.

Endogenous GLU and GABA analysis

GLU and GABA were measured by HPLC coupled with fluorometric detection as previously described (Marti *et al.* 2007). Thirty microliters of *o*-phthaldialdehyde/mercaptoethanol reagent were added to 30 μL aliquots of sample and 50 μL of the mixture was automatically injected (Triathlon autosampler; Spark Holland, Emmen, the Netherlands) onto a 5-C18 Chromsep analytical column (3 mm inner diameter, 10 cm length; Chrompack, Middelburg, the Netherlands) perfused at a flow rate of 0.48 mL/min (Beckman 125 pump; Beckman Instruments, Fullerton, CA, USA) with a mobile phase containing 0.1 M sodium acetate, 10% methanol and 2.2% tetrahydrofuran (pH 6.5). GLU and GABA were detected by means of a fluorescence spectrophotometer FP-2020 Plus (Jasco, Tokyo, Japan) with the excitation and the emission wavelengths set at 370 and 450 nm respectively. The limits of detection for GLU and GABA were ∼1 and ∼0.5 nM, respectively. Retention times for GLU and GABA were ∼3.5 and ∼18.0 min, respectively.

Histological evaluation

Mice were anaesthetized with ketamine 85 mg/kg and xylazine 15 mg/kg (i.p.), transcardially perfused with 20 mM phosphate-buffered saline (PBS) and fixed with 4% paraformaldehyde in PBS at pH 7.4. Brains were removed, post-fixed overnight and cryoprotected in 50% glycerol (solution in PBS). Serial coronal sections of 30 μm thickness were made in the striatum (−0.8 to +1.3 from bregma) and every second section processed for tyrosine hydroxylase (TH) immunohistochemistry (see below). Free-floating striatal sections were rinsed in Tris-buffered saline (TBS; 0.25 M Tris and 0.5 M NaCl, pH 7.5), incubated for 5 min TBS containing 3% H_2O_2 and 10% methanol (vol/vol), and then rinsed three times (10 min each) in TBS. After 20 min incubation in 0.2% Triton X-100 in TBS, sections were rinsed three times in TBS again. Finally, they were incubated overnight at 4°C with the anti-TH mouse monoclonal primary antibody (1 : 40; AbCam, Cambridge, UK). Following incubation, sections were rinsed three times for 10 min in TBS and incubated for 45 min with secondary antibody (1 : 200; Alexa Fluor 680 anti-mouse IgG).

TH immunoreactivity evaluation

Mouse brain sections were analyzed with a Zeiss LSM 510 (Zeiss, Oberkochem, Germany) and acquired with Plan-Neofluar 10× (Edmund Optics, Barrington, IL, USA) lens. TH-immunoreactive fiber density was analyzed using ImageJ software (Wayne Rasband, National Institute of Health, Bethesda, MD, USA). To quantify TH staining, the optical densities were corrected for non-specific background density, measured in the corpus callosum. TH-positive fiber density was calculated as the ratio between optical density in the denervated (ipsilateral) and intact (contralateral) side.

Data presentation and statistical analysis

Motor performance has been expressed as time (in seconds) on bar or rod (bar and rotarod tests), and number of steps (drag test). AIMs rating has been expressed as ALO score (magnitude × amplitude). In microdialysis studies, GABA and GLU release has been expressed as percentage ± SEM of basal values (calculated as mean of the two samples before the treatment). In Figure legends (and in Results section), basal dialysate levels of amino acids were also given as absolute values (in nM). Statistical analysis has been performed by two-way repeated measure (RM) analysis of variance (ANOVA). In case ANOVA yielded a significant *F* score, *post hoc*

© 2011 The Authors

analysis has been performed by contrast analysis to determine group differences. In case a significant time × treatment interaction was found, the sequentially rejective Bonferroni's test was used (implemented on Excel spreadsheet) to determine specific differences (i.e. at the single time-point level) between groups. p-values < 0.05 were considered to be statistically significant.

Drugs

6-OHDA hydrobromide, D-amphetamine sulphate, L-DOPA methyl ester hydrochloride, benserazide hydrochloride and amantadine hydrochloride were purchased from Sigma-Aldrich (AB, Italy). Except from 6-OHDA, all drugs were dissolved in saline and administered within 1 h at the volume of 1.0 mL/kg body weight.

Results

L-DOPA relieved akinesia, bradykinesia and motor deficit in hemi-parkinsonian mice

Basal motor scores of naïve mice ($n = 11$) were 8.0 ± 1.0 s of immobility (bar test), 15.0 ± 2.0 steps (drag test) and 1253.5 ± 122.7 s of permanence on the rod (rotarod test). Unilateral intrastriatal injections of 6-OHDA caused marked akinesia and bradykinesia mainly affecting the contralateral forepaw, and an overall reduction of motor performance. Immobility time at the contralateral paw increased by about 4-fold compared with the ipsilateral paw (Fig. 1a) whereas the number of steps was reduced by ~70% (Fig. 1b). Finally, rotarod performance was reduced by ~58% after 6-OHDA lesioning (Fig. 1c). To test the dopaminergic nature of this motor deficit, L-DOPA was systemically administered (i.p.) at a dose which was reported to attenuate hypokinesia in MPTP-treated mice (10 mg/kg in combination with 12 mg/kg benserazide; Viaro *et al.* 2008). L-DOPA normalized immobility time (Fig. 1a) and stepping activity (Fig. 1b) at the contralateral paw but was unable to attenuate deficit in rotarod performance (Fig. 1c). This behavioral phenotype was associated with a 90.3 ± 2.7% reduction of striatal TH-immunopositive fibers in the ipsilateral compared with the contralateral striatum ($n = 9$, $t = 9.367$, $p < 0.0001$, Student's t-test).

Amantadine attenuated LID expression and its neurochemical correlates in hemi-parkinsonian mice

Chronic treatment of hemi-parkinsonian mice with L-DOPA (15 mg/kg plus 12 mg/kg benserazide; i.p., once daily for 10 days) caused the development of axial, limb and orolingual AIMs having a similar temporal profile. AIMs appearance was gradual and progressive, reaching a plateau at the fifth day of treatment (Fig. 2a and b). To examine whether mouse dyskinesia was accompanied by changes of activity along the striatofugal pathways, GABA and GLU release was monitored in SNr and GP along with behavior following L-DOPA alone (15 mg/kg plus 12 mg/kg benserazide, i.p.) or in combination with amantadine. A dose of 40 mg/kg

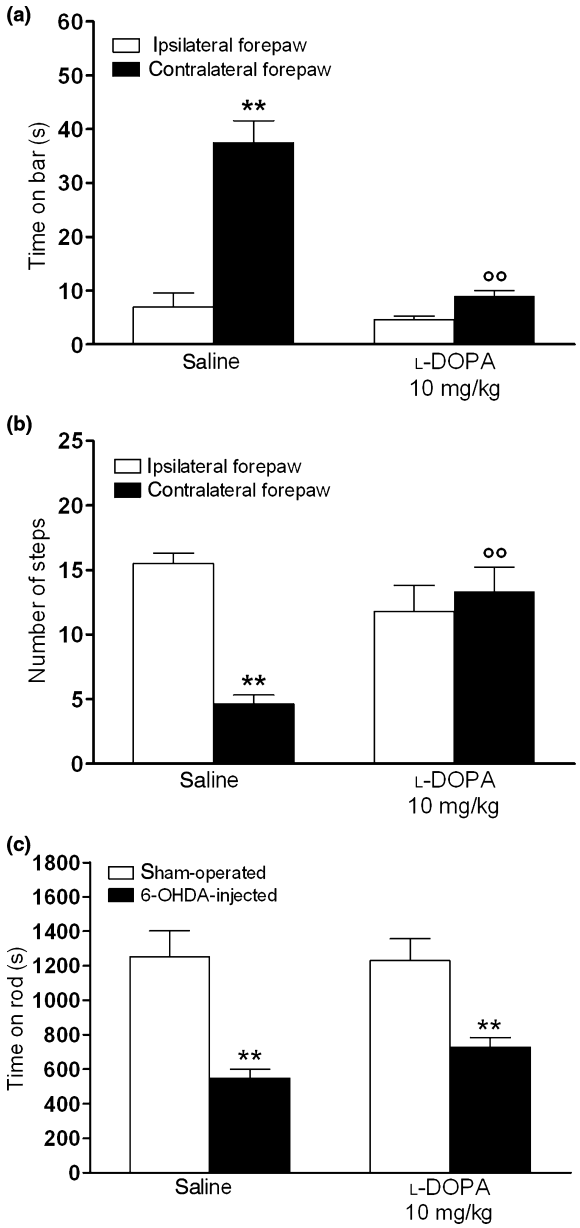

Fig. 1 L-DOPA relieved akinesia/bradykinesia in hemi-parkinsonian mice. Systemic (i.p.) administration of L-DOPA (15 mg/kg plus 12 mg/kg of benserazide) reduced the time spent on the blocks in the bar test (a), increased the number of steps of the contralateral forepaw in the drag test (b), and failed in improving overall motor performance in the rotarod test (c). Behavioral testing was performed 30 min after L-DOPA injection. Motor asymmetry was evaluated separately at the ipsilateral and contralateral (parkinsonian) paw (a, b). Data are expressed as absolute values (s, number of steps) and are mean ± SEM of 8–10 animals. Statistical analysis was performed by one-way ANOVA followed by contrast analysis and the sequentially rejective Bonferroni's test. Panel a: significant effect of treatment ($F_{3,28} = 37.70$, $p < 0.0001$). Panel b: significant effect of treatment ($F_{3,28} = 10.16$, $p = 0.0001$). Panel c: significant effect of treatment ($F_{3,24} = 20.65$, $p < 0.0001$). $^{**}p < 0.01$ versus the ipsilateral forepaw (a, b) or sham-operated mice (c), $^{\circ\circ}p < 0.01$ versus the contralateral forepaw of saline injected mice (a, b).

© 2011 The Authors

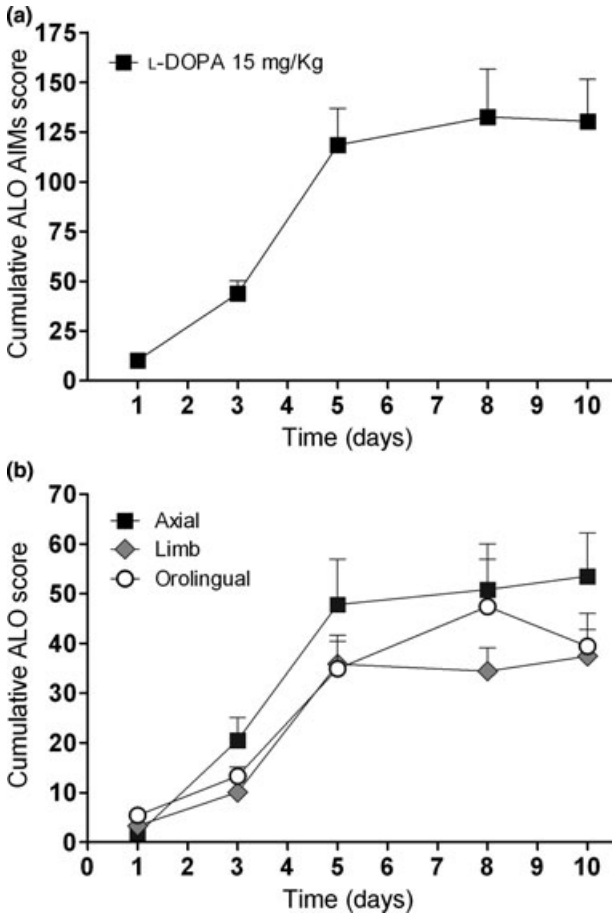

Fig. 2 Development of dyskinesia during chronic L-DOPA administration in 6-OHDA hemi-lesioned mice. Mice were treated for 10 days with L-DOPA 15 mg/kg (plus benserazide 12 mg/kg, i.p., once daily) and AIMs were evaluated at days 1, 3, 5, 8, and 10 after treatment onset. Axial, limb and orolingual (ALO) AIMs were scored every 20 min for 120 min after L-DOPA administration. Data (in arbitrary units; see Results section) have been presented either as the sum of each AIM subtype (cumulative ALO score; a) or as each AIMs subtype separately (b). Each value is the mean ± SEM of 10–11 animals.

amantadine was chosen because it proved effective in reducing ALO AIMs in mice and rats without affecting the locomotive components of AIMs (Lundblad *et al.* 2002; Dekundy *et al.* 2007) which is considered a marker of the therapeutic effect of L-DOPA (Cenci *et al.* 2002). L-DOPA caused the appearance of dyskinetic movements already at 20 min after injection. The intensity of dyskinesia remained stably at maximal levels up to 80 min after injection (Fig. 3a), after which AIMs tended to decline. Amantadine administration (1 h before L-DOPA) caused an overall (∼50%) attenuation of AIMs severity with some preference for orolingual (∼66%) over axial (∼47%) and limb (∼43%) AIMs (Fig. 3b and d). These behavioral changes were associated with different neurochemical patterns in SNr and GP (Fig. 4). A marked increase of GABA levels was observed in SNr after L-DOPA administration, with a peak (∼3-fold over basal) at 80 min (Fig. 4a). Consistent with its anti-dyskinetic effect, amantadine prevented the rise in GABA levels induced by L-DOPA (Fig. 4a) without causing *per se* any change in basal values. Nigral GLU levels were not significantly affected by L-DOPA although showing a tendency to decline over time (Fig. 4b). Amantadine, alone or in combination with L-DOPA, was also ineffective, although causing a trend for an increase (∼30% 1 h after injection, Fig. 4b). Opposite to SNr, L-DOPA alone did not cause any significant changes of GABA levels in GP (Fig. 4c). Amantadine alone was also ineffective. However, when co-administered with L-DOPA it caused a marked elevation of GABA levels up to ∼217% at the end of collection period. L-DOPA, amantadine or their combination failed to affect pallidal GLU levels (Fig. 4d).

Amantadine attenuated LID expression and its neurochemical correlates in hemi-parkinsonian rats

Rats chronically treated with L-DOPA (6 mg/kg plus 12 mg/kg of benserazide) developed a stable degree of dyskinesia already at the ninth day of treatment, scoring the maximal values at the 17th day. Axial and limb AIMs showed a similar temporal profile, reaching a similar level of intensity over the 21-day treatment. Conversely, the development of orolingual AIMs was less appreciable, and this AIM subtype was poorly represented in this group of animals (Fig. 5a and b). L-DOPA (6 mg/kg plus 12 mg/kg benserazide) induced AIM appearance already at 20 min after injection, the maximal intensity (15.5 ± 2.1) being reached after 60 min. Amantadine reduced AIMs expression by ∼53% (Fig 6a) being more effective on the axial and limb components (∼55% both) than the orolingual one (∼44%, Fig. 6c and d). As previously reported (Mela *et al.* 2007a), an increase of GABA levels was observed in the SNr of dyskinetic rats after L-DOPA challenge (6 mg/kg plus 12 mg/kg benserazide, i.p.) which reached the maximum value (∼2-fold over basal) at 60 min (Fig. 7a). Different from that observed in mice, the increase of GABA was accompanied by a quantitatively similar increase of GLU levels (Fig. 7b). Amantadine, ineffective alone, prevented the rise of both amino acids associated with AIMs. Conversely, no changes of GABA or GLU levels were observed in GP following administration of L-DOPA, amantadine or their combination (Fig. 7c and d).

Discussion

The hemi-parkinsonian mouse model of LID proves a valuable and unique tool in dyskinesia research because not only it allows interspecies comparisons of drug responses but also because it is suitable for genetic manipulations, particularly advantageous in target validation. The motor impairments observed in striatally lesioned hemi-parkinsonian mice had a dopaminergic origin because these mice showed a

© 2011 The Authors

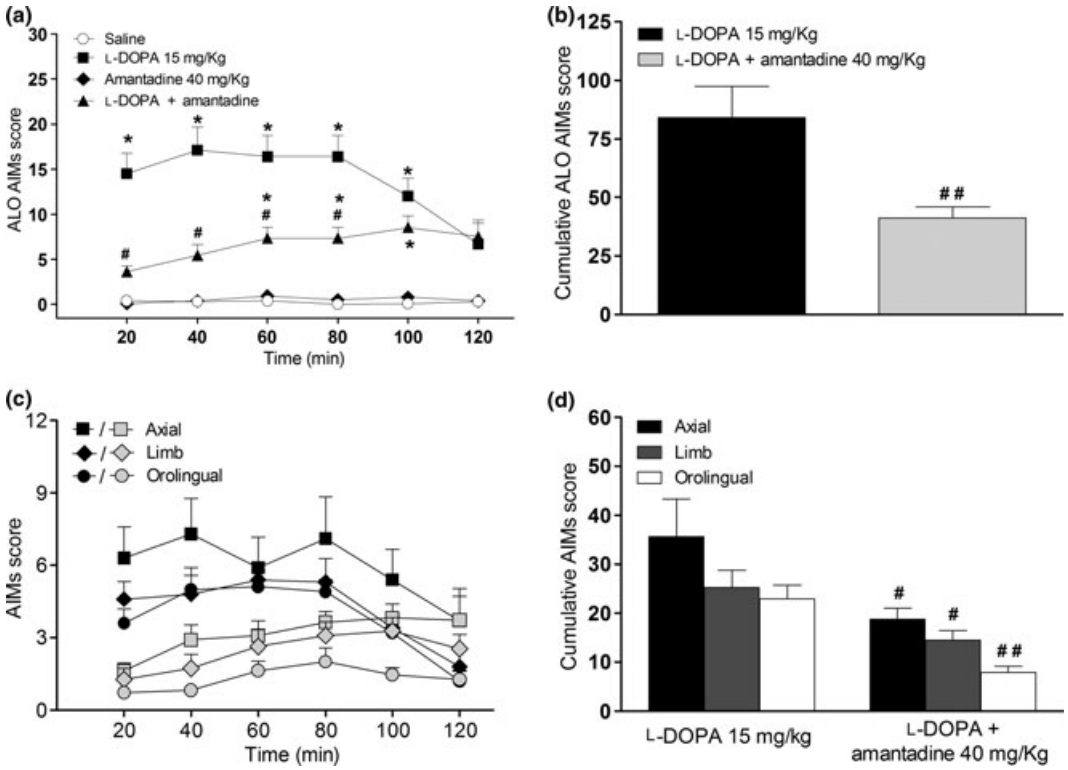

Fig. 3 Behavioral effect of L-DOPA and amantadine in dyskinetic mice undergoing microdialysis. 6-OHDA hemi-lesioned mice were made dyskinetic by chronic L-DOPA administration (15 mg/kg plus 12 mg/kg benserazide, i.p., once a day for 10 days). At the end of treatment, mice underwent surgery for microdialysis probe implantation, and 24 h later were challenged with L-DOPA alone or in combination with amantadine (40 mg/kg; i.p., 1 h in advance). Control mice were treated with either amantadine or saline alone. ALO AIMs were scored every 20 min for 120 min after L-DOPA administration. Temporal profiles of AIMs taken as a whole (ALO AIMs; a) or as separate items (c) are shown. Cumulative dyskinesia score (i.e. the sum of the scores given at each of the six observation sessions) is shown for ALO AIMs as a whole (b) or for each AIM subtype separately (d). Co-administration of amantadine reduced AIMs expression, affecting about to the same extent each AIMs subtype. Data are expressed as arbitrary units (see Results section) and are mean ± SEM of 10–11 animals. Panel a: significant effect of treatment ($F_{3,15} = 111.8$, $p < 0.0001$) but not time ($F_{5,198} = 1.68$, $p = 0.14$), and significant time × treatment interaction ($F_{15,198} = 2.31$, $p = 0.0057$), according to two-way RM ANOVA followed by contrast analysis and the sequentially rejective Bonferroni's test. Panel b: significant effect of amantadine ($t = 3.15$, df = 19, $p = 0.0052$), according to unpaired Student's *t*-test. Panel d: significant effect of amantadine; axial ($t = 2.2$, df = 19, $p = 0.0399$), limb ($t = 2.73$, df = 19, $p = 0.0133$), orolingual ($t = 5{,}0$, df = 19, $p < 0.0001$) AIMs, according to unpaired Student's *t*-test. $^{*}p < 0.05$ versus saline, $^{\#}p < 0.05$, $^{\#\#}p < 0.01$ versus L-DOPA.

marked reduction of striatal TH terminals associated with motor recovery in response to L-DOPA (Lundblad *et al.* 2004). In our hands, recovery from akinesia and bradykinesia was obtained at the same dose effective in MPTP-treated mice (10 mg/kg; Viaro *et al.* 2008), although at variance with this model, L-DOPA could not rescue rotarod performance (Marti *et al.* 2005). However, the rotarod test is a test for gross motor ability, which integrates motor and non-motor parameters (Rozas and Labandeira Garcia 1997), and therefore involves not only the dorsal motor but also the limbic striatum and other structures outside the basal ganglia (e.g. peduncolo pontine nucleus and brainstem; Nauta *et al.* 1978; Christoph *et al.* 1986; Braak and Braak 2000). The lack of response of the rotarod performance to L-DOPA may thus be related to the recruitment of dopaminergic areas less or not affected by intrastriatal 6-OHDA, in which post-synaptic DA receptor up-regulation has not fully developed.

Axial, limb and orolingual AIMs gradually developed during chronic treatment with L-DOPA, showing maximal expression after 5 days of treatment. This may reflect the homogeneity of the lesion within the dorso-lateral striatum, because this region receives somatotopic cortical projections representing trunk, forepaw and orofacial muscles (McGeorge and Faull 1989). Microdialysis setting did not influence the acute response to L-DOPA because, in line with previous studies (Lundblad *et al.* 2004; Santini *et al.* 2007), AIMs were already maximal 20 min after L-DOPA administration and tended to disappear after 120 min. Moreover, the overall response to L-DOPA recorded in the dialysis setting (i.e. after probe implantation) was not different from

© 2011 The Authors

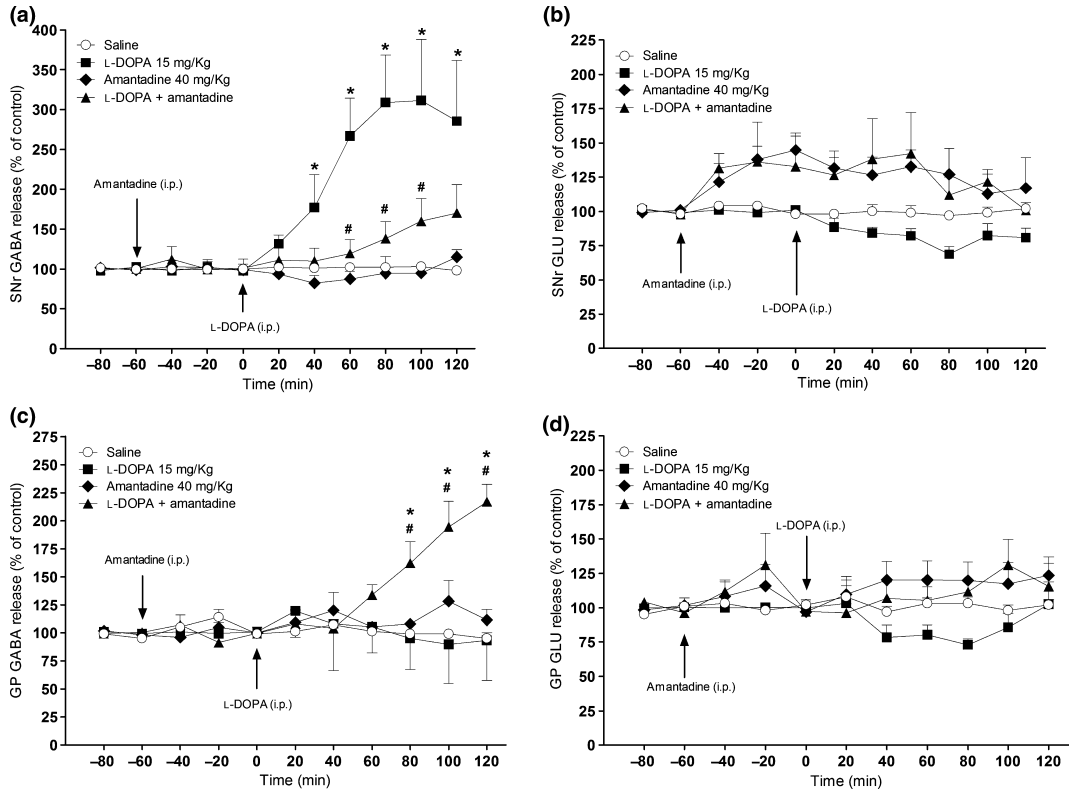

Fig. 4 Neurochemical effects of L-DOPA and amantadine in dyskinetic mice undergoing microdialysis. Dyskinetic mice (see legend to Fig. 3) were implanted with a probe in the lesioned substantia nigra reticulata (SNr; a, b) and another in ipsilateral globus pallidus (GP; c, d). Twenty-four hr later, mice received an acute challenge with L-DOPA alone (15 mg/kg plus 12 mg/kg benserazide, i.p.) or in combination with amantadine (40 mg/kg; i.p., 1 h in advance), and GABA (a, c) and GLU (b, d) levels were monitored for 120 min. Control mice were injected either with amantadine alone or saline. Data are expressed as percentage of basal pre-treatment levels (calculated as the mean of the two samples preceding the treatment) and are mean ± SEM of 7–11 animals. Basal dialysate levels of GABA and GLU were 8.0 ± 0.4 and 73.6 ± 8.0 nM, respectively, in SNr, and 7.7 ± 0.6 and 79.5 ± 8.7 nM, respectively, in GP. Statistical analysis was performed by two-way RM ANOVA followed by contrast analysis and the sequentially rejective Bonferroni's test. Panel a: significant effect of treatment ($F_{3,30} = 24.66$, $p < 0.0001$), time ($F_{10,264} = 1.94$, $p = 0.0398$) but not time × treatment interaction ($F_{30,264} = 1.09$, $p = 0.34$). Panel c: significant effect of treatment ($F_{3,30} = 9.84$, $p < 0.0001$), time ($F_{10,255} = 2.46$, $p = 0.0079$) and time × treatment interaction ($F_{30,255} = 2.75$, $p < 0.0001$). $^{*}p < 0.05$ versus saline; $^{\#}p < 0.05$ versus L-DOPA alone.

that observed in the same animal before surgery (Fig. 8). The anti-dyskinetic effect of amantadine was also quantitatively similar under the two different conditions (Fig. 8).

In keeping with that found in the rat (see also Mela *et al.* 2007a), L-DOPA caused a rise in GABA levels in the mouse SNr. Major sources of neuronal GABA levels in SNr are the striato-nigral and the pallido-nigral projections as well as GABA interneurons and collaterals of nigrofugal GABAergic neurons. Therefore, elevation of GABA levels might be related to activation of the direct striato-nigral pathway, leading to $GABA_A$ receptor-mediated overinhibition of nigro-thalamic neurons and thalamic disinhibition (Deniau and Chevalier 1985). The concomitant lack of significant changes of GABA (and GLU) levels in GP seems to exclude a contribution of the indirect pathway. This is in line with a study showing that DARPP-32 knockdown in striato-nigral neurons abolished dyskinesia whereas the same procedure in striato-pallidal neurons was ineffective (Bateup *et al.* 2010). A temporal mismatch was found between the behavioral and neurochemical responses in mice, the rise in nigral GABA being more gradual and prolonged compared with AIMs expression. As no such mismatch was observed in the rat, the lower perfusion rate through the mouse probe might be the cause for the delay of the neurochemical response. In contrast, however, we found that under the same microdialysis conditions nigral GLU levels closely matched the rapid (20 min) reduction of immobility time induced by administration of a nociceptin/orphanin FQ receptor antagonist in mice (Mabrouk *et al.* 2010; Volta *et al.* 2010). Interestingly enough, in the same studies changes in GABA levels were delayed compared with those of GLU. Therefore, the temporal dissociation observed in the mouse may reflect differences in intrinsic (e.g. uptake efficiency) mechanisms regulating extracellular GABA concentrations. Alternatively,

© 2011 The Authors

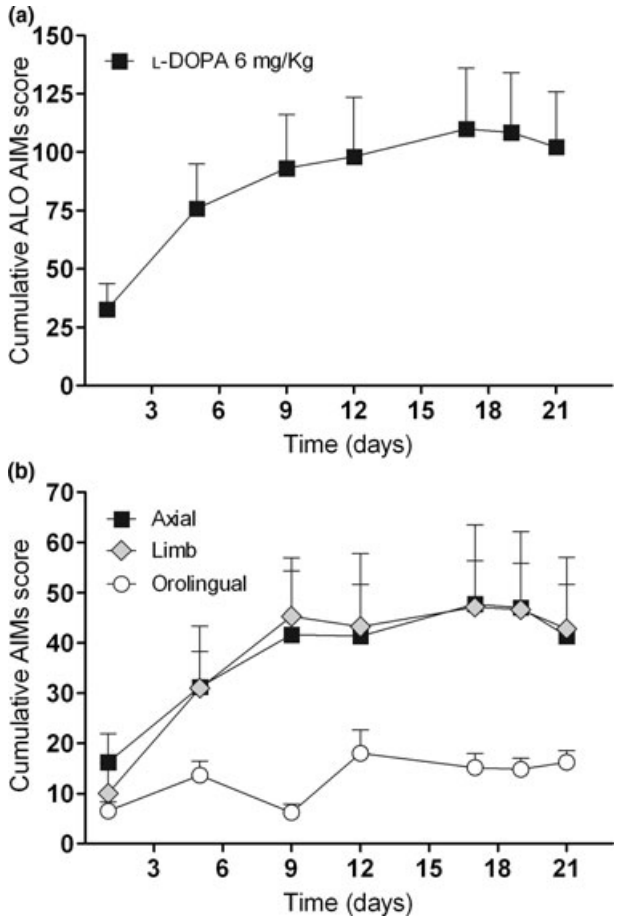

Fig. 5 Development of dyskinesia during chronic L-DOPA administration in 6-OHDA hemi-lesioned rats. Rats were treated for 21 days with L-DOPA 6 mg/kg (plus benserazide 12 mg/kg, one injection per day). AIMs were evaluated at days 1, 5, 9, 12, 17, 19, 21 after L-DOPA injection. ALO AIMs were scored every 20 min over a period of 120 min after L-DOPA administration. Data have been presented either as the sum of each AIM subtype (cumulative ALO AIMs; a) or as each AIM subtype separately (b). Data are mean ± SEM of 10–11 animals.

we have to consider the possibility that elevation of nigral GABA may not be the only trigger for dyskinesia. In support of this view, reverse dialysis of GABA alone in SNr failed to evoke AIMs (Buck *et al.* 2010). Moreover, even if amantadine prevented the rise in nigral GABA it could not completely block AIMs appearance. Larger increases in extracellular DA levels have been demonstrated in the SNr (and striatum) of dyskinetic compared with non-dyskinetic rats following L-DOPA administration (Lindgren *et al.* 2010). This suggests that nigral DA might play a role in triggering dyskinesia, via direct modulation of nigro-thalamic neurons (Zhou *et al.* 2009) or through the release of other neurotransmitters acting on the nigral output. In addition, the dyskinesiogenic action of L-DOPA may involve dopaminoceptive neurons in the thalamus or cerebellum (Rolland *et al.* 2007).

The mechanisms underlying the dual effect of amantadine, used both as anti-parkinsonian and anti-dyskinetic in combination with L-DOPA are not completely understood, also because amantadine has a complex pharmacodynamic profile. It inhibits DA reuptake (Heikkila and Cohen 1972; Mizoguchi *et al.* 1994) and increases DOPA decarboxyalase activity (Fisher *et al.* 1998; Deep *et al.* 1999). Amantadine also behaves as an antagonist at NMDA receptors (Kornhuber *et al.* 1991; Parsons *et al.* 1996), where it acts by stabilizing the 'close' state of the channel (Blanpied *et al.* 2005). Finally, it inhibits K^+ channels in the atria in a similar way to 4-aminopyridine, an action resulting in an increase in membrane excitability (Northover 1994). The mild anti-parkinsonian effect of amantadine has been related to its dopaminergic actions, in particular to the ability to potentiate the L-DOPA-induced elevation of striatal DA release (Arai *et al.* 2003). However, this effect is difficult to reconcile with its anti-dyskinetic action because a potentiation of the L-DOPA-induced DA release would also lead to stimulation of D1 receptors on the striatal cell bodies and nigral terminals of striato-nigral GABA neurons, thereby promoting LID. Interestingly, the potentiation of the L-DOPA-induced striatal DA release (Sarre *et al.* 2008) and the mild anti-parkinsonian effect (Mitchell and Carroll 1997; Nash *et al.* 1999, 2000; Steece-Collier *et al.* 2000; Loschmann *et al.* 2004) of amantadine are shared by NR2B receptor antagonists. In addition, we showed that the NR2B antagonist Ro25–6981 slightly reduced AIMs expression (maximally of ~25% at 5 mg/kg) in 6-OHDA hemi-lesioned dyskinetic rats (Mela *et al.* 2010). Therefore, based on the proposed functional segregation of NR2B and NR2A receptors along the striato-nigral and striato-pallidal pathways, respectively (Fantin *et al.* 2007, 2008), the anti-dyskinetic effect of amantadine may be accomplished via blockade of striatal NR2B receptors. However, given the mild and inconsistent (see Rylander *et al.* 2009) effect of Ro25–6981 in dyskinetic rats, it is unlikely that NR2B blockade represents the only mechanism underlying the anti-dyskinetic effect of amantadine. To support this view, the anti-dyskinetic dose of Ro25–6981 reduced GABA levels in SNr (Mela *et al.* 2010) whereas amantadine was ineffective. This might suggest that the amantadine profile is different from that of a selective NR2B antagonist. Indeed, amantadine does not display NMDA subtype receptor selectivity (Danysz *et al.* 1997). Interestingly, non-selective NMDA antagonists such as dizocilpine have been reported to prevent the L-DOPA induced GLU release in the DA-denervated striatum (Jonkers *et al.* 2002). As L-DOPA also elevated striatal GLU release in dyskinetic animals (Dupre *et al.* 2011) and dysfunction of GLU transmission is associated with LID (Calabresi *et al.* 2000; Oh and Chase 2002), reduction of striatal GLU release may result in an anti-dyskinetic effect. Amantadine may

© 2011 The Authors

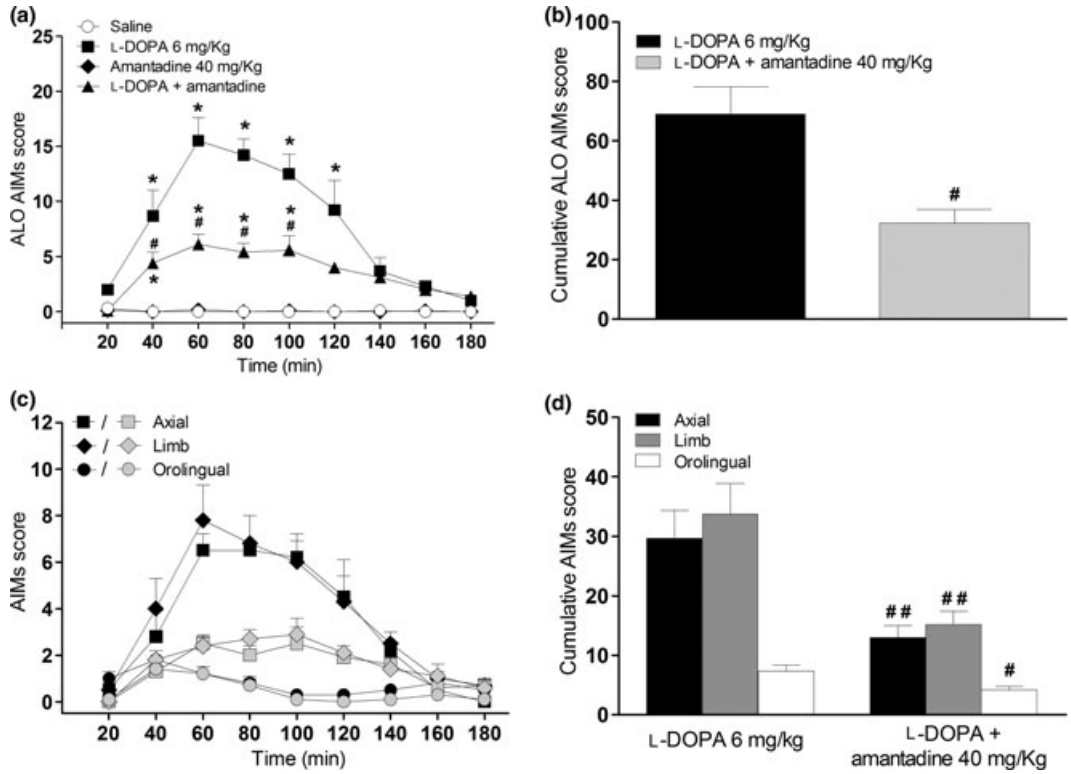

Fig. 6 Behavioral effect of L-DOPA and amantadine in dyskinetic rats undergoing microdialysis. 6-OHDA hemi-lesioned rats were made dyskinetic by chronic L-DOPA administration (6 mg/kg plus 12 mg/kg benserazide, i.p., once a day for 21 days). At the end of treatment, rats underwent surgery for microdialysis probe implantation, and were challenged with L-DOPA alone or in combination with amantadine (40 mg/kg; i.p., 1 h in advance) 24 h later. Control rats were treated with either amantadine or saline alone. ALO AIMs were scored every 20 min over 180 min after L-DOPA administration. Temporal profiles of AIMs taken as a whole (ALO AIMs; a) or as separate items (c) are shown. Cumulative dyskinesia score (i.e. the sum of the scores given at each of the nine observation sessions) is shown for ALO AIMs as a whole (b) or for each AIM subtype separately (d). Data are expressed as arbitrary units (see Results section) and are mean ± SEM of 5–7 animals. Panel a: significant effect of treatment ($F_{3,24} = 117.9$, $p < 0.0001$), time ($F_{8,171} = 14.22$, $p < 0.0001$) and time × treatment interaction ($F_{24,171} = 7.13$, $p < 0.0001$), according to two-way RM ANOVA followed by contrast analysis and the sequentially rejective Bonferroni's test. Panel b: significant effect of amantadine ($t = 3.35$, df = 5, $p = 0.0202$), according to unpaired Student's *t*-test. Panel d: significant effect of amantadine; axial ($t = 3.40$, df = 11, $p = 0.0058$), limb ($t = 3.46$, df = 11, $p = 0.0053$), orolingual ($t = 2.79$, df = 11, $p = 0.0173$) AIMs, according to unpaired Student's *t*-test. $^{*}p < 0.05$ versus saline, $^{\#}p < 0.05$, $^{\#\#}p < 0.01$ versus L-DOPA.

attenuate dyskinesia also acting in extrastriatal areas. For instance, it reduced primary motor cortex excitability in humans, an action attributed to impairment of GLU and elevation of GABA transmission (Reis *et al.* 2006). Moreover, as reported in the present study, amantadine caused a delayed and marked elevation of GABA levels in GP when challenged with L-DOPA. As neither compound alone affected amino acid levels in GP, amantadine may unravel a stimulatory effect of L-DOPA on the striato-pallidal pathway. This view is challenged by the finding that the increase in pallidal GABA was not paralleled by changes of GLU levels in GP as well as GABA and GLU levels in the downstream SNr. Moreover, an increase of the activity of the indirect pathway would result in a hypokinetic response possibly contributing to the anti-dyskinetic effect of the drug. Conversely, no accelerated extinction of dyskinesia was observed from 80 min onwards (i.e. when pallidal GABA levels rose). As NR2D (Wenzel *et al.* 1996) and DA (Weiner *et al.* 1991) receptor binding has been detected in GP, we cannot rule out that the increase in pallidal GABA levels is due to local interaction between the two drugs, with any apparent impact on AIMs appearance.

Interestingly, the increase in pallidal GABA levels following the combination of amantadine and L-DOPA was not observed in the rat. This is not the only difference observed between the two models because L-DOPA elevated nigral GLU levels in the rat but not dyskinetic mouse. At this stage, we cannot prove whether these patterns are species- or model-related. Nonetheless, the lesioning procedures (striatum vs. MFB), L-DOPA dosage (2.5-fold higher in the mouse) and treatment duration of (half shorter in the mouse) might change the responsiveness to L-DOPA by affecting the

© 2011 The Authors

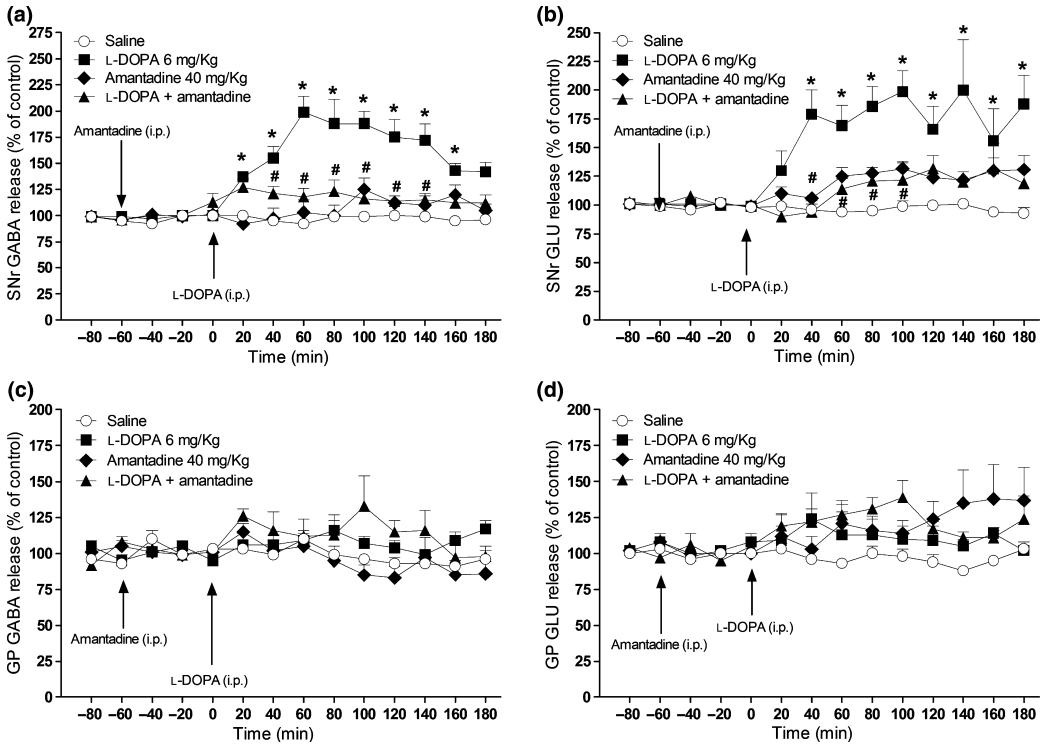

Fig. 7 Neurochemical effects of L-DOPA and amantadine in dyskinetic rats undergoing microdialysis. Dyskinetic rats (see legend to Fig. 6) were implanted with one probe in the lesioned substantia nigra reticulata (SNr; a, b) and another in ipsilateral globus pallidus (GP) (c, d). Twenty-four hours later, rats received an acute challenge with L-DOPA alone (6 mg/kg plus 12 mg/kg benserazide, i.p.) or in combination with amantadine (40 mg/kg; i.p., 1 h in advance), and GABA (a, c) and GLU (b, d) levels were monitored for 180 min. Data are expressed as percentage of basal pre-treatment levels (calculated as the mean of the two samples preceding the treatment) and are mean ± SEM of 5–7 animals. Basal dialysate levels of GABA and GLU were 10.5 ± 0.5 and 98.3 ± 5.6 nM, respectively, in SNr, and 11.9 ± 0.5 and 79.6 ± 5.3, respectively, in GP. Panel a: significant effect of treatment ($F_{3,39} = 90.23$, $p < 0.0001$), time ($F_{13,280} = 10.34$, $p < 0.0001$) and time × treatment interaction ($F_{39,280} = 5.46$, $p < 0.0001$). Panel b: significant effect of treatment ($F_{3,39} = 43.74$, $p < 0.0001$), time ($F_{13,280} = 6.43$, $p < 0.0001$) and time × treatment interaction ($F_{39,280} = 2.46$, $p < 0.0001$), according to two-way RM ANOVA followed by contrast analysis and the sequentially rejective Bonferroni's test. $^{*}p < 0.05$ versus saline; $^{\#}p < 0.05$ versus L-DOPA.

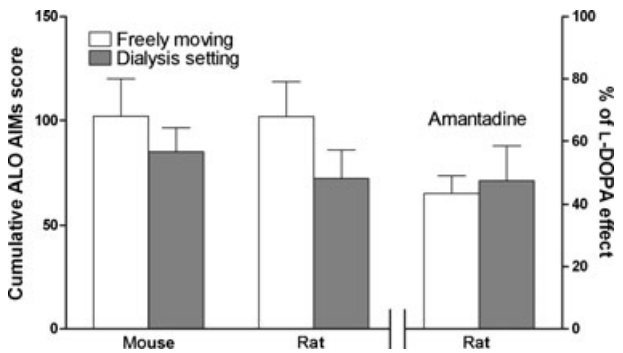

Fig. 8 Impact of microdialysis setting on the behavioral response to L-DOPA and amantadine in dyskinetic animals. AIMs were evaluated in the same animal before and after dialysis probe implantation (i.e. during microdialysis). The anti-dyskinetic effect of amantadine was evaluated in rats only. Data have been presented as cumulative ALO AIMs score or, in the case of amantadine, as percentage of L-DOPA response. Data are mean ± SEM of $n = 8$ (mice) or $n = 5$ (rats) experiments. Statistical analysis was performed by the paired Student's *t*-test.

extent of nigral lesion, and the plasticity of DA signalling and basal ganglia circuitry. In this respect, the status of the subthalamic nucleus (STN) in the two models should be considered. In fact, it has been reported that the degree of nigral cell loss reflects in a different STN firing activity (Breit *et al.* 2007). In fact, a marked (~90%) nigral cell loss, as that produced by 6-OHDA injection in SN compacta (or MFB; Marti *et al.* 2007), is associated with an increase in the firing rate of STN glutamatergic neurons whereas a milder lesion (~50%), as that produced by intrastriatal 6-OHDA injection, is not (Breit *et al.* 2007). A different activity level of the STN glutamatergic projections may help explain the different responsiveness of nigral GLU to L-DOPA in rats and mice. Indeed, we showed that striatal D1 receptor blockade prevented the rise in both GABA and GLU levels induced by L-DOPA in dyskinetic rats, indicating that this effect is a consequence of striato-nigral activation rather than extrastriatal action (Mela *et al.* 2007b). Thus, overactive GLU terminals may be more sensitive to the modulation operated

© 2011 The Authors

by the striato-nigral neurons. In fact, striato-nigral GABA terminals co-release Substance P which might elevate nigral GLU levels acting on pre-synaptic facilitatory NK1 receptors (Liu *et al.* 2002; Stacey *et al.* 2002; Bailey *et al.* 2004).

Concluding remarks

A comparative neurochemical and behavioral study in the mouse and rat models of dyskinesia revealed that AIMs appearance in response to L-DOPA challenge is accompanied by an increase of GABA release in SNr but not GP. In both models, amantadine attenuated about to the same extent the severity of dyskinesia, preventing the accompanying surge in nigral GABA. These data provide strong neurochemical support to the view that peak-dose dyskinesia involves activation of the striato-nigral GABA pathway in both models, and that amantadine opposes this effect likely via interaction with striatal NMDA receptors. Minor neurochemical differences in the response to L-DOPA and amantadine were observed between the two models, which do not appear to shape the behavioral response. Overall, this study proves the feasibility of a combined behavioral and neurochemical analysis of the dyskinetic mouse, and the consistency of the neurochemical and behavioral response to L-DOPA and amantadine among species.

Acknowledgements

This work has been supported by grants from the Italian Ministry of the University (PRIN 2008) and the S. Paolo Foundation (project title: An innovative approach to treat levodopa-induced dyskinesia based on targeting striatal intracellular signalling) to M. Morari. The authors declare no conflict of interest.

References

Albin R. L., Young A. B. and Penney J. B. (1989) The functional anatomy of basal ganglia disorders. *Trends Neurosci.* **12**, 366–375.

Andersson M., Hilbertson A. and Cenci M. A. (1999) Striatal fosB expression is causally linked with l-DOPA-induced abnormal involuntary movements and the associated upregulation of striatal prodynorphin mRNA in a rat model of Parkinson's disease. *Neurobiol. Dis.* **6**, 461–474.

Arai A., Kannari K., Shen H., Maeda T., Suda T. and Matsunaga M. (2003) Amantadine increases L-DOPA-derived extracellular dopamine in the striatum of 6-hydroxydopamine-lesioned rats. *Brain Res.* **972**, 229–234.

Bailey C. P., Maubach K. A. and Jones R. S. (2004) Neurokinin-1 receptors in the rat nucleus tractus solitarius: pre- and postsynaptic modulation of glutamate and GABA release. *Neuroscience* **127**, 467–479.

Bateup H. S., Santini E., Shen W., Birnbaum S., Valjent E., Surmeier D. J., Fisone G., Nestler E. J. and Greengard P. (2010) Distinct subclasses of medium spiny neurons differentially regulate striatal motor behaviors. *Proc. Natl. Acad. Sci. U S A* **107**, 14845–14850.

Bezard E., Ferry S., Mach U., Stark H., Leriche L., Boraud T., Gross C. and Sokoloff P. (2003) Attenuation of levodopa-induced dyskinesia by normalizing dopamine D3 receptor function. *Nat. Med.* **9**, 762–767.

Blanpied T. A., Clarke R. J. and Johnson J. W. (2005) Amantadine inhibits NMDA receptors by accelerating channel closure during channel block. *J. Neurosci.* **25**, 3312–3322.

Braak H. and Braak E. (2000) Pathoanatomy of Parkinson's disease. *J. Neurol.* **247**(Suppl. 2), II3–II10.

Breit S., Bouali-Benazzouz R., Popa R. C., Gasser T., Benabid A. L. and Benazzouz A. (2007) Effects of 6-hydroxydopamine-induced severe or partial lesion of the nigrostriatal pathway on the neuronal activity of pallido-subthalamic network in the rat. *Exp. Neurol.* **205**, 36–47.

Buck K., Voehringer P. and Ferger B. (2010) Site-specific action of L-3,4-dihydroxyphenylalanine in the striatum but not globus pallidus and substantia nigra pars reticulata evokes dyskinetic movements in chronic L-3,4-dihydroxyphenylalanine-treated 6-hydroxydopamine-lesioned rats. *Neuroscience* **166**, 355–358.

Calabresi P., Giacomini P., Centonze D. and Bernardi G. (2000) Levodopa-induced dyskinesia: a pathological form of striatal synaptic plasticity? *Ann. Neurol.* **47**, S60–68; discussion S68–S69.

Calon F., Birdi S., Rajput A. H., Hornykiewicz O., Bedard P. J. and Di Paolo T. (2002) Increase of preproenkephalin mRNA levels in the putamen of Parkinson disease patients with levodopa-induced dyskinesias. *J. Neuropathol. Exp. Neurol.* **61**, 186–196.

Carta M., Lindgren H. S., Lundblad M., Stancampiano R., Fadda F. and Cenci M. A. (2006) Role of striatal L-DOPA in the production of dyskinesia in 6-hydroxydopamine lesioned rats. *J. Neurochem.* **96**, 1718–1727.

Carta A. R., Frau L., Pontis S., Pinna A. and Morelli M. (2008) Direct and indirect striatal efferent pathways are differentially influenced by low and high dyskinetic drugs: behavioural and biochemical evidence. *Parkinsonism Relat. Disord.* **14**(Suppl. 2), S165–168.

Cenci M. A. and Lundblad M. (2007) Ratings of L-DOPA-induced dyskinesia in the unilateral 6-OHDA lesion model of Parkinson's disease in rats and mice. *Curr. Protoc. Neurosci.* **41**, 9.25.1–9.25.23.

Cenci M. A. and Ohlin K. E. (2009) Rodent models of treatment-induced motor complications in Parkinson's disease. *Parkinsonism Relat. Disord.* **15**(Suppl. 4), S13–S17.

Cenci M. A., Lee C. S. and Bjorklund A. (1998) L-DOPA-induced dyskinesia in the rat is associated with striatal overexpression of prodynorphin- and glutamic acid decarboxylase mRNA. *Eur. J. Neurosci.* **10**, 2694–2706.

Cenci M. A., Whishaw I. Q. and Schallert T. (2002) Animal models of neurological deficits: how relevant is the rat? *Nat. Rev. Neurosci.* **3**, 574–579.

Christoph G. R., Leonzio R. J. and Wilcox K. S. (1986) Stimulation of the lateral habenula inhibits dopamine-containing neurons in the substantia nigra and ventral tegmental area of the rat. *J. Neurosci.* **6**, 613–619.

Corvol J. C., Muriel M. P., Valjent E., Feger J., Hanoun N., Girault J. A., Hirsch E. C. and Herve D. (2004) Persistent increase in olfactory type G-protein alpha subunit levels may underlie D1 receptor functional hypersensitivity in Parkinson disease. *J. Neurosci.* **24**, 7007–7014.

Danysz W., Parsons C. G., Kornhuber J., Schmidt W. J. and Quack G. (1997) Aminoadamantanes as NMDA receptor antagonists and antiparkinsonian agents–preclinical studies. *Neurosci. Biobehav. Rev.* **21**, 455–468.

Darmopil S., Martin A. B., De Diego I. R., Ares S. and Moratalla R. (2009) Genetic inactivation of dopamine D1 but not D2 receptors inhibits L-DOPA-induced dyskinesia and histone activation. *Biol. Psychiatry* **66**, 603–613.

© 2011 The Authors

Deep P., Dagher A., Sadikot A., Gjedde A. and Cumming P. (1999) Stimulation of dopa decarboxylase activity in striatum of healthy human brain secondary to NMDA receptor antagonism with a low dose of amantadine. *Synapse* **34**, 313–318.

Dekundy A., Lundblad M., Danysz W. and Cenci M. A. (2007) Modulation of L-DOPA-induced abnormal involuntary movements by clinically tested compounds: further validation of the rat dyskinesia model. *Behav. Brain Res.* **179**, 76–89.

DeLong M. R. (1990) Primate models of movement disorders of basal ganglia origin. *Trends Neurosci.* **13**, 281–285.

Deniau J. M. and Chevalier G. (1985) Disinhibition as a basic process in the expression of striatal functions. II. The striato-nigral influence on thalamocortical cells of the ventromedial thalamic nucleus. *Brain Res.* **334**, 227–233.

Dupre K. B., Ostock C. Y., Eskow Jaunarajs K. L., Button T., Savage L. M., Wolf W. and Bishop C. (2011) Local modulation of striatal glutamate efflux by serotonin 1A receptor stimulation in dyskinetic, hemiparkinsonian rats. *Exp. Neurol.* **229**, 288–299.

Fahn S. (2000) The spectrum of levodopa-induced dyskinesias. *Ann. Neurol.* **47**, S2–S9; discussion S9–S11.

Fantin M., Marti M., Auberson Y. P. and Morari M. (2007) NR2A and NR2B subunit containing NMDA receptors differentially regulate striatal output pathways. *J. Neurochem.* **103**, 2200–2211.

Fantin M., Auberson Y. P. and Morari M. (2008) Differential effect of NR2A and NR2B subunit selective NMDA receptor antagonists on striato-pallidal neurons: relationship to motor response in the 6-hydroxydopamine model of Parkinsonism. *J. Neurochem.* **106**, 957–968.

Fisher A., Biggs C. S. and Starr M. S. (1998) Effects of glutamate antagonists on the activity of aromatic L-amino acid decarboxylase. *Amino Acids* **14**, 43–49.

Heikkila R. E. and Cohen G. (1972) Evaluation of amantadine as a releasing agent or uptake blocker for H 3 -dopamine in rat brain slices. *Eur. J. Pharmacol.* **20**, 156–160.

Henry B., Crossman A. R. and Brotchie J. M. (1999) Effect of repeated L-DOPA, bromocriptine, or lisuride administration on preproenkephalin-A and preproenkephalin-B mRNA levels in the striatum of the 6-hydroxydopamine-lesioned rat. *Exp. Neurol.* **155**, 204–220.

Jonkers N., Sarre S., Ebinger G. and Michotte Y. (2002) MK801 suppresses the L-DOPA-induced increase of glutamate in striatum of hemi-Parkinson rats. *Brain Res.* **926**, 149–155.

Kornhuber J., Bormann J., Hubers M., Rusche K. and Riederer P. (1991) Effects of the 1-amino-adamantanes at the MK-801-binding site of the NMDA-receptor-gated ion channel: a human postmortem brain study. *Eur. J. Pharmacol.* **206**, 297–300.

Lee C. S., Cenci M. A., Schulzer M. and Bjorklund A. (2000) Embryonic ventral mesencephalic grafts improve levodopa-induced dyskinesia in a rat model of Parkinson's disease. *Brain* **123**(Pt 7), 1365–1379.

Lindgren H. S., Andersson D. R., Lagerkvist S., Nissbrandt H. and Cenci M. A. (2010) L-DOPA-induced dopamine efflux in the striatum and the substantia nigra in a rat model of Parkinson's disease: temporal and quantitative relationship to the expression of dyskinesia. *J. Neurochem.* **112**, 1465–1476.

Liu H. L., Cao R., Jin L. and Chen L. W. (2002) Immunocytochemical localization of substance P receptor in hypothalamic oxytocin-containing neurons of C57 mice. *Brain Res.* **948**, 175–179.

Loschmann P. A., De Groote C., Smith L., Wullner U., Fischer G., Kemp J. A., Jenner P. and Klockgether T. (2004) Antiparkinsonian activity of Ro 25-6981, a NR2B subunit specific NMDA receptor antagonist, in animal models of Parkinson's disease. *Exp. Neurol.* **187**, 86–93.

Lundblad M., Andersson M., Winkler C., Kirik D., Wierup N. and Cenci M. A. (2002) Pharmacological validation of behavioural measures of akinesia and dyskinesia in a rat model of Parkinson's disease. *Eur. J. Neurosci.* **15**, 120–132.

Lundblad M., Picconi B., Lindgren H. and Cenci M. A. (2004) A model of L-DOPA-induced dyskinesia in 6-hydroxydopamine lesioned mice: relation to motor and cellular parameters of nigrostriatal function. *Neurobiol. Dis.* **16**, 110–123.

Lundblad M., Usiello A., Carta M., Hakansson K., Fisone G. and Cenci M. A. (2005) Pharmacological validation of a mouse model of l-DOPA-induced dyskinesia. *Exp. Neurol.* **194**, 66–75.

Mabrouk O. S., Marti M. and Morari M. (2010) Endogenous nociceptin/orphanin FQ (N/OFQ) contributes to haloperidol-induced changes of nigral amino acid transmission and parkinsonism: a combined microdialysis and behavioral study in naive and nociceptin/orphanin FQ receptor knockout mice. *Neuroscience* **166**, 40–48.

Marti M., Mela F., Bianchi C., Beani L. and Morari M. (2002) Striatal dopamine-NMDA receptor interactions in the modulation of glutamate release in the substantia nigra pars reticulata in vivo: opposite role for D1 and D2 receptors. *J. Neurochem.* **83**, 635–644.

Marti M., Mela F., Fantin M. *et al.* (2005) Blockade of nociceptin/orphanin FQ transmission attenuates symptoms and neurodegeneration associated with Parkinson's disease. *J. Neurosci.* **25**, 9591–9601.

Marti M., Trapella C., Viaro R. and Morari M. (2007) The nociceptin/orphanin FQ receptor antagonist J-113397 and L-DOPA additively attenuate experimental parkinsonism through overinhibition of the nigrothalamic pathway. *J. Neurosci.* **27**, 1297–1307.

McGeorge A. J. and Faull R. L. (1989) The organization of the projection from the cerebral cortex to the striatum in the rat. *Neuroscience* **29**, 503–537.

Mehta A., Bot G., Reisine T. and Chesselet M. F. (2001) Endomorphin-1: induction of motor behavior and lack of receptor desensitization. *J. Neurosci.* **21**, 4436–4442.

Mela F., Marti M., Dekundy A., Danysz W., Morari M. and Cenci M. A. (2007a) Antagonism of metabotropic glutamate receptor type 5 attenuates l-DOPA-induced dyskinesia and its molecular and neurochemical correlates in a rat model of Parkinson's disease. *J. Neurochem.* **101**, 483–497.

Mela F., Marti M., Cenci M. A. and Morari M. (2007b) Differential role of striatal and nigral D1 receptors in the expression of L-DOPA induced dyskinesia and its neurochemical correlates. *Soc. Neurosci. Abst.* 590.26.

Mela F., Dekundy A., Mabrouk O., Bido S., Gross R., Morari M. and Danysz W. (2010) Effect of selective NR2B antagonists on L-DOPA-induced dyskinesia in hemiparkinsonian rats. Mov Disorder late braking abstract LB-05. Available at: http://www.movementdisorders.org/congress/congress10/2010_late_breaking_abstracts.pdf.

Mitchell I. J. and Carroll C. B. (1997) Reversal of parkinsonian symptoms in primates by antagonism of excitatory amino acid transmission: potential mechanisms of action. *Neurosci. Biobehav. Rev.* **21**, 469–475.

Mizoguchi K., Yokoo H., Yoshida M., Tanaka T. and Tanaka M. (1994) Amantadine increases the extracellular dopamine levels in the striatum by re-uptake inhibition and by *N*-methyl-D-aspartate antagonism. *Brain Res.* **662**, 255–258.

Morari M., O'Connor W. T., Darvelid M., Ungerstedt U., Bianchi C. and Fuxe K. (1996a) Functional neuroanatomy of the nigrostriatal and striatonigral pathways as studied with dual probe microdialysis in the awake rat—I. Effects of perfusion with tetrodotoxin and low-calcium medium. *Neuroscience* **72**, 79–87.

Morari M., O'Connor W. T., Ungerstedt U., Bianchi C. and Fuxe K. (1996b) Functional neuroanatomy of the nigrostriatal and striato-

© 2011 The Authors

nigral pathways as studied with dual probe microdialysis in the awake rat—II. Evidence for striatal N-methyl-D-aspartate receptor regulation of striatonigral GABAergic transmission and motor function. *Neuroscience* **72**, 89–97.

Nash J. E., Hill M. P. and Brotchie J. M. (1999) Antiparkinsonian actions of blockade of NR2B-containing NMDA receptors in the reserpine-treated rat. *Exp. Neurol.* **155**, 42–48.

Nash J. E., Fox S. H., Henry B. *et al.* (2000) Antiparkinsonian actions of ifenprodil in the MPTP-lesioned marmoset model of Parkinson's disease. *Exp. Neurol.* **165**, 136–142.

Nauta W. J., Smith G. P., Faull R. L. and Domesick V. B. (1978) Efferent connections and nigral afferents of the nucleus accumbens septi in the rat. *Neuroscience* **3**, 385–401.

Northover B. J. (1994) Effect of pre-treating rat atria with potassium channel blocking drugs on the electrical and mechanical responses to phenylephrine. *Biochem. Pharmacol.* **47**, 2163–2169.

Obeso J. A., Olanow C. W. and Nutt J. G. (2000) Levodopa motor complications in Parkinson's disease. *Trends Neurosci.* **23**, S2–7.

Obeso J. A., Rodriguez-Oroz M., Marin C., Alonso F., Zamarbide I., Lanciego J. L. and Rodriguez-Diaz M. (2004) The origin of motor fluctuations in Parkinson's disease: importance of dopaminergic innervation and basal ganglia circuits. *Neurology* **62**, S17–S30.

Oh J. D. and Chase T. N. (2002) Glutamate-mediated striatal dysregulation and the pathogenesis of motor response complications in Parkinson's disease. *Amino Acids* **23**, 133–139.

Parent A. and Hazrati L. N. (1995a) Functional anatomy of the basal ganglia. I. The cortico-basal ganglia-thalamo-cortical loop. *Brain Res. Brain Res. Rev.* **20**, 91–127.

Parent A. and Hazrati L. N. (1995b) Functional anatomy of the basal ganglia. II. The place of subthalamic nucleus and external pallidum in basal ganglia circuitry. *Brain Res. Brain Res. Rev.* **20**, 128–154.

Parsons C. G., Panchenko V. A., Pinchenko V. O., Tsyndrenko A. Y. and Krishtal O. A. (1996) Comparative patch-clamp studies with freshly dissociated rat hippocampal and striatal neurons on the NMDA receptor antagonistic effects of amantadine and memantine. *Eur. J. Neurosci.* **8**, 446–454.

Paxinos G. and Franklin K. B. J. (2001) *The Mouse Brain in Stereotaxic Coordinates*, 2nd edn. Academic Press, San Diego.

Paxinos G. and Watson C. (1982) *The Rat Brain in Stereotaxic Coordinates*. Academic Press, Sydney.

Picconi B., Centonze D., Hakansson K., Bernardi G., Greengard P., Fisone G., Cenci M. A. and Calabresi P. (2003) Loss of bidirectional striatal synaptic plasticity in L-DOPA-induced dyskinesia. *Nat. Neurosci.* **6**, 501–506.

Reis J., John D., Heimeroth A., Mueller H. H., Oertel W. H., Arndt T. and Rosenow F. (2006) Modulation of human motor cortex excitability by single doses of amantadine. *Neuropsychopharmacology* **31**, 2758–2766.

Rolland A. S., Herrero M. T., Garcia-Martinez V., Ruberg M., Hirsch E. C. and Francois C. (2007) Metabolic activity of cerebellar and basal ganglia-thalamic neurons is reduced in parkinsonism. *Brain* **130**, 265–275.

Rozas G. and Labandeira Garcia J. L. (1997) Drug-free evaluation of rat models of parkinsonism and nigral grafts using a new automated rotarod test. *Brain Res.* **749**, 188–199.

Rylander D., Recchia A., Mela F., Dekundy A., Danysz W. and Cenci M. A. (2009) Pharmacological modulation of glutamate transmission in a rat model of L-DOPA-induced dyskinesia: effects on motor behavior and striatal nuclear signaling. *J. Pharmacol. Exp. Ther.* **330**, 227–235.

Santini E., Valjent E., Usiello A., Carta M., Borgkvist A., Girault J. A., Herve D., Greengard P. and Fisone G. (2007) Critical involvement of cAMP/DARPP-32 and extracellular signal-regulated protein kinase signaling in L-DOPA-induced dyskinesia. *J. Neurosci.* **27**, 6995–7005.

Santini E., Heiman M., Greengard P., Valjent E. and Fisone G. (2009) Inhibition of mTOR signaling in Parkinson's disease prevents L-DOPA-induced dyskinesia. *Sci. Signal.* **2**, ra36.

Sarre S., Lanza M., Makovec F., Artusi R., Caselli G. and Michotte Y. (2008) In vivo neurochemical effects of the NR2B selective NMDA receptor antagonist CR 3394 in 6-hydroxydopamine lesioned rats. *Eur. J. Pharmacol.* **584**, 297–305.

Schallert T., Fleming S. M., Leasure J. L., Tillerson J. L. and Bland S. T. (2000) CNS plasticity and assessment of forelimb sensorimotor outcome in unilateral rat models of stroke, cortical ablation, parkinsonism and spinal cord injury. *Neuropharmacology* **39**, 777–787.

Stacey A. E., Woodhall G. L. and Jones R. S. (2002) Neurokinin-receptor-mediated depolarization of cortical neurons elicits an increase in glutamate release at excitatory synapses. *Eur. J. Neurosci.* **16**, 1896–1906.

Steece-Collier K., Chambers L. K., Jaw-Tsai S. S., Menniti F. S. and Greenamyre J. T. (2000) Antiparkinsonian actions of CP-101,606, an antagonist of NR2B subunit-containing *N*-methyl-D-aspartate receptors. *Exp. Neurol.* **163**, 239–243.

Viaro R., Sanchez-Pernaute R., Marti M., Trapella C., Isacson O. and Morari M. (2008) Nociceptin/orphanin FQ receptor blockade attenuates MPTP-induced parkinsonism. *Neurobiol. Dis.* **30**, 430–438.

Volta M., Mabrouk O. S., Bido S., Marti M. and Morari M. (2010) Further evidence for an involvement of nociceptin/orphanin FQ in the pathophysiology of Parkinson's disease: a behavioral and neurochemical study in reserpinized mice. *J. Neurochem.* **115**, 1543–1555.

Weiner D. M., Levey A. I., Sunahara R. K., Niznik H. B., O'Dowd B. F., Seeman P. and Brann M. R. (1991) D_1 and D_2 dopamine receptor mRNA in rat brain. *Proc. Natl. Acad. Sci. U S A* **88**, 1859–1863.

Wenzel A., Villa M., Mohler H. and Benke D. (1996) Developmental and regional expression of NMDA receptor subtypes containing the NR2D subunit in rat brain. *J. Neurochem.* **66**, 1240–1248.

Winkler A. S., Reuter I., Harwood G. and Chaudhuri K. R. (2002) The frequency and significance of 'striatal toe' in parkinsonism. *Parkinsonism Relat. Disord.* **9**, 97–101.

Xiao Z. W., Cao C. Y., Wang Z. X., Li J. X., Liao H. Y. and Zhang X. X. (2006) Changes of dopamine transporter function in striatum during acute morphine addiction and its abstinence in rhesus monkey. *Chin. Med. J. (Engl)* **119**, 1802–1807.

Zhou F. W., Jin Y., Matta S. G., Xu M. and Zhou F. M. (2009) An ultra-short dopamine pathway regulates basal ganglia output. *J. Neurosci.* **29**, 10424–10435.

© 2011 The Authors

Journal of Neurochemistry

JOURNAL OF NEUROCHEMISTRY | 2010 | 115 | 1543–1555 doi: 10.1111/j.1471-4159.2010.07061.x

Further evidence for an involvement of nociceptin/orphanin FQ in the pathophysiology of Parkinson's disease: a behavioral and neurochemical study in reserpinized mice

Mattia Volta,*,† Omar S. Mabrouk,*,† Simone Bido,*,† Matteo Marti*,† and Michele Morari*,†

*Department of Experimental and Clinical Medicine, Section of Pharmacology, University of Ferrara, Ferrara, Italy

†Center for Neuroscience and National Institute of Neuroscience, University of Ferrara, Ferrara, Italy

Abstract

The contribution of nociceptin/orphanin FQ (N/OFQ) to reserpine-induced Parkinsonism was evaluated in mice. A battery of motor tests revealed that reserpine caused dose-dependent and long-lasting motor impairment. Endogenous N/OFQ sustained this response because N/OFQ peptide (NOP) receptor knockout ($NOP^{-/-}$) mice were less susceptible to the hypokinetic action of reserpine than wild-type ($NOP^{+/+}$) animals. Microdialysis revealed that reserpine elevated glutamate and reduced GABA levels in substantia nigra reticulata, and that resistance to reserpine in $NOP^{-/-}$ mice was accompanied by a milder increase in glutamate and lack of inhibition of GABA levels. To substantiate this genetic evidence, the NOP receptor antagonist 1-[(3R,4R)-1-cyclooctylmethyl-3-hydroxymethyl-4-piperidyl]-3-ethyl-1,3-dihydro-2H benzimidazol-2-one (J-113397) simultaneously reduced akinesia and nigral glutamate levels in reserpinized $NOP^{+/+}$ mice, being ineffective in $NOP^{-/-}$ mice. Moreover, repeated J-113397 administration in reserpinized mice resulted in faster recovery of baseline motor performance which was, however, accompanied by a loss of acute antiakinetic response. The short-term beneficial effect of J-113397 was paralleled by normalization of nigral glutamate levels, whereas loss of acute response was paralleled by loss of the ability of J-113397 to inhibit glutamate levels. We conclude that endogenous N/OFQ contributes to reserpine-induced Parkinsonism, and that sustained NOP receptor blockade produces short-term motor improvement accompanied by normalization of nigral glutamate release.

Keywords: glutamate, J-113397, microdialysis, nociceptin/orphanin FQ, Parkinson's disease, reserpine.

J. Neurochem. (2010) **115**, 1543–1555.

Nociceptin/orphanin FQ (N/OFQ; Meunier *et al.* 1995; Reinscheid *et al.* 1995) is the endogenous ligand of the NOP receptor (Mollereau *et al.* 1994), the fourth member of the opioid receptor family (Mogil and Pasternak 2001). Endogenous N/OFQ acts as a physiological constraint on motor activity (Marti *et al.* 2004a) and contributes to dopamine (DA) cell loss and motor impairment observed in neurodegeneration models of Parkinson's disease (PD; Marti *et al.* 2005). In fact, genetic deletion of the preproN/OFQ (ppN/OFQ) gene conferred mice partial protection against 1-methyl-4-phenyl-1,2,5,6-tetrahydropyridine (MPTP)-induced toxicity (Marti *et al.* 2005; Brown *et al.* 2006). Moreover, selective NOP receptor antagonists improved motor performance in 6-hydroxydopamine (6-OHDA) hemilesioned rats (Marti *et al.* 2005, 2007, 2008; Volta *et al.* 2010a) or MPTP-treated mice and non-human primates (Viaro *et al.* 2008, 2010; Visanji *et al.* 2008). N/OFQ also sustains hypokinesia following acute functional impairment of DA transmission. Indeed, NOP receptor antagonists alleviated haloperidol-induced akinesia in rats (Marti *et al.* 2004b, 2005) and mice (Mabrouk *et al.* 2010)

Received August 2, 2010; revised manuscript received September 23, 2010; accepted October 4, 2010.

Address correspondence and reprint requests to Michele Morari, Department of Experimental and Clinical Medicine, Section of Pharmacology, University of Ferrara, via Fossato di Mortara 17-19, 44100 Ferrara, Italy. E-mail: m.morari@unife.it

Abbreviations used: 6-OHDA, 6-hydroxydopamine; DA, dopamine; GLU, glutamate; J-113397, 1-[(3R,4R)-1-cyclooctylmethyl-3-hydroxymethyl-4-piperidyl]-3-ethyl-1,3-dihydro-2H benzimidazol-2-one; NOP, nociceptin/orphanin FQ peptide receptor; $NOP^{-/-}$, NOP receptor knockout; N/OFQ, nociceptin/orphanin FQ; PD, Parkinson's disease; SNr, substantia nigra reticulata.VMAT2, vesicular monoamine transporter type II.

© 2010 The Authors
Journal of Neurochemistry © 2010 International Society for Neurochemistry,

whereas NOP receptor knockout ($NOP^{-/-}$) mice were found to be more resistant to haloperidol-induced akinesia (Marti *et al.* 2005; Mabrouk *et al.* 2010). Although these studies suggest endogenous N/OFQ sustains motor impairment both in neurodegeneration and functional models of Parkinsonism, the role of N/OFQ in reserpine-induced akinesia was never investigated. Reserpine replicates some symptoms of PD, such as akinesia/hypokinesia, tremor and rigidity, without damaging DA cells in substantia nigra (SN) compacta (Schultz 1982; Gerlach and Riederer 1996; Betarbet *et al.* 2002). Motor deficits are caused by inhibition of the vesicular monoamine transporter type II (VMAT2) leading to a depletion of DA stores in nerve terminals. Reserpine also depletes noradrenaline and serotonin stores, making its action somewhat unspecific. Nevertheless, reserpine-induced hypokinesia is reversed by L-DOPA (> 100 mg/kg) or DA agonists, suggesting that these motor symptoms have dopaminergic origin (Carlsson *et al.* 1957; Colpaert 1987). Compared with the haloperidol-treated mouse, the reserpinized mouse offers the advantage of investigating also the symptomatic effect of subacute drug administration because hypokinesia and postural immobility induced by a single dose of reserpine lasts for a few days (Colpaert 1987). This is particularly relevant since previous studies with NOP receptor antagonists in Parkinsonism models were designed to specifically investigate their acute antiakinetic effects. Therefore, the present study was undertaken to investigate the contribution of endogenous N/OFQ to motor deficits in reserpinized mice, and to verify whether the acute anti-Parkinsonian effect of a NOP receptor antagonist is maintained during subacute administration. A combined neurochemical and behavioral approach allowed for the investigation of novel aspects of the mechanism of action of an old drug, reserpine, investigating changes of amino acid levels in substantia nigra reticulata (SNr), the motor output of the basal ganglia, and their behavioral correlates. A battery of behavioral tests (the bar, drag and rotarod test; Marti *et al.* 2005, 2007, 2008; Viaro *et al.* 2008) was employed to quantify the effects of reserpine in mice. To investigate the involvement of endogenous N/OFQ, the motor responses of $NOP^{-/-}$ and $NOP^{+/+}$ mice to reserpine were first studied. Microdialysis combined with a test for akinesia (the bar test) was used to investigate whether the genotype susceptibility to reserpine was associated with different dynamics of glutamate (GLU) and GABA levels in SNr. Mice treated with reserpine or saline were then administered subacutely (4 days) with the NOP receptor antagonist 1-[(3R,4R)-1-cyclooctylmethyl-3-hydroxymethyl-4-piperidyl]-3-ethyl-1,3-dihydro-2H-benzimidazol-2-one (J-113397; Kawamoto *et al.* 1999). Motor activity was monitored daily, before and after J-113397 administration, to collect information on both baseline and acute effects, respectively. Finally, microdialysis was used to verify whether the acute and short-term effects of J-113397 were associated with changes in nigral amino acid levels.

Materials and methods

Mice employed in the study (see below) were kept under regular lighting conditions (12 h light/dark cycle) and given food and water *ad libitum*. The experimental protocols performed in the present study were approved by the Italian Ministry of Health (licence n. 94-2007-B) and by the Ethics Committee of the University of Ferrara. Adequate measures were taken to limit the number of animals used and minimize animal discomfort in these studies.

Behavioral analysis

This study was performed in naïve Swiss (12–15 weeks old; Morini Italy; S. Polo d'Enza, Italy) and in CD1/C57BL6J/129 $NOP^{+/+}$ and $NOP^{-/-}$ mice (12–15 weeks old; Nishi *et al.* 1997). Motor activity was evaluated by means of three behavioral tests specific for different motor abilities, as previously described (Marti *et al.* 2005, 2007; Viaro *et al.* 2008): the bar, drag and rotarod test. The three tests were repeated in a fixed sequence (bar, drag and rotarod) before and after drug injection (starting at 10 min after treatment). Animals were trained for approximately 8 days to the specific motor tasks until their motor performance became reproducible.

Bar test

Originally developed to quantify morphine-induced catalepsy (Kuschinsky and Hornykiewicz 1972), this test measures the ability of the animal to respond to an externally imposed static posture. Also known as the catalepsy test (for a review see Sanberg *et al.* 1988), it can also be used to quantify akinesia (i.e. time to initiate a movement) also under conditions that are not characterized by increased muscle tone (i.e rigidity) as in the cataleptic/catatonic state. Mice were gently placed on a table and forepaws were placed alternatively on blocks of increasing heights (1.5, 3 and 6 cm). The time (in seconds) that each paw spent on the block (i.e. the immobility time) was recorded (cut-off time of 20 s). Akinesia was calculated as total time spent on the different blocks.

Drag test

Modification of the 'wheelbarrow test' (Schallert *et al.* 1979), this test measures the ability of the animal to balance its body posture with forelimbs in response to an externally imposed dynamic stimulus (backward dragging; Marti *et al.* 2005). It gives information regarding the time to initiate and execute (bradykinesia) a movement. Animals were gently lifted from the tail leaving the forepaws on the table, and then dragged backwards at a constant speed (about 20 cm/s) for a fixed distance (100 cm). The number of steps made by each paw was recorded. Five to 7 determinations were collected for each animal.

Rotarod test

The fixed-speed rotarod test (Rozas *et al.* 1997) measures different motor parameters such as motor coordination, gait ability, balance, muscle tone and motivation to run. It was employed according to a previously described protocol (Marti *et al.* 2004a) which allowed the detection of both facilitatory and inhibitory drug effects. Briefly, mice were tested over a wide range of increasing speeds (0–55 rpm;

© 2010 The Authors

180 s each) in a control session. One additional session was repeated 30 min after drug injection. Drug effect expressed as percent of control performance (total time spent on the rod) in a narrower time-window (25–45 rpm).

Microdialysis coupled to bar test

Concentrically designed microdialysis probes were stereotaxically implanted, under isoflurane anesthesia, into the mouse SNr (1 mm dialysing membrane, AN69, Hospal, Bologna, Italy) according to the following coordinates from bregma: AP − 3.28, ML ± 1.2, DV − 4.7 (Paxinos and Franklin 2001). Probes were secured to the skull by acrylic dental cement and metallic screws. Following surgery, mice were allowed to recover and experiments were run 24 h after probe implantation. Microdialysis probes were perfused at a flow rate of 2.1 μL/min with a modified Ringer solution (composition in mM: $CaCl_2$ 1.2; KCl 2.7, NaCl 148 and $MgCl_2$ 0.85). Samples were collected every 15 min, starting 6 h after the onset of probe perfusion. Each dialysate collection was coupled to the recording of time spent on the bar at 2 different step lengths (1.5 and 4 cm heights). Cut off for each step was 20 s (40 s maximum). For the evaluation of acute effects of reserpine, mice were implanted, perfused with Ringer then given reserpine on day 1, and tested on day 2 (i.e. 24 h after reserpine; Fig. 1). For evaluation of the chronic effects of J-113397, reserpinized mice were implanted at the second day after treatment onset (Fig. 1). At the end of each experiment, the placement of the probes was verified by microscopic examination.

Endogenous GLU and GABA analysis

Glutamate and GABA were measured by HPLC coupled with fluorometric detection as previously described (Marti *et al.* 2007). Thirty microliters of *o*-phthaldialdehyde/mercaptoethanol reagent were added to 30 μL aliquots of sample, and 50 μL of the mixture was automatically injected (Triathlon autosampler; Spark Holland, Emmen, the Netherlands) onto a 5-C18 Chromsep analytical column (3 mm inner diameter, 10 cm length; Chrompack, Middelburg, the Netherlands) perfused at a flow rate of 0.48 mL/min (Beckman 125 pump; Beckman Instruments, Fullerton, CA, USA) with a mobile phase containing 0.1 M sodium acetate, 10% methanol and 2.2% tetrahydrofuran (pH 6.5). GLU and GABA were detected by means of a fluorescence spectrophotometer FP-2020 Plus (Jasco, Tokyo, Japan) with the excitation and the emission wavelengths set at 370 and 450 nm respectively. The limits of detection for GLU and GABA were ∼1 and ∼0.5 nM, respectively. Retention times for GLU and GABA were 3.5 ± 0.2 and 18.0 ± 0.5 min respectively.

Data presentation and statistical analysis

Motor performance has been calculated as time on bar or on rod (in seconds) and number of steps (drag test) and expressed either in absolute values or as percent of the control session.

Statistical analysis has been performed by two-way repeated measure analysis of variance (ANOVA). In case ANOVA yielded a significant F score, *post hoc* analysis has been performed by contrast analysis to determine group differences. In case a significant time × treatment interaction was found, the sequentially rejective Bonferroni test was used (implemented on Excel spreadsheet) to determine specific differences (i.e. at the single time-point level) between groups. p-values < 0.05 were considered to be statistically significant.

Materials

Reserpine was purchased from Sigma Chemical Co (St Louis, MO, USA) whereas J-113397 was synthesized in the laboratory of Pharmaceutical Chemistry of the University of Ferrara as previously reported (Marti *et al.* 2004a). Reserpine was dissolved in 10% acetic acid saline solution and pH adjusted to 4.5 with NaOH. J-113397 was freshly dissolved in isoosmotic saline solution just before use. Reserpine was administered subcutaneously while J-113397 was given i.p.

Results

Behavioral effects of reserpine in Swiss mice

Basal motor activity in naïve Swiss mice was similar at the left and right paw so data were pooled together. The immobility time (bar test) was 2.5 ± 0.2 s (n = 46), the number of steps (drag test) was 17.6 ± 0.1 (n = 40) whereas the time on rod (rotarod test; 25–45 rpm range) was 234 ± 24 s (n = 38). Reserpine (0.1–3 mg/kg) impaired motor activity in a dose-dependent way, increasing the immobility time (Fig. 2a), reducing the number of steps (Fig. 2b) and impairing the rotarod performance (Fig. 2c). Motor impairment was usually maximal after 24 h and stable (although with a tendency to reverse) for 3 days following administration of reserpine ≥ 1 mg/kg. In particular, reserpine induced akinesia in the bar test (Fig. 2a) yet at 0.5 mg/kg. Immobility time increased up to 28 s at D1 and returned to control at D3. Conversely, the maximally

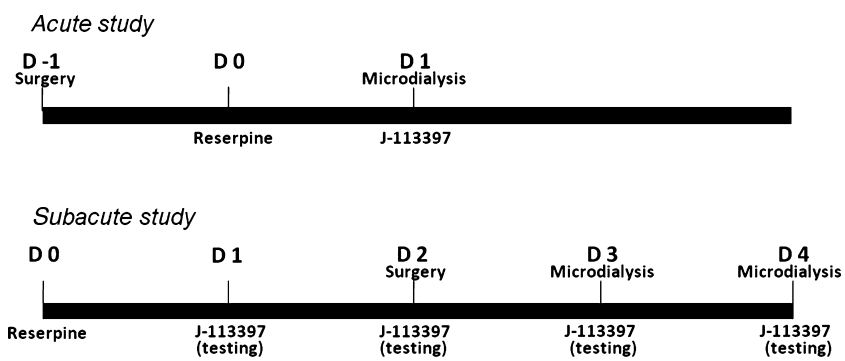

Fig. 1 Timeline of microdialysis experiments in reserpinized mice.

© 2010 The Authors

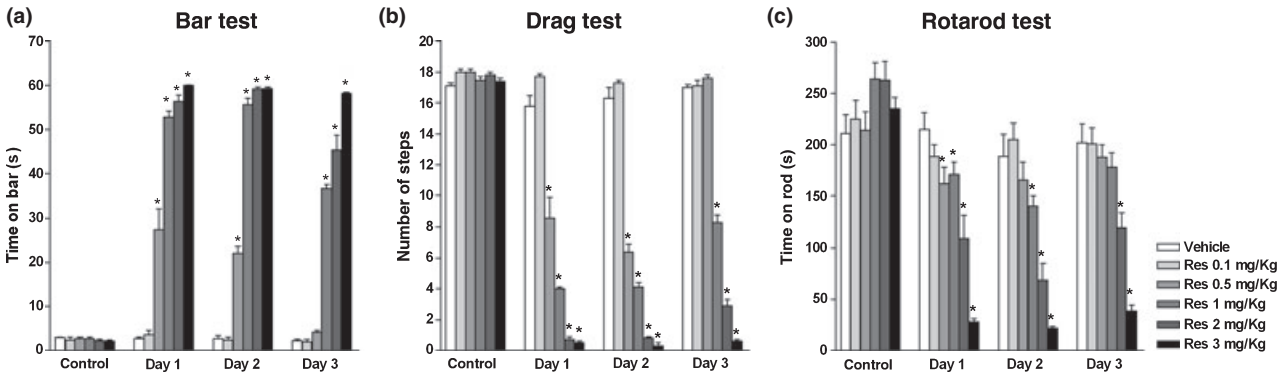

Fig. 2 Reserpine caused dose-dependent motor deficits in mice. Reserpine (0.1–3 mg/kg) or vehicle were administered s.c. and motor activity evaluated in the bar (a), drag (b) and rotarod (c) tests for 3 days after administration. Data are expressed in absolute values and are means ± SEM of seven determinations per group. Statistical analysis was performed by one-way RM ANOVA followed by contrast analysis and the sequentially rejective Bonferroni's test. (a) Significant effect of treatment ($F_{5,30}$ = 586.64, p < 0.0001), time ($F_{3,108}$ = 937.54, p < 0.0001) and time × treatment interaction ($F_{15,108}$ = 139.74, p < 0.0001). (b) Significant effect of treatment ($F_{5,30}$ = 854.56, p < 0.0001), time ($F_{3,96}$ = 826.85, p < 0.0001) and time × treatment interaction ($F_{15,96}$ = 104.06, p < 0.0001). (c) Significant effect of treatment ($F_{5,30}$ = 16.45, p < 0.0001), time ($F_{3,96}$ = 133.99, p < 0.0001) and time × treatment interaction ($F_{15,96}$ = 18.11, p < 0.0001). *p < 0.05 significantly different from basal (i.e. prior to treatment) values.

effective dose (3 mg/kg) elevated immobility time at cut-off levels (60 s) and did not show tendency to reverse over time. Also in the drag test (Fig. 2b), threshold dose was 0.5 mg/kg which caused inhibition of stepping activity at D1 (∼53%) and D2 (∼65%) but not D3. Again maximal inhibition was detected at 3 m/kg which induced a prolonged ∼95% inhibition across the different experimental sessions. Finally, 0.5 mg/kg reserpine mildly (∼23%) and transiently (only at D1) inhibited rotarod performance in the rotarod test (Fig. 2c). Maximal effect was observed at 3 mg/kg which caused a profound (∼90%) and prolonged inhibition.

Behavioral effects of reserpine in NOP$^{+/+}$ and NOP$^{-/-}$ mice

To investigate whether endogenous N/OFQ contributes to motor impairment induced by reserpine, NOP$^{+/+}$ and NOP$^{-/-}$ mice were challenged with two doses of reserpine, causing submaximal (1 mg/kg) and maximal (3 mg/kg) motor impairment. NOP$^{-/-}$ mice had immobility times comparable to NOP$^{+/+}$ mice in the bar test (1.0 ± 0.1 and 1.3 ± 0.2 s; n = 21; Fig. 3a and d) but greater (p < 0.001, Student's t-test) performance in the drag (18.5 ± 0.1 and 17.4 ± 0.2 steps, respectively, n = 21; Fig. 3b and e) and rotarod (210 ± 10 and 143 ± 6 s, n = 21; Fig. 3c and f) tests. Overall, NOP$^{-/-}$ mice were more resistant to the motor inhibition induced by both reserpine doses, although the difference was greater with reserpine 1 mg/kg. In particular, reserpine caused ∼40% less akinesia in the bar test at D1 and D2 in NOP$^{-/-}$ compared with NOP$^{+/+}$ mice (Fig. 3a). The difference in immobility time was even greater at D3, indicating a faster recovery from reserpine in NOP$^{-/-}$ mice. In the drag test (Fig. 3b), reserpine 1 mg/kg caused reduction in stepping activity which was ∼55% less in NOP$^{-/-}$ than NOP$^{+/+}$ mice. Consistently, NOP$^{-/-}$ mice were much less affected than NOP$^{+/+}$ mice in the rotarod test (Fig. 3c), with ∼50% less inhibition at D1. Different from the other tests, rotarod performance at D3 was normalized in NOP$^{-/-}$ mice still being almost maximal in NOP$^{+/+}$ mice. A different genotype response was also observed in the bar and drag test following reserpine 3 mg/kg, although it was much less pronounced (Fig. 3d and e). Conversely, no difference in rotarod performance was found with reserpine 3 mg/kg (Fig. 3f).

Neurochemical and behavioral changes in NOP$^{+/+}$ and NOP$^{-/-}$ reserpinized mice

Microdialysis coupled to behavioral testing in parkinsonian rats (Marti *et al.* 2004b, 2005, 2007, 2008) and mice (Mabrouk *et al.* 2010) revealed that endogenous N/OFQ sustains Parkinsonian-like symptoms by modulating amino acid release in SNr. We therefore used the same approach to investigate whether the different susceptibility to reserpine of NOP$^{+/+}$ and NOP$^{-/-}$ mice relied on modulation of nigral GLU and GABA release. Immobility time in mice undergoing microdialysis was higher (p < 0.05) in NOP$^{+/+}$ (4.9 ± 0.4 s) than NOP$^{-/-}$ (2.2 ± 0.3 s) mice. Conversely, SNr GLU and GABA levels did not differ between genotypes (NOP$^{+/+}$, 42.1 ± 8.7 and 2.80 ± 0.19 nM; NOP$^{-/-}$, 65.8 ± 0.3 and 2.49 ± 0.19 nM, respectively). Reserpine administration (1 mg/kg) caused a significant increase in immobility time at 24 h after administration (Fig. 4a) which was accompanied by changes in GLU ($F_{3,26}$ = 16.13, p < 0.0001; Fig. 4b) and GABA ($F_{3,25}$ = 4.49, p < 0.0001; Fig. 4c) levels. In particular, although

© 2010 The Authors

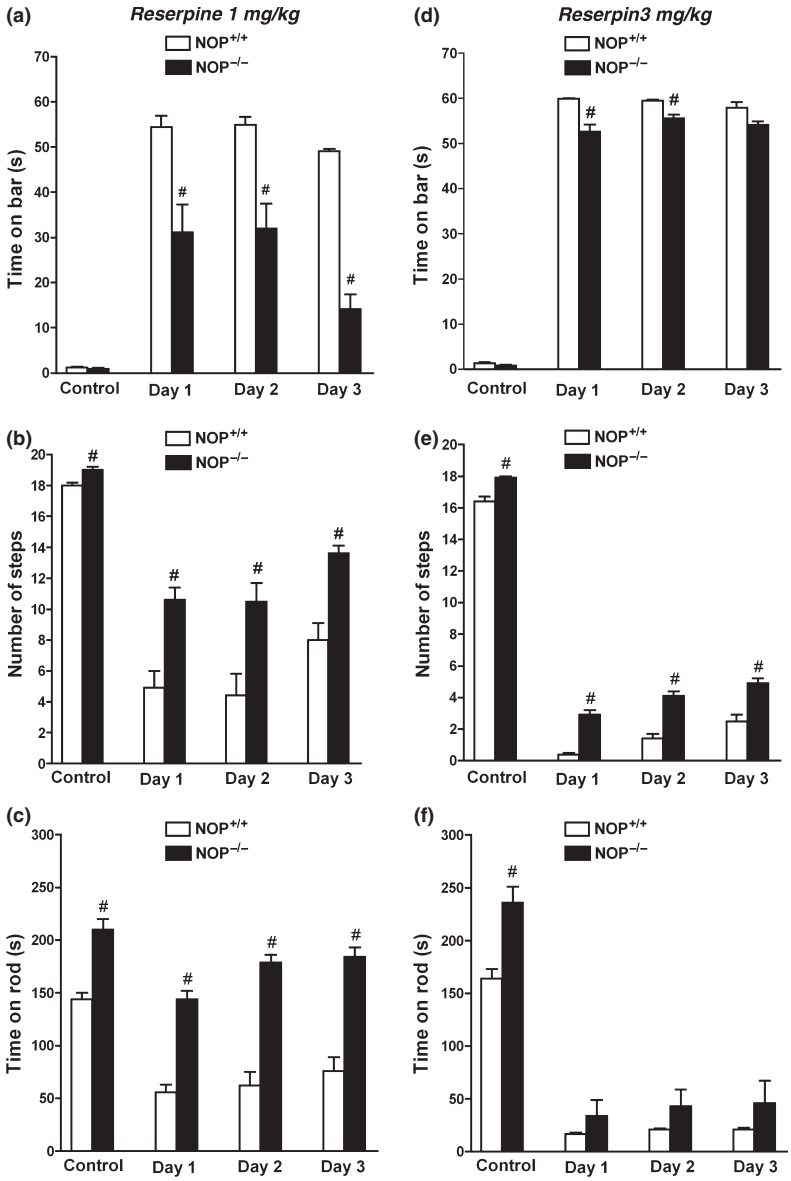

Fig. 3 NOP receptor knockout ($NOP^{-/-}$) mice were less susceptible to reserpine-induced akinesia/hypokinesia than wild-type ($NOP^{+/+}$) mice. Two doses of reserpine were administered s.c. (1 and 3 mg/kg) and motor activity evaluated in the bar (a), drag (b) and rotarod (c) tests for 3 days after administration. Data are expressed in absolute values and are means ± SEM of eight determinations per group. Statistical analysis was performed by one-way RM ANOVA followed by contrast analysis and the sequentially rejective Bonferroni's test. (a) Significant effect of treatment ($F_{1,7} = 43.37$, $p = 0.0003$), time ($F_{3,42} = 115.21$, $p < 0.0001$) and time × treatment interaction ($F_{3,42} = 15.43$, $p < 0.0001$). (b) Significant effect of treatment ($F_{1,7} = 34.25$, $p = 0.0006$), time ($F_{3,42} = 113.78$, $p < 0.0001$) and time × treatment interaction ($F_{3,42} = 6.42$, $p = 0.0011$). (c) Significant effect of treatment ($F_{1,7} = 83.8$, $p < 0.0001$), time ($F_{3,42} = 66.47$, $p < 0.0001$) and time × treatment interaction ($F_{3,42} = 8.28$, $p = 0.0002$). (d) Significant effect of treatment ($F_{1,7} = 44.27$, $p = 0.0002$), time ($F_{3,42} = 1170.21$, $p < 0.0001$) and time × treatment interaction ($F_{3,42} = 2.45$, $p = 0.0487$). (e) Significant effect of treatment ($F_{1,7} = 51.78$, $p = 0.0001$) and time ($F_{3,42} = 1165.69$, $p < 0.0001$) but not time × treatment interaction ($F_{3,42} = 1.29$, $p = 0.08$). $^{\#}p < 0.05$ significantly different from $NOP^{+/+}$ mice.

reserpine elevated immobility time in both genotypes (Fig. 4a), $NOP^{-/-}$ mice showed ∼50% less akinesia than $NOP^{+/+}$ mice. Reserpine also elevated nigral GLU levels in both genotypes, although the effect was greater in $NOP^{+/+}$ (∼440%) than $NOP^{-/-}$ (∼254%) mice. Finally, reserpine inhibited (∼35%) nigral GABA levels in $NOP^{+/+}$ mice, being ineffective in $NOP^{-/-}$ mice.

To provide additional evidence that pharmacological NOP receptor blockade attenuates reserpine-induced motor deficits, we acutely administered J-113397 to both genotypes (Fig. 5).

© 2010 The Authors

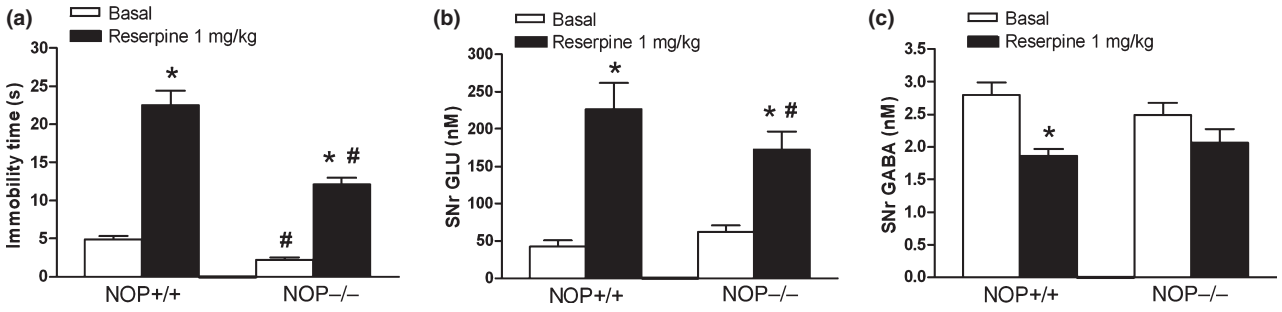

Fig. 4 Reserpine differentially modulated akinesia and amino acid release in the SNr of NOP receptor knockout ($NOP^{-/-}$) and wild-type ($NOP^{+/+}$) mice. One microdialysis probe was implanted using isoflurane anesthesia in the substantia nigra reticulata (SNr) of $NOP^{+/+}$ and $NOP^{-/-}$ mice. Immobility time (bar test; a) was measured 24 h after 1 mg/kg (s.c.) reserpine administration together with glutamate (GLU; b) and GABA (c) extracellular levels in SNr. Data are mean ± SEM of nine experiments per group and are expressed as total time spent on the bar (maximum cut-off 40 s; a) or nM (b, c). Statistical analysis was performed by one-way ANOVA followed by the Bonferroni's test. Significant effects of treatment on immobility time ($F_{3,16} = 80.67$, $p < 0.0001$; a), GLU levels ($F_{3,26} = 16.13$, $p < 0.0001$; b) and GABA levels ($F_{3,25} = 4.49$, $p < 0.0001$; c). $^{*}p < 0.05$ significantly different from basal values (i.e. prior to treatment) $^{\#}p < 0.05$ significantly different from $NOP^{+/+}$ mice.

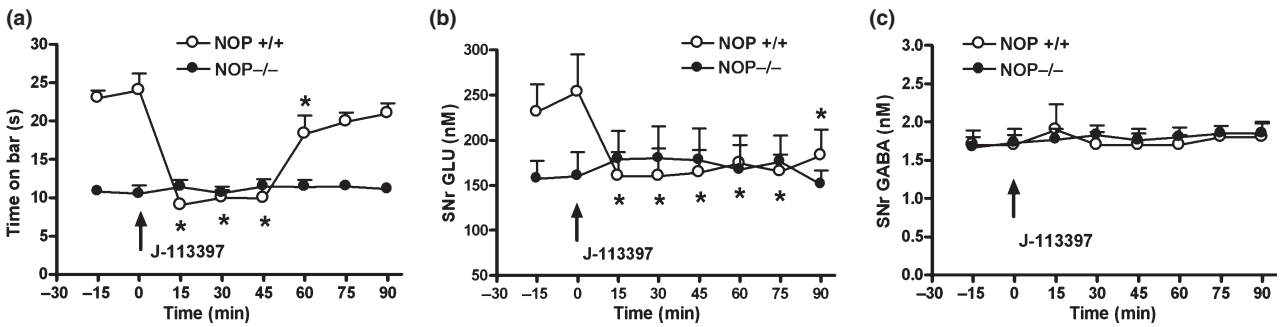

Fig. 5 J-113397 attenuated akinesia while simultaneously reducing nigral GLU release in $NOP^{+/+}$ but not $NOP^{-/-}$ reserpinized mice. One microdialysis probe was implanted using isoflurane anesthesia in the substantia nigra reticulata (SNr) of NOP receptor knockout ($NOP^{-/-}$) and wild-type ($NOP^{+/+}$) mice. Immobility time (bar test; a) was measured 24 h after 1 mg/kg (s.c.) reserpine administration together with glutamate (GLU; b) and GABA (c) extracellular levels in SNr. J-113397 (1 mg/kg) was given i.p. Data are mean ± SEM of nine experiments per group and are expressed as total time spent on the bar (maximum cut-off 40 s; a) or nM (b, c). Statistical analysis was performed by RM ANOVA followed by contrast analysis and the sequentially rejective Bonferroni's test. Significant effect of treatment on immobility time ($F_{7,49} = 23.44$; $p < 0.0001$; a) and nigral GLU levels ($F_{7,42} = 5.27$; $p < 0.0001$; b) in $NOP^{+/+}$ mice. $^{*}p < 0.05$ significantly different from control values.

J-113397 was used at a dose (1 mg/kg, i.p.) that improved motor activity in naïve mice (Viaro *et al.* 2008) and reversed Parkinsonism in haloperidol-treated mice (Mabrouk *et al.* 2010). J-113397 caused attenuation of akinesia in $NOP^{+/+}$ mice being ineffective in $NOP^{-/-}$ mice (Fig. 5a). Immobility time dropped to and remained at the same levels observed in $NOP^{-/-}$ mice for 45 min (~55% maximal reduction), progressively returning to baseline afterwards. J-113397 administration in $NOP^{+/+}$ mice was associated with significant changes in nigral GLU release being ineffective in $NOP^{-/-}$ mice (Fig. 5b). GLU levels were promptly reduced by J-113397, and remained stably below pre-stimulation levels until the end of experiment. Conversely, J-113397 did not affect GABA levels in $NOP^{+/+}$ or $NOP^{-/-}$ mice (Fig. 5c).

Behavioral effects of subacute J-113397 in reserpinized mice

To investigate whether acute beneficial effects of J-113397 were maintained over time, we administered J-113397 (1 mg/kg) to Swiss mice having received reserpine (1 mg/kg) or saline 24 h in advance. Overall, it appeared that despite evoking mild acute effects, J-113397 produced marked amelioration of basal motor performance (baseline) which translated into a faster recovery from reserpine. In the bar test (Fig. 6), no acute effect of J-113397 was observed in naïve and reserpinized mice across the different experimental sessions (i.e. from D1 to D4; Fig. 6a). Conversely, J-113397 caused significant reductions of basal immobility time at D3 and D4 in reserpinized mice (Fig. 6b).

© 2010 The Authors

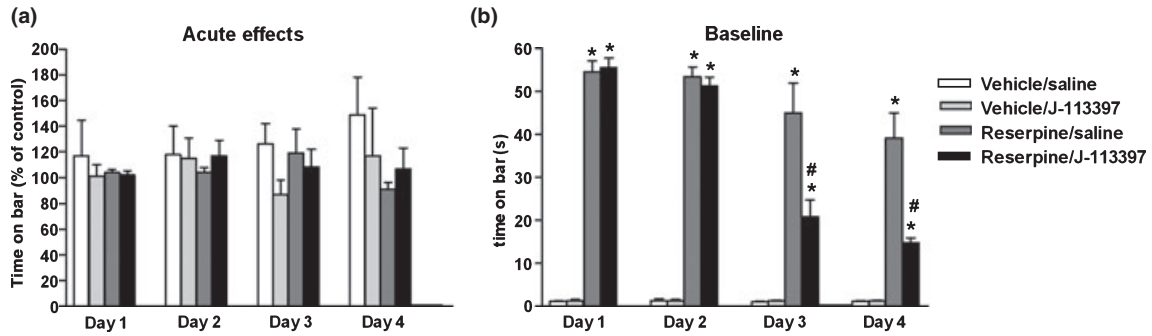

Fig. 6 Subacute administration of J-113397 ameliorated motor impairment induced by reserpine in the bar test. Reserpine (1 mg/kg) or vehicle were administered s.c. and motor activity (immobility time) evaluated in the bar test for 4 days after administration. Treatment with J-113397 (1 mg/kg, i.p., once daily) started 24 h after reserpine administration (i.e. on day 1) and continued for 4 days. Saline was also administered (i.p.) as a control. Motor activity was evaluated before ('baseline') and 10 min after ('acute effect') J-113397 administration. Data are expressed as absolute values (s; b) or percentages of motor activity in the control session (a), and are mean ± SEM of eight determinations per group. Statistical analysis was performed by two-way RM ANOVA followed by contrast analysis and the sequentially rejective Bonferroni's test. (b) Significant effect of treatment ($F_{3,15} = 155.00$, $p < 0.0001$), time ($F_{3,60} = 25.94$, $p < 0.0001$) and time × treatment interaction ($F_{9,60} = 12.30$; $p < 0.0001$). $^{*}p < 0.05$ significantly different from untreated animals (vehicle/saline); $^{\#}p < 0.05$ significantly different from saline-treated reserpinized animals.

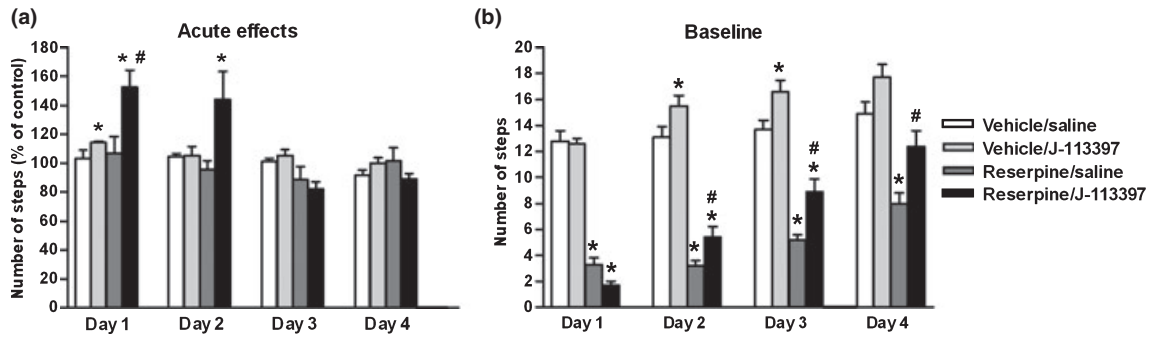

Fig. 7 Subacute administration of J-113397 ameliorated motor impairment induced by reserpine in the drag test. Reserpine (1 mg/kg) or vehicle were administered s.c. and motor activity (number of steps) evaluated in the drag test for 4 days after administration. Treatment with J-113397 (1 mg/kg, i.p., once daily) started 24 h after reserpine administration (i.e. on day 1) and continued for 4 days. Saline was also administered (i.p.) as a control. Motor activity was evaluated before ('baseline') and 20 min after ('acute effect') J-113397 administration. Data are expressed as absolute values (s; b) or percentages of motor activity in the control session (a), and are mean ± SEM of eight determinations per group. Statistical analysis was performed by two-way RM ANOVA followed by contrast analysis and the sequentially rejective Bonferroni's test. (a) Non-significant effect of treatment ($F_{3,18} = 2.87$, $p = 0.065$), but significant effect of time ($F_{3,72} = 15.85$, $p < 0.0001$) and time × treatment interaction ($F_{9,72} = 7.12$; $p < 0.0001$). (b) Significant effect of treatment ($F_{3,18} = 174.72$, $p < 0.0001$), time ($F_{3,72} = 91.61$, $p < 0.0001$) and time × treatment interaction ($F_{9,72} = 10.15$; $p < 0.0001$). $^{*}p < 0.05$ significantly different from untreated animals (vehicle/saline); $^{\#}p < 0.05$ significantly different from saline-treated reserpinized animals.

In the drag test (Fig. 7), J-113397 caused a mild and barely significant acute improvement of stepping activity in naïve mice at D1 but not later sessions (Fig. 7a). In reserpinized mice, the acute effects of J-113397 were more robust and evident at D1 and D2 but not later. Loss of acute effects was paralleled by improvement in baseline stepping activity (Fig. 7b). In naïve mice, J-113397 produced a mild increase in baseline stepping activity which reached the level of significance at D2 and D3 only. In reserpinized mice, J-113397 caused significantly greater stepping activity than saline-treated animals from D2 onward. At the end of subacute treatment, J-113397-treated reserpinized mice completely recovered from reserpine, showing stepping activity comparable to naïve mice.

In the rotarod test (Fig. 8), J-113397 caused consistent acute improvements (~40%) across the different sessions in naïve mice (Fig. 8a). Milder (~20%) improvements were also observed in reserpinized mice at D1 and D2. However, J-113397 caused mild inhibitory effects after the fourth challenge. No changes in baseline activity values were observed in naïve mice (Fig. 8b). Conversely, subacute J-113397 administration caused a dramatic and progressive

© 2010 The Authors

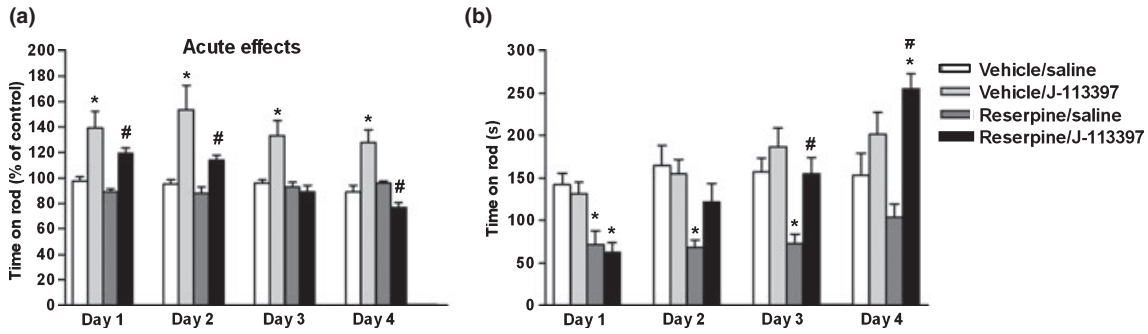

Fig. 8 Subacute administration of J-113397 ameliorated motor impairment induced by reserpine in the rotarod test. Reserpine (1 mg/kg) or vehicle were administered s.c. and motor activity (time on rod) evaluated in the rotarod test for 4 days after administration. Treatment with J-113397 (1 mg/kg, i.p., once daily) started 24-h after reserpine administration (i.e. on day 1) and continued for 4 days. Saline was also administered (i.p.) as a control. Motor activity was evaluated before ('baseline') and 30 min after ('acute effect') J-113397 administration. Data are expressed as absolute values (s; b) or percentages of motor activity in the control session (a), and are mean ± SEM of eight determinations per group. Statistical analysis was performed by two-way RM ANOVA followed by contrast analysis and the sequentially rejective Bonferroni's test. (a) Significant effect of treatment ($F_{7,21}$ = 10.54, p = 0.0002), time ($F_{3,84}$ = 6.43, p = 0.0005) and time × treatment interaction ($F_{9,84}$ = 3.91; p = 0.0003). (b) Significant effect of treatment ($F_{7,21}$ = 11.20, p = 0.0001), time ($F_{3,76}$ = 26.44, p < 0.0001) and time × treatment interaction ($F_{9,76}$ = 7.14; p < 0.0001). *p < 0.05 significantly different from untreated animals (vehicle/saline); #p < 0.05 significantly different from saline-treated reserpinized animals.

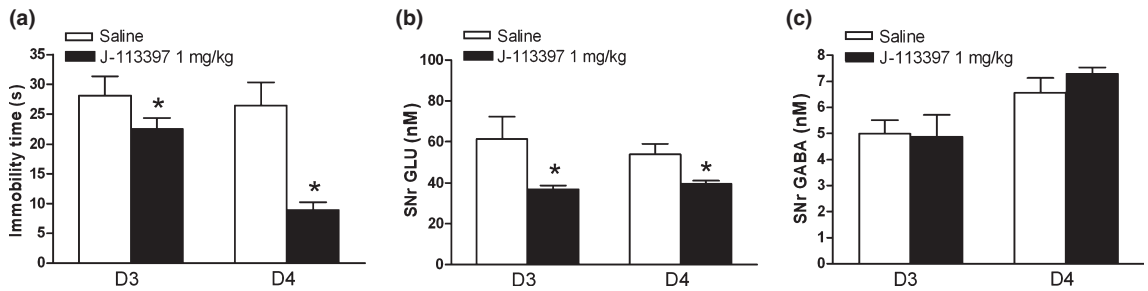

Fig. 9 Chronic treatment with J-113397 attenuated akinesia while simultaneously reducing nigral GLU release in reserpinized Swiss mice. One microdialysis probe was implanted using isoflurane anesthesia in the substantia nigra reticulata (SNr) of Swiss mice. Mice were reserpinized (1 mg/kg; s.c.) and treated daily for 4 days with J-113397 (1 mg/kg; i.p.) or saline (starting from 24 h after reserpine administration). Immobility time (bar test; a) was measured at 3 and 4 days after reserpine together with glutamate (GLU; b) and GABA (c) extracellular levels in SNr. Data are mean ± SEM of eight experiments per group and are expressed as total time spent on the bar (maximum cut-off 40 s; a) or neurotransmitter release in nM (b, c). Statistical analysis was performed by two-way RM ANOVA followed by contrast analysis and the sequentially rejective Bonferroni's test. (a) Significant effect of treatment ($F_{1,8}$ = 31.46; p = 0.0005) but not time ($F_{1,16}$ = 1.41; p = 0.25) or time × treatment interaction ($F_{1,16}$ = 0.33; p = 0.57). (b) Significant effect of treatment ($F_{1,8}$ = 72.65; p < 0.0001) but not time ($F_{1,16}$ = 0.07; p = 0.78) or time × treatment interaction ($F_{1,16}$ = 0.63; p = 0.43). *p < 0.05 significantly different from saline-treated animals.

improvement in basal activity in reserpinized mice. In particular, J-113397-treated reserpinized mice showed greater performance than saline-treated reserpinized animals from D3 onward (Fig. 8c). At the end of treatment, basal rotarod performance of J-113397-treated reserpinized animals even exceeded that of saline-treated non-reserpinized animals.

Neurochemical and behavioral changes in mice subacutely treated with J-113397

To investigate whether short term beneficial effects of J-113397 were accompanied by changes in amino acid release in SNr, microdialysis was performed in reserpinized mice subacutely treated with J-113397 or saline (Fig. 9). Mice treated with J-113397 had a greater reduction of immobility time with respect to saline-treated mice both at D3 (~20%) and D4 (~65%; Fig. 9a). Likewise, mice treated with J-113397 had significantly lower GLU levels than saline-treated mice both at D3 (~40%) and D4 (~30%; Fig. 9b). Conversely, no difference was detected in GABA levels between genotypes (Fig. 9c).

We finally monitored the acute amino acid response to J-113397 at D4 in reserpinized mice subacutely treated with J-113397 or saline (Fig. 10). J-113397 caused acute antiakinetic effect (Fig. 10a) and significantly inhibited GLU levels

© 2010 The Authors

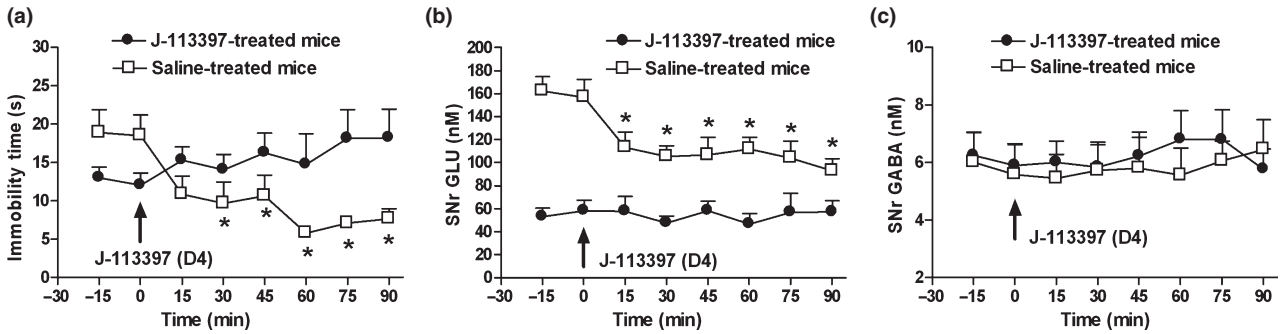

Fig. 10 Loss of the acute behavioral and neurochemical response to J-113397 after repeated treatment. One microdialysis probe was implanted using isoflurane anesthesia in the substantia nigra reticulata (SNr) of Swiss mice treated with reserpine (1 mg/kg, s.c.) or vehicle at day 0 and subsequently with a single daily injections of J-113397 or saline from day 1 to 4 (D4). Immobility time (bar test; a) was monitored at D4 simultaneously with glutamate (GLU; b) and GABA (c) extracellular levels in SNr. Data are mean ± SEM of eight experiments per group and are expressed as total time spent on the bar (maximum cut-off 40 s; a) or nM (b, c). Statistical analysis was performed by one-way RM ANOVA followed by contrast analysis and the sequentially rejective Bonferroni's test. Significant effect of J-113397 on immobility time ($F_{7,63} = 13.33$, $p < 0.0001$; a) and GLU levels ($F_{7,42} = 9.38$, $p < 0.0001$; b) in reserpinized mice pre-treated with saline. *$p < 0.05$, significantly different from control values.

(Fig. 10b) in reserpinized mice pre-treated with saline but not J-113397. However, it failed to affect GABA levels in both groups of mice (Fig. 10c).

Discussion

A battery of complementary motor tests allowed for a careful analysis of motor response to reserpine in mice. Consistent with studies in rats (Colpaert 1987; Heslop and Curzon 1994), reserpine evoked a dose- and time-dependent Parkinsonian-like syndrome which was characterized by a long lasting increase in akinesia/bradykinesia and gait disability. Hypokinesia was observed for at least 3 days after single injection, in keeping with the fact that despite being readily cleared from blood, reserpine irreversibly binds to vesicular membranes for at least 18–30 h (Stitzel 1977). Consistently, monoamine levels drop after single reserpine administration remaining below control levels for several days (Schultz 1982; Heslop and Curzon 1994). The present study provides the first evidence that reserpine caused akinesia while simultaneously elevating GLU and reducing GABA levels in SNr. This is in line with a previous microdialysis study showing that reserpine enhanced GLU levels in the rat entopeduncular nucleus (Biggs and Starr 1997), which is the homologous to the primate globus pallidus internalis and, together with SNr, the rodent motor output of the basal ganglia. SNr GLU levels may rise as a consequence of the increased activity of the subthalamic nucleus (Robledo and Feger 1991) or from disinhibition of nigral GLU terminals from a local inhibitory control mediated by D_2 receptors (Hatzipetros and Yamamoto 2006). The mechanism(s) underlying the reduction of GABA levels are more difficult to be identified since different pools of neuronal GABA are sampled in SNr, which are generated by GABAergic afferents, GABA interneurons and recurrent collaterals of nigro-thalamic projection neurons. Tentatively, the reduction of GABA levels may result from changes in basal ganglia circuitry as a consequence of reserpine-induced striatal DA depletion (reduced activity along the striato-nigral or pallido-nigral pathways; Cole and Di Figlia 1994; Harrison *et al.* 2001) or impairment of nigral GABA release caused by the loss of a D_1 receptor mediated pre-synaptic facilitation (Radnikow and Misgeld 1998). Interestingly, administration of cataleptogenic doses of haloperidol was also associated with an increase of GLU and a reduction of GABA levels in SNr (Mabrouk *et al.* 2010), supporting the view that reserpine disinhibits D_2 circuits in the basal ganglia (Cole and Di Figlia 1994). Thus, akinesia caused by functional impairment of DA transmission results from the imbalance between excitatory and inhibitory inputs converging on nigro-thalamic GABA projection neurons which regulate the thalamic filter (Deniau and Chevalier 1985).

Genetic and pharmacological evidence that endogenous N/OFQ partly sustains Parkinsonism induced by reserpine was provided for the first time. Indeed, $NOP^{-/-}$ mice displayed significantly less motor deficits than $NOP^{+/+}$ mice when administered with reserpine (1 mg/kg). The lower sensitivity may rely on a lower expression of VMAT2 in $NOP^{-/-}$ mice because VMAT2 heterozygous mice are less sensitive to reserpine than wild-type controls (Fumagalli *et al.* 1999). However, these mice also have lower striatal DA levels (Wang *et al.* 1997) and reduced locomotion (Fukui *et al.* 2007). Conversely, $NOP^{-/-}$ mice did not show changes in striatal (accumbal) DA levels (Murphy *et al.* 2002) and performed better than controls in different motor tasks (Marti *et al.* 2004a, 2005; Viaro *et al.* 2008; Mabrouk *et al.* 2010).

© 2010 The Authors

In addition, $NOP^{-/-}$ mice were also less susceptible than controls to the hypokinetic action of haloperidol (0.3 mg/kg; Marti *et al.* 2005; Mabrouk *et al.* 2010) which causes Parkinsonism through D_2 receptor blockade. Therefore, the lower sensitivity of $NOP^{-/-}$ mice to reserpine is likely caused by the removal of N/OFQ modulation at the circuit level. The finding that the lower degree of akinesia in $NOP^{-/-}$ mice was associated with a lower increase in nigral GLU levels further suggests that the akinesiogenic action of N/OFQ is accomplished by increasing an excitatory GLUergic drive on nigrothalamic neurons. Various lines of evidence have proven that endogenous N/OFQ enhances GLU levels in SNr. NOP receptor antagonists reduced GLU levels in naïve (Marti *et al.* 2002) and 6-OHDA hemilesioned (Marti *et al.* 2005, 2007, 2008; Volta *et al.* 2010a) rats as well as haloperidol-treated rats (Marti *et al.* 2004b, 2005) or mice (Mabrouk *et al.* 2010). Moreover, cataleptogenic doses of haloperidol elevated GLU levels in the SNr of $NOP^{+/+}$ mice but inhibited it in $NOP^{-/-}$ mice (Mabrouk *et al.* 2010). Finally, reverse dialysis of exogenous N/OFQ in the SNr of naïve rats increased local GLU levels (Marti *et al.* 2002). Overall, these data indicate that reserpine evokes hypokinesia and nigral GLU levels at least in part through endogenous N/OFQ. This hypothesis is further corroborated by the finding that extracellular levels of N/OFQ in SNr rise following 6-OHDA lesioning (Marti *et al.* 2005) or haloperidol administration (Marti *et al.* 2010).

Pharmacological studies substantially confirmed the link existing between N/OFQ, reserpine-induced Parkinsonism and nigral GLU levels. Indeed, J-113397 attenuated akinesia and nigral GLU rise in $NOP^{+/+}$ mice while being ineffective in $NOP^{-/-}$ mice. Moreover, both the acute and short-term antiakinetic effects of J-113397 were accompanied by an attenuation of the rise in nigral GLU levels evoked by reserpine. Finally, loss of acute antiakinetic effect of J-113397 paralleled the loss of its ability to inhibit GLU levels.

To the best of our knowledge, only two studies have investigated motor changes in response to repeated administration of a NOP receptor antagonist (Okabe and Murphy 2004; Vitale *et al.* 2009). In the former, a high dose (10 mg/kg) of compound B (the active enantiomer of J-113397) was administered systemically every other day for 5 days (three sessions) under a protocol of methamphetamine sensitization in mice. In the latter, the peptide antagonist $[Nphe^1,Arg^{14},Lys^{15}]N/OFQ\text{-}NH_2$ was given i.c.v. (10 nmol) for 21 days to investigate its antidepressant activity in rats. Both studies monitored spontaneous locomotion (horizontal activity, rearings) and reported no short-term effects of NOP receptor blockade. At variance with that, using a battery of static and dynamic motor tests, we showed that a 4-day treatment with a low dose of J-113397 (1 mg/kg) produced short-term improvements in akinesia/bradykinesia and overall motor activity. The effects in naïve mice were overall milder than those in reserpinized mice. J-113397 (1 mg/kg) barely improved stepping activity, in keeping with a previous report (Viaro *et al.* 2008). Nevertheless, no acute effect was observed from day 2 onward, that is, when J-113397 caused a small but significant increase in baseline activity. Interestingly, compound B also enhanced the facilitatory effect of methamphetamine on spontaneous locomotion only during the first challenge, failing to do so after sensitization was instated and baseline activity rose (Okabe and Murphy 2004). J-113397 also markedly elevated rotarod performance but, different from the drag test, no change in baseline performance was induced by repeated administration; therefore, this acute effect was maintained across the experimental sessions. The drag test essentially involves pathways regulating movement initiation and execution (akinesia/bradykinesia) whereas the rotarod test also measures coordination, motivation to run and endurance. Therefore the different response following subacute J-113397 may reflect adaptive changes at different motor pathways. Indeed, administration of $[Nphe^1,Arg^{14},Lys^{15}]N/OFQ\text{-}NH_2$ (a peptide NOP receptor antagonist) in SNr stimulated cortical pathways controlling forepaw but not vibrissae movements (Marti *et al.* 2009). The existence of a 'baseline' effect was more evident in reserpinized mice. At the end of subacute treatment with J-113397, reserpinized mice were still slightly akinetic, but their baseline stepping activity was normalized and rotarod performance was even greater than pre-reserpine levels. This improvement in baseline activity was accompanied by the loss of an acute response and even a reversal of the initial facilitation into inhibition (e.g. rotarod performance at day 4). This suggests that loss of acute response may not rely on receptor desensitization but rather on recruitment of inhibitory pathways which oppose (excessive) motor activation. Microdialysis showed that these behavioral changes correlated with changes in nigral GLU levels. Indeed, short-term improvement of baseline activity was accompanied by a faster recovery of nigral GLU levels, and loss of the acute behavioral response to J-113397 was accompanied by the loss of GLU release modulation. Mechanistically, reductions in extracellular DA levels following reserpine activate DA synthesis by relieving D_2 autoreceptors from negative auto feedback (Schultz 1982). Endogenous N/OFQ directly inhibits DA synthesis (Olianas *et al.* 2008) and release (Marti *et al.* 2004a). Thus, by opposing these actions, J-113397 would foster extracellular DA levels and motor recovery. However, rapid normalization of nigral DA levels may cause compensatory saturation of post-synaptic DA receptors (leading to blunting of the acute anti-akinetic response) and sensitization of D_2 autoreceptors (leading to reinstatement of negative auto feedback). Thus, sustained blockade of NOP receptors accelerates recovery from reserpine, at the same time sensitizing the system towards D_2 (auto)receptor inhibition. The finding that high doses of J-113397 inhibit motor

© 2010 The Authors

activity in MPTP-treated mice via amisulpride-dependent mechanisms may support this view (Viaro *et al.* 2010). Indeed, low doses of systemic amisulpride have been claimed to selectively bind to D_2 autoreceptors (Scatton *et al.* 1997; Schoemaker *et al.* 1997).

In contrast with that found in 6-OHDA rats (Marti *et al.* 2007) and haloperidol-treated mice (Mabrouk *et al.* 2010), the anti-akinetic effect of J-113397 in reserpinized mice and the accompanying reduction of nigral GLU levels were not accompanied by any changes in nigral GABA levels. This indicates that endogenous N/OFQ can differentially modulate the two transmitters and that the reduction in GLU levels is mediated by GABA-independent mechanisms. Although these mechanisms are presently unclear, converging lines of evidence point to an involvement of D_2 receptors. Indeed, the D_2/D_3 antagonist raclopride prevented both the increase in nigral GLU levels evoked by intranigral perfusion with N/OFQ (Marti *et al.* 2002) and the reduction induced by a NOP receptor antagonist (Volta *et al.* 2010b). Interestingly, the latter effect was observed in 6-OHDA rats, suggesting that residual transmission at nigral D_2 receptors such as the effect caused by submaximal doses of reserpine or haloperidol (Marti *et al.* 2005; Mabrouk *et al.* 2010) may be sufficient to allow J-113397 to reduce GLU levels, likely via an elevation of DA release. The fact that the J-113397-induced modulation of GABA levels was prevented by reserpine may indicate its stronger dependence on DA transmission, or the involvement of a neurotransmitter (possibly serotonin) whose action is selectively inhibited by reserpine but not haloperidol or 6-OHDA. A previous study in 6-OHDA rats demonstrated that the anti-akinetic effect of a combination of J-113397 and L-DOPA is accomplished via $GABA_A$ receptor mediated over-inhibition of nigro-thalamic neurons (Marti *et al.* 2007). The lack of changes in nigral GABA levels in reserpinized animals rather seems to emphasize the behavioral relevance of the reduction of the excitatory GLUergic input to the nigral output.

Concluding remarks

Deletion of the NOP receptor gene or acute pharmacological blockade of the NOP receptor with J-113397 resulted in amelioration of hypokinesia and attenuation of the accompanying rise of SNr GLU levels following reserpine treatment in mice. Repeated J-113397 administration also caused a faster recovery of basal motor activity and nigral GLU levels. These genetic and pharmacological data provide novel insights into the mechanism of action of reserpine suggesting that endogenous N/OFQ mediates its hypokinetic actions via elevation of SNr GLU release. The sustained beneficial response to prolonged NOP receptor blockade awaits confirmation in a neurodegeneration model of Parkinsonism where reductions of DA levels are stably attained. Nonetheless, the short-term beneficial response suggests that NOP receptor antagonists may prove effective during chronic therapy of PD (Marti *et al.* 2005, 2007; Viaro *et al.* 2008; Mabrouk *et al.* 2010).

Acknowledgements

This work has been funded by grants from the Italian Ministry of the University (FIRB Internazionalizzazione n. RBIN047W33) and the University of Ferrara (FAR 2007) to M Morari. The authors declare no conflict of interest.

References

Betarbet R., Sherer T. B. and Greenamyre J. T. (2002) Animal models of Parkinson's disease. *Bioessays* **24**, 308–318.

Biggs C. S. and Starr M. S. (1997) Dopamine and glutamate control each other's release in the basal ganglia: a microdialysis study of the entopeduncular nucleus and substantia nigra. *Neurosci. Biobehav. Rev.* **21**, 497–504.

Brown J. M., Gouty S., Iyer V., Rosenberger J. and Cox B. M. (2006) Differential protection against MPTP or metamphetamine toxicity in dopamine neurons by deletion of ppN/OFQ expression. *J. Neurochem.* **98**, 495–505.

Carlsson A., Lindqvist M. and Magnusson T. (1957) 3,4-Dihydroxyphenylalanine and 5-hydroxytryptophan as reserpine antagonists. *Nature* **180**, 1200.

Cole D. G. and Di Figlia M. (1994) Reserpine increases Fos activity in the rat basal ganglia via a quinpirole-sensitive mechanism. *Neuroscience* **60**, 115–123.

Colpaert F. C. (1987) Pharmacological characteristics of tremor, rigidity and hypokinesia induced by reserpine in rat. *Neuropharmacology* **26**, 1431–1440.

Deniau J. M. and Chevalier G. (1985) Disinhibition as a basic process in the expression of striatal functions. II. The striato-nigral influence on thalamocortical cells of the ventromedial thalamic nucleus. *Brain Res.* **334**, 227–233.

Fukui M., Rodriguiz R. M., Zhou J., Jiang S. X., Phillips L. E., Caron M. G. and Wetsel W. C. (2007) Vmat2 heterozygous mutant mice display a depressive-like phenotype. *J. Neurosci.* **27**, 10520–10529.

Fumagalli F., Gainetdinov R. R., Wang Y. M., Valenzano K. J., Miller G. W. and Caron M. G. (1999) Increased metamphetamine neurotoxicity in heterozygous vesicular monoamine transporter 2 knock-out mice. *J. Neurosci.* **19**, 2424–2431.

Gerlach M. and Riederer P. (1996) Animal models of Parkinson's disease: an empirical comparison with the phenomenology of the disease in man. *J. Neural. Transm.* **103**, 987–1041.

Harrison M. B., Kumar S., Hubbard C. A. and Trugman J. M. (2001) Early changes in neuropeptide mRNA expression in the striatum following reserpine treatment. *Exp. Neurol.* **167**, 321–328.

Hatzipetros T. and Yamamoto B. K. (2006) Dopaminergic and GABAergic modulation of glutamate release from rat subthalamic nucleus efferents to the substantia nigra. *Brain Res.* **1076**, 60–67.

Heslop K. E. and Curzon G. (1994) Depletion and repletion of cortical tissue and dialysate 5-HT after reserpine. *Neuropharmacology* **33**, 567–573.

Kawamoto H., Ozaki S., Itoh Y., Miyaji M., Arai S., Nakashima H., Kato T., Ohta H. and Iwasawa Y. (1999) Discovery of the first potent and selective small molecule opioid receptor-like (ORL1) antagonist: 1-[3R, 4R)-1-cyclooctylmethyl-3-hydroxymethyl-4-piperidyl]-3-

© 2010 The Authors

ethyl-1,3-dihydro-2H-benzimidazol-2-one (J-113397). *J. Med. Chem.* **42**, 5061–5063.

Kuschinsky K. and Hornykiewicz O. (1972) Morphine catalepsy in the rat: relation to striatal dopamine metabolism. *Eur. J. Pharmacol.* **19**, 119–122.

Mabrouk O. S., Marti M. and Morari M. (2010) Endogenous nociceptin/orphanin FQ (N/OFQ) contributes to haloperidol-induced changes of nigral amino acid transmission and Parkinsonism: a combined microdialysis and behavioral study in naive and nociceptin/orphanin FQ receptor knockout mice. *Neuroscience* **166**, 40–48.

Marti M., Guerrini R., Beani L., Bianchi C. and Morari M. (2002) Nociceptin/orphanin FQ receptors modulate glutamate extracellular levels in the substantia nigra pars reticulata. A microdialysis study in the awake freely moving rat. *Neuroscience* **112**, 153–160.

Marti M., Mela F., Veronesi C. *et al.* (2004a) Blockade of nociceptin/orphanin FQ receptor signalling in rat substantia nigra pars reticulata stimulates nigrostriatal dopaminergic transmission and motor behaviour. *J. Neurosci.* **24**, 6659–6666.

Marti M., Mela F., Guerrini R., Calò G., Bianchi C. and Morari M. (2004b) Blockade of nociceptin/orphanin FQ transmission in rat substantia nigra reverses haloperidol-induced akinesia and normalizes nigral glutamate release. *J. Neurochem.* **91**, 1501–1504.

Marti M., Mela F., Fantin M. *et al.* (2005) Blockade of nociceptin/orphanin FQ transmission attenuates symptoms and neurodegeneration associated with Parkinson's disease. *J. Neurosci.* **95**, 9591–9601.

Marti M., Trapella C., Viaro R. and Morari M. (2007) The nociceptin/orphanin FQ receptor antagonist J-113397 and L-DOPA additively attenuate experimental Parkinsonism through overinhibition of the nigrothalamic pathway. *J. Neurosci.* **27**, 1297–1307.

Marti M., Trapella C. and Morari M. (2008) The novel nociceptin/orphanin FQ receptor antagonist Trap-101 alleviates experimental Parkinsonism through inhibition of the nigro-thalamic pathway: positive interaction with L-DOPA. *J. Neurochem.* **107**, 1683–1696.

Marti M., Viaro R., Guerrini R., Franchi G. and Morari M. (2009) Nociceptin/Orphanin FQ modulates motor behavior and primary motor cortex output through receptors located in substantia nigra reticulata. *Neuropsychopharmacology* **34**, 341–355.

Marti M., Sarubbo S., Latini F. *et al.* (2010) Brain interstitial nociceptin/orphanin FQ levels are elevated in Parkinson's disease. *Mov. Disord.* **25**, 1723–1732.

Meunier J. C., Mollerau C., Toll L. *et al.* (1995) Isolation and structure of the endogenus agonist of opioid receptor-like ORL1 receptor. *Nature* **377**, 532–535.

Mogil J. S. and Pasternak G. W. (2001) The molecular and behavioral pharmacology of the orphanin FQ/nociceptin peptide and receptor family. *Pharmacol. Rev.* **53**, 381–415.

Mollereau C., Parmentier M., Mailleux P., Butour J. L., Moisand C., Chalon P., Caput D., Vassart G. and Meunier J. C. (1994) ORL1, a novel member of the opioid receptor family. Cloning, functional expression and localization. *FEBS Lett.*. **341**, 33–38.

Murphy N. P., Lam H. A., Chen Z., Pintar J. E. and Maidment N. T. (2002) Heroin-induced locomotion and mesolimbic dopamine release is unchanged in mice lacking the ORL-1 receptor gene. *Brain Res.* **953**, 276–280.

Nishi M., Houtani T., Noda Y. *et al.* (1997) Unrestrained nociceptive response and dysregulation of hearing ability in mice lacking the nociceptin/orphaninFQ receptor. *EMBO J.* **16**, 1858–1864.

Okabe C. and Murphy N. P. (2004) Short-term effects of the nociceptin receptor antagonist Compound B on the development of metamphetamine sensitization in mice: a behavioral and c-fos expression mapping study. *Brain Res.* **1017**, 1–12.

Olianas M. C., Dedoni S., Boi M. and Onali P. (2008) Activation of nociceptin/orphanin FQ-NOP receptor system inhibits tyrosine hydroxylase phosphorylation, dopamine synthesis and dopamine D1 receptor signaling in rat nucleus accumbens and dorsal striatum. *J. Neurochem.* **107**, 544–556.

Paxinos G. and Franklin K. B. J. (2001) *The Mouse Brain in Stereotaxic Coordinates*, 2nd edn. Academic Press, San Diego.

Radnikow G. and Misgeld U. (1998) Dopamine D1 receptors facilitate GABAA synaptic currents in the rat substantia nigra pars reticulata. *J. Neurosci.* **18**, 2009–2016.

Reinscheid R. K., Nothacker H. P., Bourson A. *et al.* (1995) Orphanin FQ: a neuropeptide that activates an opioid-like G protein-coupled receptor. *Science* **270**, 792–794.

Robledo P. and Feger J. (1991) Acute monoaminergic depletion in the rat potentiates the excitatory effect of the subthalamic nucleus in the substantia nigra pars reticulata but not in the pallidal complex. *J. Neural Transm. Gen. Sect.* **86**, 115–126.

Rozas G., Guerra M. J. and Labandeira-Garcia J. L. (1997) An automated rotarod method for quantitative drug-free evaluation of overall motor deficits in rat models of Parkinsonism. *Brain Res. Brain Res. Protoc.* **2**, 75–84.

Sanberg P. R., Bunsey M. D., Giordano M. and Norman A. B. (1988) The catalepsy test: its ups and downs. *Behav. Neurosci.* **102**, 748–759.

Scatton B., Claustre Y., Cudennec A., Oblin A., Perrault G., Sanger D. J. and Schoemaker H. (1997) Amisulpride: from animal pharmacology to therapeutic action. *Int. Clin. Psychopharmacol.* **12**(Suppl 2), S29–36.

Schallert T., De Ryck M., Whishaw I. Q., Ramirez V. D. and Teitelbaum P. (1979) Excessive bracing reactions and their control by atropine and L-DOPA in an animal analog of Parkinsonism. *Exp. Neurol.* **64**, 33–43.

Schoemaker H., Claustre Y., Fage D. *et al.* (1997) Neurochemical characteristics of amisulpride, an atypical D2/D3 receptor antagonist with both presynaptic and limbic selectivity. *J. Pharmacol. Exp. Ther.* **280**, 83–97.

Schultz W. (1982) Depletion of dopamine in the striatum as an experimental model of Parkinsonism: direct effects and adaptive mechanisms. *Prog. Neurobiol.* **18**, 121–166.

Stitzel R. E. (1977) The biological fate of reserpine. *Pharmacol. Rev.* **28**, 179–208.

Viaro R., Sanchez-Pernaute R., Marti M., Trapella C., Isacson O. and Morari M. (2008) Nociceptin/orphanin FQ receptor blockade attenuates MPTP-induced Parkinsonism. *Neurobiol. Dis.* **30**, 430–438.

Viaro R., Marti M. and Morari M. (2010) Dual motor response to L-dopa and nociceptin/orphanin FQ receptor antagonists in 1-methyl-4-phenyl-1,2,5,6-tetrahydropyridine (MPTP) treated mice: Paradoxical inhibition is relieved by D_2/D_3 receptor blockade. *Exp. Neurol.* **223**, 473–484.

Visanji N. P., de Bie R. M., Johnston T. H., McCreary A. C., Brotchie J. M. and Fox S. H. (2008) The nociceptin/orphanin FQ (NOP) receptor antagonist J-113397 enhances the effects of levodopa in the MPTP-lesioned nonhuman primate model of Parkinson's disease. *Mov. Disord.* **23**, 1922–1925.

Vitale G., Ruggieri V., Filaferro M. *et al.* (2009) Chronic treatment with the selective NOP receptor antagonist [Nphe 1, Arg 14, Lys 15]N/OFQ-NH2 (UFP-101) reverses the behavioural and biochemical effects of unpredictable chronic mild stress in rats. *Psychopharmacology (Berl)* **207**, 173–189.

© 2010 The Authors

Volta M., Marti M., McDonald J., Molinari S., Camarda V., Pelà M., Trapella C. and Morari M. (2010a) Pharmacological profile and antiparkinsonian properties of the novel nociceptin/orhpanin FQ receptor antagonist 1-[1-cyclooctylmethyl-5-(1-hydroxy-1-methyl-ethyl)-1,2,3,6-tetrahydro-pyridin-4-yl]-3-ethyl-1,3-dihydro-benzo-imidazol-2-one (GF-4). *Peptides* **31**, 1194–1204.

Volta M., Marti M., Chipilska L., Trapella C. and Morari M. (2010b) Dopamine D2 receptor blockade in substantia nigra pars reticulata modulates behavioral and neurochemical effects evoked by the nociceptin/orphanin FQ receptor antagonist compound 24 in 6-hydroxydopamine hemilesioned rats. 7th FENS forum of European Neuroscience, Abst n. 197.49.

Wang Y. M., Gainetdinov R. R., Fumagalli F., Xu F., Jones S. R., Bock C. B., Miller G. W., Wightman R. M. and Caron M. G. (1997) Knockout of the vesicular monoamine transporter 2 gene results in neonatal death and supersensitivity to cocaine and amphetamine. *Neuron* **19**, 1285–1296.

© 2010 The Authors